Office de la Propriété
Intellectuelle
du Canada

Un organisme
d'Industrie Canada

Canadian
Intellectual Property
Office

An agency of
Industry Canada

CA 2797941 C 2015/01/27

(11)(21) **2 797 941**

(12) **BREVET CANADIEN
CANADIAN PATENT**

(13) **C**

(22) **Date de dépôt/Filing Date:** 2010/10/01

(41) **Mise à la disp. pub./Open to Public Insp.:** 2011/04/07

(45) **Date de délivrance/Issue Date:** 2015/01/27

(62) **Demande originale/Original Application:** 2 774 869

(30) **Priorité/Priority:** 2009/10/01 (US61/247,828)

(51) **Cl.Int./Int.Cl.** *G01N 33/50* (2006.01)

(72) **Inventeurs/Inventors:**
PASTURAL, ELODIE, CA;
RITCHIE, SHAWN, CA

(73) **Propriétaire/Owner:**
PHENOMENOME DISCOVERIES INC., CA

(74) **Agent:** GOWLING LAFLEUR HENDERSON LLP

(54) **Titre :** BIOMARQUEURS SERIQUES DU CANCER DU PANCREAS ET LEURS UTILISATIONS EN VUE DE LA DETECTION ET DU DIAGNOSTIC DE LA MALADIE

(54) **Title:** SERUM-BASED BIOMARKERS OF PANCREATIC CANCER AND USES THEREOF FOR DISEASE DETECTION AND DIAGNOSIS

(57) **Abrégé/Abstract:**

Biomarkers of pancreatic cancer are described, as well as methods using these compounds for detecting pancreatic cancer. The methods can be used to diagnose a patient's health state, or change in health state, or for diagnosing risk of developing or the presence of pancreatic cancer. The method comprises analyzing a sample from a patient to obtain quantifying data for one or more than one of the metabolite markers; comparing the quantifying data to corresponding data obtained for one or more than one reference sample to identify abnormalities in the level of the metabolite marker(s) in the sample; and making a diagnosis if an abnormality is observed. Standards and kits for carrying out the method are also described.

ABSTRACT

Biomarkers of pancreatic cancer are described, as well as methods using these compounds for detecting pancreatic cancer. The methods can be used to diagnose a patient's health state, or change in health state, or for diagnosing risk of developing or the presence of pancreatic cancer. The method comprises analyzing a sample from a patient to obtain quantifying data for one or more than one of the metabolite markers; comparing the quantifying data to corresponding data obtained for one or more than one reference sample to identify abnormalities in the level of the metabolite marker(s) in the sample; and making a diagnosis if an abnormality is observed. Standards and kits for carrying out the method are also described.

SERUM-BASED BIOMARKERS OF PANCREATIC CANCER AND USES THEREOF FOR DISEASE DETECTION AND DIAGNOSIS

FIELD OF INVENTION

The present invention relates to biomarkers and methods of detecting diseases and physiological conditions. More specifically, the invention relates to biomarkers of pancreatic cancer and methods using these compounds for detecting diseases and physiological conditions, especially pancreatic cancer.

BACKGROUND OF THE INVENTION

The incidence of pancreatic cancer has increased during the past decades throughout the world, and ranks as the fourth and sixth leading causes of cancer in North America and the European Union respectively (1). This high rank is due to a very poor overall survival (OS) rate (less than 4%), which is illustrated by an annual incidence rate of pancreatic cancer almost identical to the mortality rate. In Canada for example, 3800 new cases were expected to be diagnosed in 2008 with 3700 anticipated deaths from this cancer.

Diagnosis is difficult because there are no noticeable symptoms in early stages, and signs are common with many other illnesses. Furthermore, pancreas location behind other organs renders its imaging more difficult. Diagnosis is usually performed when cancer has already disseminated to other organs. In combination with this late detection, pancreatic cancer displays a poor response to chemotherapy, radiation therapy, and surgery as conventionally used. For patients with advanced pancreatic cancer, the OS rate is less than 1% at five years, whereas for the rare patients diagnosed at an early stage, when surgery is possible, the after resection OS rate climbs to 20% (2). These numbers emphasize the need for an early detection and a new treatment concept of pancreatic cancer.

Current detection methods mostly rely on imaging and are summarized in Table 1.

Table 1. Current pancreatic cancer detection methods (adapted from cancer.gov)

Imaging	Computed Tomography (CT) Scan	
	Ultrasonography	Transabdominal Ultrasound
		Endoscopic Ultrasound
	Magnetic Resonance Imaging (MRI)	
	Endoscopic Retrograde Cholangiopancreatography	
	Percutaneous Transhepatic Cholangiography	
Biopsies	Fine-Needle Aspiration (FNA) Biopsy	
	Brush Biopsy	
	Laparoscopy	
Lab tests	Bilirubin and other substances	

The most sensitive and specific screening tool currently available seems to be the endoscopic ultrasound (3, 4), but its invasive features restrict its use to the screening of high risk populations, namely kindred with minimum two affected first-degree relatives or with known hereditary pancreatic cancer. Another inconvenience of endoscopic ultrasound is that its use is recommended to be associated to other methods such as computed tomography and endoscopic retrograde cholangiopancreatography (5). Diagnosis is confirmed exclusively on analysis of a biopsy. Thus, in addition to being invasive, this multi-step detection and diagnosis process only establishes the presence of an already developed tumor and does not identify risks of developing cancer.

New technologies such as genomics, proteomics, metabolomics and glycomics, have been used in the search for blood-based tumor markers, and have identified glycoproteins, more specifically highly glycosylated mucins, as main tumor markers in all kinds of cancer (6). Among these highly glycosylated mucins, which can be detected by specific monoclonal antibodies, the Cancer Antigen 19-9 (CA 19-9) is present primarily in pancreatic and biliary tract cancers, but also in patients with other malignancies (e.g. colorectal cancer) and benign conditions such as cirrhosis and pancreatitis. CA 19-9 is detected in most proteomics studies in pancreatic cancer serum samples (such as (7)), but its low specificity does not recommend it as a pancreatic cancer biomarker. Anecdotally so far, another glycosylation-related potential biomarker of pancreatic cancer is the core fusylation of biantennary glycans of RNase I, which displayed a 40% increase in the serum of two pancreatic cancer patients relative to two healthy controls (8).

Another well-known serum marker of pancreatic cancer is CEA (carcinoembryonic antigen), with an average reported sensitivity and specificity of both 65% (7). HIP/PAP-I and MIC-1 (macrophage inhibitory cytokine I) are also classical serum markers (9, 10). According to one study, MIC-1 and CA19-9 seem the markers with the highest sensitivity and specificity, in the sense of specificity vs. chronic pancreatitis (and not vs. colon cancer for example), when compared to osteopontin, TIMP-1 and HIP/PAP-I (9).

The use of CA19-9 as a marker is now recommended in combination with other markers, such as the mutation status of pancreatic cancer –related oncogenes like *K-ras* (2). *K-ras* is reported to be mutated in 78% of pancreatic adenocarcinomas (11). Molecular events in pancreatic carcinogenesis have been extensively studied (12), and beside *K-ras*, *p53*, *p21*, *p16*, *p27*, *SMAD4*, and *cyclin D1* are a few of these genes whose mutations or alterations in expression have been associated to pancreatic cancer (12). However, evidence regarding their application as prognostic indicators is conflicting. For instance, there is no consensus on the association between mutation in *p53* and decreased survival (12).

MicroRNA profiling has also been performed for pancreatic cancer, with the identification of some common microRNAs specifically altered (13-15).

Protein markers show the advantage of simple screening through an ELISA (Enzyme-linked immunosorbent assay) method, and research in this field is therefore very intensive. Newer proteomics studies have identified additional protein markers, such as apolipoproteins A-I and A-II, and transthyretin (7), all decreased in serum of pancreatic cancer patients, as well as MMP-9, DJ-1 and A1BG, each of which is overexpressed in pancreatic juice from cancer patients (16).

The involvement of apolipoproteins is interesting since they participate in lipid metabolism (17) and other members of this family have been associated to cancer (18).

The fatty acid composition of lipids in plasma and bile from patients with pancreatic cancer has also been analyzed (19, 20), even though neither of these studies has detailed the chemical subfamilies of the altered lipids. Plasma from pancreatic patients showed significantly lower levels of phospholipids that contain the side chain 18:2(ω6), 20:5(ω3) or 22:5(ω3), without distinction of lipid classes (19). Bile from hepatopancreaticobiliary cancer patients was found to contain a much lower level of phosphatidylcholines without distinction of side chains (20).

Since diabetes mellitus (DM) has a high prevalence in pancreatic cancer patients and is frequently of new onset, research has also been aimed at determining whether DM can be utilized as an early pancreatic cancer marker (21). A 2-fold increase of the glucagon / insulin ratio was found in the blood of pancreatic cancer patients relative to healthy controls, and at a cut-off of

7.4 ng/mU glucagon/insulin, pancreatic cancer induced new-onset DM could be discriminated from type 2 DM with 77% sensitivity and 69% specificity (21).

Overall, the methods described above are not ideally suited for large-scale population screening (either for low compliance or low sensitivity and specificity except in the case of a still-to-optimize multiple method combination), and most are capable of detecting pancreatic cancer *after* the formation of a tumor only. As a result, there still remains a need for accurate methods of detection, particularly for methods to detect early stages of the disease.

SUMMARY OF THE INVENTION

It is an object of the invention to provide diagnostic methods and diagnostic markers useful for detecting cancer in a subject.

Accordingly, the invention relates to methods and diagnostic markers for detecting or diagnosing cancer. Such methods and diagnostic markers are particularly useful for detecting pancreatic cancer.

As an aspect of the invention, a method is provided for diagnosing a subject's pancreatic cancer health state or change in health state, or for diagnosing pancreatic cancer or the risk of pancreatic cancer in a subject, comprising steps of:

a) analyzing a sample from the patient by high resolution mass spectrometry to obtain accurate mass intensity data;

b) comparing the accurate mass intensity data to corresponding data obtained from one or more than one reference sample to identify an increase or decrease in accurate mass intensity; and

c) using the increase or decrease in accurate mass intensity for diagnosing the patient's pancreatic cancer health state, or change in pancreatic cancer health state, or for diagnosing risk of developing pancreatic cancer or the presence of pancreatic cancer in the patient,

wherein the accurate mass intensity is measured, in Daltons, at or substantially equivalent to a hydrogen and electron adjusted accurate mass, or neutral accurate mass as described in further detail herein, for example in Table 5.

In an embodiment, the accurate mass intensity is measured at one or more of the following masses: 78.0516; 84.0575; 112.0974; 116.5696; 191.5055; 197.0896; 200.1389; 202.045; 203.1155; 214.1204; 214.1205; 232.1309; 233.1345; 240.0997; 243.0714; 244.0554; 254.1127;

255.1161; 256.2403; 260.0033; 262.0814; 268.1284; 270.0323; 270.0867; 276.0948; 280.2403; 280.2404; 281.2432; 281.2435; 282.2558; 282.2559; 283.2591; 283.2595; 284.9259; 300.1186; 300.2067; 302.0945; 302.222; 302.2457; 304.2375; 304.2407; 317.9613; 318.0931; 326.2048; 326.2458; 327.9902; 328.2403; 328.2408; 328.2627; 329.2439; 329.2658; 330.2559; 332.1473; 338.0189; 348.1191; 350.2222; 360.1782; 360.1792; 361.1828; 366.3593; 368.1057; 382.1083; 382.1601; 418.2204; 428.2404; 428.3647; 446.2526; 446.3395; 468.2336; 468.3581; 468.3807; 469.237; 469.3616; 481.315; 484.3527; 485.904; 494.4321; 495.3325; 496.3373; 505.3146; 508.2256; 517.3141; 518.321; 519.3295; 520.448; 522.4638; 522.4639; 523.3661; 523.4675; 538.4237; 540.4381; 541.3134; 541.3361; 542.3394; 545.3454; 562.4962; 564.5121; 565.3373; 566.3403; 569.3682; 570.372; 572.4798; 573.4833; 574.4952; 575.4985; 576.4751; 576.5113; 577.5149; 578.5169; 578.5284; 579.5313; 587.3214; 588.3269; 589.3368; 590.3408; 592.4709; 594.4852; 594.4863; 595.4892; 595.4897; 596.5017; 596.5027; 597.5066; 598.4955; 599.4993; 600.5117; 601.5151; 602.5269; 603.5297; 606.5591; 609.3259; 613.3379; 615.3535; 627.5656; 628.5438; 630.799; 631.798; 633.3245; 635.7525; 636.7532; 645.7958; 657.7337; 658.7372; 670.5696; 671.5731; 681.5858; 702.5709; 715.6959; 719.6256; 720.6272; 721.5035; 723.5203; 723.521; 724.5252; 724.5477; 725.7228; 733.5054; 735.6582; 743.5396; 744.5425; 745.5631; 746.5128; 746.5705; 748.527; 749.5374; 749.5388; 750.5425; 751.5511; 751.5539; 752.5574; 755.5497; 757.556; 757.5587; 758.562; 758.5626; 759.5383; 759.5733; 760.5792; 763.5578; 765.5678; 766.4792; 771.5699; 773.5276; 774.5419; 775.5522; 775.5532; 775.5532; 777.0402; 777.5709; 779.5405; 779.5416; 780.5452; 780.5454; 781.5029; 781.5566; 782.5612; 783.569; 783.5755; 784.5742; 784.5806; 785.5913; 785.5929; 785.5931; 786.593; 786.5972; 787.5989; 791.5841; 793.7091; 795.5181; 796.5212; 801.5147; 801.5262; 801.5523; 802.5291; 803.5373; 803.5414; 803.5677; 804.5422; 804.5456; 804.5714; 804.7208; 805.5549; 806.5632; 807.5734; 807.5739; 807.5764; 808.5783; 808.5791; 809.5796; 810.5867; 811.5729; 811.608; 812.6774; 813.5888; 819.5177; 823.5411; 824.69; 825.5522; 826.5561; 826.7047; 827.5401; 827.5678; 827.7082; 828.5397; 828.5721; 829.5516; 829.5532; 829.5843; 830.5591; 830.5879; 831.5652; 831.572; 831.5997; 832.6031; 833.5864; 834.5868; 835.598; 837.7209; 838.7284; 838.7435; 839.7464; 847.531; 850.7061; 850.7326; 851.6694; 851.7107; 851.7337; 852.7368; 853.573; 854.7358; 854.7397; 855.5721; 855.7392; 855.7436; 856.7505; 856.754; 857.6923; 857.7543; 857.7574; 858.7644; 861.749; 865.752; 866.7585; 867.7649; 868.7704; 871.5547; 873.7819; 874.7066; 874.787; 875.7108; 879.7629; 889.7537; 889.8147; 894.7911; 898.7043; 898.7325; 902.7629; 903.7636; 907.7847; 908.7907; 909.7882; 910.7272; 916.7735; 919.6496; 921.813; 922.7081; 922.7285; 922.8222; 923.7295; 924.7233; 925.727; 933.8137; 937.7542; 946.8194; 947.8263; 948.836; 950.7364; 960.7432; 970.733; 972.7481; 973.7482; 984.7406; 986.7568;

996.7518; 997.7397; 998.7566; 999.7632; 1010.765; 1011.669; 1011.77; 1012.781; 1016.931; 1017.935; 1018.944; 1019.951; 1020.957; 1038.915; 1039.705; 1039.921; 1040.933; 1041.935; 1199.084; 1200.088; 1201.09; 1202.098; 1223.09; 1224.096; 1225.096; 1226.599; 1227.112; 1228.117; 1229.12; 1230.125; 1247.084; 1249.105; 1250.108; 1251.119; 1252.12; 1253.123; 1253.134; 1254.137 and 1255.153.

In a further non-limiting embodiment of the invention, the accurate mass intensity is measured at an accurate mass of 519.3295, 523.3661, 541.3134, 702.5709, 724.5477, 757.556, 779.5405, 783.569, 785.5913, 803.5373, 805.5549, 807.5734, 809.5796, 812.6774, 829.5516, 833.5864, 576.4751, 594.4863, 596.5017 or combinations thereof. In such embodiments a decrease in accurate mass intensity is generally identified in the comparing step (b).

In a further exemplary embodiment, the accurate mass is measured at an accurate mass of 600.5117. In such an embodiment an increase in accurate mass intensity is identified in the comparing step (b).

In the above-described method, the term "substantially equivalent" may in certain non-limiting embodiments refer to ± 5 ppm of the hydrogen and electron adjusted accurate mass, or neutral accurate mass, and in further embodiments, ± 1 ppm of the hydrogen and electron adjusted accurate mass, or neutral accurate mass.

As a further aspect of the invention, there is provided a method for diagnosing a patient's pancreatic cancer health state, or change in pancreatic cancer health state, or for diagnosing risk of developing pancreatic cancer or the presence of pancreatic cancer in a patient, comprising the steps of:

> a) analyzing a sample from the patient to obtain quantifying data for one or more than one metabolite marker;
> b) comparing the quantifying data for the one or more than one metabolite marker to corresponding data obtained for one or more than one reference sample to identify an increase or decrease in the level of the one or more than one metabolite marker in the sample; and
> c) using the increase or decrease in the level of the one or more than one metabolite marker in the sample for diagnosing the patient's pancreatic cancer health state, or change in pancreatic cancer health state, or for diagnosing risk of developing pancreatic cancer or the presence of pancreatic cancer in the patient,

wherein the one or more metabolite marker is as described herein.

In an embodiment, the one or more metabolite marker comprises one or more molecule having a molecular formula as follows: $C_{36}H_{62}O_4$, $C_{36}H_{62}O_5$, $C_{36}H_{64}O_5$, $C_{36}H_{66}O_5$, $C_{36}H_{64}O_6$, $C_{36}H_{66}O_6$, $C_{36}H_{68}O_6$, $C_{22}H_{46}NO_7P$, $C_{22}H_{48}NO_7P$, $C_{24}H_{50}NO_7P$, $C_{24}H_{48}NO_7P$, $C_{24}H_{46}NO_7P$, $C_{26}H_{54}NO_7P$, $C_{26}H_{52}NO_7P$, $C_{26}H_{50}NO_7P$, $C_{26}H_{48}NO_7P$, $C_{28}H_{56}NO_7P$, $C_{28}H_{54}NO_7P$, $C_{28}H_{52}NO_7P$, $C_{28}H_{50}NO_7P$, $C_{28}H_{48}NO_7P$, $C_{28}H_{46}NO_7P$, $C_{30}H_{56}NO_7P$, $C_{30}H_{54}NO_7P$, $C_{30}H_{52}NO_7P$, $C_{30}H_{50}NO_7P$, $C_{32}H_{58}NO_7P$, $C_{32}H_{54}NO_7P$, $C_{38}H_{76}NO_7P$, $C_{40}H_{82}NO_7P$, $C_{40}H_{80}NO_7P$, $C_{40}H_{78}NO_7P$, $C_{40}H_{70}NO_7P$, $C_{42}H_{78}NO_8P$, $C_{42}H_{80}NO_8P$, $C_{42}H_{82}NO_8P$, $C_{42}H_{84}NO_8P$, $C_{44}H_{78}NO_8P$, $C_{44}H_{80}NO_8P$, $C_{44}H_{82}NO_8P$, $C_{44}H_{84}NO_8P$, $C_{44}H_{86}NO_8P$, $C_{44}H_{88}NO_8P$, $C_{46}H_{78}NO_8P$, $C_{46}H_{80}NO_8P$, $C_{46}H_{82}NO_8P$, $C_{46}H_{84}NO_8P$, $C_{48}H_{80}NO_8P$, $C_{48}H_{82}NO_8P$, $C_{48}H_{84}NO_8P$, $C_{48}H_{86}NO_8P$, $C_{42}H_{80}NO_7P$, $C_{42}H_{82}NO_7P$, $C_{42}H_{84}NO_7P$, $C_{44}H_{82}NO_7P$, $C_{44}H_{84}NO_7P$, $C_{44}H_{86}NO_7P$, $C_{44}H_{88}NO_7P$, $C_{46}H_{82}NO_7P$, $C_{46}H_{84}NO_7P$, $C_{46}H_{86}NO_7P$, $C_{48}H_{84}NO_7P$, $C_{48}H_{86}NO_7P$, $C_{39}H_{79}N_2O_6P$ (or $C_{39}H_{80}N_2O_6P^+$), or $C_{41}H_{81}N_2O_6P$ (or $C_{41}H_{82}N_2O_6P^+$), or $C_{41}H_{83}N_2O_6P$ (or $C_{41}H_{84}N_2O_6P^+$), or $C_{47}H_{93}N_2O_6P$ (or $C_{47}H_{94}N_2O_6P^+$), or $C_{47}H_{95}N_2O_6P$ (or $C_{47}H_{96}N_2O_6P^+$), including combinations thereof.

In further non-limiting embodiments, the metabolite marker may be a diacylphosphatidylcholine, plasmanylphosphocholine or plasmenylphosphocholine as defined in Formula (I):

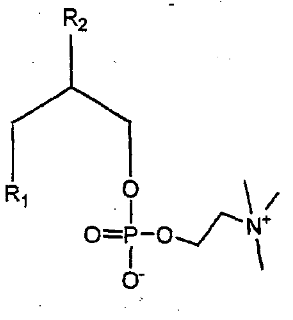

(I)

including adducts or salts thereof, wherein

R_1 is a 16:0, 16:1, 18:0, 18:1, 18:2, 18:3, 20:3, 20:4, 20:5, 22:5 or 22:6 fatty acid or alcohol moiety bonded to the glycerol backbone, the bond being an acyl linkage when the metabolite marker is a diacylphosphatidylcholine, an ether linkage when the metabolite marker is a plasmanylphosphocholine, or a vinyl-ether linkage when the metabolite marker is a plasmenylphosphocholine; and

R_2 is a 16:0, 16:1, 18:0, 18:1, 18:2, 18:3, 20:3, 20:4, 20:5, 22:5, or 22:6 fatty acid moiety bonded to the glycerol backbone through an acyl linkage.

In further embodiments, the metabolite marker may be a 2-lysophosphatidylcholine as defined in Formula (II) or a 1-lysophosphatidylcholine as defined in Formula (III):

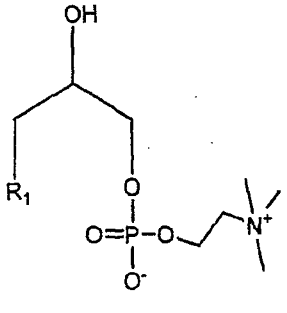

(II)

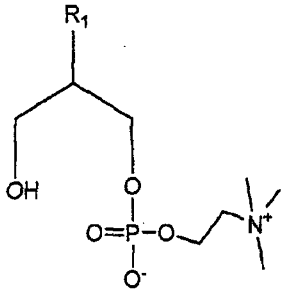

(III)

including adducts or salts thereof, wherein

R_1 is a 14:0, 14:1, 16:0, 16:1, 16:2, 18:0, 18:1, 18:2, 18:3, 20:1, 20:2, 20:3, 20:4, 20:5, 20:6, 22:3, 22:4, 22:5, 22:6, 24:4, 24:6, 30:1, 32:0, 32:1, 32:2 or 32:6 fatty acid moiety bonded to the glycerol backbone through an acyl linkage.

In other non-limiting embodiments, the metabolite marker may be a sphingomyelin as defined in Formula (IV):

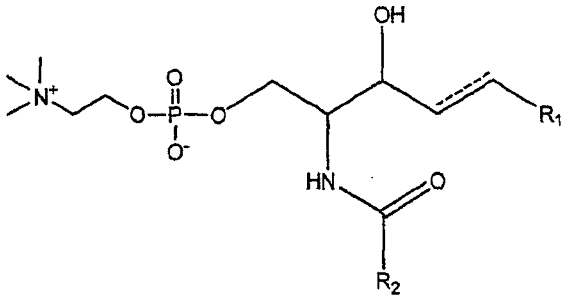

(IV)

including adducts or salts thereof, wherein the dashed line represents an optional double bond;

R_1 is a C_{13} alkyl group; and

R_2 is a C_{11} to C_{25} alkyl or alkenyl group, the alkenyl group having from 1 to 3 double bonds.

In certain non-limiting embodiments, R_2 of the sphingomyelin of Formula (IV) may be a C_{11} alkyl group, a C_{13} alkyl group, a C_{15} alkyl group, a C_{17} alkyl group, a C_{17} alkenyl group with 3 double bonds, a C_{19} alkyl group, a C_{21} alkyl group, a C_{23} alkenyl group with 1 double bond, a C_{23} alkyl group, a C_{24} alkyl group, a C_{25} alkenyl group with 1 double bond, a C_{25} alkyl group.

The above described methods may further include steps of: analyzing a sample from the patient to obtain quantifying data for one or more than one internal standard molecule; and obtaining a ratio for each of the levels of the one or more than one metabolite marker to the level obtained for the one or more than one internal standard molecule; wherein the comparing step (b) comprises comparing each ratio to one or more corresponding ratios obtained for the one or more than one reference sample.

Without wishing to be limiting in any way, it will be appreciated that the above-described methods can be carried out, at least in part, with the assistance of a computer. In such embodiments the computer may be integrated with the instrument used to perform the analysis, or it may be a separate computer adapted to receive data output from the instrument according to the knowledge and skill of those in the art. The analyzing step (a) will typically be carried out using the instrument, for example but not limited to a mass spectrometer, and the comparing step (b) carried out using the computer or other processing means programmed to receive the accurate mass intensity data or quantifying data from the instrument and perform the calculations required to identify an increase or decrease in the level of the one or more than one metabolite marker in the sample. This data from step (b) may be output for use by an individual trained to identify the noted increase or decrease and make the diagnosis of step (c), or alternatively the computer or processing means may be further programmed to generate an output of a diagnosis. In the latter case, the output may comprise a positive or negative diagnosis factor, and may optionally include additional details including but not limited to statistical data, threshold data, patient data and other details. The data may be output to a display, such as a monitor, to a printer for generating a copy of the details of diagnosis, to a data receiving centre or directly to a service provider, or in any other way as would be understood by one skilled in the art.

In certain embodiments, the metabolite may be a lysophosphatidylcholine (LysoPC), including LysoPC 14:0, LysoPC 14:1, LysoPC 16:0, LysoPC 16:1, LysoPC 16:2, LysoPC 18:0, LysoPC 18:1, LysoPC 18:2, LysoPC 18:3, LysoPC 20:1, LysoPC 20:2, LysoPC 20:3, LysoPC 20:4, LysoPC 20:5, LysoPC 20:6, LysoPC 22:3, LysoPC 22:4, LysoPC 22:5, LysoPC 22:6, LysoPC 24:4, LysoPC 24:6, LysoPC 30:1, LysoPC 32:0, LysoPC 32:1, LysoPC 32:2, LysoPC 32:6, or combinations thereof.

In other embodiments the metabolite may be a phosphatidylcholine, including phosphatidylcholine molecules having a molecular formula of $C_{42}H_{78}NO_8P$, $C_{42}H_{80}NO_8P$, $C_{42}H_{82}NO_8P$, $C_{42}H_{84}NO_8P$, $C_{44}H_{78}NO_8P$, $C_{44}H_{80}NO_8P$, $C_{44}H_{82}NO_8P$, $C_{44}H_{84}NO_8P$, $C_{44}H_{86}NO_8P$, $C_{44}H_{88}NO_8P$, $C_{46}H_{78}NO_8P$, $C_{46}H_{80}NO_8P$, $C_{46}H_{82}NO_8P$, $C_{46}H_{84}NO_8P$, $C_{48}H_{80}NO_8P$, $C_{48}H_{82}NO_8P$, $C_{48}H_{84}NO_8P$, $C_{48}H_{86}NO_8P$, or combinations thereof.

In other embodiments the metabolite may be a plasmenylphosphocholine, including plasmenylphosphocholine molecules having a formula of $C_{42}H_{80}NO_7P$, $C_{42}H_{82}NO_7P$, $C_{42}H_{84}NO_7P$, $C_{44}H_{82}NO_7P$, $C_{44}H_{84}NO_7P$, $C_{44}H_{86}NO_7P$, $C_{44}H_{88}NO_7P$, $C_{46}H_{82}NO_7P$, $C_{46}H_{84}NO_7P$, $C_{46}H_{86}NO_7P$, $C_{48}H_{84}NO_7P$, $C_{48}H_{86}NO_7P$, or combinations thereof.

In yet further embodiments the metabolite may be a sphingomyelin, including sphingomyelin molecules having a molecular formula of $C_{39}H_{79}N_2O_6P$ (or $C_{39}H_{80}N_2O_6P^+$), $C_{41}H_{81}N_2O_6P$ (or $C_{41}H_{82}N_2O_6P^+$), or $C_{41}H_{83}N_2O_6P$ (or $C_{41}H_{84}N_2O_6P^+$), or $C_{47}H_{93}N_2O_6P$ (or $C_{47}H_{94}N_2O_6P^+$), or $C_{47}H_{95}N_2O_6P$ (or $C_{47}H_{96}N_2O_6P^+$), or combinations thereof.

As described herein, alterations in the levels of the metabolite markers may be detected by MS/MS transition. For instance, a metabolite marker of molecular formula $C_{36}H_{64}O_5$ may be monitored for level fluctuations of organic extracts in negative ionization mode (such as atmospheric pressure chemical ionization (APCI)) at a MS/MS transition of 575.5 / 513.5, 575.5 / 557.5, 575.5 / 539.5, 575.5 / 531.5, 575.5 / 499.5, 575.5 / 495.5, 575.5 / 459.4, 575.5 / 417.4, 575.5 / 415.3, 575.5 / 413.3, 575.5 / 403.3, 575.5 / 295.2, 575.5 / 279.2, 575.5 / 260.2, 575.5 / 251.2, 575.5 / 197.9, 575.5 / 119.4, 575.5 / 113.1, and 575.5 / 97.0, or combinations thereof.

Other useful MS/MS transitions for organic extracts in negative ionization mode (e.g. APCI mode) for the metabolite markers described herein include: 593.5 / 557.5, 593.5 / 575.4, 593.5 / 549.4, 593.5 / 531.5, 593.5 / 513.4, 593.5 / 495.4, 593.5 / 433.3, 593.5 / 421.4, 593.5 / 415.2, 593.5 / 391.4, 593.5 / 371.3, 593.5 / 315.3, 593.5 / 311.1, 593.5 / 297.2, 593.5 / 281.2, 593.5 / 277.2, 593.5 / 251.2, 593.5 / 201.1, 593.5 / 195.3, 593.5 / 171.1, 593.5 / 139.1 and 593.5 / 133.5, or combinations thereof for $C_{36}H_{66}O_6$; 595.5 / 559.5, 595.5 / 577.4, 595.5 / 551.4, 595.5 / 533.4, 595.5 / 515.5, 595.5 / 497.4, 595.5 / 478.4, 595.5 / 433.3, 595.5 / 423.4, 595.5 / 391.3, 595.5 / 372.3, 595.5 / 595.5 / 315.3, 595.5 / 313.2, 595.5 / 298.2, 595.5 / 297.2, 595.5 / 281.2, 595.5 / 279.2, 595.5 / 239.2, 595.5 / 232.9, 595.5 / 171.1, 595.5 / 169.1 and 595.5 / 141.1, or combinations thereof for $C_{36}H_{68}O_6$; 557.4 / 495.4, 557.4 / 539.4, 557.4 / 513.3, 557.4 / 279.2, 557.4 / 277.2, 557.4 / 220.7 and 557.4 / 111.2, or combinations thereof for $C_{36}H_{62}O_4$; 573.5 / 511.4, 573.5 / 555.3, 573.5 / 537.4, 573.5 / 529.4, 573.5 / 519.4, 573.5 / 493.3, 573.5 / 457.4, 573.5 / 455.3, 573.5 / 443.4, 573.5 / 415.4, 573.5 / 413.3, 573.5 / 411.3, 573.5 / 399.3, 573.5 / 397.3, 573.5 / 389.7, 573.5 / 295.2, 573.5 / 279.2, 573.5 / 277.2, 573.5 / 251.2, 573.5 / 231.1, 573.5 / 223.1, 573.5 / 201.1, 573.5 / 171.1, 573.5 / 169.1, 573.5 / 125.1 and 573.5 / 113.1, or combinations thereof for $C_{36}H_{62}O_5$; 577.5 / 515.4, 577.5 / 559.4, 577.5 / 546.5, 577.5 / 533.5, 577.5 / 497.4, 577.5 / 419.4, 577.5 / 405.5, 577.5 / 297.2 and 577.5 / 281.2, or combinations thereof for $C_{36}H_{66}O_5$; 591.5 / 573.4, 591.5 / 555.4, 591.5 / 528.3, 591.5 / 511.2, 591.5 / 476.1, 591.5 / 419.3, 591.5 / 403.1, 591.5 / 387.3, 591.5 / 297.2, 591.5 / 295.2, 591.5 / 274.0, 591.5 / 255.3, 591.5 / 223.6, 591.5 / 203.5, 591.5 / 201.1, 591.5 / 171.0 and 591.5 / 125.3, or combinations thereof for $C_{36}H_{64}O_6$.

Other useful MS/MS transitions for aqueous extracts in positive ionization mode (e.g. positive Electrospray Ionization (ESI)) for the metabolite markers described herein include: 520.3 / 184.2 for $C_{26}H_{50}NO_7P$; 524.3 / 184.2 for $C_{26}H_{54}NO_7P$; 542.3 / 184.2 for $C_{28}H_{48}NO_7P$; 758.6 / 184.2 for $C_{42}H_{80}NO_8P$; 784.6 / 184.2 for $C_{44}H_{82}NO_8P$; 786.6 / 184.2 for $C_{44}H_{84}NO_8P$; 788.6 / 184.2 for $C_{44}H_{86}NO_8P$; 790.6 / 184.2 for $C_{44}H_{88}NO_8P$; 806.6 / 184.2 for $C_{46}H_{80}NO_8P$; 808.6 / 184.2 for $C_{46}H_{82}NO_8P$; 810.6 / 184.2 for $C_{46}H_{84}NO_8P$; 834.6 / 184.2 for $C_{48}H_{84}NO_8P$; 836.6 / 184.2 for $C_{48}H_{86}NO_8P$; 703.6 / 184.2 for $C_{39}H_{79}N_2O_6P$; 729.6 / 184.2 for $C_{41}H_{81}N_2O_6P$; 731.6 / 184.2 for $C_{41}H_{83}N_2O_6P$; 813.6 / 184.2 for $C_{47}H_{93}N_2O_6P$; or 815.6 / 184.2 for $C_{47}H_{95}N_2O_6P$. Additional

MS/MS transition details and other features of the metabolites described herein are evident from the following detailed description of the invention and may also be used in further non limiting embodiments of the invention.

Other useful MS/MS transitions for aqueous extracts in negative ionization mode (e.g. negative ESI) for the metabolite markers described herein include: 564.3 / 504.3 / 279.3 for $C_{26}H_{50}NO_7P$; 568.3 / 508.4 / 283.3 for $C_{26}H_{54}NO_7P$; 586.3 / 526.3 / 301.2 for $C_{28}H_{48}NO_7P$; 802.6 / 742.6 / 279.2, 802.6 / 742.6 / 281.2, 802.6 / 742.6 / 253.2 or 802.6 / 742.6 / 255.2 for $C_{42}H_{80}NO_8P$; 828.6 / 768.6 / 305.3, 828.6 / 768.6 / 279.2, 828.6 / 768.6 / 281.2 or 828.6 / 768.6 / 255.2 for $C_{44}H_{82}NO_8P$; 830.6 / 770.6 / 279.2, 830.6 / 770.6 / 281.2 or 830.6 / 770.6 / 283.2 for $C_{44}H_{84}NO_8P$; 832.6 / 772.6 / 281.2 or 832.6 / 772.6 / 283.2 for $C_{44}H_{86}NO_8P$; 834.6 / 774.6 / 283.2 for $C_{44}H_{88}NO_8P$; 850.6 / 790.6 / 327.3, 850.6 / 790.6 / 279.2, 850.6 / 790.6 / 303.2 or 850.6 / 790.6 / 255.2 for $C_{46}H_{80}NO_8P$; 852.6 / 792.6 / 329.3, 852.6 / 792.6 / 301.3, 852.6 / 792.6 / 303.2, 852.6 / 792.6 / 281.2, 852.6 / 792.6 / 283.2 or 852.6 / 792.6 / 255.2 for $C_{46}H_{82}NO_8P$; 854.6 / 794.6 / 331.3, 854.6 / 794.6 / 303.2, 854.6 / 794.6 / 283.2 or 854.6 / 794.6 / 255.2 for $C_{46}H_{84}NO_8P$; 878.6 / 818.6 / 327.3 or 878.6 / 818.6 / 283.2 for $C_{48}H_{84}NO_8P$; 880.6 / 820.6 / 329.3 or 880.6 / 820.6 / 283.2 for $C_{44}H_{86}NO_8P$; 747.6 / 687.6 / 168.1 for $C_{39}H_{79}N_2O_6P$; 773.6 / 713.6 / 168.1 for $C_{41}H_{81}N_2O_6P$; 775.6 / 715.6 / 168.1 for $C_{41}H_{83}N_2O_6P$; 857.6 / 797.6 / 168.1 for $C_{47}H_{93}N_2O_6P$; or 859.6 / 799.6 / 168.1 for $C_{47}H_{95}N_2O_6P$. Additional MS/MS transition details and other features of the metabolites described herein are evident from the following detailed description of the invention and may also be used in further non limiting embodiments of the invention.

In the above-described methods, the step of comparing accurate mass intensity data to reference data to identify an increase or decrease in accurate mass intensity; or the step of comparing quantifying data for a metabolite marker to reference data to identify an increase or decrease in the level of the metabolite marker, can in certain non-limiting embodiments comprise or otherwise relate to a step of determining the level of the specified markers, metabolites or molecules, either by determining a change in accurate mass intensity or by other analytical means.

The invention further relates to an assay standard comprising a metabolite marker as described herein labeled with a detection agent. The standard will be useful for carrying out a diagnostic method as described herein, and may include one or more of the following non-limiting detection agents: a stable isotope, an enzyme, or a protein that enables detection *in vitro*.

In certain non-limiting embodiments, the assay standard may comprise as the metabolite marker a diacylphosphatidylcholine, plasmanylphosphocholine or plasmenylphosphocholine as defined in Formula (I):

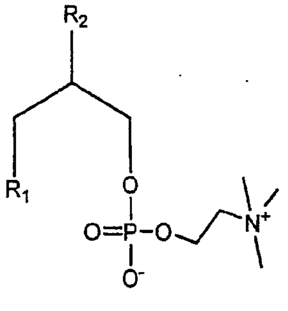

(I)

including adducts or salts thereof, wherein

R_1 is a 16:0, 16:1, 18:0, 18:1, 18:2, 18:3, 20:3, 20:4, 20:5, 22:5 or 22:6 fatty acid or alcohol moiety bonded to the glycerol backbone, the bond being an acyl linkage when the metabolite marker is a diacylphosphatidylcholine, an ether linkage when the metabolite marker is a plasmanylphosphocholine, or a vinyl-ether linkage when the metabolite marker is a plasmenylphosphocholine; and

R_2 is a 16:0, 16:1, 18:0, 18:1, 18:2, 18:3, 20:3, 20:4, 20:5, 22:5, or 22:6 fatty acid moiety bonded to the glycerol backbone through an acyl linkage.

In further embodiments, the assay standard may comprise as the metabolite marker a 2-lysophosphatidylcholine as defined in Formula (II) and a 1-lysophosphatidylcholine in Formula (III):

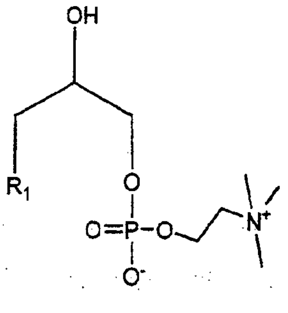

(II)

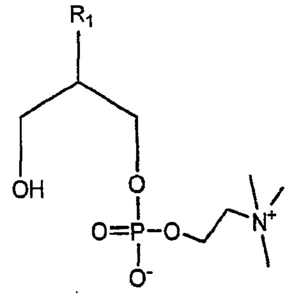

(III)

including adducts or salts thereof, wherein

R$_1$ is a 14:0, 14:1, 16:0, 16:1, 16:2, 18:0, 18:1, 18:2, 18:3, 20:1, 20:2, 20:3, 20:4, 20:5, 20:6, 22:3, 22:4, 22:5, 22:6, 24:4, 24:6, 30:1, 32:0, 32:1, 32:2 or 32:6 fatty acid moiety bonded to the glycerol backbone through an acyl linkage.

In other non-limiting embodiments, the assay standard may comprise as the metabolite marker a sphingomyelin as defined in Formula (IV):

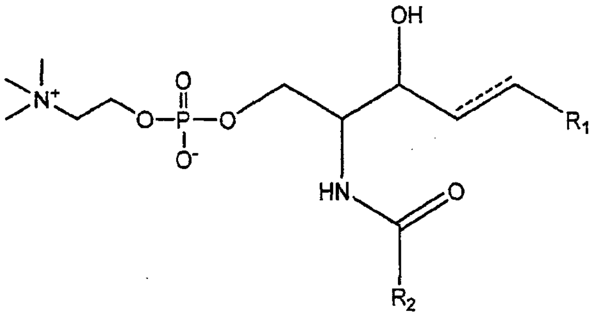

(IV)

including adducts or salts thereof, wherein the dashed line represents an optional double bond,

R$_1$ is a C$_{13}$ alkyl group; and

R$_2$ is a C$_{11}$ to C$_{25}$ alkyl or alkenyl group, the alkenyl group having from 1 to 3 double bonds.

In certain non-limiting embodiments, R$_2$ of the sphingomyelin of Formula (IV) may be a C$_{11}$ alkyl group, a C$_{13}$ alkyl group, a C$_{15}$ alkyl group, a C$_{17}$ alkyl group, a C$_{17}$ alkenyl group with 3 double bonds, a C_{19} alkyl group, a C_{21} alkyl group, a C_{23} alkenyl group with 1 double bond, a C_{23} alkyl group, a C_{24} alkyl group, a C_{25} alkenyl group with 1 double bond, or a C_{25} alkyl group.

In further embodiments of the standard, which are also considered to be non-limiting, the assay standard may comprise as the metabolite marker a lysophosphatidylcholine (LysoPC, either 1-LysoPC or 2-LysoPC) including LysoPC 14:0, LysoPC 14:1, LysoPC 16:0, LysoPC 16:1, LysoPC 16:2, LysoPC 18:0, LysoPC 18:1, LysoPC 18:2, LysoPC 18:3, LysoPC 20:1, LysoPC 20:2, LysoPC 20:3, LysoPC 20:4, LysoPC 20:5, LysoPC 20:6, LysoPC 22:3, LysoPC 22:4, LysoPC 22:5, LysoPC 22:6, LysoPC 24:4, LysoPC 24:6, LysoPC 30:1, LysoPC 32:0, LysoPC 32:1, LysoPC 32:2, or LysoPC 32:6.

The invention further relates to a kit or commercial package comprising the above-described standard and instructions for quantitating an analyte or performing a diagnostic test as described herein.

BRIEF DESCRIPTION OF THE DRAWINGS

These and other features of the invention will become more apparent from the following description in which reference is made to the following figures.

Figure 1 provides a schematic description of the studies performed.

Figure 2 illustrates a Principal Component Analysis on all masses differentiating pancreatic cancer from controls with p-value < 0.05 showing a clear separation between pancreatic cancer samples (grey) and controls (black).

Figure 3 illustrates a Principal Component Analysis on the 20 best biomarkers showing a clear separation between pancreatic cancer samples (grey) and controls (black) (a), and the relative level intensities of these 20 biomarkers in the serum of pancreatic cancer patients relative to controls (b).

Figure 4 illustrates a ROC and variability chart for the first six best biomarkers by FTICR, namely 594.4863 (AUC=0.96) (a), 785.5913 (AUC=0.93) (b), 702.5709 (AUC=0.91) (c), 807.5734 (AUC=0.93) (d), 576.4751 (AUC=0.93) (e) and 541.3134 (AUC=0.92) (f).

Figure 5 shows a logistic regression analysis of the combination of the six FTICR best biomarkers, with ROC curve (a) and classification table (b).

Figure 6 illustrates the fragmentation pattern of C36 compound "576".

Figure 7 illustrates the fragmentation pattern of C36 compound “594”.

Figure 8 illustrates the fragmentation pattern of C36 compound “596”.

Figure 9 illustrates the fragmentation pattern of C36 compound “558”.

Figure 10 illustrates the fragmentation pattern of C36 compound “574”.

Figure 11 illustrates the fragmentation pattern of C36 compound “578”

Figure 12 illustrates the fragmentation pattern of C36 compound “592”.

Figure 13 shows the ^{1}H NMR spectrum of the fraction rich in C36 markers “594” and “596”.

Figure 14 illustrates the fragmentation patterns of 519.3 in positive aqueous ESI mode. (a) and (b) correspond to the fragmentation patterns at different retention times.

Figure 15 illustrates the fragmentation patterns of 523.3 in positive aqueous ESI mode. (a) and (b) correspond to the fragmentation patterns at different retention times.

Figure 16 illustrates the fragmentation patterns of 541.3 in positive aqueous ESI mode. (a), (b), (c) and (d) correspond to fragmentation patterns at different retention times.

Figure 17 illustrates the fragmentation pattern of 757.6 in positive aqueous ESI mode.

Figure 18 illustrates the fragmentation pattern of 779.5 in positive aqueous ESI mode.

Figure 19 illustrates the fragmentation pattern of 783.6 in positive aqueous ESI mode, showing three retention times with choline fragments (a), (b), (c).

Figure 20 illustrates the fragmentation pattern of 785.6 in positive aqueous ESI mode.

Figure 21 illustrates the fragmentation pattern of 803.5 in positive aqueous ESI mode.

Figure 22 illustrates the fragmentation pattern of 805.6 in positive aqueous ESI mode.

Figure 23 illustrates the fragmentation pattern of 807.6 in positive aqueous ESI mode showing two retention times with choline fragments (a), (b).

Figure 24 illustrates the fragmentation pattern of 809.6 in positive aqueous ESI mode.

Figure 25 illustrates the fragmentation pattern of 829.6 in positive aqueous ESI mode.

Figure 26 illustrates the fragmentation pattern of 833.6 in positive aqueous ESI mode.

Figure 27 illustrates the fragmentation pattern of "757.6" as a formic acid adduct in negative aqueous ESI mode, showing two main side chains, 16:0 (m/z 255.2) and 18:2 (m/z 279.2). "757.6" is therefore PtdCho 16:0/18:2 and PtdCho 18:2/16:0.

Figure 28 illustrates the fragmentation pattern of "779.6" as a formic acid adduct in negative aqueous ESI mode, showing the side chains 16:0 (m/z 255.2), 20:5 (m/z 301.2) and 20:4 (m/z 303.2) as the most abundant. "779.6" is therefore mostly PtdCho 16:0/20:5, PtdCho 20:5/16:0 and PtdCho 18:2/20:4.

Figure 29 illustrates the fragmentation pattern of "783.6" as a formic acid adduct in negative ESI aqueous mode, showing the side chains 20:3 (m/z 305.2), 18:2 (m/z 279.2), 18:1 (m/z 281.2) and 16:0 (m/z 255.2) as the most abundant. "783.6" therefore mostly is PtdCho 16:0/20:3 and PtdCho 18:1/18:2.

Figure 30 illustrates the fragmentation pattern of "785.6" as a formic acid adduct in negative aqueous ESI mode, showing two side chains, 18:0 (m/z 283.3) and 18:2 (m/z 279.2) in one pattern (a) and one main side chain, 18:1 (m/z 281.2) in the other (b). "785.6" is therefore PtdCho 18:0/18:2 and PtdCho18:1/18:1.

Figure 31 illustrates the fragmentation pattern of "805.6" as a formic acid adduct in negative aqueous ESI mode at different retention times (a-d). The different side chains, 16:0 (m/z 255.2), 22:6 (m/z 327.3), 18:2 (m/z 279.3) and 20:4 (m/z 303.2), identify "805.6" as PtdCho 22:6/16:0 and, PtdCho 20:4/18:2).

Figure 32 illustrates the fragmentation patterns of "807.6" as a formic acid adduct in negative aqueous ESI mode at different retention times (a-c). The different side chains, 18:0 (m/z 283.2), 20:5 (m/z 301.2), 16:0 (m/z 255.2), 22:5 (m/z 329.3), 18:1 (m/z 281.3) and 20:4 (m/z 303.2) identify "807.6" as PtdCho 18:0/20:5, PtdCho 16:0/22:5, PtdCho 22:5/16:0 and PtdCho 18:1/20:4.

Figure 33 illustrates the fragmentation pattern of 702.6 in positive aqueous ESI mode.

Figure 34 illustrates the fragmentation pattern of 812.7 in positive aqueous ESI mode.

Figure 35 illustrates the fragmentation pattern of 724.6 in positive aqueous ESI mode

Figure 36 illustrates the fragmentation pattern of 702.6 as a formic acid adduct in negative ESI analysis mode in control sample aqueous extracts (m/z 747.6).

Figure 37 illustrates the fragmentation pattern of synthetic SM(d18:1/16:0) (from Avanti Polar Lipids, cat. 860584) as a formic acid adduct in negative ESI analysis mode (m/z 747.6).

Figure 38 illustrates the fragmentation pattern of 812.7 as a formic acid adduct in negative ESI analysis mode in control sample aqueous extracts (m/z 857.7).

Figure 39 illustrates the fragmentation pattern of synthetic SM(d18:1/24:1(15Z)) (from Avanti Polar Lipids, cat. 860593) as a formic acid adduct in negative ESI analysis mode (m/z 857.7).

Figure 40 illustrates the fragmentation of 600.5117 organic extract in positive APCI.

Figure 41 shows the relative levels of LysoPC18:0 (mass 523.4), LysoPC18:2 (mass 519.3) and LysoPC20:5 (mass 541.3) and of additional LysoPC in the serum of pancreatic cancer patients relative to controls by Electrospray Ionization (ESI) analysis. (a) LysoPC with 14, 16 and 18 carbons on the side chain, (b) LysoPC with 20, 22 and 24 carbons on the side chain, (c) LysoPC with 30 and 32 carbons on the side chain, and (d) LysoPC with 14, 16, 18, 20 and 22 carbons on the side chain. (a) to (c) in positive ESI analysis mode and (d) in negative ESI analysis mode.

Figure 42 shows the relative MRM levels of 13 PtdCho named by their parent mass in positive ESI analysis mode (a) 27 PtdCho in negative ESI mode (b), and 12 PlsCho named by their parent mass in positive ESI mode (c) in the serum of pancreatic cancer patients relative to controls.

Figure 43 shows the relative MRM levels of five sphingomyelins in the serum of pancreatic cancer patients relative to controls.

Figure 44 shows the relative levels of C36 markers in the serum of pancreatic cancer patients relative to controls.

Figure 45 shows the relative intensities of biomarkers for pancreatic cancer at different stages in three LysoPC (a), seven PtdCho (b), five sphingomyelins (c) and three C36 markers (d).

Figure 46 shows the relative intensities of biomarkers for pancreatic cancer chemoradiation therapy status in three LysoPC (a), seven PtdCho (b), five sphingomyelins (c) and three C36 markers (d).

DETAILED DESCRIPTION

The present inventors have identified cancer-specific biomarkers in human serum, and accordingly present herein a non-invasive cancer detection method that is useful for monitoring an individual's susceptibility to disease, and that may be used either alone or in combination with other known diagnostic methods. The methods described are particularly useful for detecting or diagnosing pancreatic cancer.

A "non-targeted" approach was developed for the identification of biomarkers specific to pancreatic cancer. This discovery platform incorporated the use of Fourier transform ion cyclotron resonance mass spectrometry (FTICR-MS), which is capable of detecting ions with mass accuracy below 1 part per million (ppm). Using this method, liquid sample extracts can be directly infused, for instance using electrospray ionization (ESI) and atmospheric pressure chemical ionization (APCI), without chromatographic separation. Ions with differing mass to charge (M/Z) ratios are then simultaneously resolved using a Fourier transformation. This combination of liquid extraction, flow injection, high resolution and informatics affords a unique opportunity to broadly characterize the biochemical composition of samples without *a priori* knowledge.

When analyzing the serum metabolomic profiles of pancreatic cancer patients and healthy asymptomatic subjects included in their study, the inventors identified specific biomarkers that had significantly altered serum levels in pancreatic cancer patients when compared to controls in a set of 90 samples. Structural characterization was performed by MS/MS technology, and some of the markers were found to be choline-related compounds. Alterations in the serum levels of these biomarkers were confirmed by targeted mass spectrometry using a targeted high-throughput triple-quadrupole MRM (TQ-MRM) method on the same samples.

The inventors have accordingly developed methods to monitor levels of these biomarkers in a subject in a specific and sensitive manner, and to use this information as a useful tool for the early detection and screening of pancreatic cancer.

The present invention accordingly relates to a method of diagnosing cancer by measuring the levels of specific biomarkers present in human serum and comparing them to "normal" reference levels. The described method may be used for the early detection and diagnosis of cancer as well as for monitoring the effects of treatment on cancer patients.

The method also may be incorporated into a high-throughput screening method for testing large numbers of individuals, and further enables longitudinal screening throughout the lifetime of a subject to assess risk and detect disease early on. The method therefore has the potential to detect disease progression prior to that detectable by conventional methods, which is critical to positive treatment outcome.

According to the described method, biological samples taken from one or more subjects of a particular health-state category are compared to the same samples taken from the normal population to identify differences in the levels of the described biomarkers. The samples are extracted and analyzed using various analytical platforms including, but not limited to, Fourier transform ion cyclotron resonance mass spectrometry (FTMS) and liquid chromatography mass spectrometry (LC-MS).

The biological samples could originate from anywhere within the body, for example but not limited to, blood (serum/plasma), cerebral spinal fluid (CSF), bile, urine, stool, breath, saliva, or biopsy of any solid tissue including tumor, adjacent normal, smooth and skeletal muscle, adipose tissue, liver, skin, hair, brain, kidney, pancreas, lung, colon, stomach, or other. Of particular interest are samples that are serum or CSF. While the term "serum" is used herein, those skilled in the art will recognize that plasma or whole blood or a sub-fraction of whole blood may be used.

When a blood sample is drawn from a patient there are several ways in which the sample can be processed. The range of processing can be as little as none (i.e. frozen whole blood) or as complex as the isolation of a particular cell type. The most common and routine procedures involve the preparation of either serum or plasma from whole blood. All blood sample processing methods, including spotting of blood samples onto solid-phase supports, such as filter paper or other immobile materials, are also contemplated by the invention.

Without wishing to be limiting, the processed blood or plasma sample described above may then be further processed to make it compatible with the methodical analysis technique to be employed in the detection and measurement of the metabolites contained within the processed blood sample. The types of processing can range from as little as no further processing to as complex as differential extraction and chemical derivatization. Extraction methods may include sonication, soxhlet extraction, microwave assisted extraction (MAE), supercritical fluid extraction (SFE), accelerated solvent extraction (ASE), pressurized liquid extraction (PLE), pressurized hot water extraction (PHWE) and/or surfactant assisted extraction (PHWE) in common solvents such as methanol, ethanol, mixtures of alcohols and water, or organic solvents such as ethyl acetate or hexane. A method of particular interest for extracting metabolites for FTMS non-targeted analysis and for flow injection LC-MS/MS analysis is to perform a liquid/liquid extraction whereby non-polar metabolites dissolve in an organic solvent and polar metabolites dissolve in an aqueous solvent.

The extracted samples may be analyzed using any suitable method including those known in the art. For example, and without wishing to be limiting, extracts of biological samples are amenable to analysis on essentially any mass spectrometry platform, either by direct injection or following chromatographic separation. Typical mass spectrometers are comprised of a source that ionizes molecules within the sample, and a detector for detecting the ionized molecules or fragments of molecules. Non-limiting examples of common sources include electron impact, electrospray ionization (ESI), atmospheric pressure chemical ionization (APCI), atmospheric pressure photo ionization (APPI), matrix assisted laser desorption ionization (MALDI), surface enhanced laser desorption ionization (SELDI), and derivations thereof. Common mass separation and detection systems can include quadrupole, quadrupole ion trap, linear ion trap, time-of-flight (TOF), magnetic sector, ion cyclotron (FTMS), Orbitrap, and derivations and combinations thereof. The advantage of FTMS over other MS-based platforms is its high resolving capability that allows for the separation of metabolites differing by only hundredths of a Dalton, many of which would be missed by lower resolution instruments.

By the term "metabolite", it is meant specific small molecules, the levels or intensities of which are measured in a sample, and that may be used as markers to diagnose a disease state. These small molecules may also be referred to herein as "metabolite marker", "metabolite component", "biomarker", or "biochemical marker".

The metabolites are generally characterized by their accurate mass, as measured by mass spectrometry technique. The accurate mass may also be referred to as "accurate neutral mass" or "neutral mass". The accurate mass of a metabolite is given herein in Daltons (Da), or a mass substantially equivalent thereto. By "substantially equivalent thereto", it is meant that a +/- 5 ppm difference in the accurate mass would indicate the same metabolite. The accurate mass is given as the mass of the neutral metabolite. During the ionization of the metabolites, which occurs during analysis of the sample, the metabolite will cause either a loss or gain of one or more hydrogen atoms and a loss or gain of an electron. This changes the accurate mass to the "ionized mass", which differs from the accurate mass by the mass of hydrogen atoms and electrons lost or gained during ionization. Unless otherwise specified, the accurate neutral mass will be referred to herein.

Similarly, when a metabolite is described by its molecular formula, the molecular formula of the neutral metabolite will be given. Naturally, the molecular formula of the ionized metabolite will differ from the neutral molecular formula by the number of hydrogen atoms lost or gained during ionization or due to the addition of a non-hydrogen adduct ion.

Data is collected during analysis and quantifying data for one or more than one metabolite is obtained. "Quantifying data" is obtained by measuring the levels or intensities of specific metabolites present in a sample.

The quantifying data is compared to corresponding data from one or more than one reference sample. The "reference sample" is any suitable reference sample for the particular disease state. For example, and without wishing to be limiting in any manner, the reference sample may be a sample from a control individual, i.e., a person not suffering from cancer with or without a family history of cancer (also referred to herein as a " 'normal' counterpart"); the reference sample may also be a sample obtained from a patient clinically diagnosed with cancer. As would be understood by a person of skill in the art, more than one reference sample may be used for comparison to the quantifying data. For example and without wishing to be limiting, the one or more than one reference sample may be a first reference sample obtained from a non-cancer control individual. In the case of monitoring a subject's change in disease state, the reference sample may include a sample obtained at an earlier time period either pre-therapy or during therapy to compare the change in disease state as a result of therapy.

An "internal control metabolite" refers to an endogenous metabolite naturally present in the patient. Any suitable endogenous metabolite that does not vary over the disease states can be used as the internal control metabolite.

Use of a ratio of the metabolite marker to the internal control metabolite offers measurement that is more stable and reproducible than measurement of absolute levels of the metabolite marker. As the internal control metabolite is naturally present in all samples and does not appear to vary significantly over disease states, the sample-to-sample variability (due to handling, extraction, etc) is minimized.

As discussed above the biomarkers described herein were identified by a method known as non-targeted analysis. Non-targeted analysis involves the measurement of as many molecules in a sample as possible, without any prior knowledge or selection of the components prior to the analysis (see WO 01/57518, published August 9, 2001). Therefore, the potential for non-targeted analysis to discover novel metabolite biomarkers is high versus targeted methods, which detect a predefined list of molecules. The present inventors used a non-targeted method to identify metabolite components that differ between cancer-positive and healthy individuals, followed by the development of a high-throughput targeted assay for a subset of the metabolites identified from the non-targeted analysis.

According to this analysis small molecules, metabolites, or metabolite fragments were identified that have differential abundances between cancer-positive serum and normal serum. As listed in Table 5, the inventors found 362 metabolite masses to have statistically significant differential abundances between cancer-positive serum and normal serum. All of these features, which differ statistically between the two populations, have potential diagnostic utility. However, the incorporation of 362 signals into a commercially diagnostic assay is in many cases impractical, so an optimum diagnostic set of markers or metabolites may be selected, for instance in a panel for a high-throughput screening (HTS) assay.

There are multiple types of HTS assay platform options currently available depending on the molecules being detected. These include, but are not limited to, colorimetric chemical assays (UV, or other wavelength), antibody-based enzyme-linked immunosorbant assays (ELISAs), chip-based and polymerase-chain reaction for nucleic acid detection assays, bead-based nucleic-acid detection methods, dipstick chemical assays, image analysis such as MRI, petscan, CT scan, and various mass spectrometry-based systems.

In a non-limiting embodiment, the HTS assay is based upon conventional triple-quadrupole mass spectrometry technology. The HTS assay works by directly injecting a serum extract into the triple-quad mass spectrometer, which then individually isolates each of the parent molecules by single-ion monitoring (SIM). This is followed by the fragmentation of each molecule using an inert gas (called a collision gas, collectively referred to as collision-induced dissociation or CID). The intensity of a specific fragment from each parent biomarker is then measured and recorded, through a process called multiple-reaction monitoring (MRM). In addition, an internal standard molecule is also added to each sample and subjected to fragmentation as well. This internal standard fragment should have the same intensity in each sample if the method and instrumentation is operating correctly. When all biomarker fragment intensities, as well as the internal standard fragment intensities are collected, a ratio of the biomarker to IS fragment intensity is calculated, and the ratio log-transformed. The values for each patient sample are then compared to a previously determined distribution of disease-positive and controls, to determine the relative likelihood that the person is positive or negative for the disease.

A commercial method for screening patients for cancer using the described assay methods is also envisioned. There are numerous options for the deployment of the assay world-wide. These include, but are not limited to: 1, the development of MS/MS methods compatible with current laboratory instrumentation and triple-quadrupole mass spectrometers which are readily in place in many labs around the world, and/or 2, the establishment of a testing facility where samples could be shipped and analyzed at one location, and the results sent back to the patient or patient's physician.

Structural elucidation of the identified metabolites was carried out using a series of physical and chemical property investigations. The principal characteristics that are normally used for this identification are accurate mass and molecular formula determination, polarity, acid/base properties, NMR spectra, and MS/MS or MSn spectra.

One group of diagnostic biomarkers, referred to herein as the C36 markers (558.4, 574.5, 576.5, 578.5, 592.5, 594.5, 596.5), were determined to have the following molecular formulae, respectively: $C_{36}H_{62}O_4$, $C_{36}H_{62}O_5$, $C_{36}H_{64}O_5$, $C_{36}H_{66}O_5$, $C_{36}H_{64}O_6$, $C_{36}H_{66}O_6$, and $C_{36}H_{68}O_6$. MS/MS transitions for each of these biomarkers for organic extracts in negative APCI were observed as follows: $C_{36}H_{62}O_4$: 557.4 / 495.4, 557.4 / 539.4, 557.4 / 513.3, 557.4 / 279.2, 557.4 / 277.2, 557.4 / 220.7 and 557.4 / 111.2; $C_{36}H_{62}O_5$: 573.5 / 511.4, 573.5 / 555.3, 573.5 / 537.4, 573.5 / 529.4, 573.5 / 519.4, 573.5 / 493.3, 573.5 / 457.4, 573.5 / 455.3, 573.5 / 443.4, 573.5 / 415.4, 573.5 / 413.3, 573.5 / 411.3, 573.5 / 399.3, 573.5 / 397.3, 573.5 / 389.7, 573.5 / 295.2, 573.5 / 279.2, 573.5 / 277.2, 573.5 / 251.2, 573.5 / 231.1, 573.5 / 223.1, 573.5 / 201.1, 573.5 / 171.1, 573.5 / 169.1, 573.5 / 125.1 and 573.5 / 113.1; $C_{36}H_{64}O_5$: 575.5 / 513.5, 575.5 / 557.5, 575.5 / 531.5, 575.5 / 499.5, 575.5 / 495.4, 575.5 / 447.3, 575.5 / 417.4, 575.5 / 415.4, 575.5 / 413.3, 575.5 / 371.3, 575.5 / 295.2, 575.5 / 279.2, 575.5 / 260.2, 575.5 / 251.2, 575.5 / 459.4, 575.5 / 403.3, 575.5 / 197.9, 575.5 / 119.4, 575.5 / 113.1, 575.5 / 97.0 and 575.5 / 539.5; $C_{36}H_{66}O_5$: 577.5 / 515.4, 577.5 / 559.4, 577.5 / 546.5, 577.5 / 533.5, 577.5 / 497.4, 577.5 / 419.4, 577.5 / 405.5, 577.5 / 297.2 and 577.5 / 281.2; $C_{36}H_{64}O_6$: 591.5 / 573.4, 591.5 / 555.4, 591.5 / 528.3, 591.5 / 511.2, 591.5 / 476.1, 591.5 / 419.3, 591.5 / 403.1, 591.5 / 387.3, 591.5 / 297.2, 591.5 / 295.2, 591.5 / 274.0, 591.5 / 255.3, 591.5 / 223.6, 591.5 / 203.5, 591.5 / 201.1, 591.5 / 171.0 and 591.5 / 125.3; $C_{36}H_{66}O_6$: 593.5 / 557.5, 593.5 / 513.4, 593.5 / 495.4, 593.5 / 371.3, 593.5 / 315.3, and 593.5 / 277.2; $C_{36}H_{68}O_6$: 595.5 / 577.5, 595.5 / 559.5, 595.5 / 551.5, 595.5 / 549.7, 595.5 / 533.5, 595.5 / 279.2, 595.5 / 391.3, 595.5 / 515.4, 595.5 / 478.4, 595.5 / 423.4, 595.5 / 372.5, 595.5 / 315.3, 595.5 / 313.2, 595.5 / 433.3, 595.5 / 298.2, 595.5 / 239.2, 595.5 / 232.9, 595.5 / 171.1, 595.5 / 169.1, 595.5 / 141.1 and 595.5 / 497.4.

A second group of choline-related diagnostic biomarkers, including lysophosphatidylcholines, phosphatidylcholines and sphingomyelins were also identified. The lysophosphatidylcholines include: LysoPC 14:0; LysoPC 14:1; LysoPC 16:0; LysoPC 16:1; LysoPC 16:2; LysoPC 18:0; LysoPC 18:1; LysoPC 18:2; LysoPC 18:3; LysoPC 20:1; LysoPC 20:2; LysoPC 20:3; LysoPC 20:4; LysoPC 20:5; LysoPC 20:6; LysoPC 22:3; LysoPC 22:4; LysoPC 22:5; LysoPC 22:6; LysoPC 24:4; LysoPC 24:6; LysoPC 30:1; LysoPC 32:0; LysoPC 32:1; LysoPC 32:2; and LysoPC 32:6. The molecular weight, formulae and MS/MS transitions for each of these biomarkers are described in further detail below.

The phosphatidylcholines (755.55; 757.56; 759.58; 761.59; 779.54; 781.56; 783.58; 785.59; 787.61; 803.54; 805.56; 807.58; 809.59; 829.55; 831.58; and 833.59), were determined to have the following molecular formulae, respectively: $C_{42}H_{78}NO_8P$; $C_{42}H_{80}NO_8P$; $C_{42}H_{82}NO_8P$; $C_{42}H_{84}NO_8P$; $C_{44}H_{78}NO_8P$; $C_{44}H_{80}NO_8P$; $C_{44}H_{82}NO_8P$; $C_{44}H_{84}NO_8P$; $C_{44}H_{86}NO_8P$; $C_{46}H_{78}NO_8P$; $C_{46}H_{80}NO_8P$; $C_{46}H_{82}NO_8P$; $C_{46}H_{84}NO_8P$; $C_{48}H_{80}NO_8P$; $C_{48}H_{82}NO_8P$; and $C_{48}H_{84}NO_8P$. The molecular weight, formulae and MS/MS transitions for each of these biomarkers are described in further detail below.

The sphingomyelins 702.57 and 812.68 were determined to have the respective formulae $C_{39}H_{72}N_2O_6P$ and $C_{47}H_{93}N_2O_6P$. The molecular weight, formulae and MS/MS transitions for each of these biomarkers are described in further detail below.

The present invention is further defined with reference to the following examples that are not to be construed as limiting.

EXAMPLES

Materials & Methods:

1. **Patient Sample Selection**

Clinical samples were obtained from Osaka Medical University, Japan. Samples were collected, processed and stored in a consistent manner by teams of physicians. All samples were properly consented and were accompanied by detailed pathology reports.

The samples included 50 controls and 40 pancreatic cancer patients, among them 20 had undergone chemoradiation therapy (CRT) and 20 had not at the time of sampling. Four patients were in stage I, four in stage II, five in stage III, 16 in stage IVa and 11 in stage IVb (Table 2).

Table 2. Clinical characteristics of the studied population.

	Stage I	Stage II	Stage III	Stage IVa	Stage IVb
CRT	4	2	2	7	5
no CRT	0	2	3	9	6

All samples were processed and analyzed in a randomized manner and the results unblinded following analysis.

2. Sample extraction

Serum samples were stored at -80°C until thawed for analysis, and were only thawed once. All extractions were performed on ice. Serum samples were prepared for FTICR-MS analysis by first sequentially extracting equal volumes of serum with 1% ammonium hydroxide and ethyl acetate (EtOAc) in the ratio of 1:1:5 respectively three times. Samples were centrifuged between extractions at 4°C for 10 min at 3500 rpm, and the organic layer removed and transferred to a new tube (extract A). After the third EtOAc extraction, 0.33 % formic acid was added, followed by two more EtOAc extractions. Following the final organic extraction, the remaining aqueous component was further extracted twice with water, and protein removed by precipitation with 3:1 acetonitrile (extract B). A 1:5 ratio of EtOAc to butanol (BuOH) was then evaporated under nitrogen to the original BuOH starting volume (extract C). All extracts were stored at -80°C until FTICR-MS analysis.

3. FTICR-MS analysis

Extracts were diluted either three or six-fold in methanol:0.1%(v/v) ammonium hydroxide (50:50, v/v) for negative ionization modes, or in methanol:0.1% (v/v) formic acid (50:50, v/v) for positive ionization modes. For APCI, sample extracts were directly injected without diluting. All analyses were performed on a Bruker Daltonics APEX III Fourier transform ion cyclotron resonance mass spectrometer equipped with a 7.0 T actively shielded superconducting magnet (Bruker Daltonics, Billerica, MA). Samples were directly injected using electrospray ionization (ESI) and atmospheric pressure chemical ionization (APCI) at a flow rate of 600 μL per hour. Details of instrument tuning and calibration conditions have been previously reported (22).

Although different sample extracts were analyzed separately, the mass spectral data for each sample were combined following spectral processing. All sample peaks were calibrated using internal standards such that each internal standard mass peak had a mass error of <1 ppm relative to the theoretical mass.

4. Full-scan Q-TOF and HPLC-coupled tandem mass spectrometry

4.1 Organic extracts

500 µL of ethyl acetate extracts of serum from five pancreatic cancer samples and five normal samples were evaporated separately under nitrogen gas and each reconstituted in 50 µL of isopropanol:methanol:formic acid (10:89.9:0.1, v/v/v). For both LC/MS full scan and MS/MS, 20 µL of the reconstituted samples were subjected to HPLC (Agilent 1100, Agilent Technologies) analyses with Hypersil ODS column (5 µm, 150 x 4.6 mm), mobile phase: Solvent A: 94.9% H_2O, 5% MeOH and 0.1% Formic acid, Solvent B: 100% MeOH, gradient 100% A to 79% A and 21% B at 15 min, then to 100% B at 25 min, and then held up to 30 min at a flow rate of 1 mL/min. Eluate from the HPLC was analyzed using an ABI QSTAR® XL mass spectrometer fitted with an APCI source and data were collected in negative mode. The scan type in full scan mode was time-of-flight (TOF-MS) with a scan time of 1.0000 second, mass range between 50 and 1500 Da, and duration time of 30 min. Source parameters were as follows: Ion source gas 1 (GS1) 80; Ion source gas 2 (GS2) 10; Curtain gas (CUR) 30; Nebulizer Current (NC) -3.0; Temperature 400°C; Declustering Potential (DP) -60; Focusing Potential (FP) -265; Declustering Potential 2 (DP2) -15. In MS/MS mode, scan type was Product Ion, scan time was 1.0000 second, scan range was 50 to 1500 Da and duration time was 30 min. All source parameters are the same as above, with collision energies (CE) of - 35 V and collision gas (CAD, nitrogen) of 5.

4.2 Aqueous extracts

10 µL of C-ACN fractions (aqueous extracts) of serum from five pancreatic cancer samples and five normal samples were directly injected into HPLC (Agilent 1100) equipped with a Meta Sil AQ column (3 µm, 100 x 2.0 mm, Varian) for full scan and product ion scan (MS/MS) at a flow rate of 0.18 mL/min. Solvent A: H_2O- MeOH-formic acid (94.9 : 5 : 0.1, v/v/v) and solvent B: MeOH-formic acid (99.9 : 0.1, v/v) were used as the mobile phase; the gradient solvent program was applied starting from 100% of A to 80% of B and 20% of A at 11 min, then held up to 20 min, then to 100% of B at 30 min, then held up to 45 min. Eluate from the HPLC was analyzed

in negative and positive modes, using an Applied Biosystem (AB) QSTAR® XL mass spectrometer fitted with an ESI source. The scan type in full scan mode was time-of-flight (TOF-MS) with a scan time of 1.0000 second, mass range between 50 and 1500 Da, and duration time of 60 min. Source parameters are as follows: Ion source gas 1 (GS1), 65; Ion source gas 2 (GS2), 75; Curtain gas (CUR), 30; Temperature 425°C; for negative mode: Ion Spray (IS), -4200V; Declustering Potential (DP), -60; Focusing Potential (FP), -265; Declustering Potential 2 (DP2), -15; and for positive mode: Ion Spray (IS), 5500V; Declustering Potential (DP), 60; Focusing Potential (FP), 265; Declustering Potential 2 (DP2), 15. In MS/MS mode, the scan type was Product Ion, scan time was set as 1.0000 second, scan range was 50 to 1500 Da and duration time was 60 min. All source parameters are the same as above, with collision energy (CE) of -30 V and +30V, respectively, and collision gas (CAD, nitrogen) of 5.

5. LC-MS/MS flow injection analyses.

All LC-MS/MS analyses were performed according to Goodenowe *et al.* (23) with the following modifications. Specifically, analyses were performed using a triple quadrupole mass spectrometer (4000 Q TRAP, Applied Biosystems) coupled with an Agilent 1100 LC system.

5.1 MRM for C36 markers

Sample was prepared by adding 15 μL of internal standard (0.1 μg/mL of (24-^{13}C)-Cholic Acid (Cambridge Isotope Laboratories, Andover, MA) in methanol) to 120 μL ethyl acetate fraction of each sample. 100 μL of sample was injected by flow injection analysis (FIA), and monitored under negative Atmospheric Pressure Chemical Ionization (APCI) mode. The method was based on multiple reaction monitoring (MRM) of one parent/fragment transition for each metabolite and (24-^{13}C)-Cholic Acid (Table 3).

Table 3. List of C36 markers monitored in negative mode (organic fraction) with their formulae and transitions

Name	Mass	Predicted formula	MRM transitions
"558"	558.4	$C36H62O4$	557.4 / 495.4
"574"	574.5	$C36H62O5$	573.5 / 511.4
"576"	576.5	$C36H64O5$	575.5 / 513.5
"578"	578.5	$C36H66O5$	577.5 / 515.4
"592"	592.5	$C36H64O6$	591.5 / 555.4
"594"	594.5	$C36H66O6$	593.5 / 557.5
"596"	596.5	$C36H68O6$	595.5 / 559.5

Each transition was scanned for 70 ms. 100% MeOH at a flow rate of 360 µL/min was used as the mobile phase. The source parameters were set as follows: CUR: 10.0, CAD: 8.0, NC: -4.0, TEM: 400, GS1: 30, GS2: 50, interface heater on. A standard curve was generated for all analytes to verify instrument linearity by serial dilution of (24-^{13}C)-Cholic Acid in extracted commercial serum matrix (ethyl acetate fraction). All samples were analyzed in a randomized blinded manner and were bracketed by known serum standard dilutions. All standard curves had r^2 values > 0.98.

5.2 MRM for choline-related compounds

12 µL of C-ACN fraction was mixed with 108 µL mobile phase and 15 µL reserpine as an internal standard. Mobile phase consists of 75% acetonitrile and 25% of 1% formic acid in ddH_2O. 100 µL of sample was injected by flow injection analysis (FIA), and monitored under positive or negative Ion Electrospray (ESI) mode. The method was based on multiple reaction monitoring (MRM) of one parent / fragment transition for each metabolite and reserpine (Table 4). The negative ESI mode transitions for phosphatidylcholines have been selected as follows: formate adduct and qualifier (both common to same mass phosphatidylcholines), and sn-2 fatty acid (specific to individual phosphatidylcholines).

Table 4. List of choline-related markers with their formulae and transitions monitored in positive mode (a) and in negative mode (b), both with aqueous fractions

(a)

	Name	Mass (neutral)	Formula	MRM transitions (M+H)
Lysophosphatidylcholines	LysoPC 14:0	467.3	C22H46NO7P	468.3 / 184.2
	LysoPC 14:1	465.3	C22H48NO7P	466.3 / 184.2
	LysoPC 16:0	495.3	C24H50NO7P	496.3 / 184.2
	LysoPC 16:1	493.3	C24H48NO7P	494.3 / 184.2
	LysoPC 16:2	491.3	C24H46NO7P	492.3 / 184.2
	LysoPC 18:0	523.3	C26H54NO7P	524.3 / 184.2
	LysoPC 18:1	521.3	C26H52NO7P	522.3 / 184.2
	LysoPC 18:2	519.3	C26H50NO7P	520.3 / 184.2
	LysoPC 18:3	517.3	C26H48NO7P	518.3 / 184.2
	LysoPC 20:1	549.4	C28H56NO7P	550.4 / 184.2
	LysoPC 20:2	547.4	C28H54NO7P	548.4 / 184.2
	LysoPC 20:3	545.3	C28H52NO7P	546.3 / 184.2
	LysoPC 20:4	543.3	C28H50NO7P	544.3 / 184.2
	LysoPC 20:5	541.3	C28H48NO7P	542.3 / 184.2
	LysoPC 20:6	539.3	C28H46NO7P	540.3 / 184.2
	LysoPC 22:3	573.4	C30H56NO7P	574.4 / 184.2
	LysoPC 22:4	571.4	C30H54NO7P	572.4 / 184.2
	LysoPC 22:5	569.4	C30H52NO7P	570.4 / 184.2
	LysoPC 22:6	567.3	C30H50NO7P	568.3 / 184.2
	LysoPC 24:4	599.4	C32H58NO7P	600.4 / 184.2
	LysoPC 24:6	595.4	C32H54NO7P	596.4 / 184.2
	LysoPC 30:1	689.5	C38H76NO7P	690.5 / 184.2
	LysoPC 32:0	719.6	C40H82NO7P	720.6 / 184.2
	LysoPC 32:1	717.6	C40H80NO7P	718.6 / 184.2
	LysoPC 32:2	715.6	C40H78NO7P	716.6 / 184.2
	LysoPC 32:6	707.5	C40H70NO7P	708.5 / 184.2

	Name	Mass (neutral)	Formula	MRM transitions (M+H)
Phosphatidylcholines	755.6	755.55	C42H78NO8P	756.6 / 184.2
	757.6	757.56	C42H80NO8P	758.6 / 184.2
	759.6	759.58	C42H82NO8P	760.6 / 184.2
	761.6	761.59	C42H84NO8P	762.6 / 184.2
	781.6	781.56	C44H80NO8P	782.6 / 184.2
	783.6	783.58	C44H82NO8P	784.6 / 184.2
	785.6	785.59	C44H84NO8P	786.6 / 184.2
	787.6	787.61	C44H86NO8P	788.6 / 184.2
	805.6	805.56	C46H80NO8P	806.6 / 184.2
	807.6	807.58	C46H82NO8P	808.6 / 184.2
	809.6	809.59	C46H84NO8P	810.6 / 184.2
	831.6	831.58	C48H82NO8P	832.6 / 184.2
	833.6	833.59	C48H84NO8P	834.6 / 184.2

	Name	Mass (neutral)	Formula	MRM transitions (M+H)
Plasmenylcholines	742.6	741.57	C42H80NO7P	742.6 / 184.2
	744.6	743.58	C42H82NO7P	744.6 / 184.2
	746.6	745.60	C42H84NO7P	746.6 / 184.2
	768.6	767.58	C44H82NO7P	768.6 / 184.2
	770.6	769.60	C44H84NO7P	770.6 / 184.2
	772.6	771.61	C44H86NO7P	772.6 / 184.2
	774.6	773.63	C44H88NO7P	774.6 / 184.2
	792.6	791.58	C46H82NO7P	792.6 / 184.2
	794.6	793.60	C46H84NO7P	794.6 / 184.2
	796.6	795.61	C46H86NO7P	796.6 / 184.2
	818.6	817.60	C48H84NO7P	818.6 / 184.2
	820.6	819.61	C48H86NO7P	820.6 / 184.2

	Metabolite Name	**Molecular Formula**	**Mass (neutral)**	**MRM Transition**
Sphingomyelins	SM(d18:1/16:0)	$C_{39}H_{79}N_2O_6P$	702.6	703.6 / 184.2
	SM(d18:1/18:1)	$C_{41}H_{81}N_2O_6P$	728.6	729.6 / 184.2
	SM(d18:1/18:0)	$C_{41}H_{83}N_2O_6P$	730.6	731.6 / 184.2
	SM(d18:1/24:1 (15Z))	$C_{47}H_{93}N_2O_6P$	812.6	813.6 / 184.2
	SM(d18:1/24:0)	$C_{47}H_{95}N_2O_6P$	814.6	815.6 / 184.2

(b)

	Metabolite Name	**Molecular Formula**	**Parent Mass (neutral)**	**[M+FA-H] Mass**	**MRM Transitions**
Lysophosphatidylcholines	LysoPC 14:0	C22H46NO7P	467.3	512.3	512.3 / 452.3 / 227.2
	LysoPC 14:1	C22H44NO7P	465.3	510.3	510.3 / 450.3 / 225.2
	LysoPC 16:0	C24H50NO7P	495.3	540.3	540.3 / 480.3 / 255.2
	LysoPC 16:1	C24H48NO7P	493.3	538.3	538.3 / 478.3 / 253.2
	LysoPC 16:2	C24H46NO7P	491.3	536.3	536.3 / 476.3 / 251.2
	LysoPC 18:0	C26H54NO7P	523.4	568.4	568.4 / 508.4 / 283.3
	LysoPC 18:1	C26H52NO7P	521.3	566.3	566.3 / 506.3 / 281.3
	LysoPC 18:2	C26H50NO7P	519.3	564.3	564.3 / 504.3 / 279.3
	LysoPC 18:3	C26H48NO7P	517.3	562.3	562.3 / 502.3 / 277.3
	LysoPC 20:1	C28H56NO7P	549.4	594.4	594.4 / 534.4 / 309.3
	LysoPC 20:2	C28H54NO7P	547.4	592.4	592.4 / 532.4 / 307.3
	LysoPC 20:3	C28H52NO7P	545.3	590.3	590.3 / 530.3 / 305.2
	LysoPC 20:4	C28H50NO7P	543.3	588.3	588.3 / 528.3 / 303.2
	LysoPC 20:5	C28H48NO7P	541.3	586.3	586.3 / 526.3 / 301.2
	LysoPC 20:6	C28H46NO7P	539.3	584.3	584.3 / 524.3 / 299.2
	LysoPC 22:3	C30H56NO7P	573.4	618.4	618.4 / 558.4 / 333.3
	LysoPC 22:4	C30H54NO7P	571.4	616.4	616.4 / 556.4 / 331.3
	LysoPC 22:5	C30H52NO7P	569.3	614.3	614.3 / 554.3 / 329.2
	LysoPC 22:6	C30H50NO7P	567.3	612.3	612.3 / 552.3 / 327.2
	LysoPC 24:4	C32H58NO7P	599.4	644.4	644.4 / 584.4 / 359.3
	LysoPC 24:6	C32H54NO7P	595.4	640.4	640.4 / 580.4 / 355.3
	LysoPC 30:1	C38H76NO7P	689.5	734.5	734.5 / 674.5 / 449.4
	LysoPC 32:0	C40H82NO7P	719.6	764.6	764.6 / 703.6 / 479.5
	LysoPC 32:1	C40H80NO7P	717.6	762.6	762.6 / 702.6 / 477.4
	LysoPC 32:2	C40H78NO7P	715.6	760.6	760.6 / 700.6 / 475.4
	LysoPC 32:6	C40H70NO7P	707.5	752.5	752.5 / 692.5 / 467.4

	Metabolite Name	Parent Mass	Molecular Formula	[Parent + FA -H]	MRM Transitions
Phosphatidyl cholines	PtdCho 16:0/18:3	755.6	C42H78NO8P	800.6	800.6 / 740.6 / 277.2
	PtdCho 16:1/18:2	755.6	C42H78NO8P	800.6	800.6 / 740.6 / 279.2
	PtdCho 18:2/16:1	755.6	C42H78NO8P	800.6	800.6 / 740.6 / 253.2
	PtdCho 18:3/16:0	755.6	C42H78NO8P	800.6	800.6 / 740.6 / 255.2
	PtdCho 16:0/18:2	757.6	C42H80NO8P	802.6	802.6 / 742.6 / 279.2
	PtdCho 16:1/18:1	757.6	C42H80NO8P	802.6	802.6 / 742.6 / 281.2
	PtdCho 18:1/16:1	757.6	C42H80NO8P	802.6	802.6 / 742.6 / 253.2
	PtdCho 18:2/16:0	757.6	C42H80NO8P	802.6	802.6 / 742.6 / 255.2
	PtdCho 16:0/18:1	759.6	C42H82NO8P	804.6	804.6 / 744.6 / 281.2
	PtdCho 18:1/16:0	759.6	C42H82NO8P	804.6	804.6 / 744.6 / 255.2
	PtdCho 18:0/16:0	761.6	C42H84NO8P	806.6	806.6 / 746.6 / 255.2
	PtdCho 16:0/18:0	761.6	C42H84NO8P	806.6	806.6 / 746.6 / 281.2
	PtdCho 16:0/20:5	779.6	C44H78NO8P	824.6	824.6 / 764.6 / 301.2
	PtdCho 18:3/18:2	779.6	C44H78NO8P	824.6	824.6 / 764.6 / 279.2
	PtdCho 20:5/16:0	779.6	C44H78NO8P	824.6	824.6 / 764.6 / 255.2
	PtdCho 16:0/20:4	781.6	C44H80NO8P	826.6	826.6 / 766.6 / 303.2
	PtdCho 18:2/18:2	781.6	C44H80NO8P	826.6	826.6 / 766.6 / 279.2
	PtdCho 20:4/16:0	781.6	C44H80NO8P	826.6	826.6 / 766.6 / 255.2
	PtdCho 16:0/20:3	783.6	C44H82NO8P	828.6	828.6 / 768.6 / 305.3
	PtdCho 18:1/18:2	783.6	C44H82NO8P	828.6	828.6 / 768.6 / 279.2
	PtdCho 18:2/18:1	783.6	C44H82NO8P	828.6	828.6 / 768.6 / 281.2
	PtdCho 20:3/16:0	783.6	C44H82NO8P	828.6	828.6 / 768.6 / 255.2
	PtdCho 18:0/18:2	785.6	C44H84NO8P	830.6	830.6 / 770.6 / 279.2
	PtdCho 18:1/18:1	785.6	C44H84NO8P	830.6	830.6 / 770.6 / 281.2
	PtdCho 18:2/18:0	785.6	C44H84NO8P	830.6	830.6 / 770.6 / 283.2
	PtdCho 18:0/18:1	787.6	C44H86NO8P	832.6	832.5 / 772.6 / 281.2
	PtdCho 18:1/18:0	787.6	C44H86NO8P	832.6	832.5 / 772.6 / 283.2
	PtdCho 18:0/18:0	789.6	C44H88NO8P	834.6	834.6 / 774.6 / 283.2
	PtdCho 16:1/22:6	803.6	C46H78NO8P	848.6	848.6 / 788.6 / 327.3
	PtdCho 20:5/18:2	803.6	C46H78NO8P	848.6	848.6 / 788.6 / 279.2
	PtdCho 16:0/22:6	805.6	C46H80NO8P	850.6	850.6 / 790.6 / 327.3
	PtdCho 18:2/20:4	805.6	C46H80NO8P	850.6	850.6 / 790.6 / 303.2
	PtdCho 20:4/18:2	805.6	C46H80NO8P	850.6	850.6 / 790.6 / 279.2
	PtdCho 22:6/16:0	805.6	C46H80NO8P	850.6	850.6 / 790.6 / 255.2
	PtdCho 16:0/22:5	807.6	C46H82NO8P	852.6	852.6 / 792.6 / 329.3
	PtdCho 18:0/20:5	807.6	C46H82NO8P	852.6	852.6 / 792.6 / 301.3
	PtdCho 18:1/20:4	807.6	C46H82NO8P	852.6	852.6 / 792.6 / 303.2
	PtdCho 20:4/18:1	807.6	C46H82NO8P	852.6	852.6 / 792.6 / 281.2
	PtdCho 20:5/18:0	807.6	C46H82NO8P	852.6	852.6 / 792.6 / 283.2
	PtdCho 22:5/16:0	807.6	C46H82NO8P	852.6	852.6 / 792.6 / 255.2
	PtdCho 16:0/22:4	809.6	C46H84NO8P	854.6	854.6 / 794.6 / 331.3
	PtdCho 18:0/20:4	809.6	C46H84NO8P	854.6	854.6 / 794.6 / 303.2
	PtdCho 20:4/18:0	809.6	C46H84NO8P	854.6	854.6 / 794.6 / 283.2
	PtdCho 22:4/16:0	809.6	C46H84NO8P	854.6	854.6 / 794.6 / 255.2
	PtdCho 18:1/22:6	831.6	C48H82NO8P	876.6	876.6 / 916.6 / 327.3
	PtdCho 22:6/18:1	831.6	C48H82NO8P	876.6	876.6 / 916.6 / 281.2
	PtdCho 18:0/22:6	833.6	C48H84NO8P	878.6	878.6 / 818.6 / 327.3
	PtdCho 22:6/18:0	833.6	C48H84NO8P	878.6	878.6 / 818.6 / 283.2
	PtdCho 18:0/22:5	835.6	C48H86NO8P	880.6	880.6 / 820.6 / 329.3
	PtdCho 22:5/18:0	835.6	C48H86NO8P	880.6	880.6 / 820.6 / 283.2

	Metabolite Name	Molecular Formula	Parent Mass	[M+FA-H] Mass	MRM Transitions
Sphingo myelins	SM(d18:1/16:0)	$C_{39}H_{79}N_2O_6P$	702.6	747.6	747.6 / 687.6 / 168.1
	SM(d18:1/18:1)	$C_{41}H_{81}N_2O_6P$	728.6	773.6	773.6 / 713.6 / 168.1
	SM(d18:1/18:0)	$C_{41}H_{83}N_2O_6P$	730.6	775.6	775.6 / 715.6 / 168.1
	SM(d18:1/24:1 (15Z))	$C_{47}H_{93}N_2O_6P$	812.6	857.6	857.6 / 797.6 / 168.1
	SM(d18:1/24:0)	$C_{47}H_{95}N_2O_6P$	814.6	859.6	859.6 / 799.6 / 168.1

Each transition was scanned for 70 ms. Mobile phase was used at a flow rate of 60 µL/min. The source parameters were set as follows: CUR: 10.0, IS: 5500.0, CAD: 10.0, TEM: 500, GS1: 30, GS2: 50, interface heater on. A standard curve was generated for all analytes to verify instrument linearity by serial dilution of C-ACN fraction of Randox (Human Serum Precision Control Level II) with constant concentration of reserpine. All samples were analyzed in a randomized blinded manner and were bracketed by known serum standard dilutions. All standard curves had r^2 values > 0.98. For sphingomyelins, both MRM transitions were run and similarity was verified; the MRM transitions with m/z 168 were selected for the graphs reported.

6. Statistical Analysis

FTICR-MS accurate mass array alignments were performed using *DISCOVAmetrics*™ (Phenomenome Discoveries Inc., Saskatoon). Initial statistical analysis and graphs of FTICR-MS data were carried out using Microsoft Office Excel 2007. Two-tailed unpaired Student's *t*-tests were used for determination of significant difference between pancreatic cancer and controls. *P*-values of less than 0.05 were considered significant. ROC curves were generated from logistic regression analysis using SAS Enterprise Guide 4.2.

Results

FTICR Metabolomic Profiling

1A. FTICR data analysis

The experimental workflow generated for the studies described here is summarized in Figure 1.

Serum metabolites were captured through a liquid extraction process (see methods) and extracts were directly infused by electrospray ionization (ESI) or atmospheric pressure chemical ionization (APCI) on an FTICR mass spectrometer. In total six separate analyses comprising combinations of extracts and ionization modes were obtained for each sample:

Aqueous Extract
1. Positive ESI (analysis mode 1101)
2. Negative ESI (analysis mode 1102)

Organic Extract
3. Positive ESI (analysis mode 1201)
4. Negative ESI (analysis mode 1202)
5. Positive APCI (analysis mode 1203)
6. Negative APCI (analysis mode 1204)

Separately for each project, the resulting spectral data of all the subjects was aligned within 1 ppm mass accuracy, background peaks were subtracted, and a two-dimensional array table comprising the intensities of each of the sample-specific spectral peaks was created using custom informatics software *DISCOVAmetrics*™.

In the metabolomic profile thus created, a Boolean filtering sorted the masses that differentiate the "pancreatic cancer" condition from the "control" condition. Table 5 lists the 362 masses that discriminate the pancreatic cancer samples from the control samples with a *p*-value lower than 0.05.

Table 5: Accurate mass features differing between clinically diagnosed pancreatic cancer patients and controls ($p<0.05$).

Detected Mass	Analysis Mode	P value	Ratio pancreatic cancer / control	AVG controls	AVG pancreatic cancer
786.593	1101	5.24E-14	0.30	15.59	4.61
595.4897	1202	7.48E-14	0.36	5.30	1.88
594.4863	1202	9.91E-14	0.31	14.02	4.40
785.5913	1101	1.39E-13	0.27	33.03	8.93
808.5783	1101	1.63E-13	0.30	15.62	4.75
702.5709	1101	2.39E-13	0.47	9.60	4.48
780.5452	1101	3.57E-13	0.30	22.48	6.68
807.5734	1101	5.49E-13	0.28	34.47	9.70
576.4751	1202	5.61E-13	0.40	4.85	1.93
541.3134	1101	6.66E-13	0.37	6.27	2.30
804.5422	1101	2.04E-12	0.34	6.56	2.26
779.5405	1101	2.66E-12	0.26	53.60	13.93
812.6774	1101	3.81E-12	0.54	5.11	2.77
758.5626	1101	1.17E-11	0.31	23.80	7.28
783.569	1101	1.19E-11	0.36	13.94	4.98
596.5017	1202	2.03E-11	0.36	11.29	4.04
803.5373	1101	2.11E-11	0.33	13.46	4.48
810.5867	1101	3.75E-11	0.39	7.46	2.90
724.5477	1101	3.75E-11	0.49	8.07	3.98
519.3295	1101	7.30E-11	0.41	6.62	2.71
757.556	1101	1.04E-10	0.27	58.48	16.01
600.5117	1203	2.61E-10	1.40	124.61	174.25
809.5796	1101	2.67E-10	0.43	15.81	6.73
829.5516	1101	2.82E-10	0.41	7.32	2.98
523.3661	1101	3.97E-10	0.49	4.95	2.44
784.5742	1101	4.29E-10	0.42	6.06	2.54
806.5632	1101	4.47E-10	0.37	13.07	4.77
601.5151	1203	5.26E-10	1.39	52.15	72.62
805.5549	1101	6.17E-10	0.35	27.28	9.66

833.5864	1101	9.05E-10	0.43	9.23	4.01
723.5203	1202	1.35E-09	0.55	6.92	3.80
749.5374	1202	1.36E-09	0.46	11.63	5.39
782.5612	1101	1.71E-09	0.37	19.17	7.08
827.5401	1101	1.73E-09	0.39	12.52	4.83
801.5147	1101	2.21E-09	0.39	6.00	2.34
834.5868	1101	2.61E-09	0.45	4.76	2.16
781.5566	1101	4.33E-09	0.33	44.71	14.95
828.5397	1101	4.68E-09	0.41	6.34	2.61
831.5652	1101	4.96E-09	0.51	8.53	4.33
592.4709	1202	5.85E-09	0.37	4.97	1.85
759.5383	1101	9.35E-09	0.53	11.72	6.21
240.0997	1202	1.36E-08	0.45	15.83	7.05
1038.915	1203	1.58E-08	0.39	6.28	2.45
588.3269	1202	1.79E-08	0.54	6.01	3.25
587.3214	1202	2.93E-08	0.50	19.54	9.71
545.3454	1101	4.01E-08	0.54	4.67	2.53
382.1601	1201	4.69E-08	1.94	12.90	24.98
326.2048	1202	5.08E-08	2.58	3.05	7.87
360.1782	1201	7.10E-08	1.52	5.83	8.85
280.2404	1202	7.61E-08	2.44	16.22	39.65
281.2432	1202	9.00E-08	2.38	3.68	8.77
214.1204	1203	1.01E-07	1.67	6.67	11.12
302.222	1201	1.19E-07	2.58	13.20	34.07
282.2558	1202	1.47E-07	2.40	31.82	76.36
575.4985	1203	1.73E-07	1.25	61.51	76.85
855.5721	1101	1.74E-07	0.39	4.56	1.77
283.2591	1202	1.89E-07	2.45	6.15	15.06
759.5733	1101	2.33E-07	0.39	31.65	12.32
760.5792	1101	2.65E-07	0.45	13.99	6.28
574.4952	1203	2.84E-07	1.25	162.04	201.84
517.3141	1101	4.79E-07	0.57	16.74	9.61
283.2595	1204	5.17E-07	1.41	11.22	15.84
262.0814	1201	5.40E-07	0.44	10.65	4.71
811.5729	1202	5.45E-07	0.65	6.67	4.34
1040.933	1203	6.01E-07	0.58	10.18	5.93
328.2627	1202	6.71E-07	2.06	16.89	34.73
326.2458	1202	7.57E-07	2.06	7.72	15.91
282.2559	1204	8.36E-07	1.46	56.00	81.98
564.5121	1202	9.99E-07	3.32	3.17	10.53
276.0948	1201	1.00E-06	1.22	9.93	12.12
775.5522	1202	1.02E-06	0.51	7.83	4.02
811.608	1101	1.38E-06	0.49	4.23	2.09
824.69	1203	1.74E-06	0.61	5.01	3.03
495.3325	1101	2.06E-06	0.58	17.63	10.17
508.2256	1201	2.26E-06	1.43	4.64	6.65
562.4962	1202	2.46E-06	2.91	3.06	8.90
329.2658	1202	2.48E-06	1.99	3.85	7.68

518.321	1101	2.57E-06	0.63	4.70	2.95
1016.931	1203	3.03E-06	0.57	58.00	32.85
1017.935	1203	3.05E-06	0.57	45.70	26.16
360.1792	1202	5.30E-06	1.49	36.91	54.94
566.3403	1202	5.63E-06	0.67	29.61	19.78
565.3373	1202	5.77E-06	0.65	118.24	77.43
300.2067	1201	6.14E-06	2.41	2.57	6.20
771.5699	1202	7.10E-06	0.69	6.90	4.76
116.5696	1202	7.19E-06	1.22	5.54	6.78
468.3807	1202	8.42E-06	0.64	5.22	3.33
361.1828	1202	8.72E-06	1.50	7.05	10.58
428.3647	1201	9.73E-06	0.66	10.24	6.78
1255.153	1203	1.04E-05	0.59	7.38	4.36
1200.088	1203	1.52E-05	0.55	8.45	4.64
540.4381	1202	1.58E-05	0.61	5.38	3.27
851.7107	1203	1.63E-05	0.72	8.61	6.17
1018.944	1203	1.71E-05	0.64	38.50	24.48
505.3146	1202	1.95E-05	0.73	6.13	4.50
496.3373	1101	2.20E-05	0.65	4.79	3.10
569.3682	1202	2.30E-05	0.72	39.22	28.31
330.2559	1202	2.43E-05	2.07	4.21	8.70
808.5791	1201	2.54E-05	0.71	46.64	33.33
572.4798	1203	3.15E-05	1.20	18.65	22.42
765.5678	1201	3.27E-05	0.77	5.30	4.06
786.5972	1201	3.39E-05	0.72	29.54	21.13
1228.117	1203	3.63E-05	0.64	24.71	15.87
791.5841	1201	4.14E-05	0.75	5.81	4.35
1229.12	1203	4.19E-05	0.61	13.11	7.98
850.7061	1203	4.30E-05	0.72	13.39	9.66
830.5591	1201	4.47E-05	0.70	13.41	9.34
1201.09	1203	4.63E-05	0.50	9.82	4.92
802.5291	1201	4.75E-05	0.60	12.32	7.38
1041.935	1203	5.64E-05	0.65	7.35	4.79
260.0033	1101	6.07E-05	1.35	7.68	10.34
785.5929	1201	6.59E-05	0.71	70.58	50.30
1227.112	1203	6.68E-05	0.65	32.33	20.98
826.5561	1202	7.07E-05	0.50	15.42	7.74
1199.084	1203	7.39E-05	0.63	10.34	6.53
825.5522	1202	8.54E-05	0.47	32.08	15.06
244.0554	1101	8.97E-05	1.36	8.98	12.19
602.5269	1203	9.14E-05	1.26	208.79	262.81
570.372	1202	9.17E-05	0.76	11.10	8.43
599.4993	1203	9.78E-05	1.25	15.04	18.83
1019.951	1203	9.91E-05	0.67	21.64	14.54
1039.705	1201	1.01E-04	0.73	4.53	3.29
573.4833	1203	1.03E-04	1.19	7.23	8.57
801.5262	1201	1.06E-04	0.55	30.09	16.68
603.5297	1203	1.09E-04	1.25	86.64	108.65

1230.125	1203	1.10E-04	0.50	5.34	2.69
317.9613	1101	1.28E-04	1.39	5.16	7.18
807.5739	1201	1.34E-04	0.74	115.80	86.22
598.4955	1203	1.47E-04	1.25	37.42	46.65
368.1057	1202	1.61E-04	1.35	4.89	6.61
280.2403	1204	1.62E-04	1.24	31.44	39.14
823.5411	1201	1.65E-04	0.77	5.10	3.95
1039.921	1203	1.68E-04	0.52	4.79	2.48
284.9259	1203	1.69E-04	1.26	6.30	7.96
270.0867	1201	1.72E-04	1.19	20.78	24.82
578.5169	1203	1.75E-04	1.33	21.27	28.33
948.836	1204	1.83E-04	0.67	10.17	6.85
446.3395	1202	1.85E-04	0.70	5.27	3.69
577.5149	1203	1.90E-04	1.23	119.24	147.02
633.3245	1202	2.02E-04	0.68	8.26	5.63
590.3408	1202	2.15E-04	0.75	11.13	8.39
837.7209	1204	2.38E-04	0.61	6.81	4.19
469.3616	1201	2.44E-04	0.72	5.54	3.97
468.3581	1201	2.46E-04	0.69	17.82	12.36
856.7505	1203	2.49E-04	1.22	205.07	250.07
576.5113	1203	2.52E-04	1.23	316.44	388.31
522.4639	1203	2.60E-04	0.62	16.82	10.39
787.5989	1101	2.64E-04	0.63	9.66	6.13
589.3368	1202	2.93E-04	0.74	35.28	26.06
300.1186	1202	3.03E-04	1.28	11.97	15.32
831.5997	1202	3.11E-04	0.66	72.40	47.60
270.0323	1101	3.20E-04	1.34	13.66	18.30
281.2435	1204	3.34E-04	1.23	6.03	7.44
84.0575	1202	3.34E-04	1.22	6.64	8.13
856.754	1204	3.41E-04	1.22	44.96	54.67
922.8222	1204	3.47E-04	0.53	8.16	4.32
832.6031	1202	3.48E-04	0.67	34.86	23.36
1202.098	1203	3.56E-04	0.58	7.40	4.27
829.5532	1201	3.74E-04	0.69	34.32	23.60
857.7543	1203	3.97E-04	1.21	114.80	138.68
327.9902	1101	4.25E-04	1.36	5.92	8.05
304.2407	1202	4.27E-04	1.46	8.00	11.67
538.4237	1202	4.40E-04	0.63	6.33	3.97
1020.957	1203	4.47E-04	0.69	7.99	5.52
1250.108	1203	4.49E-04	0.56	5.60	3.16
1253.134	1203	4.55E-04	0.63	11.69	7.34
847.531	1201	4.82E-04	0.78	5.86	4.56
200.1389	1202	5.57E-04	1.34	6.87	9.21
350.2222	1201	5.59E-04	1.74	4.00	6.97
857.7574	1204	5.87E-04	1.20	25.77	30.92
203.1155	1101	6.19E-04	1.49	7.01	10.46
197.0896	1101	7.68E-04	1.34	5.71	7.68
523.4675	1203	8.74E-04	0.64	5.97	3.84

191.5055	1203	9.26E-04	1.31	9.55	12.54
1011.669	1201	9.48E-04	0.78	6.76	5.27
838.7284	1204	9.60E-04	0.62	4.89	3.04
338.0189	1101	9.69E-04	1.34	7.96	10.70
202.045	1101	1.04E-03	1.32	33.71	44.61
302.0945	1201	1.06E-03	1.26	10.37	13.02
873.7819	1203	1.08E-03	1.23	8.50	10.45
1225.096	1203	1.15E-03	0.71	25.00	17.85
446.2526	1204	1.15E-03	2.33	2.87	6.69
898.7043	1203	1.31E-03	0.56	3.34	1.86
382.1083	1101	1.33E-03	1.56	5.59	8.70
970.733	1204	1.38E-03	0.55	6.35	3.49
715.6959	1101	1.42E-03	2.04	5.53	11.27
302.2457	1202	1.45E-03	1.23	9.18	11.33
851.7337	1204	1.56E-03	0.65	5.80	3.78
874.787	1203	1.64E-03	1.29	4.60	5.92
721.5035	1204	1.69E-03	0.48	3.57	1.70
630.799	1101	1.70E-03	2.32	25.23	58.48
1252.12	1203	1.70E-03	0.64	7.72	4.94
268.1284	1201	1.77E-03	1.34	8.63	11.54
780.5454	1201	1.80E-03	0.77	71.95	55.17
750.5425	1204	1.91E-03	0.46	8.04	3.67
749.5388	1204	1.96E-03	0.43	17.32	7.50
947.8263	1204	1.97E-03	0.77	15.18	11.72
853.573	1202	2.04E-03	0.67	26.48	17.62
779.5416	1201	2.06E-03	0.80	169.63	135.27
1224.096	1203	2.07E-03	0.70	9.01	6.26
838.7435	1203	2.13E-03	1.21	8.28	10.01
1226.599	1203	2.20E-03	0.73	20.59	15.07
635.7525	1101	2.21E-03	2.25	34.61	77.78
871.5547	1202	2.24E-03	0.80	8.04	6.45
743.5396	1202	2.25E-03	0.80	14.69	11.72
924.7233	1203	2.30E-03	0.61	9.77	5.92
801.5523	1202	2.44E-03	0.72	7.08	5.07
615.3535	1202	2.48E-03	0.77	7.10	5.50
541.3361	1202	2.58E-03	0.79	104.55	82.62
921.813	1204	2.60E-03	0.75	19.33	14.41
520.448	1203	2.72E-03	0.69	6.51	4.49
903.7636	1204	2.80E-03	1.19	105.15	125.04
744.5425	1202	2.99E-03	0.78	6.66	5.18
318.0931	1202	3.14E-03	0.82	20.17	16.54
758.562	1201	3.16E-03	0.77	64.96	49.94
1254.137	1203	3.19E-03	0.71	8.83	6.24
868.7704	1204	3.38E-03	0.68	3.94	2.67
606.5591	1203	3.47E-03	0.44	4.80	2.11
998.7566	1204	3.50E-03	0.74	10.82	7.99
329.2439	1202	3.53E-03	1.46	7.29	10.65
594.4852	1204	3.63E-03	0.59	11.81	7.00

757.5587	1201	3.64E-03	0.80	161.90	129.94
925.727	1203	3.69E-03	0.58	6.16	3.57
996.7518	1204	3.73E-03	0.67	11.29	7.51
804.5714	1202	3.76E-03	0.74	81.05	59.96
595.4892	1204	3.81E-03	0.61	4.70	2.86
328.2408	1202	3.92E-03	1.46	28.17	41.15
1223.09	1203	4.15E-03	0.73	9.81	7.16
803.5677	1202	4.22E-03	0.74	169.16	125.07
752.5574	1204	4.28E-03	0.54	7.20	3.87
328.2403	1204	4.36E-03	1.40	5.10	7.15
332.1473	1202	4.52E-03	1.21	7.74	9.34
631.798	1101	4.72E-03	1.92	3.52	6.76
775.5532	1204	5.06E-03	0.46	14.20	6.58
777.5709	1204	5.40E-03	0.54	6.39	3.44
636.7532	1101	5.40E-03	2.05	4.43	9.09
867.7649	1204	5.52E-03	0.71	7.81	5.51
597.5066	1204	5.52E-03	0.62	4.55	2.81
908.7907	1204	5.56E-03	0.68	9.63	6.54
763.5578	1204	5.62E-03	0.57	3.17	1.79
596.5027	1204	5.84E-03	0.60	11.58	6.97
777.0402	1204	6.01E-03	0.52	6.89	3.59
542.3394	1202	6.53E-03	0.83	23.67	19.76
723.521	1204	6.76E-03	0.57	7.41	4.19
627.5656	1203	6.89E-03	1.26	5.47	6.87
657.7337	1101	6.92E-03	2.06	20.13	41.54
255.1161	1201	7.01E-03	1.14	27.21	30.97
751.5511	1202	7.02E-03	0.64	7.10	4.57
751.5539	1204	7.02E-03	0.53	15.18	8.11
827.5678	1202	7.35E-03	0.71	67.73	47.91
658.7372	1101	7.35E-03	1.91	2.70	5.15
804.5456	1201	7.48E-03	0.79	26.05	20.68
670.5696	1203	7.50E-03	0.68	10.09	6.81
628.5438	1203	7.58E-03	1.18	7.10	8.39
613.3379	1202	7.62E-03	0.81	36.81	29.89
645.7958	1101	7.76E-03	2.00	3.94	7.88
850.7326	1204	7.89E-03	0.70	6.57	4.60
923.7295	1204	7.93E-03	0.83	13.51	11.27
579.5313	1203	8.30E-03	0.70	12.95	9.10
748.527	1204	8.77E-03	0.52	5.95	3.07
783.5755	1201	9.29E-03	0.79	37.00	29.41
828.5721	1202	9.38E-03	0.73	31.90	23.31
578.5284	1203	9.41E-03	0.71	33.06	23.56
894.7911	1204	9.58E-03	0.77	18.12	14.02
910.7272	1204	9.85E-03	0.83	10.17	8.45
112.0974	1201	1.01E-02	1.19	7.97	9.46
857.6923	1204	1.02E-02	0.49	2.58	1.26
1012.781	1204	1.03E-02	0.71	7.04	4.99
733.5054	1204	1.06E-02	1.35	6.61	8.91

829.5843	1202	1.08E-02	0.75	38.25	28.65
855.7436	1204	1.09E-02	1.15	12.81	14.70
997.7397	1204	1.09E-02	0.69	10.03	6.88
984.7406	1204	1.13E-02	0.73	7.01	5.09
735.6582	1204	1.13E-02	0.74	7.76	5.74
830.5879	1202	1.18E-02	0.77	18.18	13.95
775.5532	1203	1.19E-02	0.57	2.87	1.64
902.7629	1204	1.28E-02	1.16	113.63	131.44
874.7066	1203	1.29E-02	0.76	8.79	6.67
861.749	1203	1.30E-02	0.79	7.93	6.25
243.0714	1101	1.32E-02	1.24	7.52	9.33
256.2403	1202	1.33E-02	1.21	10.40	12.63
766.4792	1204	1.34E-02	0.70	5.88	4.13
214.1205	1201	1.34E-02	1.15	22.10	25.34
854.7397	1204	1.41E-02	1.15	19.42	22.33
1249.105	1203	1.45E-02	0.72	6.51	4.67
795.5181	1201	1.46E-02	0.84	11.33	9.57
854.7358	1203	1.48E-02	1.17	164.45	192.27
946.8194	1204	1.55E-02	0.81	26.05	21.20
719.6256	1204	1.56E-02	1.30	8.46	10.99
919.6496	1101	1.56E-02	1.57	1.25	1.96
1251.119	1203	1.58E-02	0.72	9.37	6.76
855.7392	1203	1.60E-02	1.17	95.69	111.76
671.5731	1203	1.67E-02	0.72	5.22	3.74
839.7464	1203	1.71E-02	1.19	5.07	6.01
933.8137	1204	1.72E-02	0.80	21.43	17.14
725.7228	1101	1.74E-02	1.76	4.71	8.28
916.7735	1204	1.78E-02	1.15	137.59	158.45
468.2336	1201	1.80E-02	1.36	22.33	30.32
804.7208	1203	1.91E-02	0.70	5.47	3.81
304.2375	1201	1.92E-02	1.71	7.28	12.43
922.7285	1204	1.92E-02	0.81	15.80	12.85
609.3259	1202	1.93E-02	0.83	8.39	6.98
755.5497	1201	1.98E-02	0.84	5.36	4.49
972.7481	1204	2.01E-02	0.79	9.99	7.91
827.7082	1203	2.03E-02	0.85	9.17	7.79
494.4321	1203	2.04E-02	0.59	3.30	1.96
232.1309	1202	2.05E-02	1.09	227.50	248.81
803.5414	1201	2.06E-02	0.81	66.42	53.85
826.7047	1203	2.17E-02	0.85	15.48	13.19
720.6272	1204	2.20E-02	1.27	4.46	5.67
807.5764	1203	2.20E-02	0.71	3.47	2.46
922.7081	1203	2.29E-02	0.62	2.64	1.62
986.7568	1204	2.29E-02	0.83	9.18	7.65
348.1191	1201	2.29E-02	0.79	5.78	4.58
813.5888	1202	2.33E-02	0.84	5.27	4.43
233.1345	1202	2.41E-02	1.10	27.50	30.33
784.5806	1201	2.48E-02	0.85	14.21	12.08

973.7482	1204	2.50E-02	0.83	9.22	7.69
724.5252	1204	2.56E-02	0.69	3.95	2.71
1011.77	1204	2.62E-02	0.72	6.37	4.59
858.7644	1203	2.64E-02	1.15	121.34	139.48
835.598	1201	2.84E-02	0.86	6.87	5.90
469.237	1201	2.88E-02	1.28	5.11	6.54
773.5276	1204	2.94E-02	0.74	12.51	9.32
889.7537	1204	2.97E-02	1.13	79.81	90.07
819.5177	1201	3.10E-02	0.86	5.89	5.09
875.7108	1203	3.11E-02	0.78	5.01	3.89
781.5029	1204	3.18E-02	0.75	6.97	5.26
793.7091	1101	3.19E-02	1.68	4.56	7.67
866.7585	1204	3.28E-02	0.79	17.66	13.95
785.5931	1203	3.30E-02	0.78	5.98	4.67
485.904	1101	3.46E-02	1.14	7.86	8.96
1253.123	1201	3.47E-02	0.69	3.56	2.45
481.315	1202	3.56E-02	0.90	9.09	8.20
745.5631	1203	3.64E-02	1.47	7.05	10.35
851.6694	1101	3.64E-02	1.59	1.78	2.84
1010.765	1204	3.71E-02	0.72	8.26	5.97
999.7632	1204	3.72E-02	0.81	8.01	6.52
907.7847	1204	3.78E-02	0.81	23.16	18.73
254.1127	1201	3.80E-02	1.13	215.52	243.63
898.7325	1204	3.80E-02	0.88	13.60	11.95
418.2204	1204	4.01E-02	0.61	12.12	7.44
522.4638	1201	4.01E-02	0.67	3.86	2.59
937.7542	1204	4.06E-02	0.88	18.10	15.92
484.3527	1201	4.09E-02	0.74	11.34	8.43
366.3593	1101	4.15E-02	1.81	2.10	3.80
852.7368	1204	4.16E-02	0.88	7.42	6.52
831.572	1201	4.16E-02	0.84	30.16	25.20
746.5128	1204	4.27E-02	1.27	10.08	12.78
796.5212	1201	4.29E-02	0.85	4.71	3.98
1247.084	1203	4.37E-02	0.71	3.97	2.83
889.8147	1203	4.41E-02	0.65	1.97	1.28
681.5858	1204	4.42E-02	0.78	4.60	3.60
746.5705	1204	4.44E-02	1.31	7.89	10.30
865.752	1204	4.49E-02	0.81	28.03	22.72
960.7432	1204	4.59E-02	0.87	10.60	9.21
950.7364	1203	4.73E-02	0.72	14.31	10.32
78.0516	1202	4.75E-02	1.09	4.89	5.32
774.5419	1204	4.76E-02	0.72	6.38	4.61
428.2404	1201	4.93E-02	1.35	3.83	5.15
879.7629	1204	4.97E-02	0.79	24.59	19.43
909.7882	1203	4.98E-02	1.12	18.12	20.25

Principal Component Analysis was then performed on the whole populations (90 samples) upon the 362 markers through *DISCOVAmetrics*™. Figure 2 illustrates the separation resulting from this unsupervised classification between pancreatic cancer (with individual samples in grey) and controls (in black).

^{13}C isotopic peaks were identified, such as the first two markers, 786.593 and 595.4897, which are the isotopic peaks of the fourth and third markers respectively, 785.5913 and 594.4863. Table 6 lists the 20 best biomarkers without ^{13}C isotopic peaks. All of these markers except 600.5117 have decreased levels in the pancreatic cancer cohort relative to controls.

Table 6. List of the 20 best FTICR biomarkers of pancreatic cancer, sorted by mass within their analysis mode.

Analysis Mode	Detected Mass	*P* value	Ratio pancreatic cancer / control
1101	519.3295	7.30E-11	0.41
	523.3661	3.97E-10	0.49
	541.3134	6.66E-13	0.37
	702.5709	2.39E-13	0.47
	724.5477	3.75E-11	0.49
	757.556	1.04E-10	0.27
	779.5405	2.66E-12	0.26
	783.569	1.19E-11	0.36
	785.5913	1.39E-13	0.27
	803.5373	2.11E-11	0.33
	805.5549	6.17E-10	0.35
	807.5734	5.49E-13	0.28
	809.5796	2.67E-10	0.43
	812.6774	3.81E-12	0.54
	829.5516	2.82E-10	0.41
	833.5864	9.05E-10	0.43
1202	576.4751	5.61E-13	0.40
	594.4863	9.91E-14	0.31
	596.5017	2.03E-11	0.36
1203	600.5117	2.61E-10	1.40

Principal Component Analysis was then performed on the whole populations upon these 20 markers through *DISCOVAmetrics*™. Figure 3 illustrates (a) the separation resulting from this unsupervised classification between pancreatic cancer (with individual samples in grey) and controls (in black), as well as (b) the relative intensities of these 20 biomarkers in both populations.

1B. Logistic regression analysis

Receiver Operating Characteristic (ROC) analysis was performed on these 20 best FTICR biomarkers. Table 7 summarizes the resulting Areas Under the Curves (AUCs).

Table 7. List of FTICR biomarkers sorted by *p*-values with corresponding AUCs.

Masses	P-value	Area Under the Curve
594.4863	9.91E-14	0.961
785.5913	1.39E-13	0.932
702.5709	2.39E-13	0.909
807.5734	5.49E-13	0.933
576.4751	5.61E-13	0.925
541.3134	6.66E-13	0.921
779.5405	2.66E-12	0.934
812.6774	3.81E-12	0.895
783.569	1.19E-11	0.906
596.5017	2.03E-11	0.932
803.5373	2.11E-11	0.924
724.5477	3.75E-11	0.878
519.3295	7.30E-11	0.899
757.556	1.04E-10	0.916
600.5117	2.61E-10	0.855
809.5796	2.67E-10	0.895
829.5516	2.82E-10	0.877
523.3661	3.97E-10	0.877
805.5549	6.17E-10	0.897
833.5864	9.05E-10	0.888

At least nine markers display AUC>0.90, which indicates an excellent specificity and sensitivity. Figure 4 illustrates each ROC along with the distribution of sample values for the first six best biomarkers (*p*-value < E-12).

There are multiple ways of combining the best biomarkers in the perspective of obtaining a very high sensitivity and specificity with few of them. For example the combination of the six best biomarkers as classified by *p*-values displays an AUC of 0.985 (Figure 5), with an optimal specificity and sensitivity pair of 92.5% and 88% respectively.

1C. Formula prediction

Computational assignments of reasonable molecular formulae were performed for the 20 best biomarkers. The assignments were based on a series of mathematical and chemometric rules as previously described (24), which rely on high mass accuracy for precise prediction. The algorithm computes the number of carbons, hydrogens, oxygens, and other elements, based on their exact mass, which can be assigned to a detected accurate mass within defined constraints. Logical putative molecular formulae were computed in Table 8.

Table 8. Putative molecular formulae for the 20 best FTICR biomarkers.

Analysis Mode	Detected Mass	Putative formula	P value	Ratio pancreatic cancer / control
1101	519.3295	$C_{26}H_{60}NO_7P$	7.30E-11	0.41
	523.3661	$C_{26}H_{54}NO_7P$	3.97E-10	0.49
	541.3134	$C_{28}H_{48}NO_7P$ or $C_{26}H_{49}NO_7PNa$	6.66E-13	0.37
	702.5709	$C_{39}H_{79}N_2O_6P$	2.39E-13	0.47
	724.5477	$C_{41}H_{77}N_2O_6P$ or $C_{39}H_{78}N_2O_6PNa$	3.75E-11	0.49
	757.556	$C_{42}H_{80}NO_8P$	1.04E-10	0.27
	779.5405	$C_{44}H_{78}NO_8P$	2.66E-12	0.26
	783.569	$C_{44}H_{82}NO_8P$	1.19E-11	0.36
	785.5913	$C_{44}H_{84}NO_8P$	1.39E-13	0.27
	803.5373	$C_{46}H_{78}NO_8P$ or $C_{44}H_{79}NO_8PNa$	2.11E-11	0.33
	805.5549	$C_{46}H_{80}NO_8P$	6.17E-10	0.35
	807.5734	$C_{46}H_{82}NO_8P$	5.49E-13	0.28
	809.5796	$C_{46}H_{84}NO_8P$	2.67E-10	0.43
	812.6774	$C_{47}H_{93}N_2O_6P$	3.81E-12	0.54
	829.5516	$C_{48}H_{80}NO_8P$ or $C_{46}H_{81}NO_8PNa$	2.82E-10	0.41
	833.5864	$C_{48}H_{84}NO_8P$ or $C_{46}H_{85}NO_8PNa$	9.05E-10	0.43
1202	576.4751	$C_{36}H_{64}O_5$	5.61E-13	0.40
	594.4863	$C_{36}H_{66}O_6$	9.91E-14	0.31
	596.5017	$C_{36}H_{68}O_6$	2.03E-11	0.36
1203	600.5117	$C_{39}H_{68}O_4$	2.61E-10	1.40

Four main families seem to emerge, three in 1101 analysis mode and one in 1202 analysis mode. In 1101 mode they are reminiscent of choline-related compounds, namely lysophosphatidylcholines for compounds in NO_7P, phosphatidylcholines for compounds in NO_8P, and sphingomyelins for compounds in N_2O_6P. The next step was the structural validation of these 16 putative choline-related compounds, the three compounds in C36 and the additional compound in 1203 mode.

HPLC-Coupled Tandem Mass Spectrometry

Tandem mass spectrometric fragmentation fingerprints were generated for the markers mentioned above.

2A. 1202/1204 compounds in C36

Selected ethyl acetate extracts of serum from the control cohort used in the FTICR-MS work were re-analyzed using HPLC coupled to a quadrupole time-of-flight (Q-TOF) mass spectrometer in APCI negative ion mode (1202 mode) for the three C36 biomarkers, "576", "594" and "596". For a retention time around 25-27 minutes, the MS/MS and MS3 fragmentation data were dominated by peaks resulting from losses of H_2O (m/z 557, 575 and 577 respectively) and losses of two molecules of H_2O (m/z 539, 557 and 559 respectively), with smaller peaks corresponding to losses of CO_2 (m/z 531, 549 and 551 respectively) and losses of CO_2 and H_2O (m/z 513, 531 and 533) (Table 9; figures 6 to 12).

Table 9. Fragmentation pattern of biomarkers "576", "594" and "596" in negative APCI mode (with m/z 575, 593 and 595 respectively), with daughter ion relative abundance.

Parent mass	576.5	Parent mass	594.5	Parent mass	596.5
Predicted formula	C36H64O5	Predicted formula	C36H66O6	Predicted formula	C36H68O6
m/z575		m/z593		m/z595	
Mass	Intensity	Mass	Intensity	Mass	Intensity
495.4234	100	593.4734	100	279.2176	100
575.5086	100	575.4275	94	595.4591	86
513.4442	80	513.4442	65	315.2409	64
557.4564	80	371.3305	53	577.4549	55
539.4565	60	557.4476	53	515.4361	41
575.3825	60	315.2542	47	297.2472	36
97.0558	40	277.2144	41	559.452	36
403.3057	40	171.1025	35	595.6056	36
415.3021	40	201.101	35	281.228	27
459.3655	40	575.5266	35	313.2118	27
531.4755	40	279.2113	29	171.0829	23
71.0055	20	297.2407	24	576.4453	23
89.0176	20	513.5378	24	141.1259	18
101.0108	20	531.4495	24	577.5812	18
113.0104	20	557.5539	24	169.1396	14
119.0578	20	593.638	24	251.2339	14
123.0715	20	200.091	18	277.2081	14
125.0865	20	281.2217	18	373.3293	14

185.1142	20	313.2716	18	391.3588	14
197.1239	20	415.2715	18	594.507	14
205.193	20	433.3294	18	594.6352	14
251.2101	20	113.0862	12	125.0949	9
277.2081	20	139.1091	12	127.1136	9
279.2301	20	155.1033	12	153.1139	9
295.2963	20	195.1371	12	155.1126	9
297.2213	20	199.0942	12	207.214	9
371.2799	20	233.2058	12	239.2276	9
373.3873	20	251.2279	12	253.2247	9
387.3672	20	261.2057	12	261.2179	9
389.3049	20	263.2417	12	278.2338	9
417.3544	20	295.1996	12	295.2189	9
429.3153	20	311.1893	12	298.2186	9
431.3005	20	391.3737	12	372.3292	9
441.3348	20	403.3434	12	423.3793	9
445.3017	20	421.3739	12	497.4302	9
463.2347	20	495.4067	12	514.4141	9
529.4355	20	549.4484	12	515.5639	9
539.352	20	111.0599	6	516.4506	9
557.5893	20	125.0949	6	533.424	9
		127.1051	6	558.4582	9
		141.0992	6	559.6117	9
		169.1103	6	595.6698	9
		183.0976	6	115.0181	5
		185.1039	6	143.099	5
		221.1523	6	185.1091	5
		283.2708	6	201.1223	5
		289.2268	6	202.1455	5
		309.3185	6	233.2287	5
		331.3406	6	235.147	5
		353.3364	6	239.0883	5
		373.322	6	249.1502	5
		389.3346	6	249.2509	5
		401.2808	6	263.2417	5
		417.3774	6	265.2183	5
		446.3477	6	281.3413	5
		451.3569	6	314.2888	5
		453.4963	6	361.3032	5
		514.4737	6	371.3305	5
		549.5451	6	373.5324	5
		559.0969	6	387.3451	5
		564.3806	6	405.3583	5
		568.1941	6	407.3632	5
		576.3011	6	433.306	5
		592.3951	6	438.3753	5
		594.26	6	483.4343	5
		594.4887	6	497.5474	5

531.4495	5
532.5142	5
533.554	5
533.6667	5
540.2675	5
541.4458	5
549.6155	5
551.5353	5
558.3518	5
560.3933	5
561.2821	5
577.7255	5
594.9372	5

Among FTICR biomarkers in Table 5, the presence of other compounds in 1202 mode with a mass differing from the masses above only by two or four suggested that a whole family may be altered in pancreatic cancer. We therefore performed the same analysis as above for 574.5, 578.5, 592.5 and 558.4, respectively predicted to have a formula of $C_{36}H_{62}O_5$, $C_{36}H_{66}O_5$, $C_{36}H_{64}O_6$ and $C_{36}H_{62}O_4$ (Table 10; figures 9 to 12).

Table 10. Fragmentation pattern of biomarkers "558", "574", "578" and "592" in negative APCI mode, with daughter ion relative abundance.

Parent mass	592.5	Parent mass	558.5	Parent mass	574.5	Parent mass	578.5
Predicted formula	C36H64O6	Predicted formula	C36H62O4	Predicted formula	C36H62O5	Predicted formula	C36H66O5
m/z591		m/z 557		m/z573		m/z577	
Mass	Intensity	Mass	Intensity	Mass	Intensity	Mass	Intensity
591.3998	100	495.4401	100	573.3857	100	515.402	100
171.0927	75	539.3868	40	125.0991	80	497.4302	67
201.0903	75	557.4298	40	511.3968	80	533.4673	67
511.3543	75	111.0836	30	555.3937	80	541.4196	67
573.4127	75	539.5089	30	171.1025	40	559.4431	67
125.0907	50	279.2176	20	223.1101	40	577.464	67
223.1661	50	97.0632	10	277.1956	40	251.1982	33
255.2113	50	205.1823	10	279.2301	40	283.2393	33
279.1987	50	221.1467	10	457.3247	40	297.1955	33
295.206	50	373.3365	10	493.3789	40	405.4037	33
403.3358	50	494.5049	10	511.5665	40	515.5469	33
497.4637	50	495.5737	10	529.3751	40	576.4904	33
515.4105	50	513.4187	10	537.3752	40		
529.4701	50			555.5264	40		
555.4025	50			113.0782	20		
559.4253	50			205.1823	20		

573.5834	50
591.6189	50
111.0639	25
113.0263	25
127.0882	25
203.1713	25
275.1623	25
277.2144	25
297.2213	25
313.245	25

295.2447	20
385.3239	20
389.3346	20
401.3484	20
415.3709	20
429.3309	20
443.3555	20
519.3887	20
574.2218	20

Several classes of metabolites, including various forms of steroids (or bile acids), fatty acids and fat soluble vitamins theoretically fit these elemental compositions.

Preliminary Isolation of C36 Markers and NMR Analysis

Ethyl acetate extracts of commercial serum subjected to reverse phase flash column chromatography with a step gradient elution; acetonitrile – water 25:75 to 100% acetonitrile resulted in a fraction found to be very rich in two pancreatic cancer C36 markers (m/z 594 and 596) when analyzed by LC/MS and MS/MS. The proton nuclear magnetic resonance (^{1}H NMR) spectrum (Figure 13) of this fraction showed resonances characteristic of compounds with condensed ring systems thought to be pregnane ring. These two markers are thought to have a steroidal backbone and may probably belong to a class of compounds known as bile acids.

2B. Putative choline-related compounds

In table 6, 16 compounds showed putative formulas belonging to three choline-related families, namely lysophosphatidylcholines (LysoPC) for 519.3, 523.3, and 541.3, phosphatidylcholines (PtdCho) for 757.6, 779.5, 783.6, 785.6, 803.5, 805.6, 807.6, 809.6, 829.6 and 833.6, and sphingomyelins for 702.6, 724.5 and 812.7.

Selected aqueous extracts of serum from the control cohort used in the FTICR-MS work were re-analyzed using HPLC coupled to a quadrupole time-of-flight (Q-TOF) mass spectrometer in ESI positive ion mode (1101 mode). Multiple fragmentation patterns were observed for the three putative lysophosphatidylcholines (Figures 14 to 16).

Table 11. Fragmentation pattern of putative lysophosphatidylcholines in positive ESI mode, with daughter ion relative abundance.

Accurate / Exact Mass	MS/MS Parent ion (% intensity)	Daughter ions (% intensity)	Collision Energy
519.3295	520 (6%)	283 (8%), 209 (3%), 184 (100%), 177 (3%), 175 (8%), 130 (11%), 125 (8%), 109 (6%), 104 (14%), 86 (11%)	40V
523.3661	524 (20%)	506 (11%), 185 (3%), 184 (100%), 401 (62%), 86 (2%)	30V
541.3134	542 (14%) Na adduct	483 (88%), 439 (6%), 359 (8%), 337 (22%), 177 (6%), 147 (72%), 421 (6%), 104 (100%), 86 (28%)	40V

The compound with a mass of 519.3 is confirmed to be a lysophosphatidylcholine with a fatty acid moiety of C18:2, and the two different retention times correspond to two different subspecies: the lower time shows the fragmentation pattern of the 1-linoleoyl-*sn*-glycero-3-phosphocholine (Figure 14a) whereas the higher shows the fragmentation pattern of the 2-linoleoyl-*sn*-glycero-3-phosphocholine (Figure 14b).

The compound with a mass of 523.3 is confirmed to be a lysophosphatidylcholine with a fatty acid moiety of C18:0, and different retention times correspond to two different subspecies: the lower time shows the fragmentation pattern of the 2-stearoyl-*sn*-glycero-3-phosphocholine (Figure 15a) whereas the higher shows the fragmentation pattern of the 1-stearoyl-*sn*-glycero-3-phosphocholine (Figure 15b).

The compounds with a mass of 541.3 seem to be a mixture of the lysophosphatidylcholines with a fatty acid moiety of C20:5 and of the sodium adduct of the compounds with a mass of 519.3 above mentioned (Figure 16). The lowest retention time shows indeed two fragmentation patterns corresponding to 1-eicosapentaenoyl-*sn*-glycero-3-phosphocholine (Figure 16a) and 2-eicosapentaenoyl-*sn*-glycero-3-phosphocholine (Figure 16b). The two higher retention times observed reflect the two retention times observed for 519.3, with the lower corresponding to the fragmentation pattern of the sodium adduct of the 1-linoleoyl-*sn*-glycero-3-phosphocholine (Figure 16c), and the higher corresponding to the fragmentation pattern of the sodium adduct of the 2-linoleoyl-*sn*-glycero-3-phosphocholine (Figure 16d).

In order to further validate the chemical family of these putative lysophosphatidylcholines, the same samples were run in aqueous negative ESI mode (Table 12).

Table 12. Fragmentation pattern of putative lysophosphatidylcholines in negative ESI mode, with daughter ion relative abundance.

Accurate / Exact Mass	MS/MS Formic acid adduct (% intensity)	Daughter ions (% intensity)	Collision Energy
519.3295	564.3 (1%)	504 (5%), 279 (100%), 242 (2%), 224 (6%)	-35V
523.3661	568.3 (1%)	508 (14%), 283 (100%), 242 (2%), 224 (6%)	-35V

Selected aqueous extracts of serum from the control cohort used in the FTICR-MS work were re-analyzed using HPLC coupled to a Q-TOF mass spectrometer in ESI positive ion mode (1101 mode) for the putative PtdCho (Table 13).

Table 13. Fragmentation pattern of putative phosphatidylcholines in positive ESI mode, with daughter ion relative abundance.

Accurate / Exact Mass	MS/MS Parent ion (% intensity)	Daughter ions (% intensity)	Collision Energy
757.5560	758 (47%)	184 (100%)	30V
779.5405	780 (68%)	721 (7%), 712 (4%), 597 (4%), 184 (100%)	30V
783.5690	784 (55%)	184 (100%)	30V
785.5913	786 (66%)	184 (100%)	30V
803.5373	804 26%) (Na adduct)	745 (49%), 621 (100%), 599 (6%), 313 (4%), 147 (17%)	40V
805.5549	806 (95%)	747 (10%), 623 (6%), 184 (100%)	30V
807.5734	808 (80%)	749 (5%), 624 (5%), 184 (100%)	30V
809.5796	810 (100%)	751 (8%), 627 (6%), 184 (89%)	30V
829.5516	830 (47%) (Na adduct)	771 (53%), 647 (100%), 625 (10%), 147 (22%), 86 (7%)	40V
833.5864	834 (96%)	775 (6%), 651 (3%), 415, (2%), 184 (100%)	30V

Fragmentation pattern of all compounds seems restricted to one main fragment (m/z 184) for all masses, which likely corresponds to choline phosphate (Figures 17 to 20, 22 to 26), except for 803.5 (Figure 21). The fragmentation pattern of 803.5 rather suggests the majority of the compounds at this mass to be the sodium adducts of 781.5566.

In order to confirm the chemical family of these putative phosphatidylcholines, the same samples were run in aqueous negative ESI mode (Table 14). Fragmentation patterns are shown in figures 27 to 32 that show how to determine the PtdCho side chains.

Table 14. Fragmentation pattern of putative phosphatidylcholines in negative ESI mode, with daughter ion relative abundance.

Accurate / Exact Mass	MS/MS Formic acid adduct (% intensity)	Daughter ions (% intensity)	Collision Energy
757.5560	802.5 (1%)	745 (9%), 480 (9%), 279 (100%), 255 (26%)	-35V
779.5405	824.5 (12%)	764 (100%), 480 (4%), 301 (30%), 255 (19%)	-35V
783.5690	828.6 (16%)	768 (100%), 480 (5%), 305 (15%), 279 (9%), 255 (9%), 224 (2%)	-35V
785.5913	830.6 (1%)	770 (11%), 283 (22%), 281 (11%), 279 (100%)	-45V
803.5373	848.5 (1%)	788 (100%), 576 (8%), 508 (8%), 492 (8%), 474 (8%), 440 (16%), 301 (16%)	-35V
805.5549	850.6 (1%)	790 (33%), 255 (100%)	-35V
807.5734	852.6 (1%)	792 (32%), 508 (16%), 480 (12%), 329 (52%), 301 (100%), 283 (56%), 257 (48%), 255 (336%), 224 (16%), 203 12%)	-45V
809.5796	854.6 (5%)	794 (23%), 508 (12%), 378 (7%), 303 (100%), 283 (41%), 259 (17%), 242 (9%), 227 (7%), 205 (9%), 168 (7%)	-45V
829.5516	852.6 (1%)	792 (32%), 508 (16%), 480 (12%), 329 (52%), 301 (100%), 283 (56%), 257 (48%), 255 (336%), 224 (16%), 203 12%)	-45V
833.5864	878.6 (1%)	818 (33%), 508 (33%), 490 (33%), 327 (67%), 283 (100%)	-35V

Side chain combinations may be unique, such as in 757.6, corresponding to both PtdCho 16:0/18:2 and PtdCho 18:2/16:0 (Figure 27), or multiple, such as in 807.6, corresponding to PtdCho 18:0/20:5, PtdCho 16:0/22:5 and PtdCho 18:1/20:4, all with the same chemical formula $C_{46}H_{82}NO_8P$ (Figure 32). Confirmed side chains for all PtdCho biomarkers are reported in Table 15.

Table 15. Assignment of side chains to PtdCho according to MS/MS data analysis

Mass	Formula	Identity			
757.556	$C_{42}H_{80}NO_8P$	PtdCho16:0/18:2	PtdCho18:2/16:0		
779.5405	$C_{44}H_{78}NO_8P$	PtdCho18:3/18:2	PtdCho16:0/20:5	PtdCho20:5/16:0	PtdCho20:4/18:1
783.569	$C_{44}H_{82}NO_8P$	PtdCho16:0/20:3	PtdCho18:1/18:2	PtdCho18:0/18:3	
785.5913	$C_{44}H_{84}NO_8P$	PtdCho18:0/18:2	PtdCho18:1/18:1		
803.5373	$C_{46}H_{78}NO_8P$	PtdCho20:5/18:2	PtdCho16:1/22:6	PtdCho22:6/16:1	
805.5549	$C_{46}H_{80}NO_8P$	PtdCho22:6/16:0	PtdCho18:2/20:4		
807.5734	$C_{46}H_{82}NO_8P$	PtdCho18:0/20:5	PtdCho16:0/22:5	PtdCho18:1/20:4	PtdCho22:5/16:0
809.5796	$C_{46}H_{84}NO_8P$	PtdCho18:0/20:4	PtdCho18:1/20:3	PtdCho18:2/20:2	PtdCho16:0/22:4
827.5401	$C_{48}H_{78}NO_8P$	Na adduct of 805.55	PtdCho18:3/22:6		
829.5516	$C_{48}H_{80}NO_8P$	PtdCho18:2/22:6	Na adduct of 807.57	PtdCho18:3/22:5	
833.5864	$C_{48}H_{84}NO_8P$	PtdCho22:6/18:0	Na adduct of 811.6	PtdCho18:1/22:5	PtdCho16:0/24:6

The fragmentation pattern of the putative sphingomyelins confirmed the presence of a choline phosphate fragment as the major peak for 702.6 and 812.7, suggesting that these two compounds respectively are the common sphingomyelins SM(d18:1/16:0) and SM(d18:1/24:1(15Z)) with the sphingosine (18:1) as the sphingoid base (Figures 33 and 34). The fragmentation pattern of 724.5 suggests that the compound is the sodium adduct of 702.6 above mentioned (Figure 35).

The sphingomyelin identity of these two compounds was confirmed by a further analysis in aqueous negative ESI mode, through the comparison between the serum compounds with a mass of 702.6 and 812.7 and the commercially available sphingomyelins SM(d18:1/16:0) and SM(d18:1/24:1(15Z)). The fragmentation pattern of the serum compound with a mass of 702.6 detected as a formic acid adduct in negative ESI mode (Figure 36) is indeed identical to the fragmentation pattern of the synthetic SM(d18:1/16:0) (Figure 37). Similarly, the fragmentation pattern of the serum compound with a mass of 812.7 detected as a formic acid adduct in negative ESI mode (Figure 38) is identical to the fragmentation pattern of the synthetic SM(d18:1/24:1(15Z)) (Figure 39).

2C. Other compound

600.5117 compound in 1203 analysis mode was further analyzed by tandem mass spectrometry mass fragmentation. The fragmentation pattern, dominated by peaks at 545.5, 527.5 and 263.3, confirms that a compound with the molecular formula indicated in table 6 is present and can be classified as 1-alkenyl-2-acylglycerol with 18:2 at both side chains (Figure 40).

Validation using Multiple Reaction Monitoring Methodology

Reduced levels of choline-related compounds and C36 biomarkers in the blood of pancreatic cancer patients were further confirmed using a tandem mass spectrometry approach (see methods) in the same populations. The approach is based upon the measurement of parent-daughter fragment ion combinations (referred to as multiple-reaction monitoring; MRM) for quantifying analytes.

3A. MRM for lysophosphatidylcholines

A tandem-MS approach based upon multiple reaction monitoring was used to confirm differences in LysoPC levels between patients and controls using the same aqueous extracts as for the FTICR-MS analysis, in both positive and negative ElectroSpray Ionization modes (see methods for formulae and transitions). Figure 41 reports the confirmation that the levels in the 3 lysophosphatidylcholines listed in Table 6 and in 20 additional LysoPC are significantly decreased in pancreatic cancer patients relative to controls. The lowest *p*-values among all

LysoPC tested by MRM are obtained for LysoPC present in the 20 best FTICR biomarkers as could be expected, with the minimal value in positive ESI analysis mode, 2.69E-15, obtained for LysoPC18:2, the second best putative LysoPC by FTICR. Overall, the significant decreases observed in 23 LysoPC suggest that the whole family is down-regulated in pancreatic cancer serum.

3B. MRM for PtdCho and Plasmenylphosphocholine (PlsCho)

The same aqueous extracts as for the FTICR-MS analysis were analyzed by a targeted method for 7 PtdCho out of the 10 listed in Table 6 and 6 additional PtdCho in positive analysis mode, and for 9 PtdCho out of the 10 listed in Table 6 and many additional PtdCho in negative analysis mode. Figures 42a and 42b report the confirmation that the serum levels of all PtdCho tested in both positive and negative ESI analysis modes are significantly decreased in pancreatic cancer patients relative to controls. The best putative PtdCho among FTICR best biomarkers, "785.6", is also the best PtdCho among all tested by MRM in positive ESI analysis mode, with a *p*-value of 5.77E-18. It is interesting to note that *all* PtdCho tested are decreased in pancreatic cancer serum independently of their side chains, with a maximal *p*-value of 5.31E-10 in positive ESI analysis mode, demonstrating that the whole phosphatidylcholine family is collectively down-regulated in pancreatic cancer serum.

The decrease in PtdCho family incited us to assess the levels of their vinyl ether counterparts, plasmenylphosphocholines (PlsCho), in the same samples. Figure 42c reports that the serum levels of all PlsCho tested in positive Electrospray Ionization analysis mode are very significantly decreased in pancreatic cancer patients relative to controls. PlsCho with a mass of 793.6, which likely is PlsCho 18:0/20:4, shows the lowest p-value, 3.9E-17.

3D. MRM for sphingomyelins

A tandem-MS approach based upon multiple reaction monitoring was developed to confirm differences in sphingomyelin levels between patients and controls using the same aqueous extracts as for the FTICR-MS analysis. Figure 43 reports that the serum levels of the five sphingomyelins tested (including the two identified by FTICR analysis, SM(d18:1/16:0) and SM(d18:1/24:1(15Z)) are very significantly decreased in pancreatic cancer patients relative to controls. SM(d18:1/24:0), which had not been detected by FTICR, shows the strongest decrease with a *p*-value of 7.81E-15.

3D. MRM for C36 biomarkers

A tandem-MS approach based upon multiple reaction monitoring was developed to confirm differences in C36 biomarker levels between patients and controls using the same ethyl acetate extracts as for the FTICR-MS analysis. As explained in 2A, among all masses listed in Table 5, several seemed to belong to a same family in C36, only differing by an H_2O molecule or the number of unsaturations, and the tandem-MS method was extended to the whole "C36 family" (see methods for formulae and transitions).

Figure 44 reports the confirmation that the levels in the seven C36 markers tested are significantly decreased in pancreatic cancer patients relative to controls. The best putative C36 marker among all FTICR biomarkers (which is also the best biomarker of pancreatic cancer), "594", is also the best biomarker among all C36 tested by MRM, with a *p*-value of 1.42E-11. Again, it is interesting to note that as a whole family, the C36 markers seem down-regulated in pancreatic cancer serum.

Disease stage analysis

Information regarding disease progression status was included. It was therefore determined whether there were a correlation between disease progression and biomarker decrease. MRM data for the 3 LysoPC, 7 PtdCho and 3 C36 markers of interest were re-analyzed according to cancer stage (Figure 45). This preliminary study on a small amount of patients per stage does not seem to indicate any trends.

Chemoradiation therapy effects on biomarkers

Information regarding chemoradiation therapy status was included. It was therefore determined whether there was a correlation between this kind of therapy and biomarker decrease. MRM data for the 3 LysoPC, 7 PtdCho and 3 C36 markers of interest were re-analyzed according to therapy status (Figure 46). This preliminary study on a small amount of patients seems to indicate that there is no effect of chemoradiation therapy on biomarkers.

Discussion

We have performed a comprehensive non-targeted metabolomic profiling of pancreatic cancer serum samples and have identified a very strong signature of this cancer as illustrated by most AUCs above 0.90. The families of markers identified by FTICR as discriminating were validated by targeted analysis. Four families have been identified whose decrease is associated to pancreatic cancer: phosphatidylcholines, lysophosphatidylcholines, sphingomyelins and C36 markers that may be steroidal-like compounds.

Lysophosphatidylcholines 18:2, 18:3 and 20:5 show the strongest decrease of all LysoPC tested. All 27 PtdCho tested (with nine included in the top list of Table 6) show significantly decreased levels in pancreatic cancer patients relative to controls (Figure 42a,b). Most of the 10 PtdCho in Table 8 are predicted or shown to have 18:2, 20:5 or 22:5 as one of the two side chains, as seen in Table 15. In summary, phosphatidylcholines and lysophosphatidylcholines that contain 18:2, 18:3, 20:5 and in a lesser extent, 22:5, show the strongest decrease.

The presence of sphingomyelins among the best biomarkers is extremely interesting. The role of sphingomyelin in cell death, growth and differentiation, and therefore in cancer, is well documented (25, 26) and cancer therapeutics targeted to their signaling pathways give very promising preliminary results (27, 28). For example, sphingomyelin addition to pancreatic cancer cell lines has been shown to drastically enhance chemosensitivity to anticancer agents, presumably by redirecting the cell to enter the apoptotic pathway (29).

Without wishing to be bound in any way by theory, the alteration observed in both phosphatidylcholines and sphingomyelins suggests a role for choline kinase; this cytosolic enzyme is indeed important for the generation of both species and subsequently for cell division (11). The involvement of the choline kinase during tumorigenesis (mediated by Ras effectors serine/threonine kinase (Raf-1), Ral-GDS and PI3K) and the success of its specific inhibitors in antitumoral activity make this kinase a very attractive target in cancer (11, 30). The present results therefore suggest an involvement of choline kinase in pancreatic carcinogenesis.

The C36 markers described herein have not, to our knowledge, yet been associated to pancreatic cancer. Preliminary NMR studies suggest that these compounds may be steroidal-like or conjugated bile acids. This is very interesting since bile acids are emerging as an important family in cancers of the gastrointestinal tract (31). Mechanistically speaking, although without wishing to be bound by theory, there is a complex balance in the bile between bile salts and phospholipids; the reduced levels in phosphatidylcholines observed in pancreatic cancer may be caused by a reduced export into bile, which could be reflective of *MDR3* gene polymorphisms (20). An unbalance observed between phosphatidylcholines and bile acids may therefore reflect some genetic alterations underlying carcinogenesis.

A major effect of clinical variables on the alterations of biomarkers has not been identified on the whole pancreatic cancer population. Disease stages do not seem to affect the decrease in biomarkers. The observation that there are no stage effects suggests that the metabolic deficiency may precede the development of pancreatic cancer, and therefore supports the utility as an early detection risk screening method. A chemoradiation therapy effect on biomarkers was also not observed, suggesting that this therapy does not affect the underlying mechanism of pancreatic cancer; a normalization of biomarkers after treatment would therefore be a good efficacy indicator of new therapeutics.

Statistical analysis revealed how discriminating a few biomarkers could be between pancreatic cancer and healthy controls. For example, the six FTICR best biomarkers all present with a p-value lower than 1E-12 and individual AUCs above 0.90. They have been afterwards identified as most likely being a lysophosphatidylcholine, a sphingomyelin, two phosphatidylcholines and two C36 markers (one being the best biomarker, “594”, with $p = 9.9E\text{-}14$ and the highest AUC). When these markers are combined, the AUC reaches 0.985, with a specificity of 92.5% and a sensitivity of 88%, illustrating how a blood draw can be a powerful diagnostic tool in pancreatic cancer.

In summary, we have identified a metabolic dysregulation specific to pancreatic cancer. The characteristic decrease in two main metabolite families, glycerophosphocholine-related compounds (sub grouped in three subfamilies) and previously uncharacterized C36 markers. These metabolites represent useful biomarkers for sensitive and specific detection of pancreatic cancer, which remains the most dreaded cancer because of its extremely low survival rate. The described diagnostic methods, when conducted in conjunction with therapeutic optimization steps, may also be used to design more efficacious drug therapies for the disease.

One or more currently preferred embodiments have been described by way of example. It will be apparent to persons skilled in the art that a number of variations and modifications can be made without departing from the scope of the invention as defined in the claims.

References

1. Boyle, P., and J. Ferlay. 2005. Cancer incidence and mortality in Europe, 2004. *Ann Oncol* **16**: 481-488.
2. Däbritz, J., R. Preston, J. Hänfler, and H. Oettle. 2009. Follow-up study of K-ras mutations in the plasma of patients with pancreatic cancer: correlation with clinical features and carbohydrate antigen 19-9. *Pancreas* **38**: 534-541.
3. Klapman, J., and M. P. Malafa. 2008. Early detection of pancreatic cancer: why, who, and how to screen. *Cancer Control.* **15**: 280-287.
4. Helmstaedter, L., and J. F. Riemann. 2008. Pancreatic cancer--EUS and early diagnosis. *Langenbecks Arch Surg* **393**: 923-927.
5. Gemmel, C., A. Eickhoff, L. Helmstädter, and J. F. Riemann. 2009. Pancreatic cancer screening: state of the art. *Expert Rev Gastroenterol Hepatol.* **3**: 89-96.
6. Peracaula, R., S. Barrabés, A. Sarrats, P. M. Rudd, and R. de Llorens. 2008. Altered glycosylation in tumours focused to cancer diagnosis. *Dis Markers* **25**: 207-218.
7. Ehmann, M., K. Felix, D. Hartmann, M. Schnölzer, M. Nees, S. Vorderwülbecke, R. Bogumil, M. W. Büchler, and H. Friess. 2007. Identification of potential markers for the detection of pancreatic cancer through comparative serum protein expression profiling. *Pancreas* **34**: 205-214.
8. Barrabés, S., L. Pagès-Pons, C. M. Radcliffe, G. Tabarés, E. Fort, L. Royle, D. J. Harvey, M. Moenner, R. A. Dwek, P. M. Rudd, R. De Llorens, and R. Peracaula. 2008. Glycosylation of serum ribonuclease 1 indicates a major endothelial origin and reveals an increase in core fucosylation in pancreatic cancer. *Glycobiology* **17**: 388-400.
9. Koopmann, J., C. N. White Rosenzweig, Z. Zhang, M. I. Canto, D. A. Brown, M. Hunter, C. Yeo, D. W. Chan, S. N. Breit, and M. Goggins. 2006. Serum Markers in Patients with Resectable Pancreatic Adenocarcinoma: Macrophage Inhibitory Cytokine 1 versus CA19-9 *Clinical Cancer Research* **12**: 442-446.
10. Rosty, C., L. Christa, S. Kuzdzal, B. W.M., M. L. Zahurak, F. Carnot, D. W. Chan, M. Canto, K. D. Lillemoe, J. L. Cameron, C. J. Yeo, R. H. Hruban, and M. Goggins. 2002. Identification of hepatocarcinoma-intestine-pancreas/pancreatitis-associated protein I as a biomarker for pancreatic ductal adenocarcinoma by protein biochip technology. *Cancer research* **62**: 1868-1875.
11. Janardhan, S., P. Srivani, and G. N. Sastry. 2006. Choline kinase: an important target for cancer. *Curr Med Chem* **13**: 1169-1186.
12. Garcea, G., C. P. Neal, C. J. Pattenden, W. P. Steward, and D. P. Berry. 2005. Molecular prognostic markers in pancreatic cancer: a systematic review. *Eur J Cancer* **41**: 2213-2236.
13. Bloomston, M., W. L. Frankel, F. Petrocca, S. Volinia, H. Alder, J. P. Hagan, C. G. Liu, D. Bhatt, C. Taccioli, and C. M. Croce. 2007. MicroRNA expression patterns to differentiate pancreatic adenocarcinoma from normal pancreas and chronic pancreatitis. *JAMA* **297**: 1901-1908.
14. Szafranska, A. E., T. S. Davison, J. John, T. Cannon, B. Sipos, A. Maghnouj, E. Labourier, and S. A. Hahn. 2007. MicroRNA expression alterations are linked to tumorigenesis and non-neoplastic processes in pancreatic ductal adenocarcinoma. *Oncogene* **26**: 4442-4452.
15. Lee, E. J., Y. Gusev, J. Jiang, G. J. Nuovo, M. R. Lerner, W. L. Frankel, D. L. Morgan, R. G. Postier, D. J. Brackett, and T. D. Schmittgen. 2007. Expression profiling identifies microRNA signature in pancreatic cancer. *Int J Cancer* **120**: 1046-1054.
16. Tian, M., Y. Z. Cui, G. H. Song, M. J. Zong, X. Y. Zhou, Y. R. Chen, and J. X. Han. 2008. Proteomic analysis identifies MMP-9, DJ-1 and A1BG as overexpressed proteins in pancreatic juice from pancreatic ductal adenocarcinoma patients

BMC Cancer **8**: 241.
17. Warden, C. H., A. Daluiski, X. Bu, D. A. Purcell-Huynh, C. De Meester, B. H. Shieh, D. L. Puppione, R. M. Gray, G. M. Reaven, Y. D. Chen, and **e. al.** 1993. Evidence for linkage of the apolipoprotein A-II locus to plasma apolipoprotein A-II and free fatty acid levels in mice and humans. *Proceedings of the National Academy of Sciences of the United States of America* **90**: 10886-10890.
18. Trougakos, I. P., and E. S. Gonos. 2002. Clusterin/apolipoprotein J in human aging and cancer. *The international journal of biochemistry & cell biology* **34**: 1430-1448.
19. Zuijdgeest-van Leeuwen, S. D., M. S. van der Heijden, T. Rietveld, J. W. van den Berg, H. W. Tilanus, J. A. Burgers, J. H. Wilson, and P. C. Dagnelie. 2002. Fatty acid composition of plasma lipids in patients with pancreatic, lung and oesophageal cancer in comparison with healthy subjects. *Clinical Nutrition* **21**: 225-230.
20. Khan, S. A., I. J. Cox, A. V. Thillainayagam, D. S. Bansi, H. C. Thomas, and S. D. Taylor-Robinson. 2005. Proton and phosphorus-31 nuclear magnetic resonance spectroscopy of human bile in hepatopancreaticobiliary cancer. *Eur J Gastroenterol Hepatol* **17**: 733-738.
21. Kolb, A., S. Rieder, D. Born, N. A. Giese, T. Giese, G. Rudofsky, J. Werner, M. W. Büchler, H. Friess, I. Esposito, and J. Kleeff. 2009. Glucagon/insulin ratio as a potential biomarker for pancreatic cancer in patients with new-onset diabetes mellitus. *Cancer Biol Ther* **8**.
22. Gray, G. R., and D. Heath. 2005. A global reorganization of the metabolome in Arabidopsis during cold acclimation is revealed by metabolic fingerprinting. *Physiologia Plantarum* **124**: 236-248.
23. Goodenowe, D. B., L. L. Cook, J. Liu, Y. Lu, D. A. Jayasinghe, P. W. Ahiahonu, D. Heath, Y. Yamazaki, J. Flax, K. F. Krenitsky, D. L. Sparks, A. Lerner, R. P. Friedland, T. Kudo, K. Kamino, T. Morihara, M. Takeda, and P. L. Wood. 2007. Peripheral ethanolamine plasmalogen deficiency: a logical causative factor in Alzheimer's disease and dementia. *Journal of lipid research* **48**: 2485-2498.
24. Aharoni, A., C. H. Ric de Vos, H. A. Verhoeven, C. A. Maliepaard, G. Kruppa, R. Bino, and D. B. Goodenowe. 2002. Nontargeted metabolome analysis by use of Fourier Transform Ion Cyclotron Mass Spectrometry. *Omics* **6**: 217-234.
25. Dyatlovitskaya, E. V., and A. G. Kandyba. 2006. Role of biologically active sphingolipids in tumor growth. *Biochemistry (Mosc).* **71**: 10-17.
26. Clària, J. 2006. Regulation of cell proliferation and apoptosis by bioactive lipid mediators. *Recent Pat Anticancer Drug Discov.* **1**: 369-382.
27. Billich, A., and T. Baumruker. 2008. Sphingolipid metabolizing enzymes as novel therapeutic targets. *Subcell Biochem* **49**: 487-522.
28. Modrak, D. E., D. V. Gold, and D. M. Goldenberg. 2006. Sphingolipid targets in cancer therapy. *Mol Cancer Ther* **5**: 200-208.
29. Modrak, D. E., E. Leon, D. M. Goldenberg, and D. V. Gold. 2009. Ceramide regulates gemcitabine-induced senescence and apoptosis in human pancreatic cancer cell lines. *Mol Cancer Res* **7**: 890-896.
30. Ramírez de Molina, A., D. Gallego-Ortega, J. Sarmentero-Estrada, D. Lagares, T. Gómez Del Pulgar, E. Bandrés, J. García-Foncillas, and J. C. Lacal. 2008. Choline kinase as a link connecting phospholipid metabolism and cell cycle regulation: implications in cancer therapy. *The international journal of biochemistry & cell biology* **40**: 1753-1763.
31. Bernstein, H., C. Bernstein, C. M. Payne, and K. Dvorak. 2009. Bile acids as endogenous etiologic agents in gastrointestinal cancer. *World J Gastroenterol* **15**: 3329-3340.

WHAT IS CLAIMED IS:

1. A standard for use in a method to detect pancreatic cancer, or to quantitate a pancreatic cancer marker, comprising:

(i) a diacylphosphatidylcholine, plasmanylphosphocholine or plasmenylphosphocholine of Formula (I):

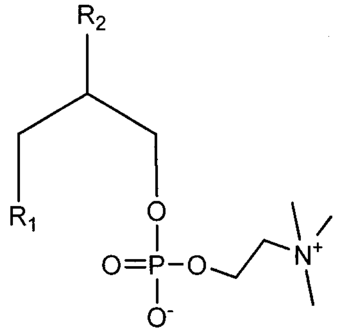

(I)

including adducts or salts thereof, wherein

R_1 is a 16:0, 16:1, 18:0, 18:1, 18:2, 18:3, 20:3, 20:4, 20:5 or 22:5 fatty acid or alcohol moiety bonded to the glycerol backbone, the bond being an acyl linkage when the standard comprises a diacylphosphatidylcholine, an ether linkage when the standard comprises a plasmanylphosphocholine, or a vinyl-ether linkage when the standard comprises a plasmenylphosphocholine; and

R_2 is a 16:0, 16:1, 18:0, 18:1, 18:2, 18:3, 20:3, 20:4, 20:5, 22:5, or 22:6 fatty acid moiety bonded to the glycerol backbone through an acyl linkage;

(ii) a 2-lysophosphatidylcholine of Formula (II) or a 1-lysophosphatidylcholine of Formula (III):

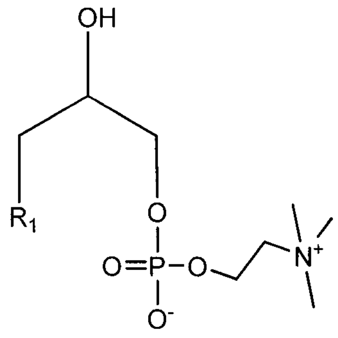

(II)

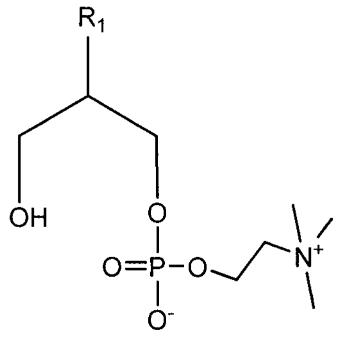

(III)

including adducts or salts thereof, wherein

R_1 is a 14:0, 14:1, 16:0, 16:1, 16:2, 18:0, 18:1, 18:2, 18:3, 20:1, 20:2, 20:3, 20:4, 20:5, 20:6, 22:3, 22:4, 22:5, 22:6, 24:4, 24:6, 30:1, 32:0, 32:1, 32:2 or 32:6 fatty acid moiety bonded to the glycerol backbone through an acyl linkage; or

(iii) a sphingomyelin as defined in Formula (IV):

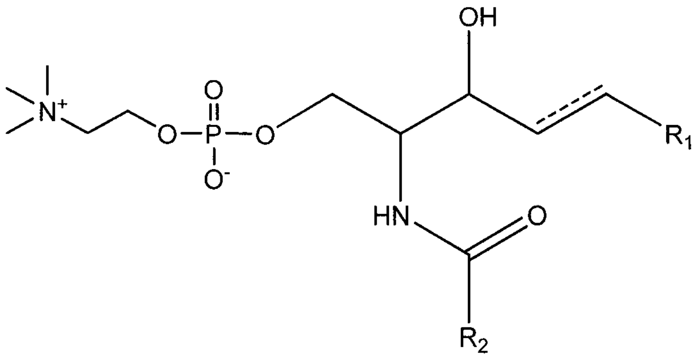

(IV)

including adducts or salts thereof, wherein the dashed line represents an optional double bond;

R_1 is a C_{13} alkyl group; and

R_2 is a C_{11} to C_{25} alkyl or alkenyl group, said alkenyl group having from 1 to 3 double bonds,

wherein the diacylphosphatidylcholine, plasmanylphosphocholine, plasmenylphosphocholine, lysophosphatidylcholine or sphingomyelin is labeled with a detectable marker.

2. The standard of claim 1, wherein R_2 of the sphingomyelin is a C_{11} alkyl group, a C_{13} alkyl group, a C_{15} alkyl group, a C_{17} alkyl group, a C_{17} alkenyl group with 3 double bonds, a C_{19} alkyl group, a C_{21} alkyl group, a C_{23} alkenyl group with 1 double bond, a C_{23} alkyl group, a C_{24} alkyl group, a C_{25} alkenyl group with 1 double bond, or a C_{25} alkyl group.

3. The standard of claim 1, wherein the lysophosphatidylcholine is selected from the group consisting of LysoPC 14:0, LysoPC 14:1, LysoPC 16:0, LysoPC 16:1, LysoPC 16:2, LysoPC 18:0, LysoPC 18:1, LysoPC 18:2, LysoPC 18:3, LysoPC 20:1, LysoPC 20:2, LysoPC 20:3, LysoPC 20:4, LysoPC 20:5, LysoPC 20:6, LysoPC 22:3, LysoPC 22:4, LysoPC 22:5, LysoPC 22:6, LysoPC 24:4, LysoPC 24:6, LysoPC 30:1, LysoPC 32:0, LysoPC 32:1, LysoPC 32:2, and LysoPC 32:6.

4. The standard of claim 1, wherein the diacylphosphatidylcholine has a molecular formula selected from the group consisting of $C_{42}H_{78}NO_8P$, $C_{42}H_{80}NO_8P$, $C_{42}H_{82}NO_8P$, $C_{42}H_{84}NO_8P$, $C_{44}H_{78}NO_8P$, $C_{44}H_{80}NO_8P$, $C_{44}H_{82}NO_8P$, $C_{44}H_{84}NO_8P$, $C_{44}H_{86}NO_8P$, $C_{44}H_{86}NO_8P$, $C_{46}H_{78}NO_8P$, $C_{46}H_{80}NO_8P$, $C_{46}H_{82}NO_8P$, $C_{46}H_{84}NO_8P$, $C_{48}H_{80}NO_8P$, $C_{48}H_{82}NO_8P$, $C_{48}H_{84}NO_8P$ and $C_{48}H_{86}NO_8P$.

5. The standard of claim 1, wherein the plasmenylphosphocholine has a molecular formula selected from the group consisting of $C_{42}H_{80}NO_7P$, $C_{42}H_{82}NO_7P$, $C_{42}H_{84}NO_7P$, $C_{44}H_{82}NO_7P$, $C_{44}H_{84}NO_7P$, $C_{44}H_{86}NO_7P$, $C_{44}H_{88}NO_7P$, $C_{46}H_{82}NO_7P$, $C_{46}H_{84}NO_7P$, $C_{46}H_{86}NO_7P$, $C_{48}H_{84}NO_7P$, and $C_{48}H_{86}NO_7P$.

6. The standard of claim 1, wherein the sphingomyelin has a molecular formula selected from the group consisting of $C_{39}H_{79}N_2O_6P$, $C_{39}H_{80}N_2O_6P^+$, $C_{41}H_{81}N_2O_6P$, $C_{41}H_{82}N_2O_6P^+$, $C_{41}H_{83}N_2O_6P$, $C_{41}H_{84}N_2O_6P^+$, $C_{47}H_{93}N_2O_6P$, $C_{47}H_{94}N_2O_6P^+$, $C_{47}H_{95}N_2O_6P$, and $C_{47}H_{96}N_2O_6P^+$.

7. The standard of any one of claims 1 to 6, wherein the detectable marker is a stable isotope, an enzyme or a protein that enables detection *in vitro*.

8. A kit for use in a method to detect pancreatic cancer, or to quantitate a pancreatic cancer marker, comprising a standard according to any one of claims 1 to 7, a dilution medium, and instructions for quantitating said marker or performing said detection method.

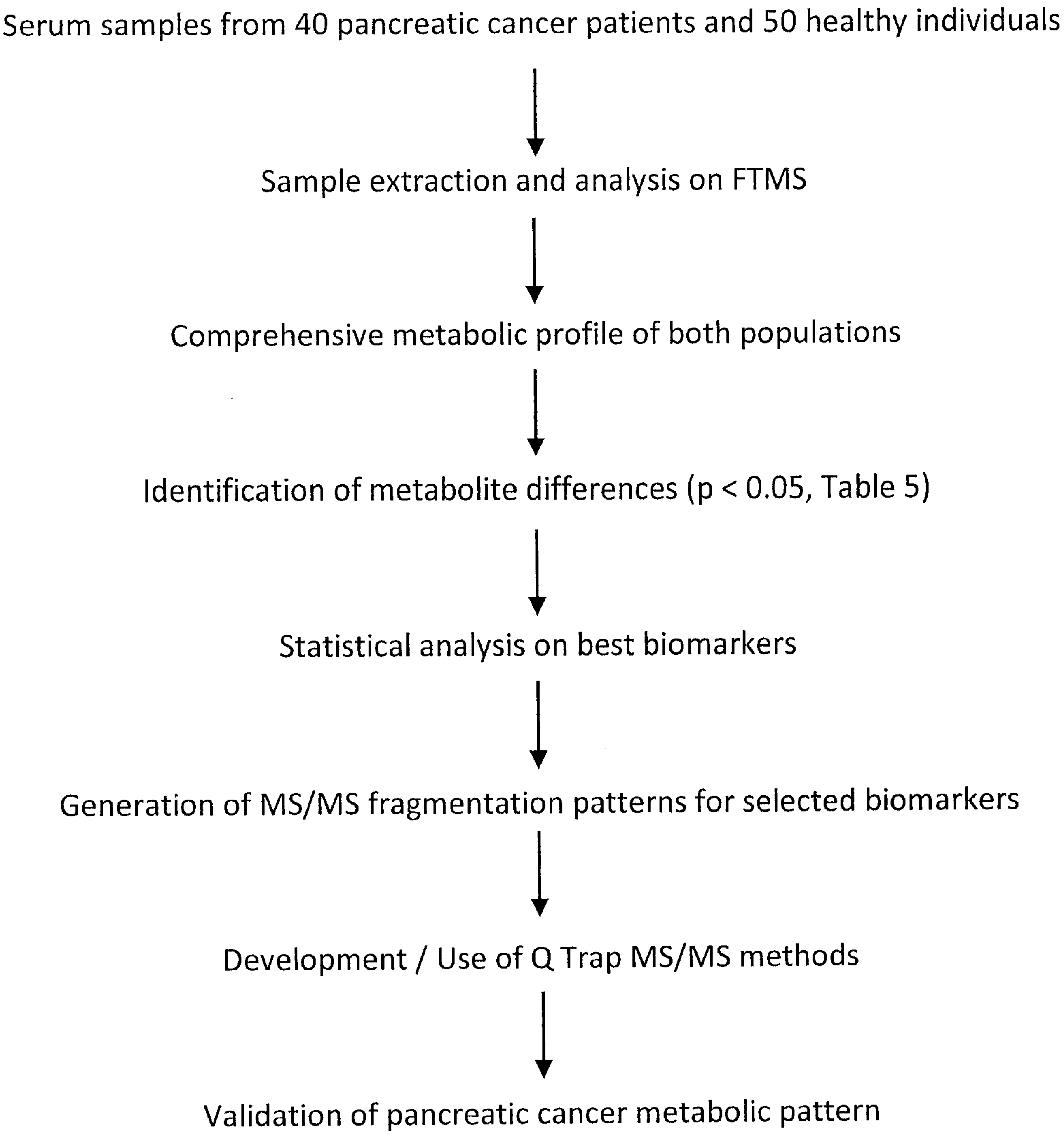
Serum samples from 40 pancreatic cancer patients and 50 healthy individuals
Sample extraction and analysis on FTMS
Comprehensive metabolic profile of both populations
Identification of metabolite differences (p < 0.05, Table 5)
Statistical analysis on best biomarkers
Generation of MS/MS fragmentation patterns for selected biomarkers
Development / Use of Q Trap MS/MS methods
Validation of pancreatic cancer metabolic pattern

Figure 1

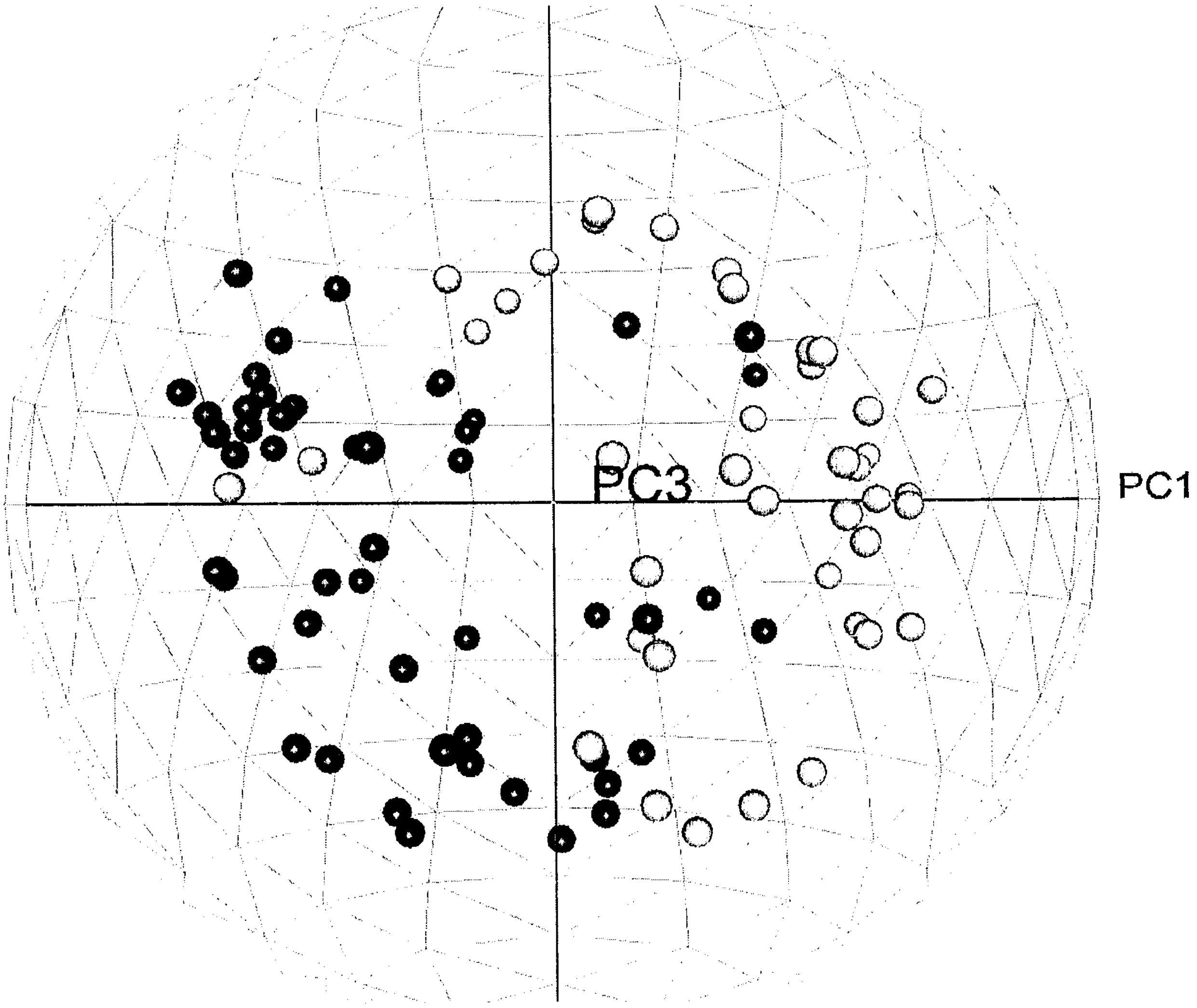

Figure 2

a)

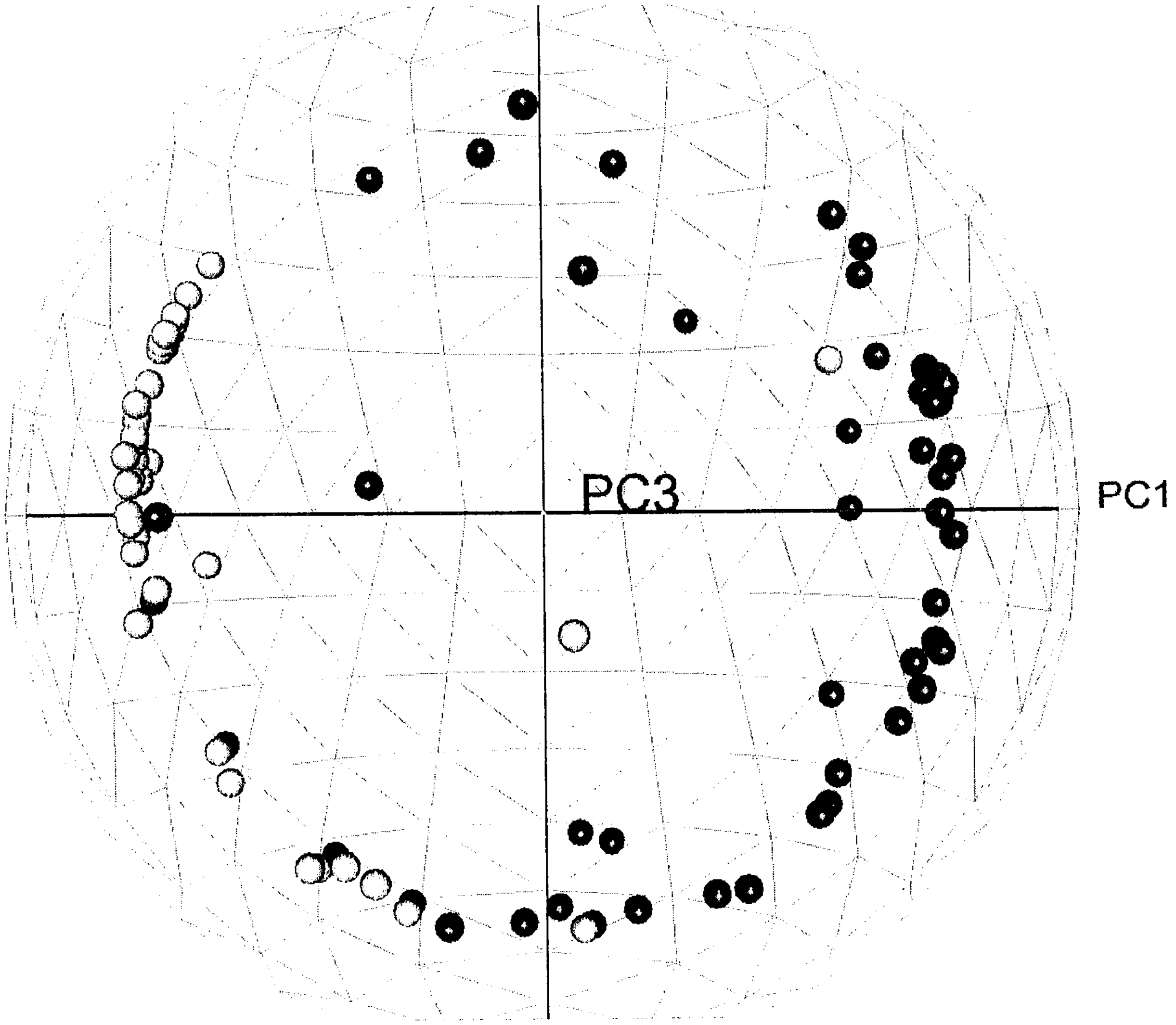

Figure 3

b)

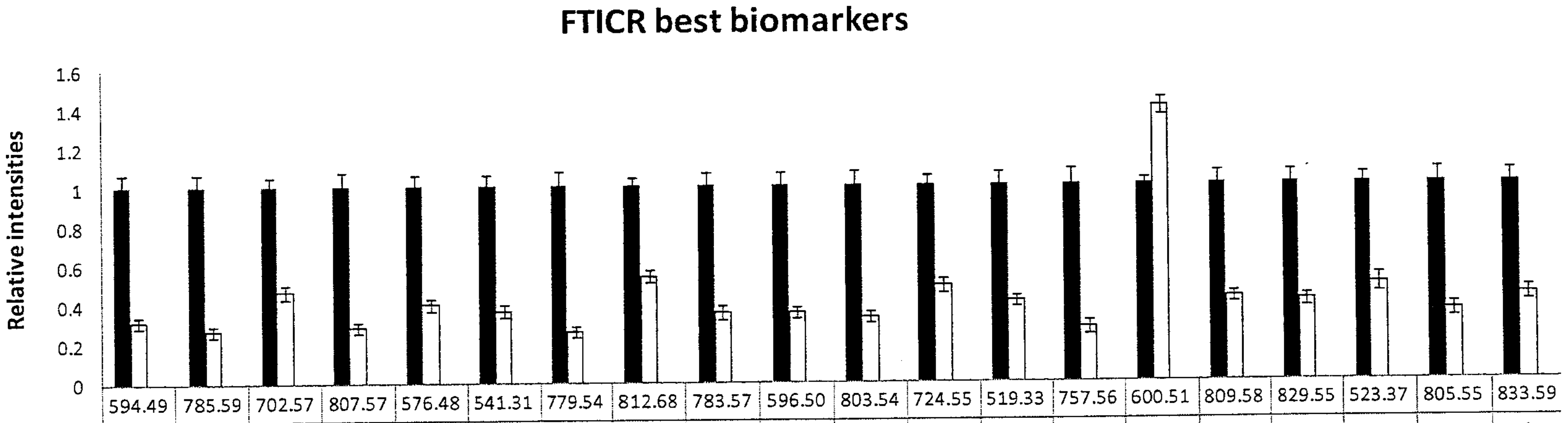

	594.49	785.59	702.57	807.57	576.48	541.31	779.54	812.68	783.57	596.50	803.54	724.55	519.33	757.56	600.51	809.58	829.55	523.37	805.55	833.59
■ Controls	1	1	1	1	1	1	1	1	1	1	1	1	1	1	1	1	1	1	1	1
□ Pancreatic cancer	0.31	0.27	0.47	0.28	0.40	0.37	0.26	0.54	0.36	0.36	0.33	0.49	0.41	0.27	1.40	0.43	0.41	0.49	0.35	0.43
▨ P-value	9.9E-14	1.4E-13	2.4E-13	5.5E-13	5.6E-13	6.7E-13	2.7E-12	3.8E-12	1.2E-11	2.0E-11	2.1E-11	3.8E-11	7.3E-11	1.0E-10	2.6E-10	2.7E-10	2.8E-10	4.0E-10	6.2E-10	9.0E-10

Figure 3 (Cont.)

(a)

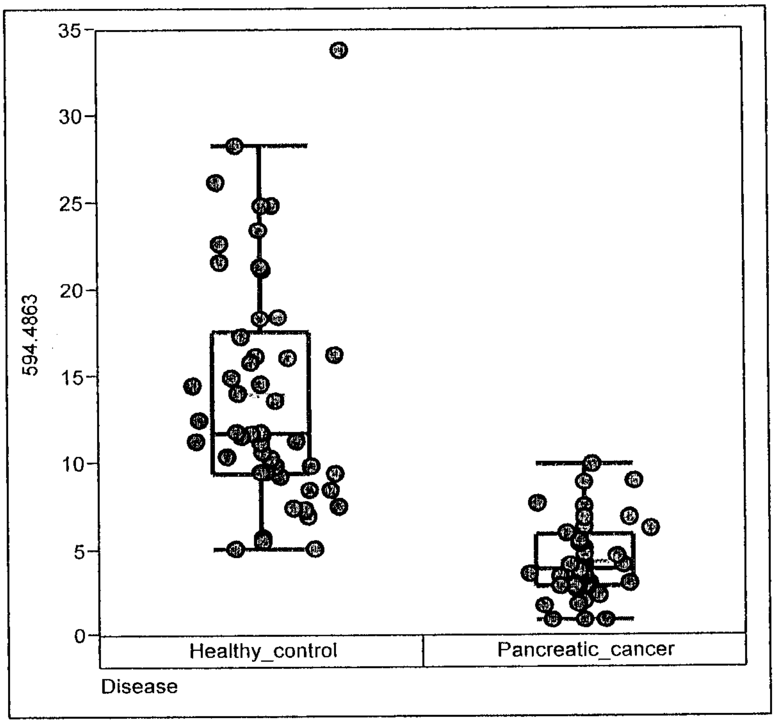
35
30
25
20
15
10
5
0
594.4863
Healthy_control
Pancreatic_cancer
Disease

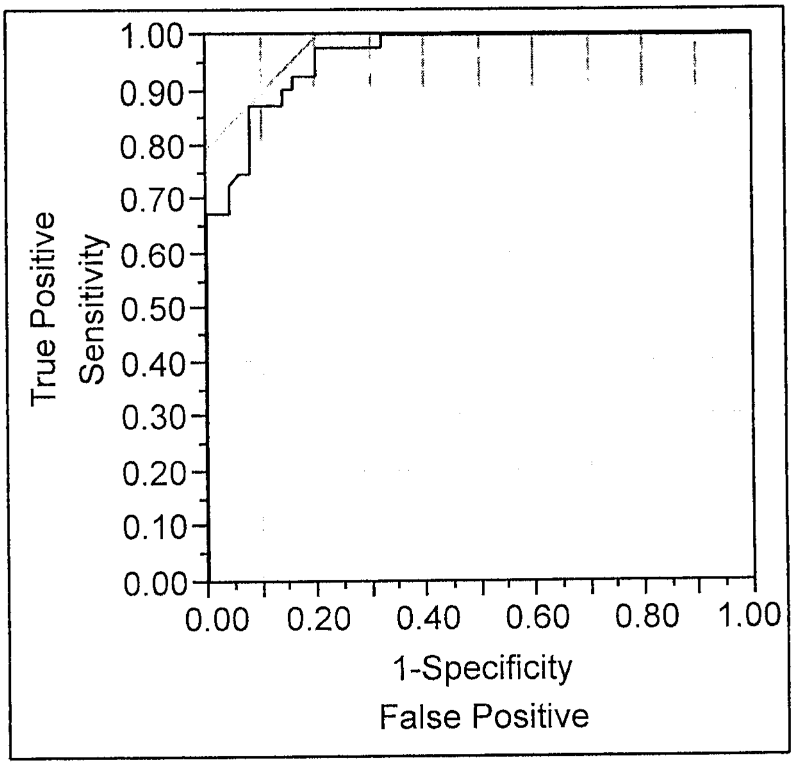
1.00
0.90
0.80
0.70
0.60
0.50
0.40
0.30
0.20
0.10
0.00
True Positive
Sensitivity
0.00
0.20
0.40
0.60
0.80
1.00
1-Specificity
False Positive

Figure 4

(b)

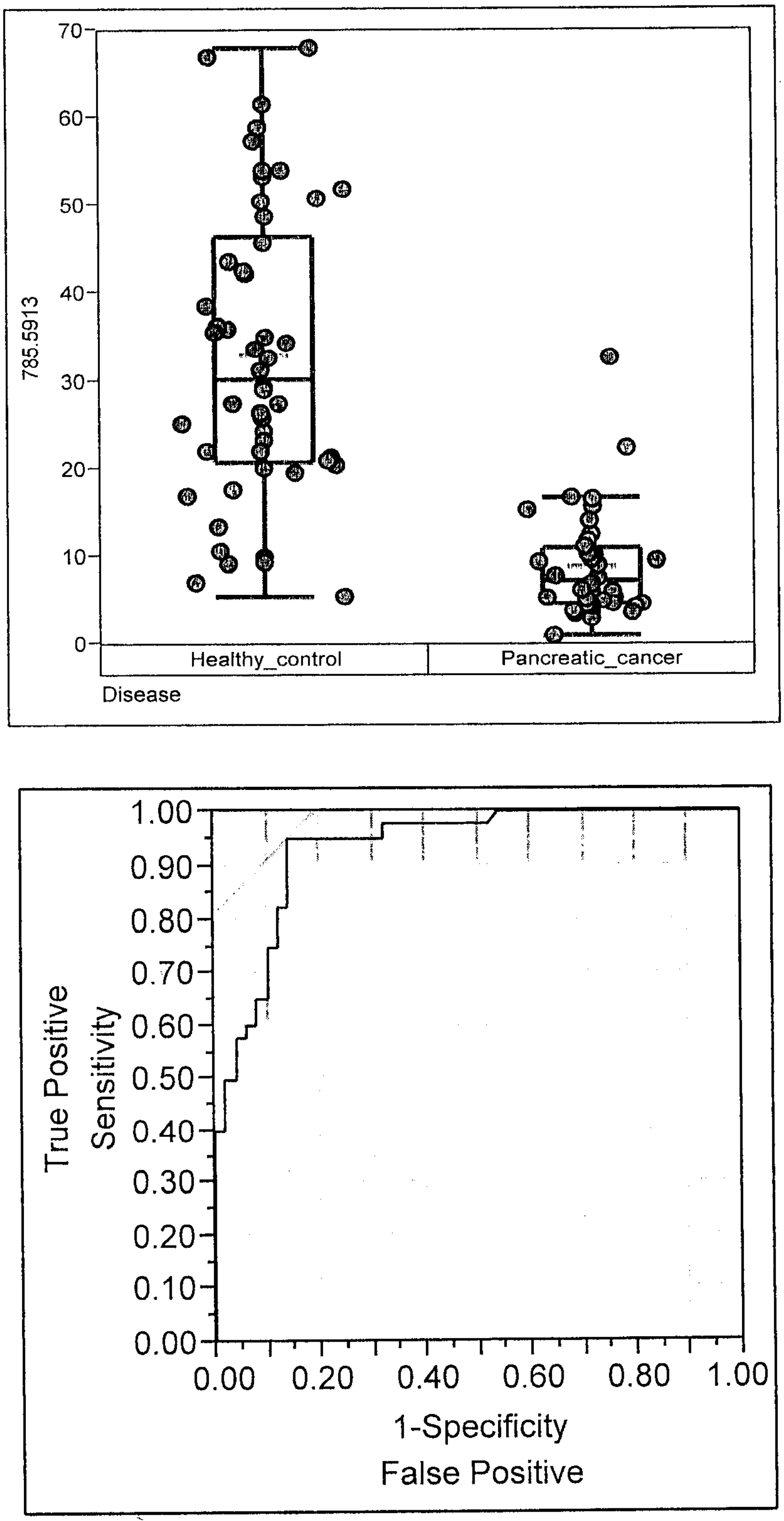

Figure 4 (cont.)

(c)

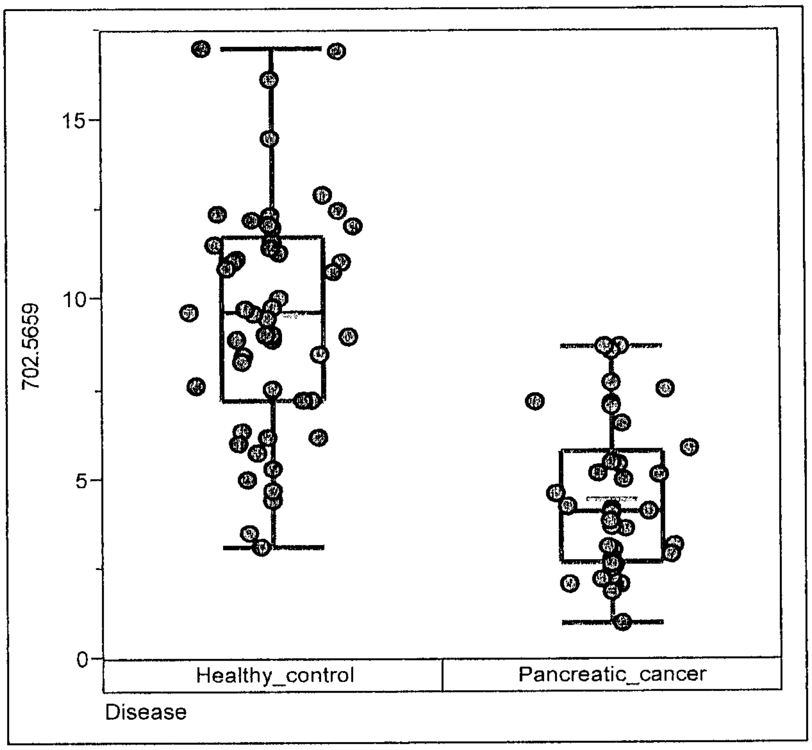

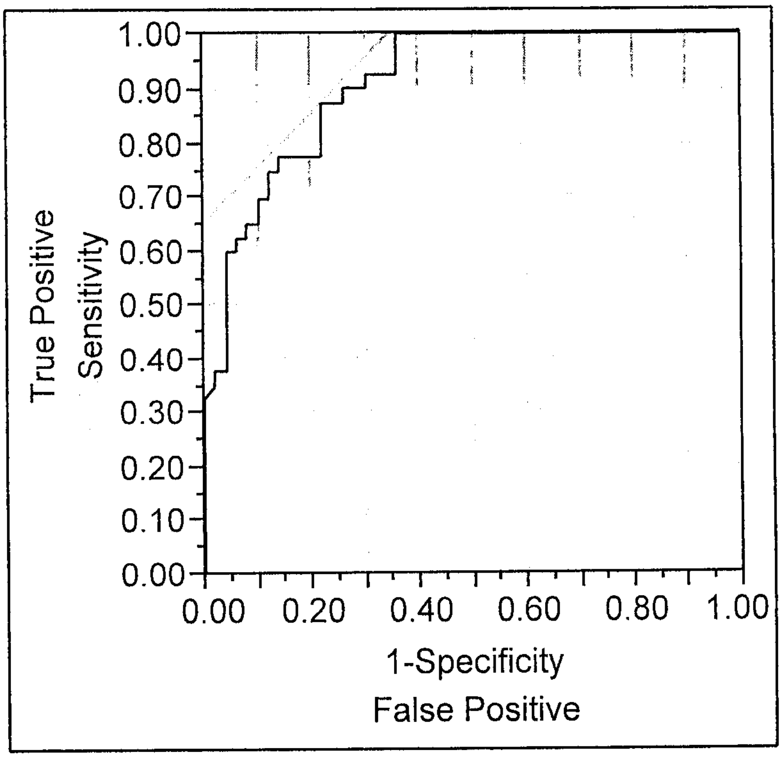

Figure 4 (cont.)

(d)

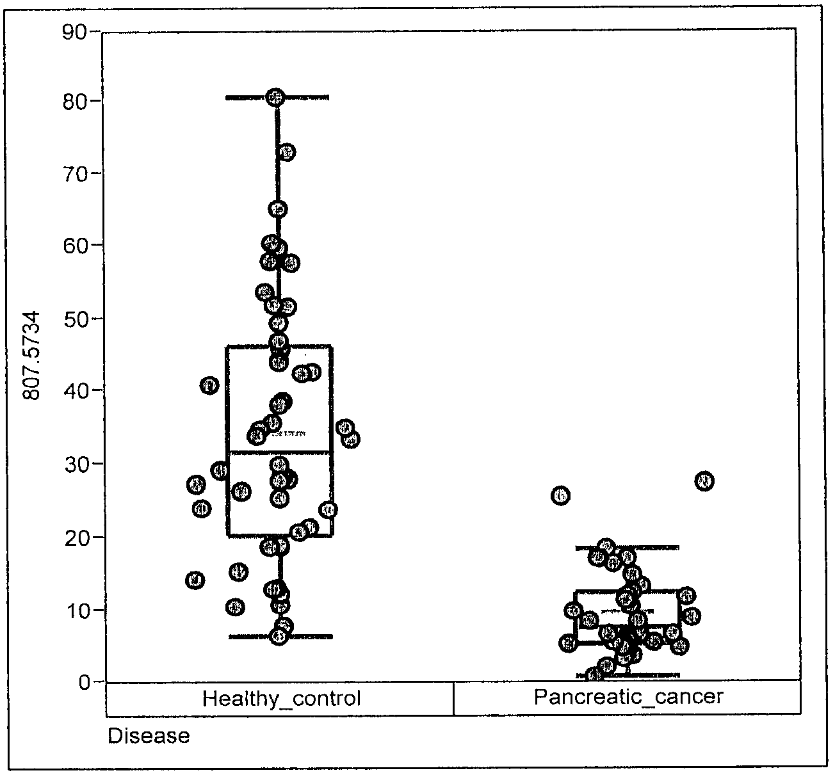

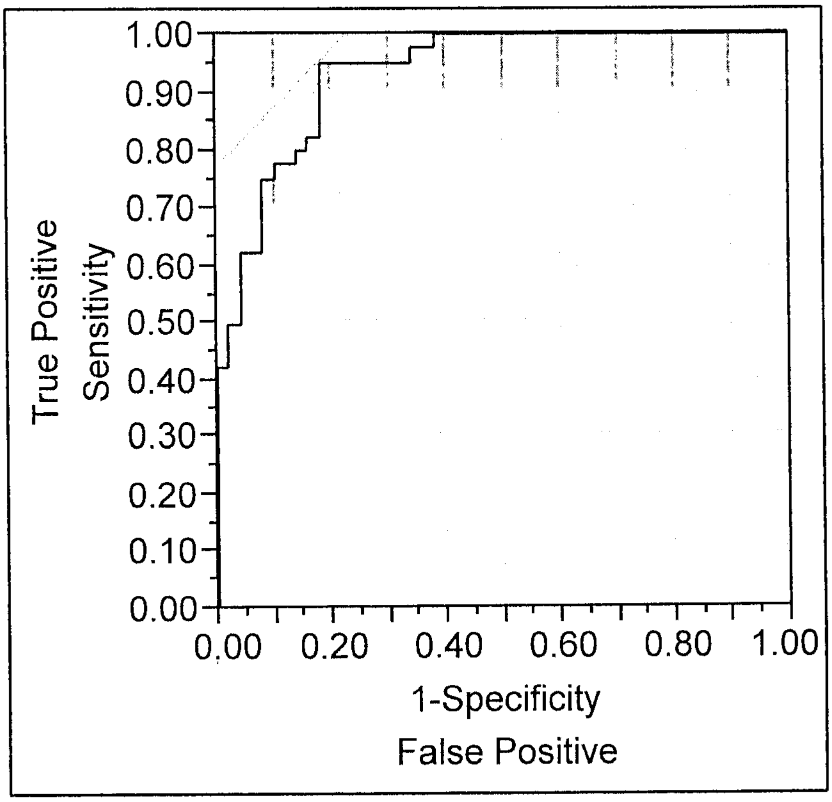

Figure 4 (cont.)

(e)

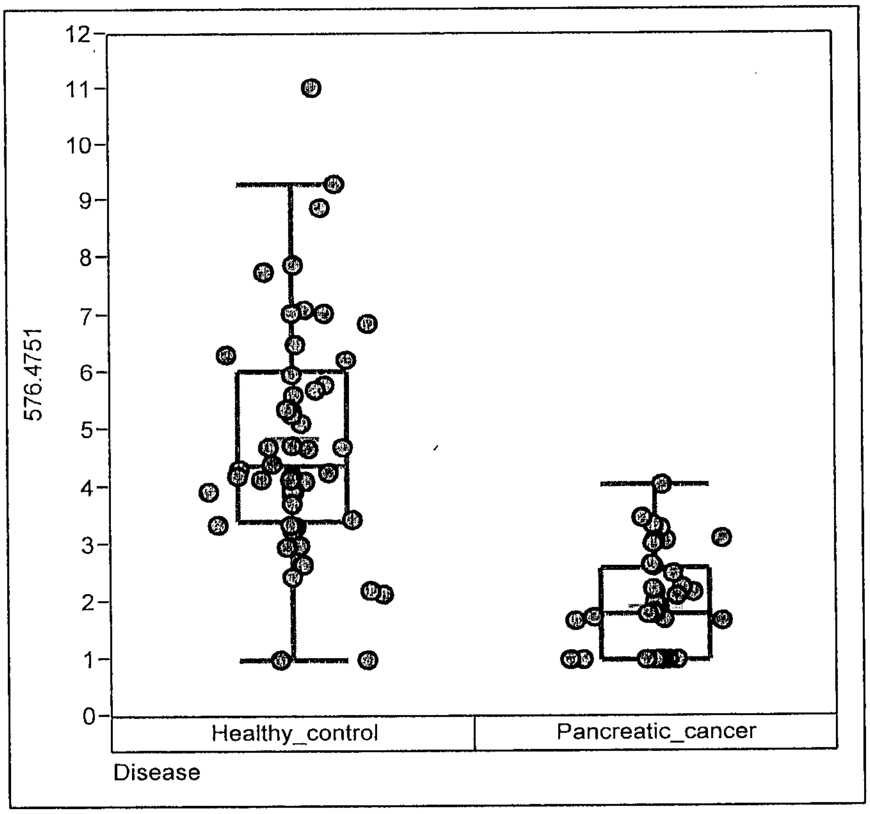

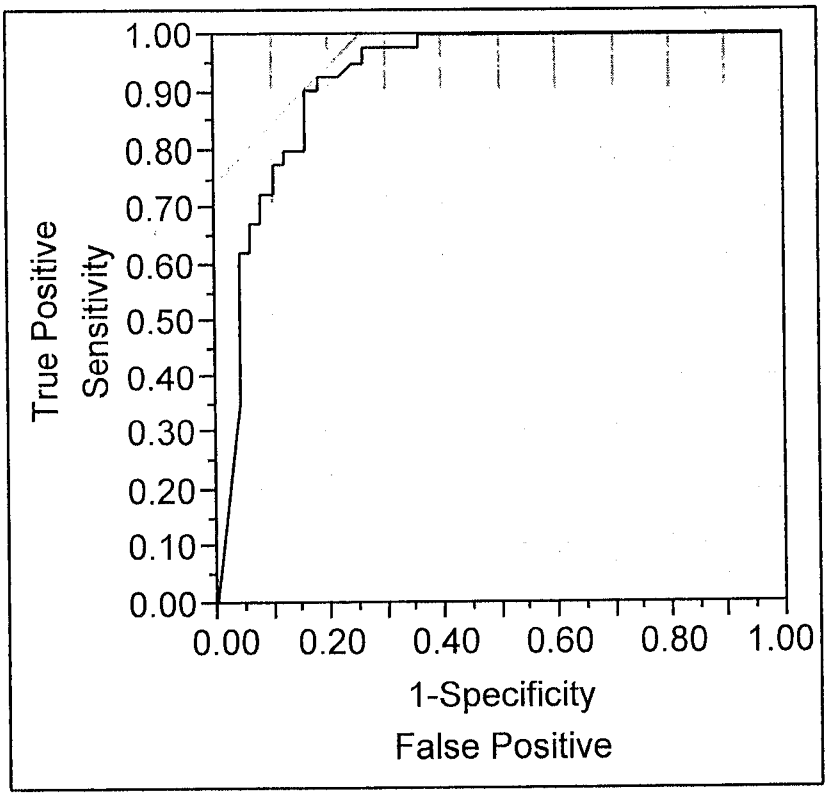

Figure 4 (cont.)

(f)

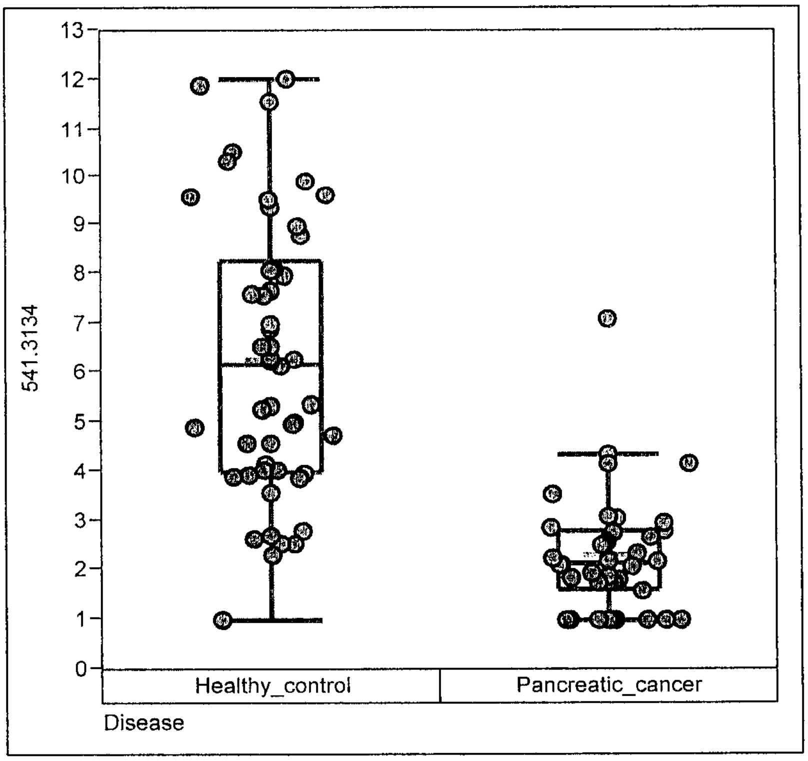

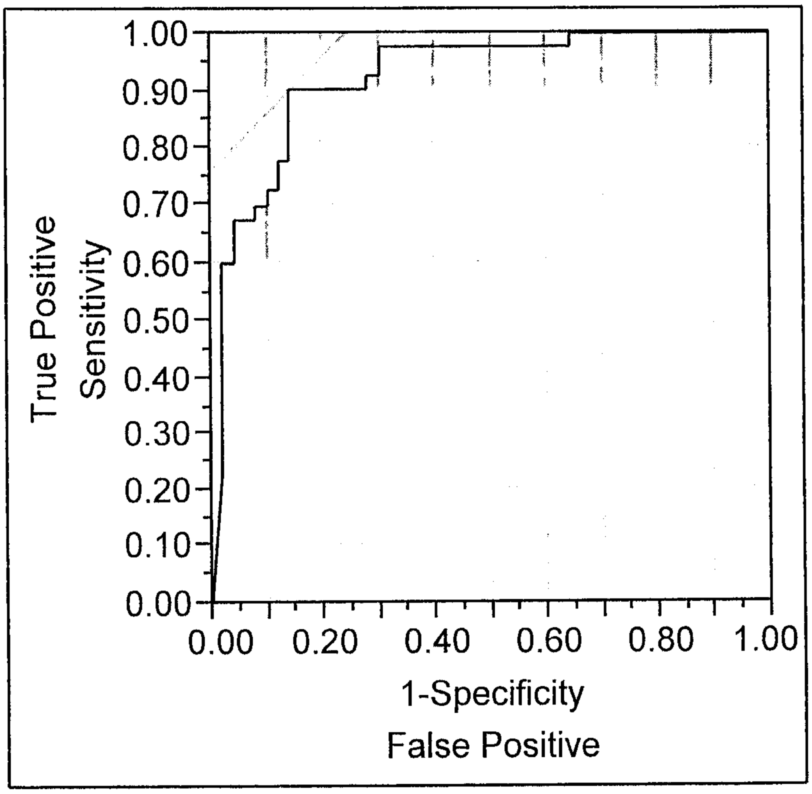

Figure 4 (cont.)

(a)

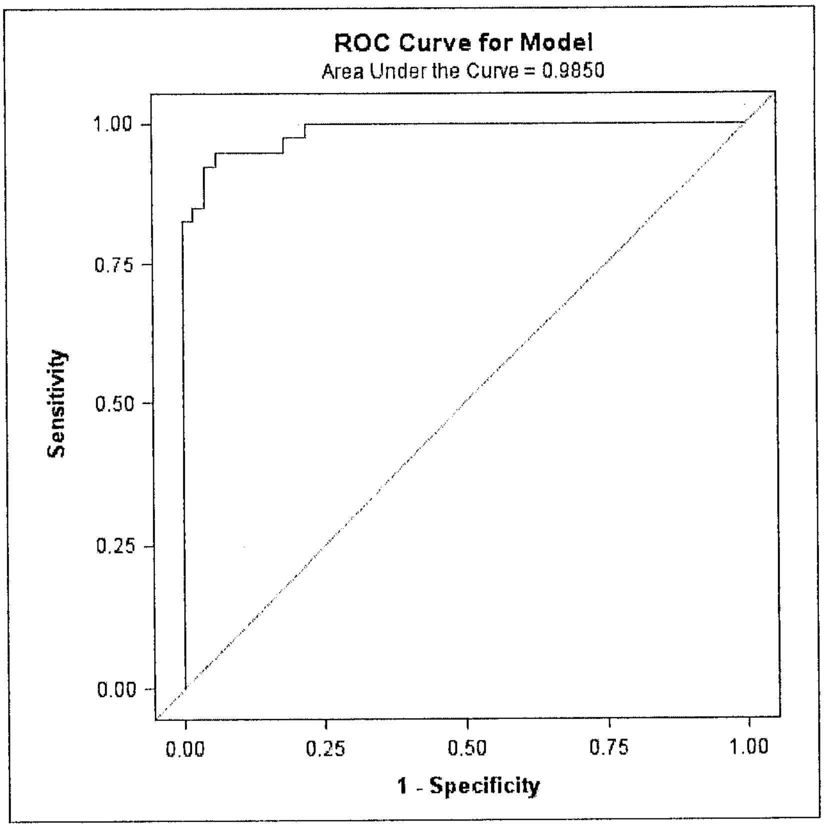

(b)

Classification Table									
Prob Level	Correct		Incorrect		Percentages				
	Event	Non-Event	Event	Non-Event	Correct	Sensitivity	Specificity	FALSE	FALSE NEG
0.05	38	36	14	2	82.2	95	72	26.9	5.3
0.1	38	40	10	2	86.7	95	80	20.8	4.8
0.15	38	41	9	2	87.8	95	82	19.1	4.7
0.2	38	42	8	2	88.9	95	84	17.4	4.5
0.25	38	42	8	2	88.9	95	84	17.4	4.5
0.3	38	42	8	2	88.9	95	84	17.4	4.5
0.35	38	42	8	2	88.9	95	84	17.4	4.5
0.4	37	43	7	3	88.9	92.5	86	15.9	6.5
0.45	37	43	7	3	88.9	92.5	86	15.9	6.5
0.5	37	44	6	3	90	92.5	88	14	6.4
0.55	36	44	6	4	88.9	90	88	14.3	8.3
0.6	34	45	5	6	87.8	85	90	12.8	11.8
0.65	34	45	5	6	87.8	85	90	12.8	11.8
0.7	33	46	4	7	87.8	82.5	92	10.8	13.2
0.75	33	48	2	7	90	82.5	96	5.7	12.7
0.8	33	48	2	7	90	82.5	96	5.7	12.7
0.85	31	48	2	9	87.8	77.5	96	6.1	15.8
0.9	28	48	2	12	84.4	70	96	6.7	20
0.95	25	49	1	15	82.2	62.5	98	3.8	23.4
1	0	50	0	40	55.6	0	100	.	44.4

Figure 5

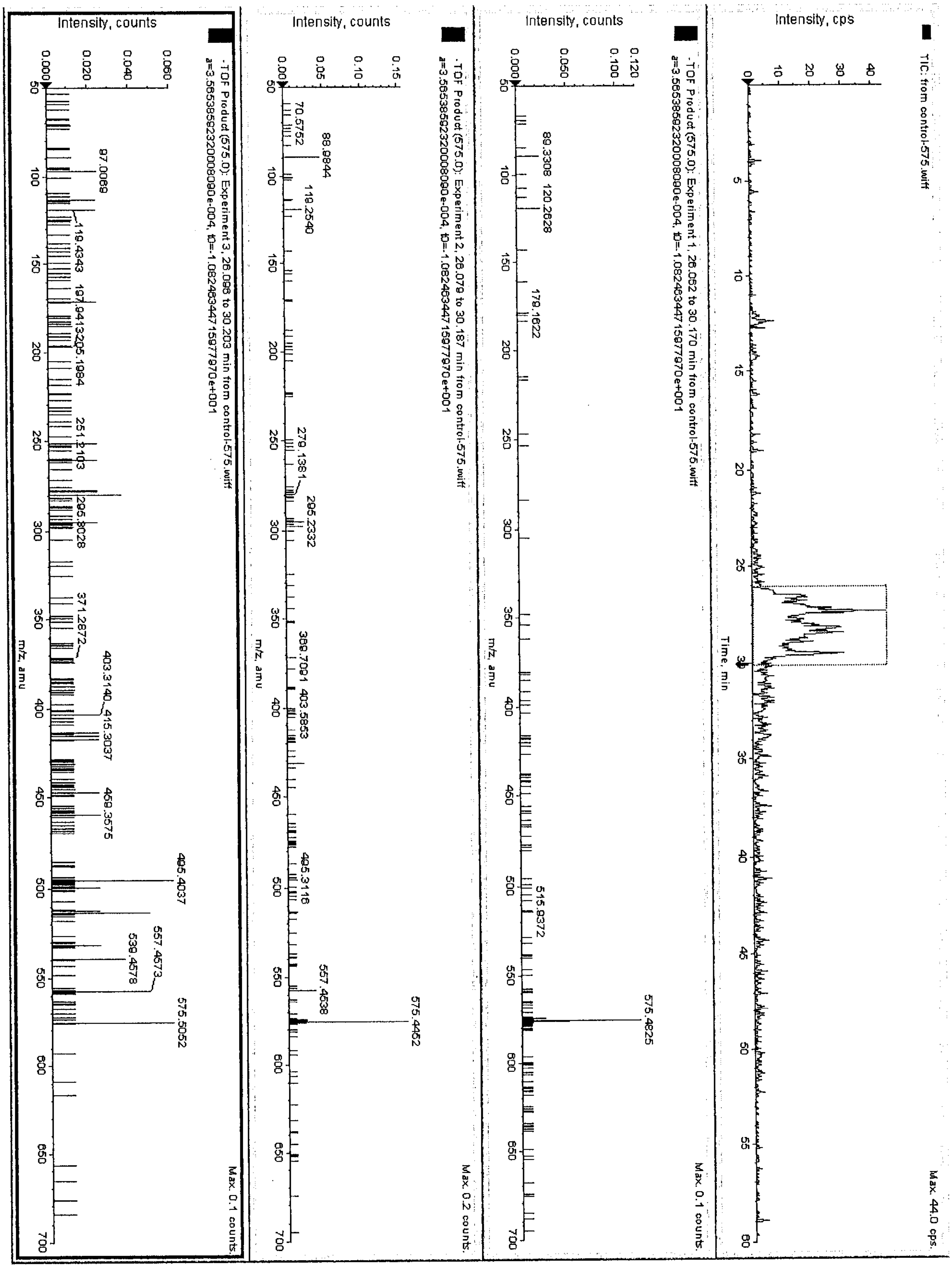
TIC: from control-575.wiff
Max. 44.0 cps.
Intensity, cps
0
10
20
30
40
5
10
15
20
25
30
35
40
45
50
55
60
Time, min
-TOF Product (575.0): Experiment 1, 26.062 to 30.170 min from control-575.wiff
a=3.56538592320008090e-004, t0=-1.08246344715977970e+001
Max. 0.1 counts.
Intensity, counts
0.000
0.050
0.100
0.120
89.3308
120.2628
179.1622
515.9372
575.4825
m/z, amu
-TOF Product (575.0): Experiment 2, 26.079 to 30.187 min from control-575.wiff
a=3.56538592320008090e-004, t0=-1.08246344715977970e+001
Max. 0.2 counts.
Intensity, counts
0.00
0.05
0.10
0.15
70.5752
88.9844
119.2540
279.1361
295.2332
386.7091
403.5853
495.3116
557.4538
575.4462
m/z, amu
-TOF Product (575.0): Experiment 3, 26.096 to 30.203 min from control-575.wiff
a=3.56538592320008090e-004, t0=-1.08246344715977970e+001
Max. 0.1 counts.
Intensity, counts
0.000
0.020
0.040
0.060
87.0069
119.4343
197.9413
205.1984
251.2103
295.3028
371.2872
403.3140
415.3037
469.3575
495.4037
539.4578
557.4573
575.5052
m/z, amu
50
100
150
200
250
300
350
400
450
500
550
600
650
700

Figure 6

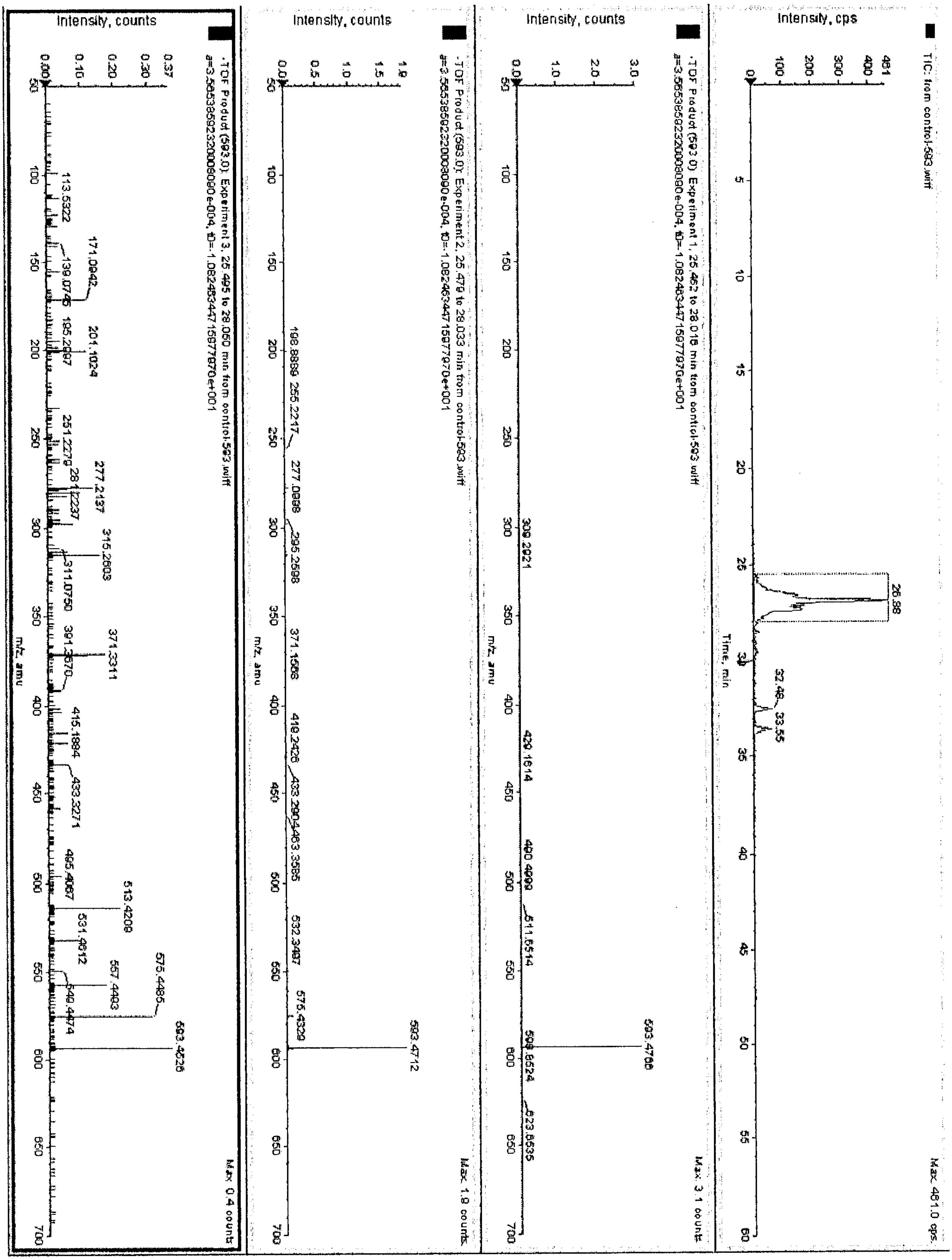
TIC: from control-593.wiff
Intensity, cps
Max. 461.0 cps.
Time, min
26.88
32.48
33.55
-TOF Product (593.0): Experiment 1, 25.462 to 28.016 min from control-593.wiff
Intensity, counts
Max. 3.1 counts.
309.2921
420.1614
490.4090
511.5514
593.4708
599.5524
623.5535
-TOF Product (593.0): Experiment 2, 25.479 to 28.033 min from control-593.wiff
Intensity, counts
Max. 1.9 counts.
198.8889
255.2247
277.0886
295.2598
371.1586
418.2426
433.2904
463.3585
532.3487
575.4329
593.4712
-TOF Product (593.0): Experiment 3, 25.495 to 28.050 min from control-593.wiff
Intensity, counts
Max. 0.4 counts.
113.5322
171.0942
139.0745
195.2097
201.1024
251.2279
277.2137
281.2237
315.2603
311.0750
371.3311
391.3670
415.1884
433.3271
465.4067
513.4209
531.4612
557.4403
549.4474
575.4485
593.4526
m/z, amu

Figure 7

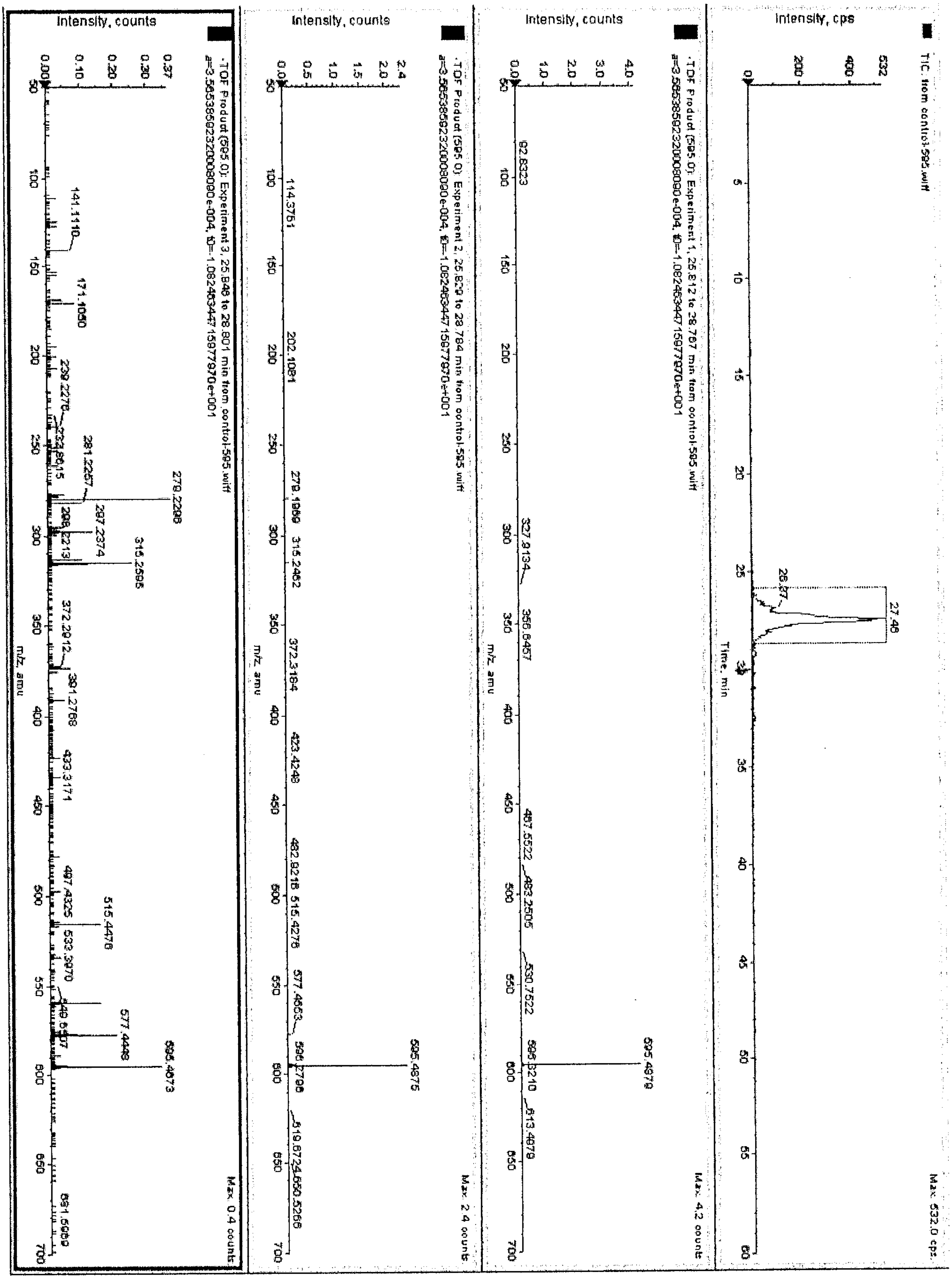
TIC from control-595.wiff
Intensity, cps
Time, min
27.48
26.87
Max 532.0 cps.
+TOF Product (595.0): Experiment 1, 25.812 to 28.767 min from control-595.wiff
a=3.58538592320008090e-004, t0=-1.08246344715977970e+001
Intensity, counts
Max 4.2 counts
92.8323
327.9134
356.6457
487.5522
483.2505
530.7522
595.4879
599.3210
613.4879
+TOF Product (595.0): Experiment 2, 25.829 to 28.784 min from control-595.wiff
Max 2.4 counts
114.3761
202.1081
278.1989
315.2462
372.3184
423.4248
482.8218
515.4276
577.4663
595.4875
596.2798
619.8724
650.5266
+TOF Product (595.0): Experiment 3, 25.846 to 28.801 min from control-595.wiff
Max 0.4 counts
141.1110
171.1050
239.2276
263.2015
281.2257
279.2298
297.2374
299.2213
315.2565
372.2912
391.2768
433.3171
497.4325
515.4476
533.3970
549.6507
577.4448
595.4873
681.5660
m/z, amu

Figure 8

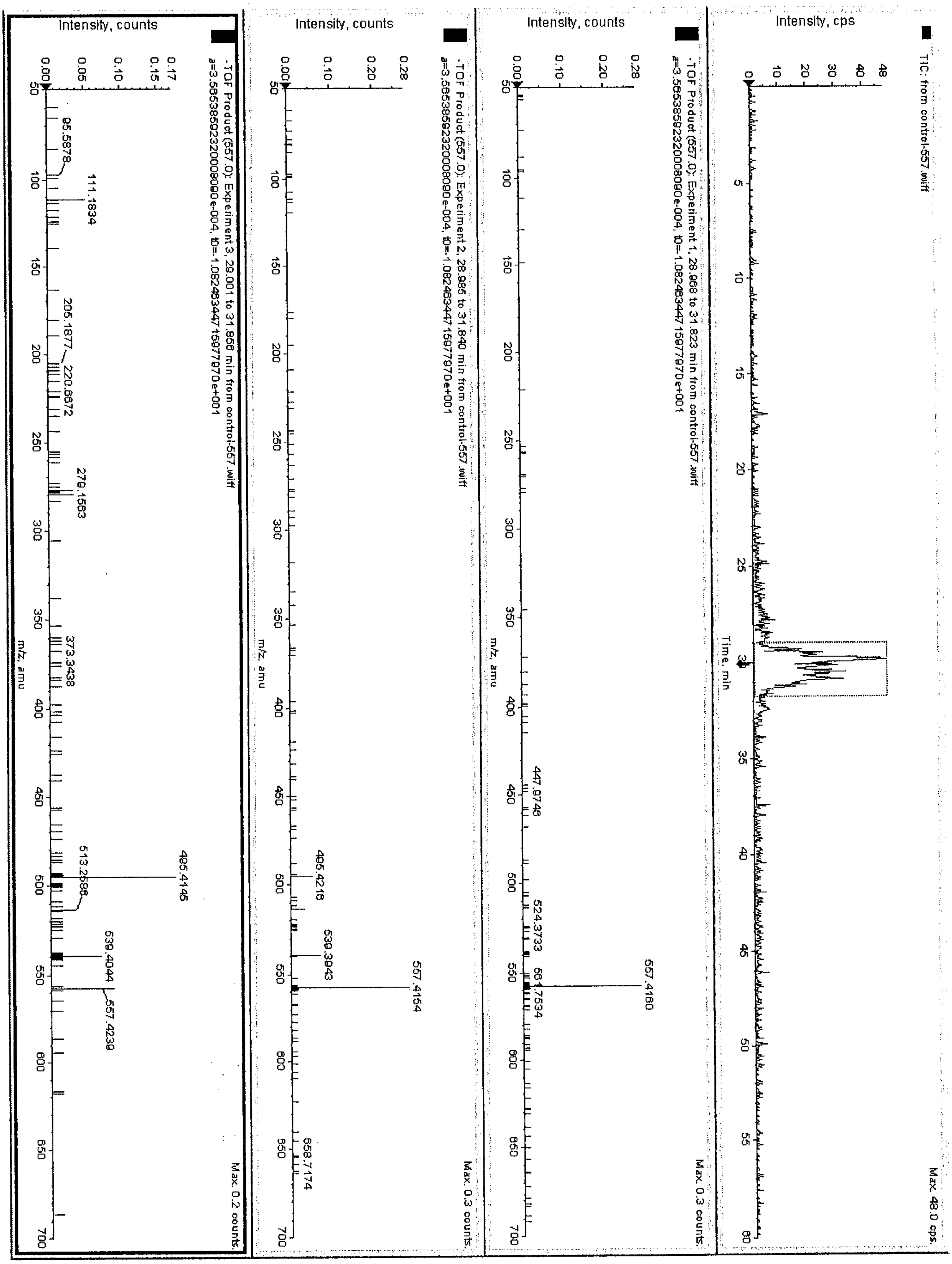
TIC: from control-557.wiff
Max. 48.0 cps.
Intensity, cps
0
10
20
30
40
48
Time, min
5
10
15
20
25
30
35
40
45
50
55
60
-TOF Product (557.0): Experiment 1, 28.908 to 31.823 min from control-557.wiff
a=3.56538592320008090e-004, t0=1.08248344715977970e+001
Max. 0.3 counts.
Intensity, counts
0.00
0.10
0.20
0.28
447.8746
524.3733
557.4180
561.7534
m/z, amu
-TOF Product (557.0): Experiment 2, 28.985 to 31.840 min from control-557.wiff
a=3.56538592320008090e-004, t0=1.08248344715977970e+001
Max. 0.3 counts.
Intensity, counts
0.00
0.10
0.20
0.28
495.4216
539.3943
557.4154
668.7174
m/z, amu
-TOF Product (557.0): Experiment 3, 29.001 to 31.856 min from control-557.wiff
a=3.56538592320008090e-004, t0=1.08248344715977970e+001
Max. 0.2 counts.
Intensity, counts
0.00
0.05
0.10
0.15
0.17
95.5878
111.1834
205.1877
220.6672
279.1563
373.3438
495.4145
513.2686
539.4044
557.4239
m/z, amu
50
100
150
200
250
300
350
400
450
500
550
600
650
700

Figure 9

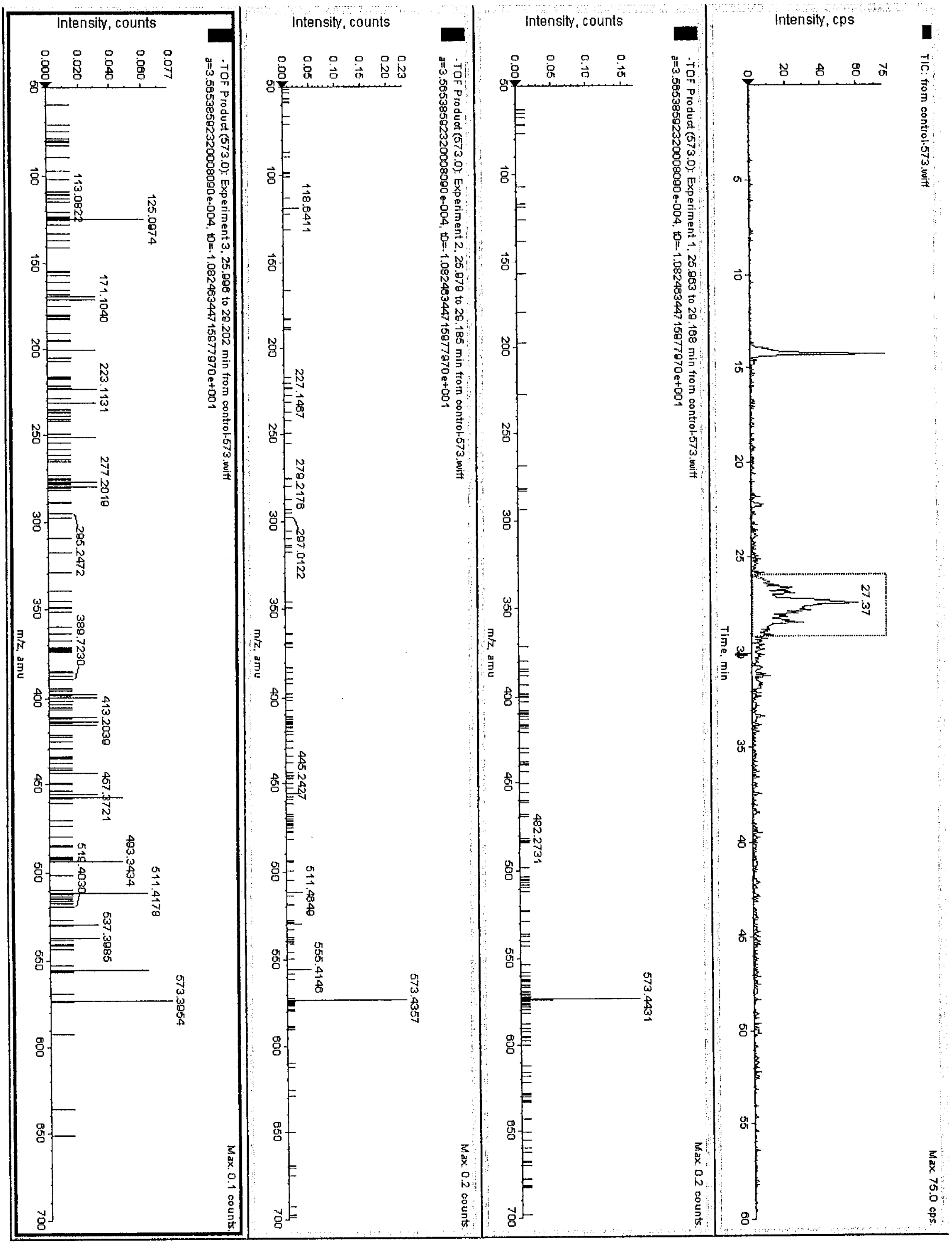
TIC: from control-573.wiff
Max. 75.0 cps.
Intensity, cps
Time, min
27.37
+TOF Product (573.0): Experiment 1, 25.803 to 29.168 min from control-573.wiff
a=3.56538592320008090e-004, t0=-1.08246344715977970e+001
Max. 0.2 counts.
Intensity, counts
573.4431
482.2731
m/z, amu
+TOF Product (573.0): Experiment 2, 25.879 to 29.185 min from control-573.wiff
a=3.56538592320008090e-004, t0=-1.08246344715977970e+001
Max. 0.2 counts.
Intensity, counts
118.6411
227.1467
279.2176
297.0122
445.2427
511.4649
555.4146
573.4357
m/z, amu
+TOF Product (573.0): Experiment 3, 25.906 to 29.202 min from control-573.wiff
a=3.56538592320008090e-004, t0=-1.08246344715977970e+001
Max. 0.1 counts.
Intensity, counts
113.0822
125.0974
171.1040
223.1131
277.2019
295.2472
389.7230
413.2039
457.3721
493.3434
511.4178
519.4030
537.3985
573.3954
m/z, amu

Figure 10

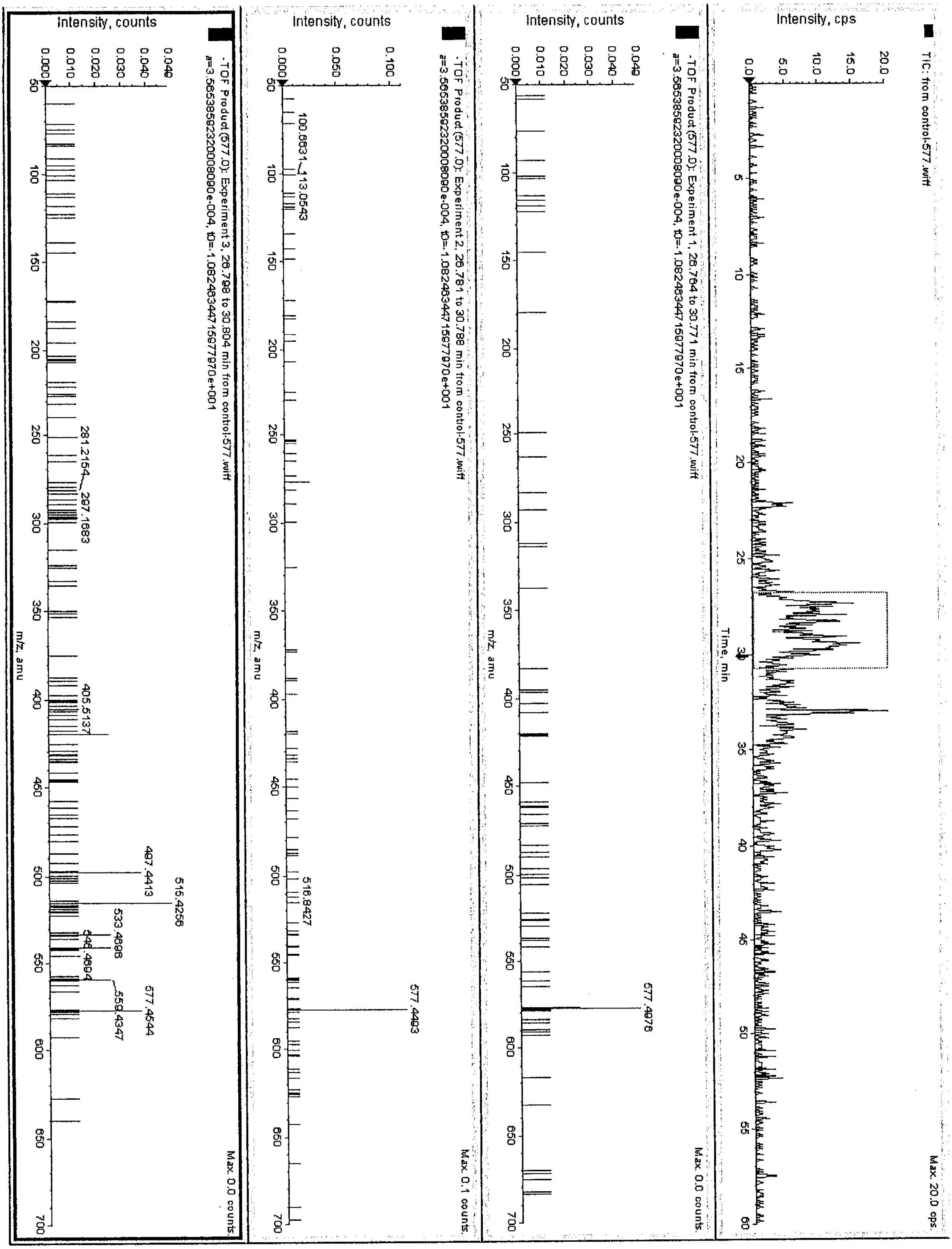
TIC: from control-577.wiff
Intensity, cps
20.0
15.0
10.0
5.0
0.0
Time, min
5
10
15
20
25
30
35
40
45
50
55
60
Max. 20.0 cps.
-TOF Product (577.0): Experiment 1, 26.764 to 30.771 min from control-577.wiff
a=3.56538582320008090e-004, t0=1.08248344715677970e+001
Intensity, counts
0.049
0.040
0.030
0.020
0.010
0.000
577.4876
Max. 0.0 counts.
m/z, amu
-TOF Product (577.0): Experiment 2, 26.781 to 30.788 min from control-577.wiff
a=3.56538582320008090e-004, t0=1.08248344715677970e+001
Intensity, counts
0.100
0.050
0.000
100.8831
113.0543
516.8427
577.4403
Max. 0.1 counts.
m/z, amu
-TOF Product (577.0): Experiment 3, 26.798 to 30.804 min from control-577.wiff
a=3.56538582320008090e-004, t0=1.08248344715677970e+001
Intensity, counts
0.049
0.040
0.030
0.020
0.010
0.000
281.2154
297.1683
405.5137
497.4413
515.4256
533.4888
546.4804
559.4347
577.4544
Max. 0.0 counts.
m/z, amu
50
100
150
200
250
300
350
400
450
500
550
600
650
700

Figure 11

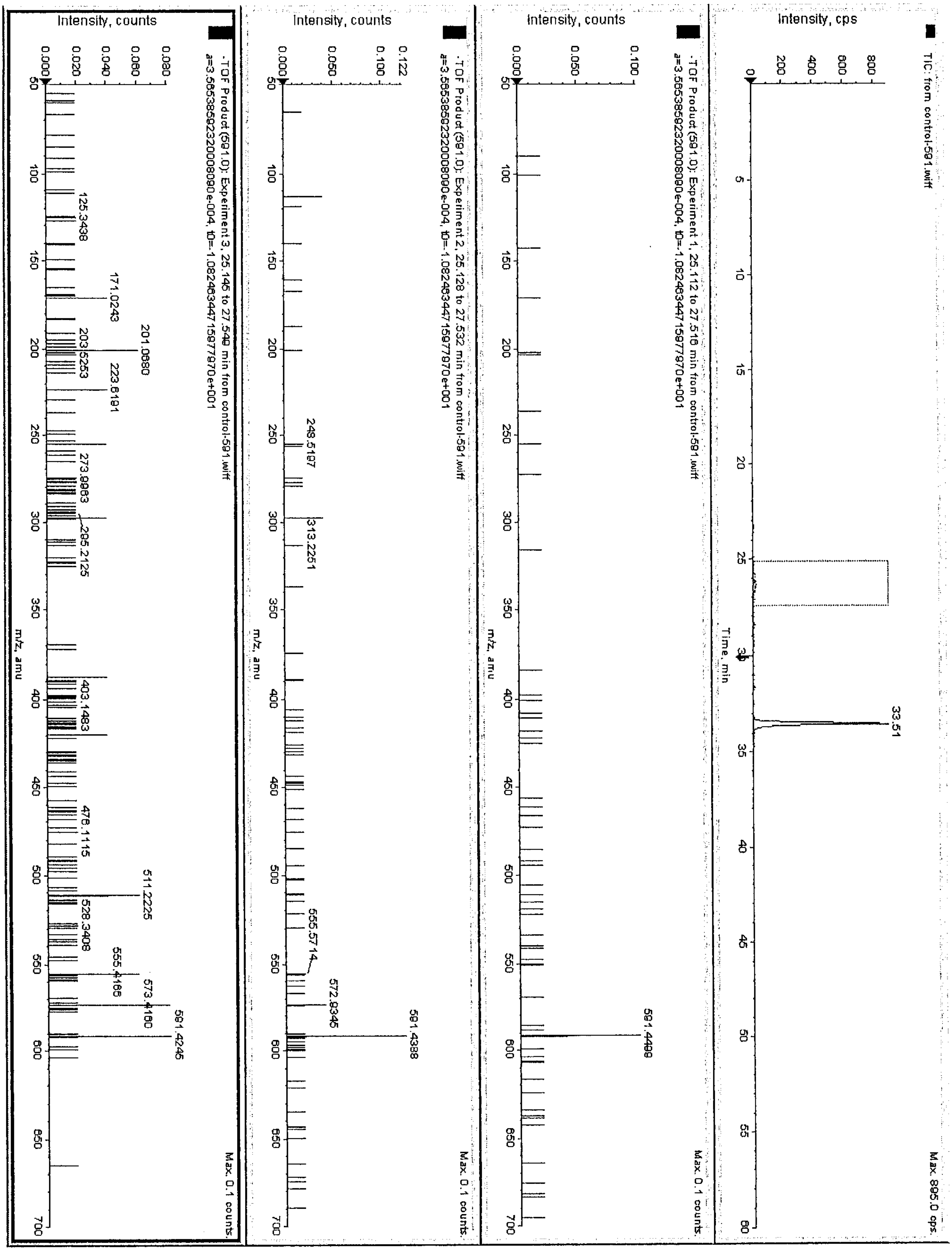
TIC: from control-591.wiff
Max. 895.0 cps.
Intensity, cps
Time, min
33.51
-TOF Product (591.0): Experiment 1, 25.112 to 27.516 min from control-591.wiff
a=3.56538592320008090e-004, t0=-1.08246344715987970e+001
Max. 0.1 counts.
Intensity, counts
m/z, amu
591.4499
-TOF Product (591.0): Experiment 2, 25.128 to 27.532 min from control-591.wiff
a=3.56538592320008090e-004, t0=-1.08246344715987970e+001
Max. 0.1 counts.
Intensity, counts
m/z, amu
248.5187
313.2251
555.5714
572.8345
591.4388
-TOF Product (591.0): Experiment 3, 25.146 to 27.549 min from control-591.wiff
a=3.56538592320008090e-004, t0=-1.08246344715987970e+001
Max. 0.1 counts.
Intensity, counts
m/z, amu
125.3438
171.0243
201.0680
203.5253
223.8191
273.9983
295.2125
403.1483
476.1115
511.2225
528.3408
555.4166
573.4180
591.4245

Figure 12

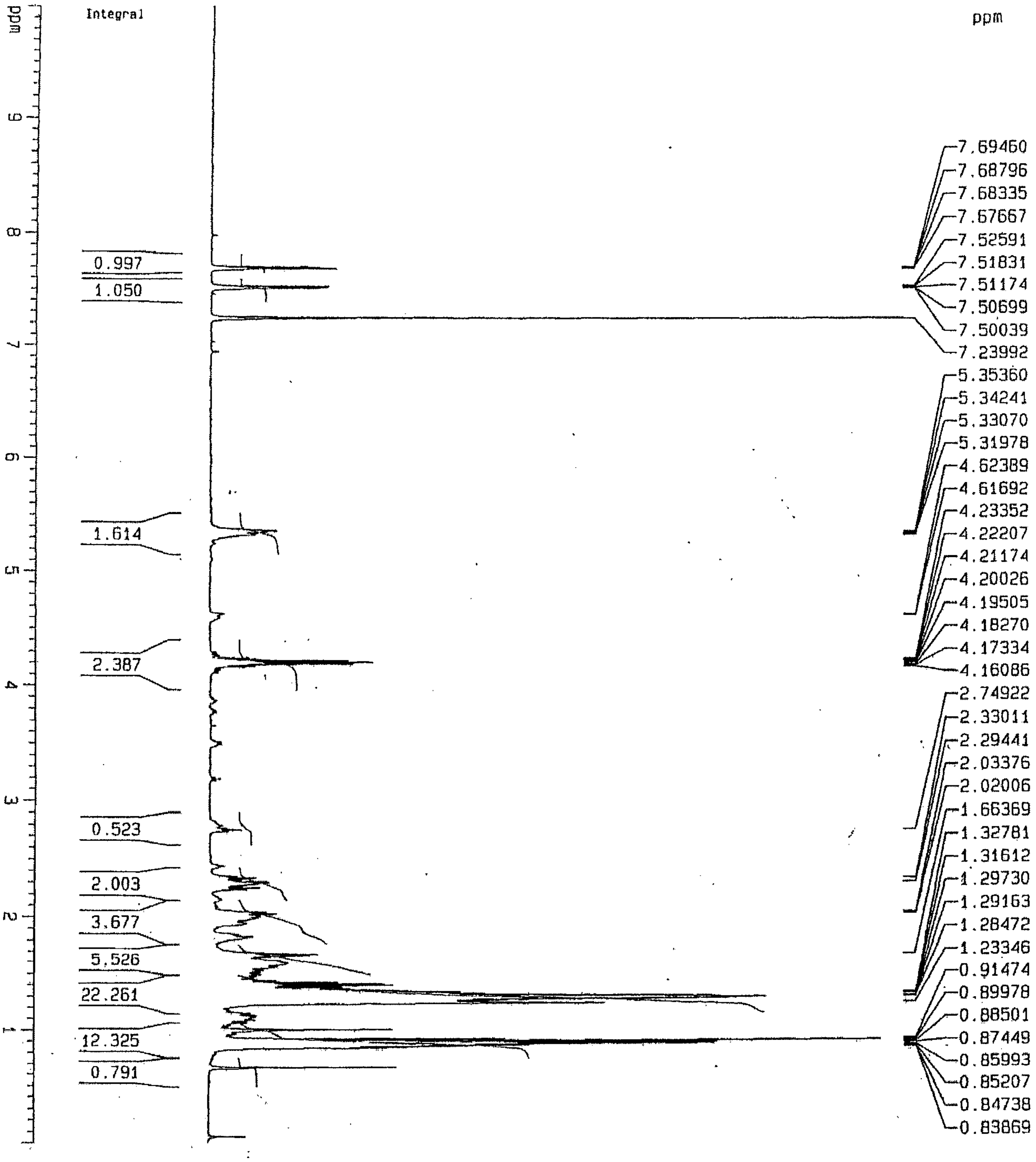
ppm
Integral
9
8
7
6
5
4
3
2
1
0.997
1.050
1.614
2.387
0.523
2.003
3.677
5.526
22.261
12.325
0.791
ppm
7.69460
7.68796
7.68335
7.67667
7.52591
7.51831
7.51174
7.50699
7.50039
7.23992
5.35360
5.34241
5.33070
5.31978
4.62389
4.61692
4.23352
4.22207
4.21174
4.20026
4.19505
4.18270
4.17334
4.16086
2.74922
2.33011
2.29441
2.03376
2.02006
1.66369
1.32781
1.31612
1.29730
1.29163
1.28472
1.23346
0.91474
0.89978
0.88501
0.87449
0.85993
0.85207
0.84738
0.83869

Figure 13

(a)

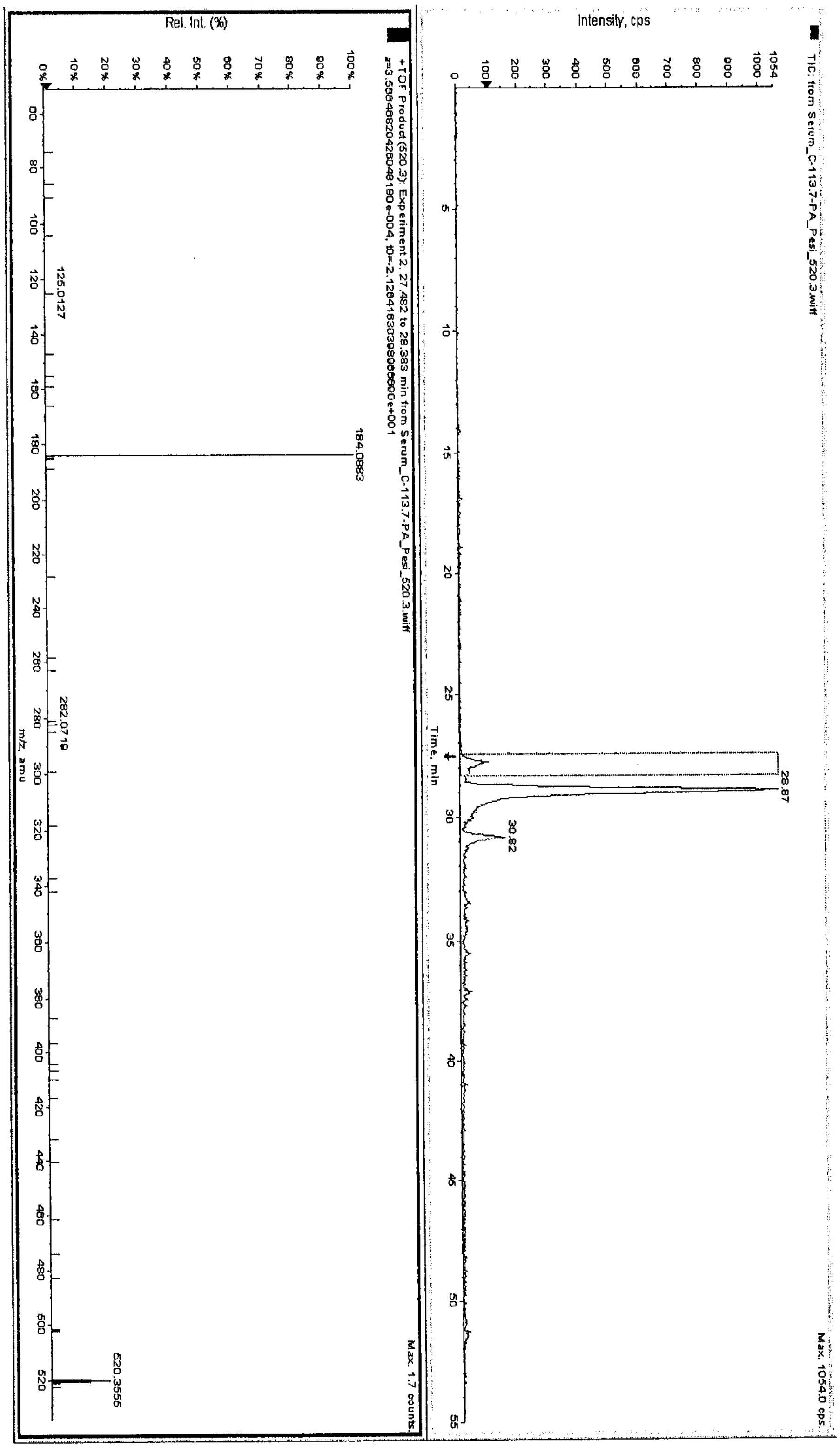
TIC: from Serum_C-113.7-PA_Pesi_520.3.wiff
Max. 1054.0 cps.
Intensity, cps
0
100
200
300
400
500
600
700
800
900
1000
1054
5
10
15
20
25
30
35
40
45
50
55
Time, min
28.87
30.82
+TOF Product (520.3): Experiment 2, 27.482 to 28.383 min from Serum_C-113.7-PA_Pesi_520.3.wiff
a=3.56846820426048180e-004, t0=-2.12841630398066680e+001
Max. 1.7 counts.
Rel. Int. (%)
0%
10%
20%
30%
40%
50%
60%
70%
80%
90%
100%
60
80
100
120
140
160
180
200
220
240
260
280
300
320
340
360
380
400
420
440
460
480
500
520
m/z, amu
125.0127
184.0883
282.0719
520.3555

Figure 14

(b)

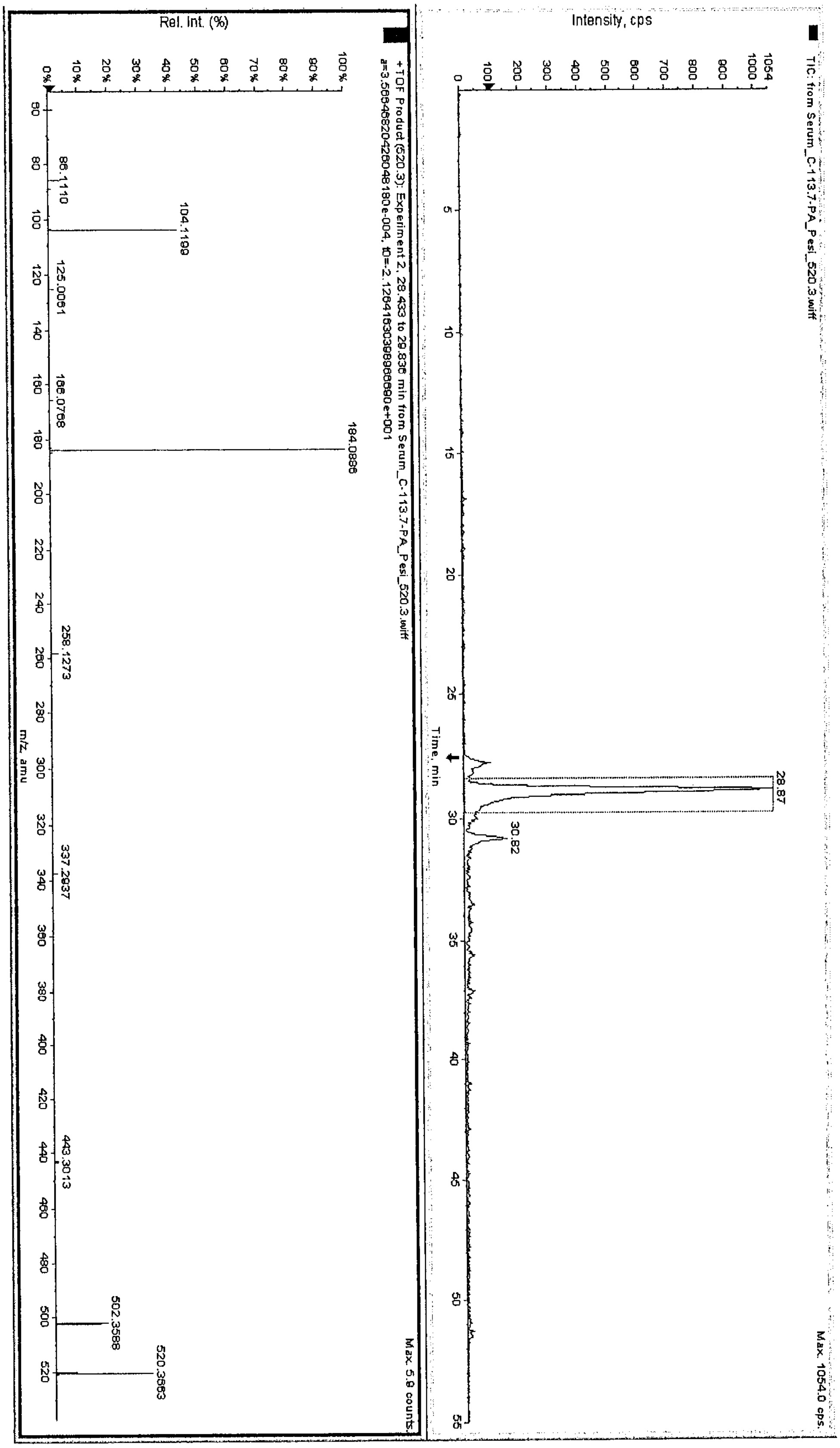

Figure 14 (cont.)

(a)

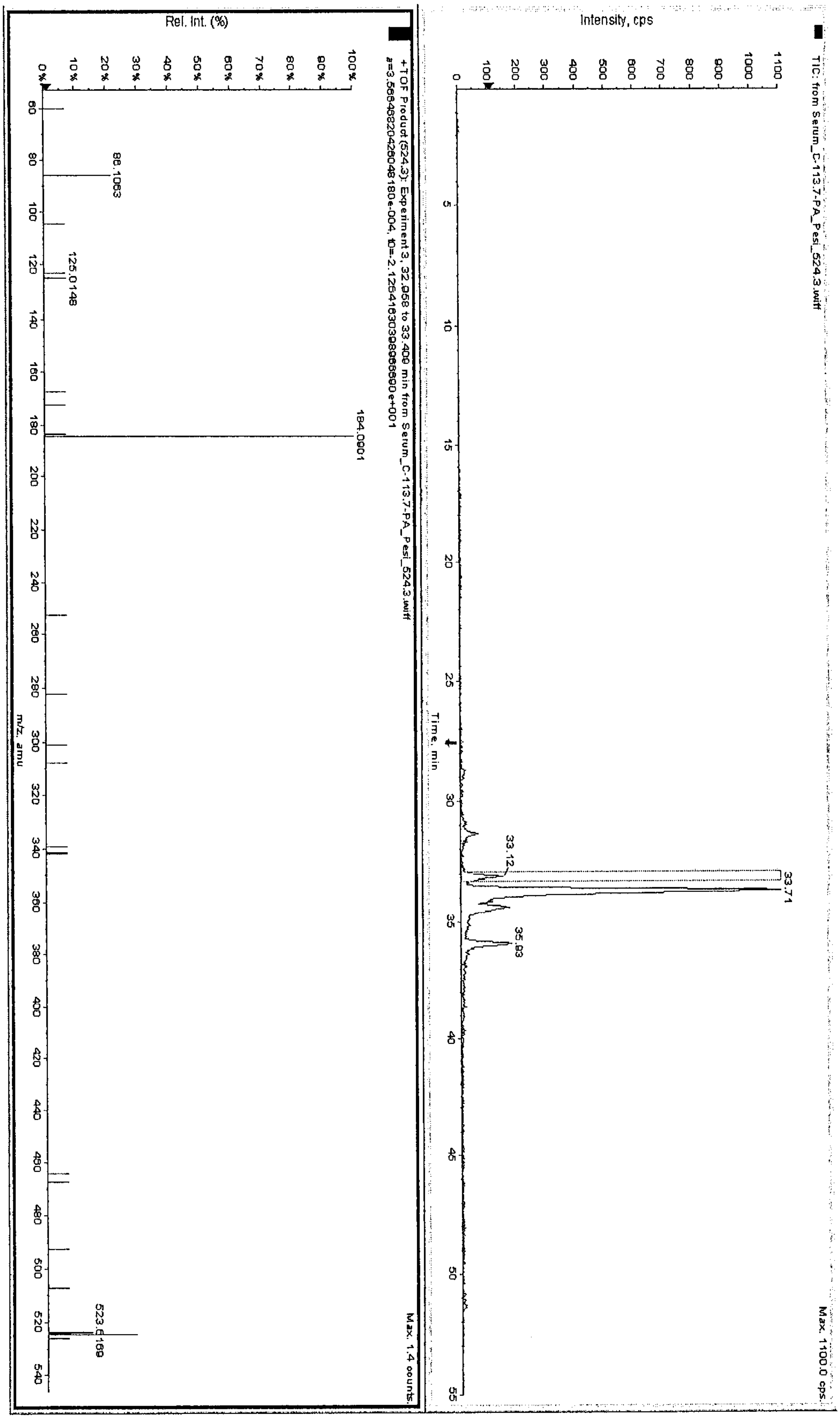
TIC: from Serum_C-113.7-PA_Pesi_524.3.wiff
Max. 1100.0 cps.
Intensity, cps
0
100
200
300
400
500
600
700
800
900
1000
1100
5
10
15
20
25
30
35
40
45
50
55
Time, min
33.12
33.71
35.83
+TOF Product (524.3): Experiment 3, 32.958 to 33.409 min from Serum_C-113.7-PA_Pesi_524.3.wiff
#=3.56846820426048180e-004, t0=-2.1264163039886880e+001
Max. 1.4 counts.
Rel. Int. (%)
0%
10%
20%
30%
40%
50%
60%
70%
80%
90%
100%
60
80
100
120
140
160
180
200
220
240
260
280
300
320
340
360
380
400
420
440
460
480
500
520
540
m/z, amu
86.1063
125.0148
184.0801
523.8169

Figure 15

(b)

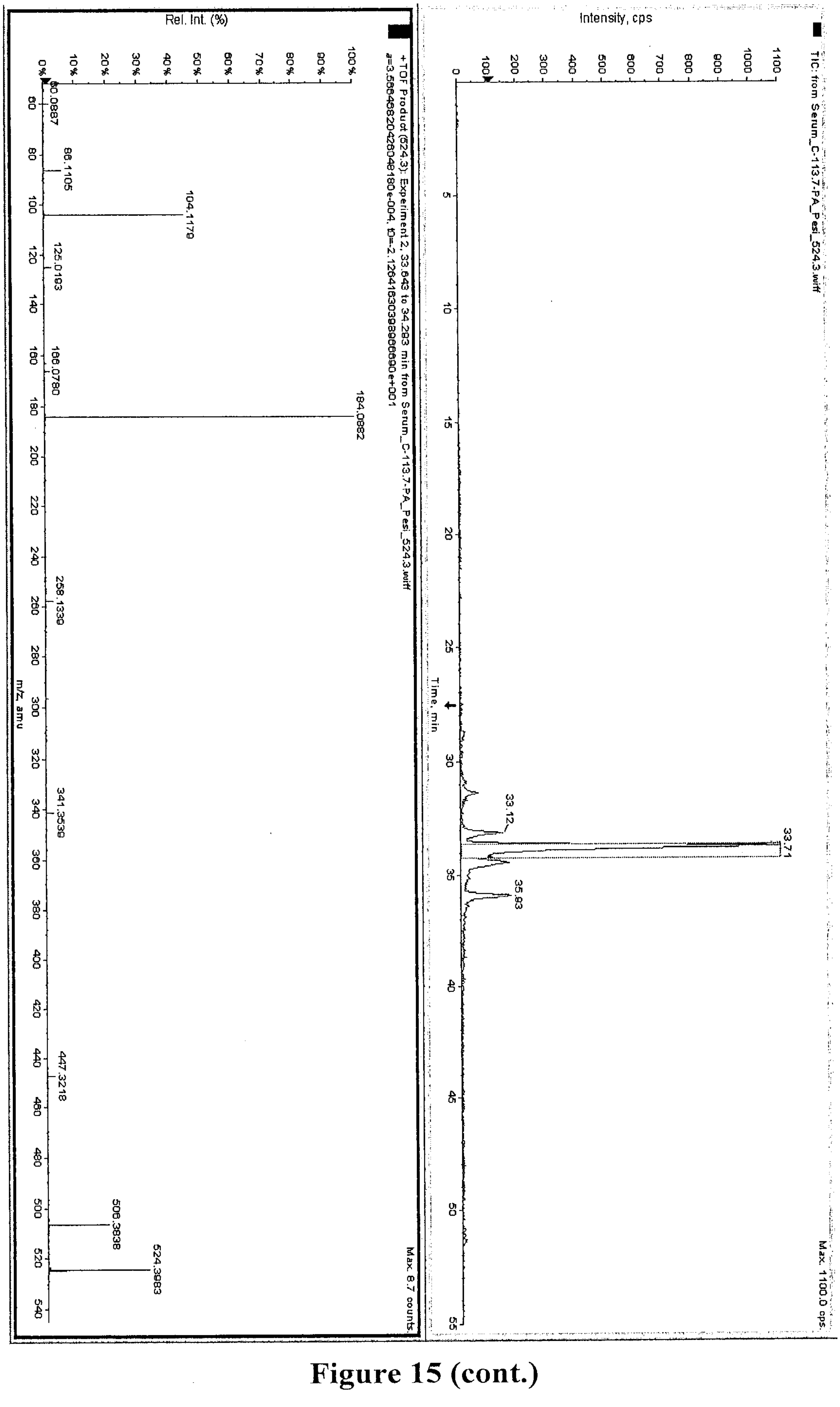

Figure 15 (cont.)

(a)

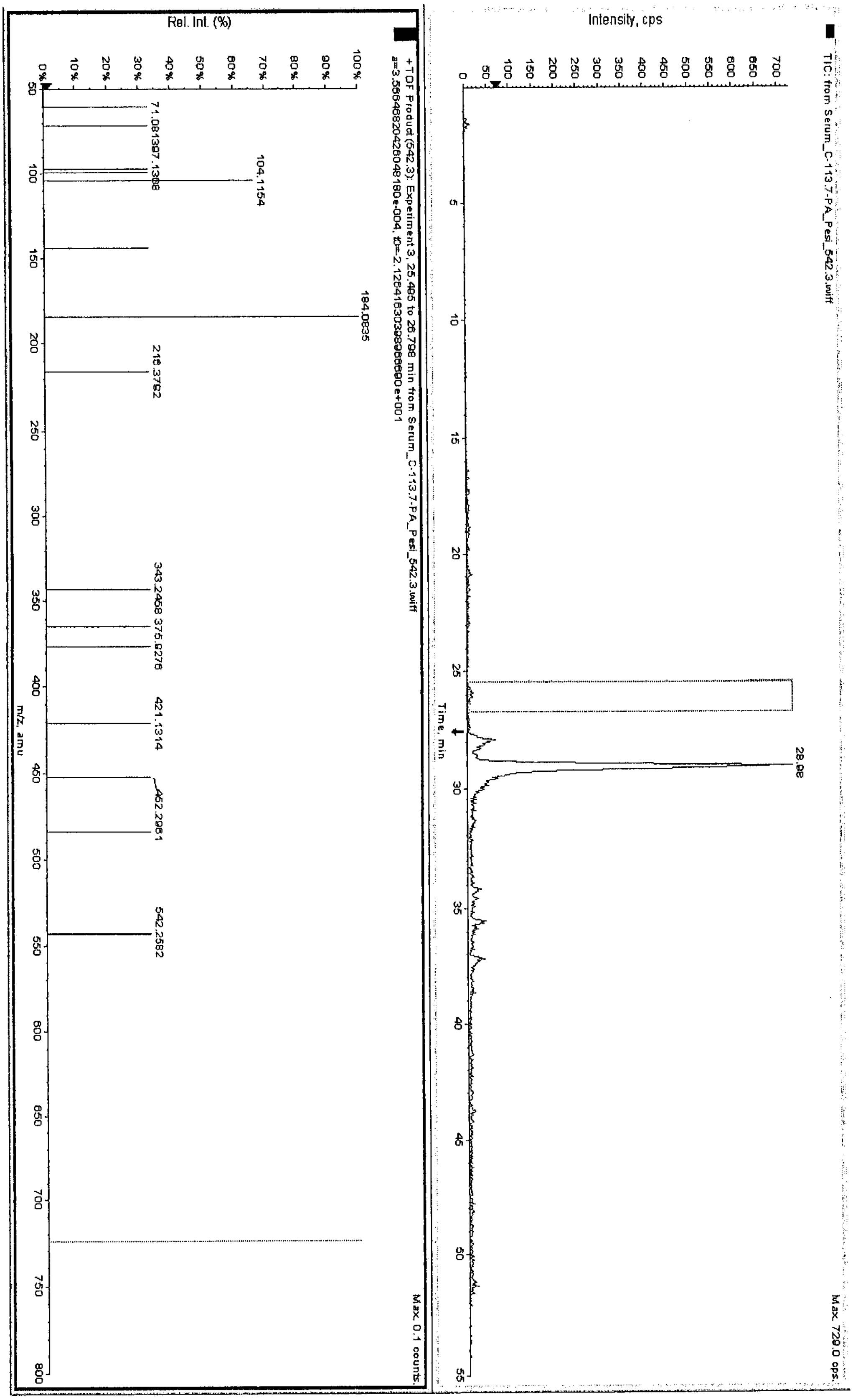
TIC: from Serum_C-113.7-PA_Pesi_542.3.wiff
Max. 729.0 cps.
Intensity, cps
0
50
100
150
200
250
300
350
400
450
500
550
600
650
700
Time, min
5
10
15
20
25
30
35
40
45
50
55
28.98
+TOF Product (542.3): Experiment 3, 25.485 to 26.798 min from Serum_C-113.7-PA_Pesi_542.3.wiff
a=3.56648820426048180e-004, t0=2.12641630398860000e+001
Max. 0.1 counts
Rel. Int. (%)
0%
10%
20%
30%
40%
50%
60%
70%
80%
90%
100%
71.081397.1308
104.1154
184.0835
216.3782
343.2458 375.9276
421.1314
462.2961
542.2582
m/z, amu
50
100
150
200
250
300
350
400
450
500
550
600
650
700
750
800

Figure 16

(b)

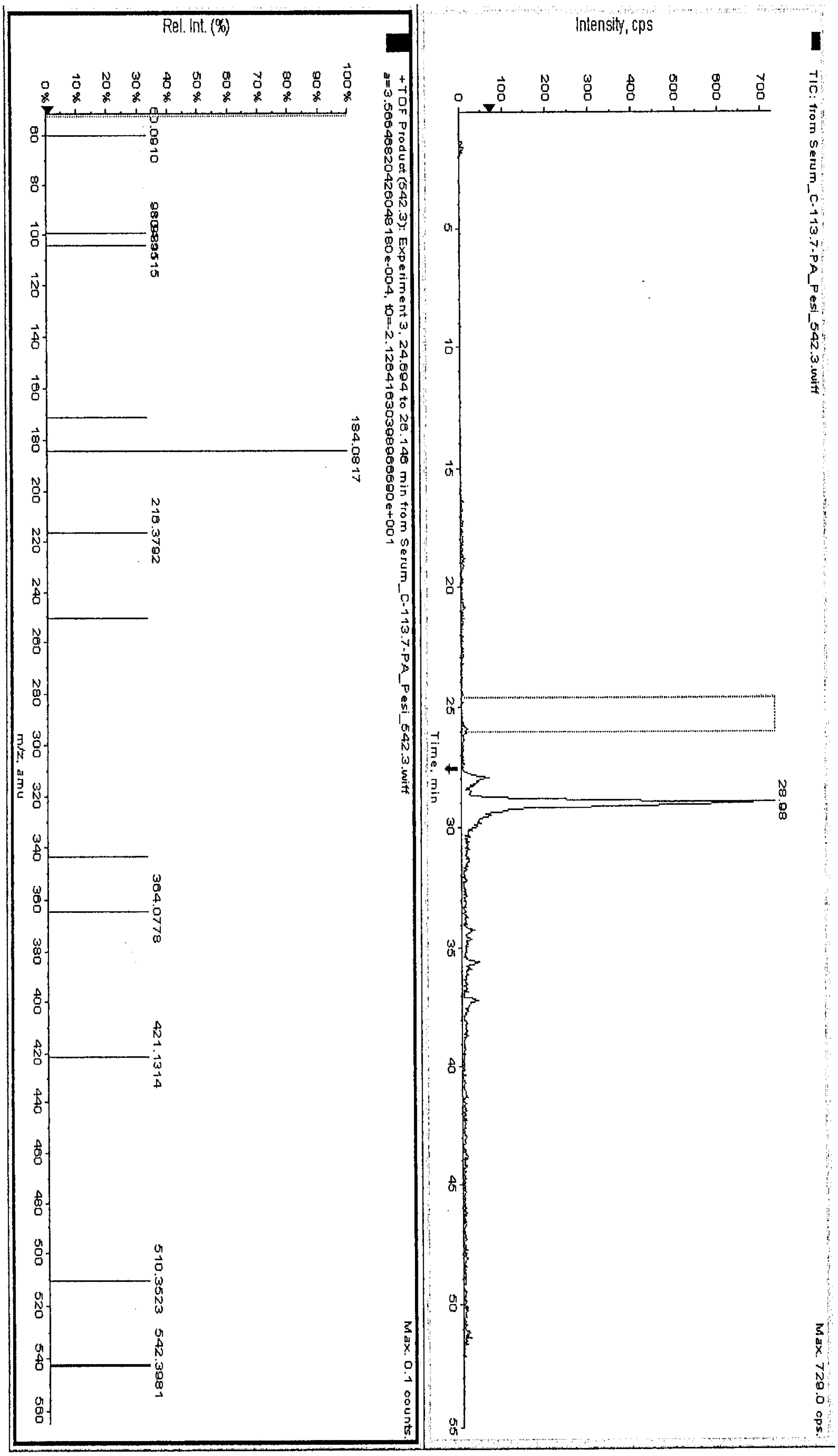

Figure 16 (cont.)

(c)

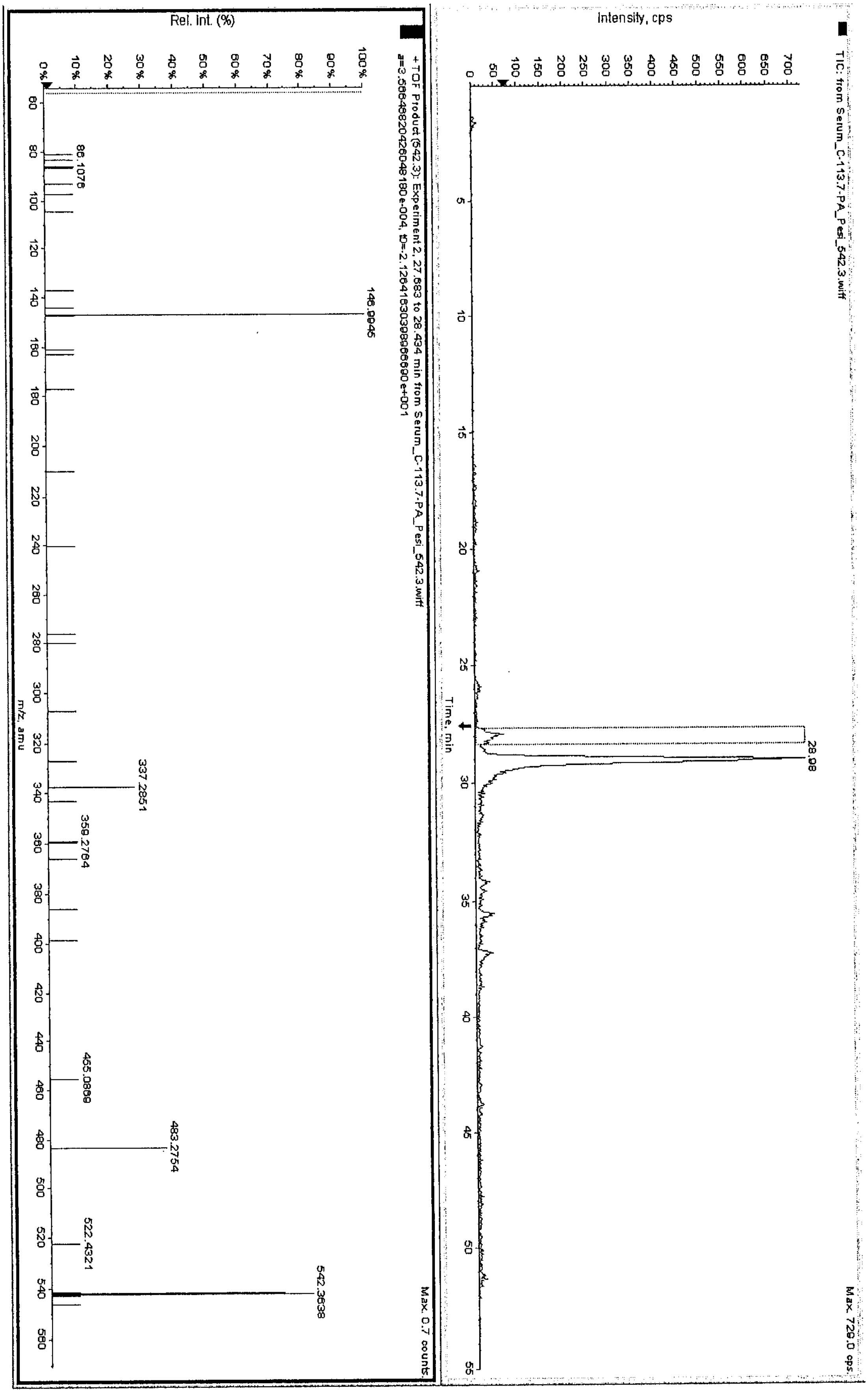

Figure 16 (cont.)

(d)

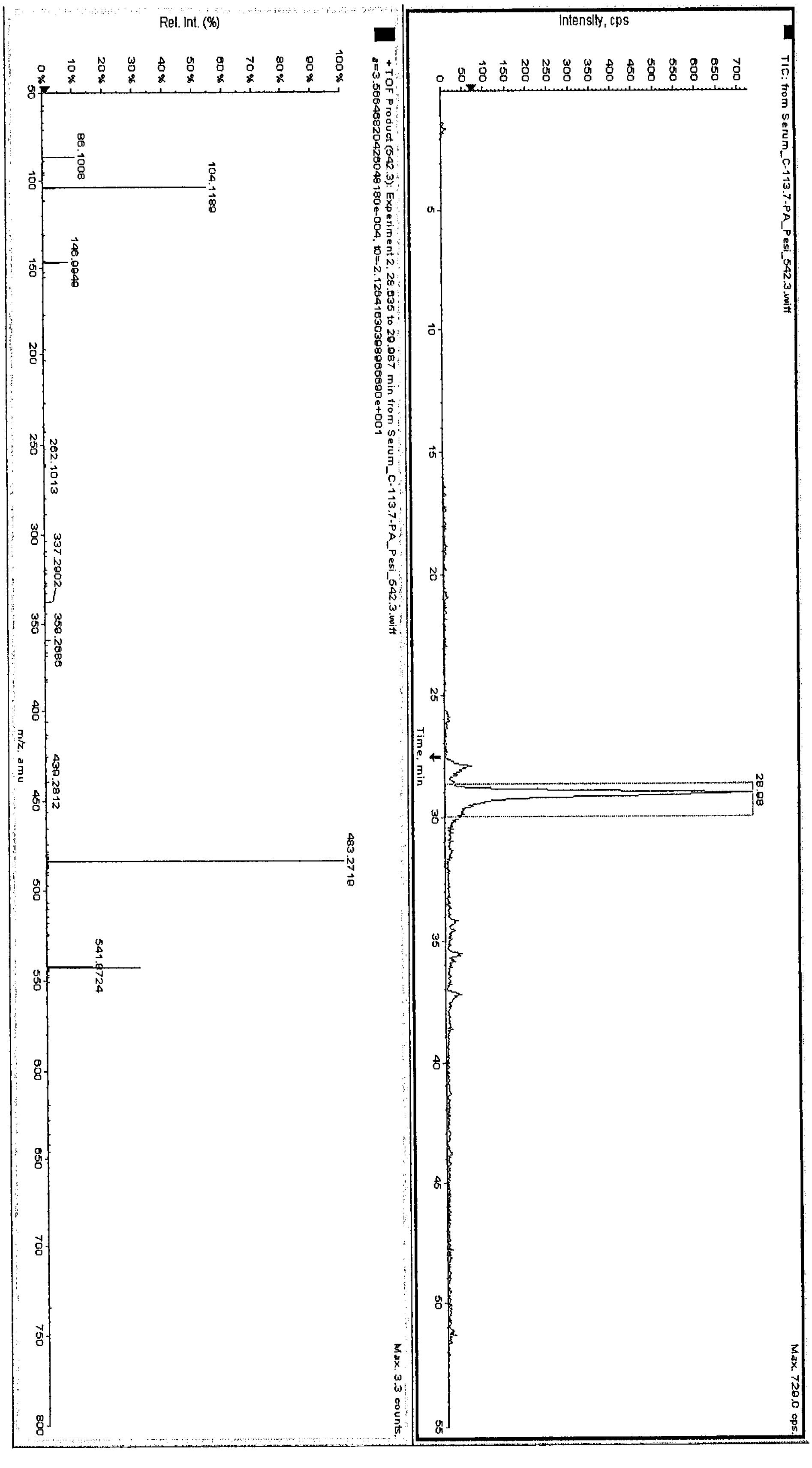

Figure 16 (cont.)

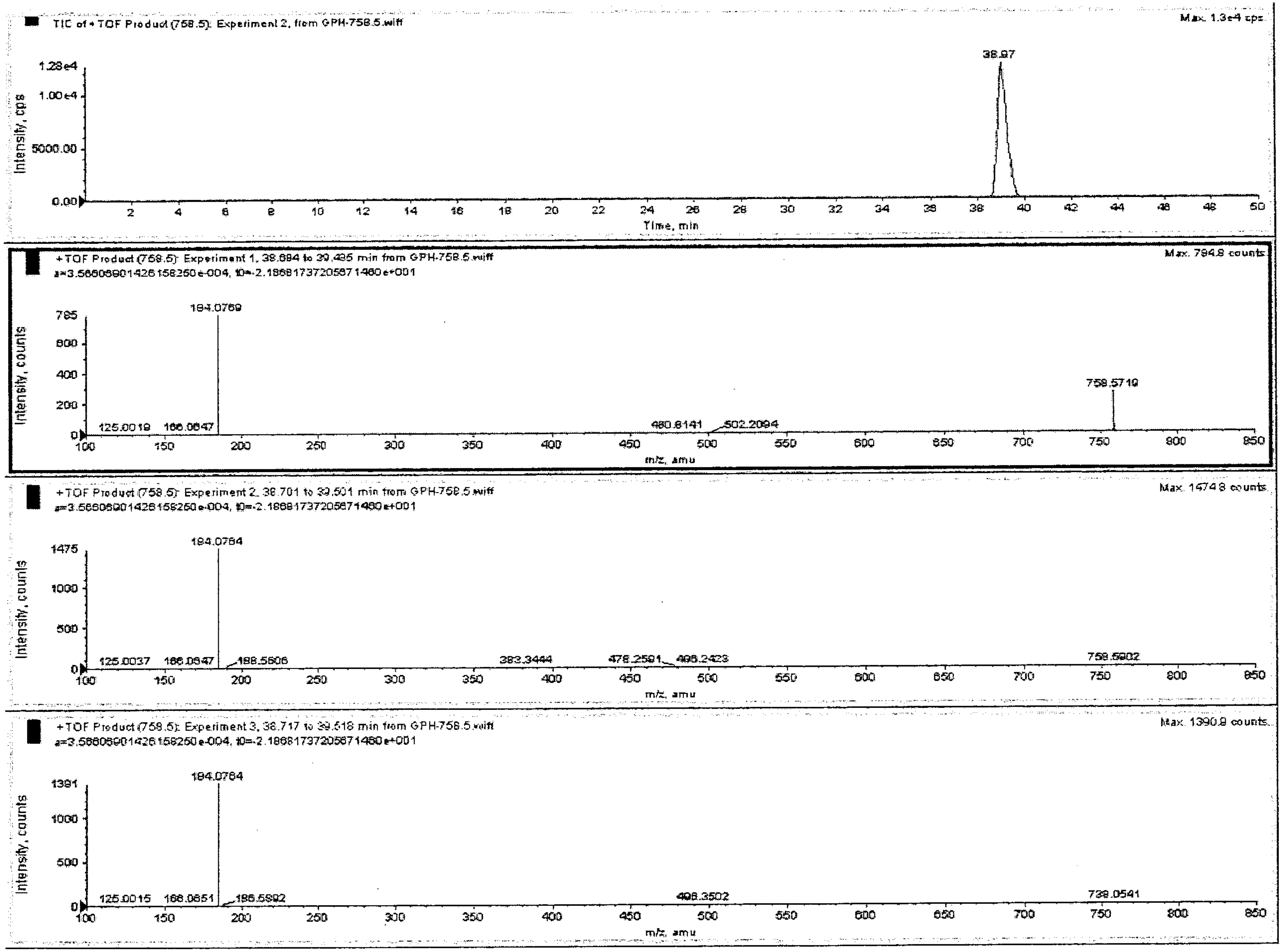
TIC of +TOF Product (758.5): Experiment 2, from GPH-758.5.wiff
Max. 1.3e4 cps
Intensity, cps
1.28e4
1.00e4
5000.00
0.00
38.97
2
4
6
8
10
12
14
16
18
20
22
24
26
28
30
32
34
36
38
40
42
44
46
48
50
Time, min
+TOF Product (758.5): Experiment 1, 38.684 to 39.495 min from GPH-758.5.wiff
a=3.56606901426158260e-004, t0=-2.18681737205871480e+001
Max. 794.8 counts
Intensity, counts
785
600
400
200
0
184.0769
125.0019
166.0647
480.8141
502.2094
758.5719
m/z, amu
+TOF Product (758.5): Experiment 2, 38.701 to 39.501 min from GPH-758.5.wiff
a=3.56606901426158260e-004, t0=-2.18681737205871480e+001
Max. 1474.8 counts
Intensity, counts
1475
1000
500
0
184.0764
125.0037
166.0647
188.5606
383.3444
478.2591
496.2423
758.5902
m/z, amu
+TOF Product (758.5): Experiment 3, 38.717 to 39.518 min from GPH-758.5.wiff
a=3.56606901426158260e-004, t0=-2.18681737205871480e+001
Max. 1390.9 counts
Intensity, counts
1391
1000
500
0
184.0764
125.0015
166.0651
186.5992
498.3502
738.0541
100
150
200
250
300
350
400
450
500
550
600
650
700
750
800
850
m/z, amu

Figure 17

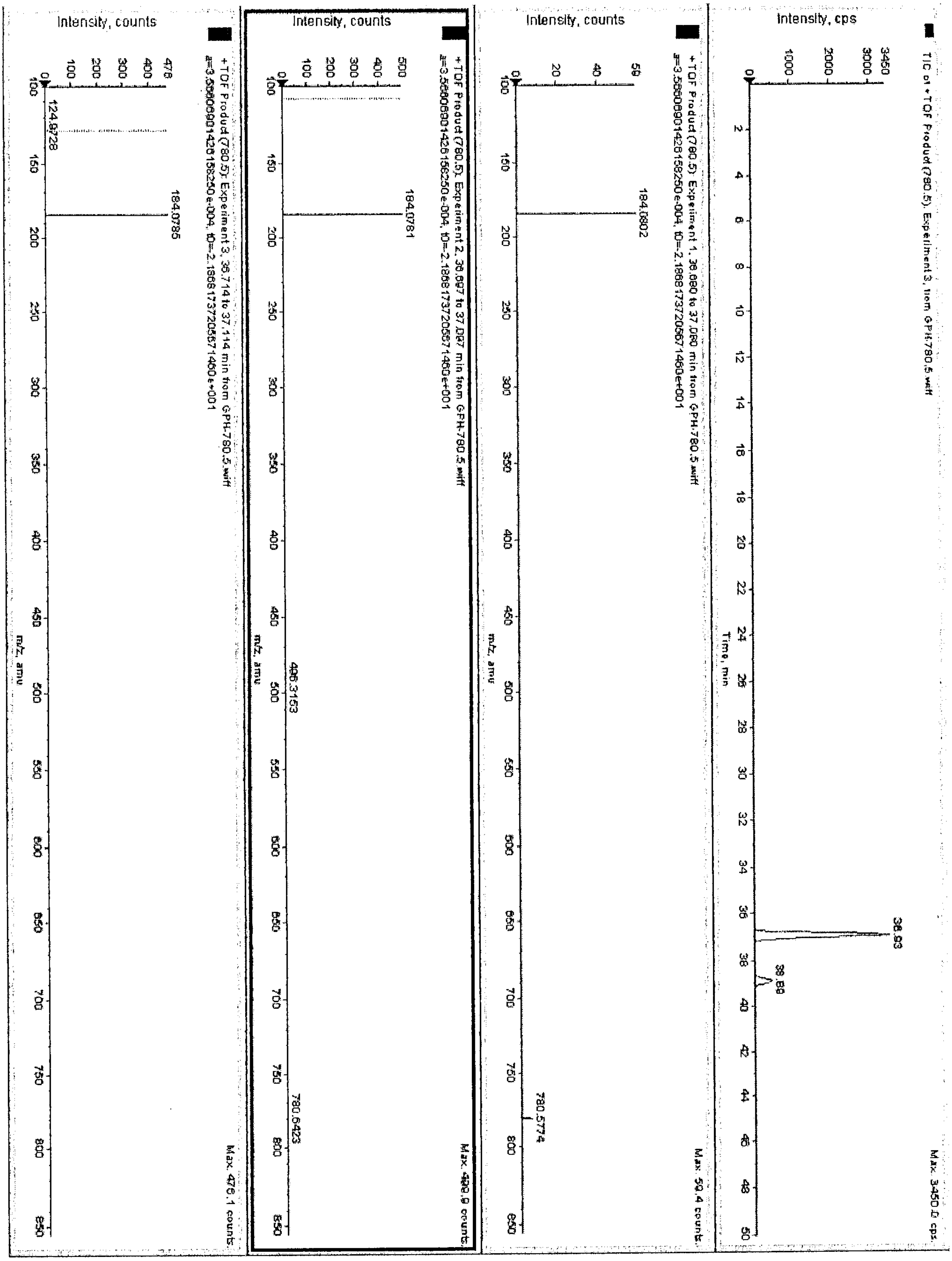
TIC of +TOF Product (780.5): Experiment 3, from GPH-780.5.wiff
Max. 3450.0 cps.
Intensity, cps
36.93
38.88
Time, min
+TOF Product (780.5): Experiment 1, 36.880 to 37.080 min from GPH-780.5.wiff
a=3.56606901426156250e-004, t0=2.18681737205671460e+001
Max. 59.4 counts.
Intensity, counts
184.0802
780.5774
m/z, amu
+TOF Product (780.5): Experiment 2, 36.697 to 37.097 min from GPH-780.5.wiff
a=3.56606901426156250e-004, t0=2.18681737205671460e+001
Max. 499.9 counts.
Intensity, counts
184.0781
496.3153
780.6423
m/z, amu
+TOF Product (780.5): Experiment 3, 36.714 to 37.114 min from GPH-780.5.wiff
a=3.56606901426156250e-004, t0=2.18681737205671460e+001
Max. 476.1 counts.
Intensity, counts
124.9728
184.0785
m/z, amu

Figure 18

(a)

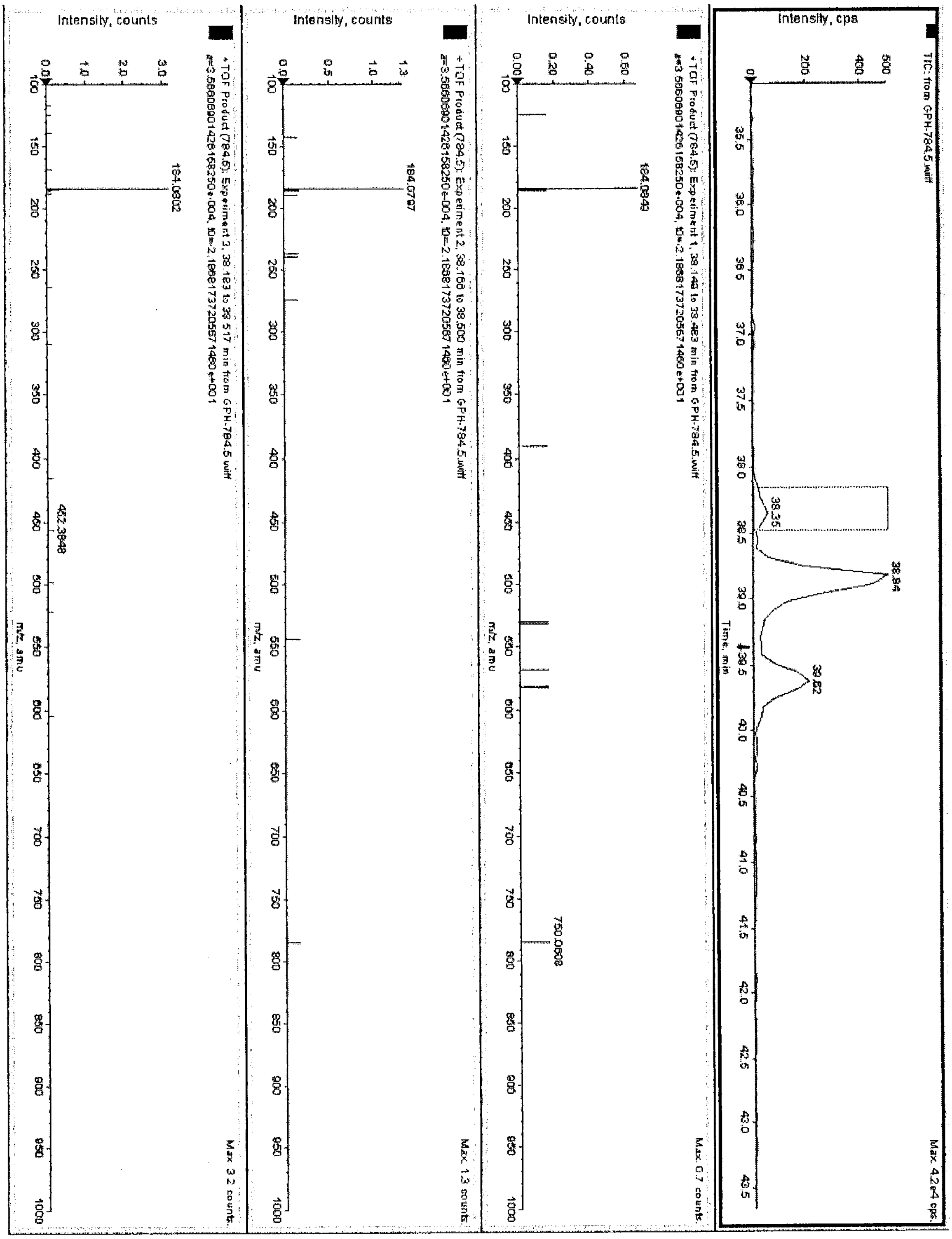
TIC: from GPH-784.5.wiff
Intensity, cps
Max. 4.2e4 cps.
38.35
38.84
39.62
Time, min
+TOF Product (784.5): Experiment 1, 38.149 to 38.483 min from GPH-784.5.wiff
Max. 0.7 counts.
Intensity, counts
184.0849
750.0808
m/z, amu
+TOF Product (784.5): Experiment 2, 38.166 to 38.500 min from GPH-784.5.wiff
Max. 1.3 counts.
Intensity, counts
184.0787
m/z, amu
+TOF Product (784.5): Experiment 3, 38.183 to 38.517 min from GPH-784.5.wiff
Max. 3.2 counts.
Intensity, counts
184.0802
452.3848
m/z, amu

Figure 19

(b)

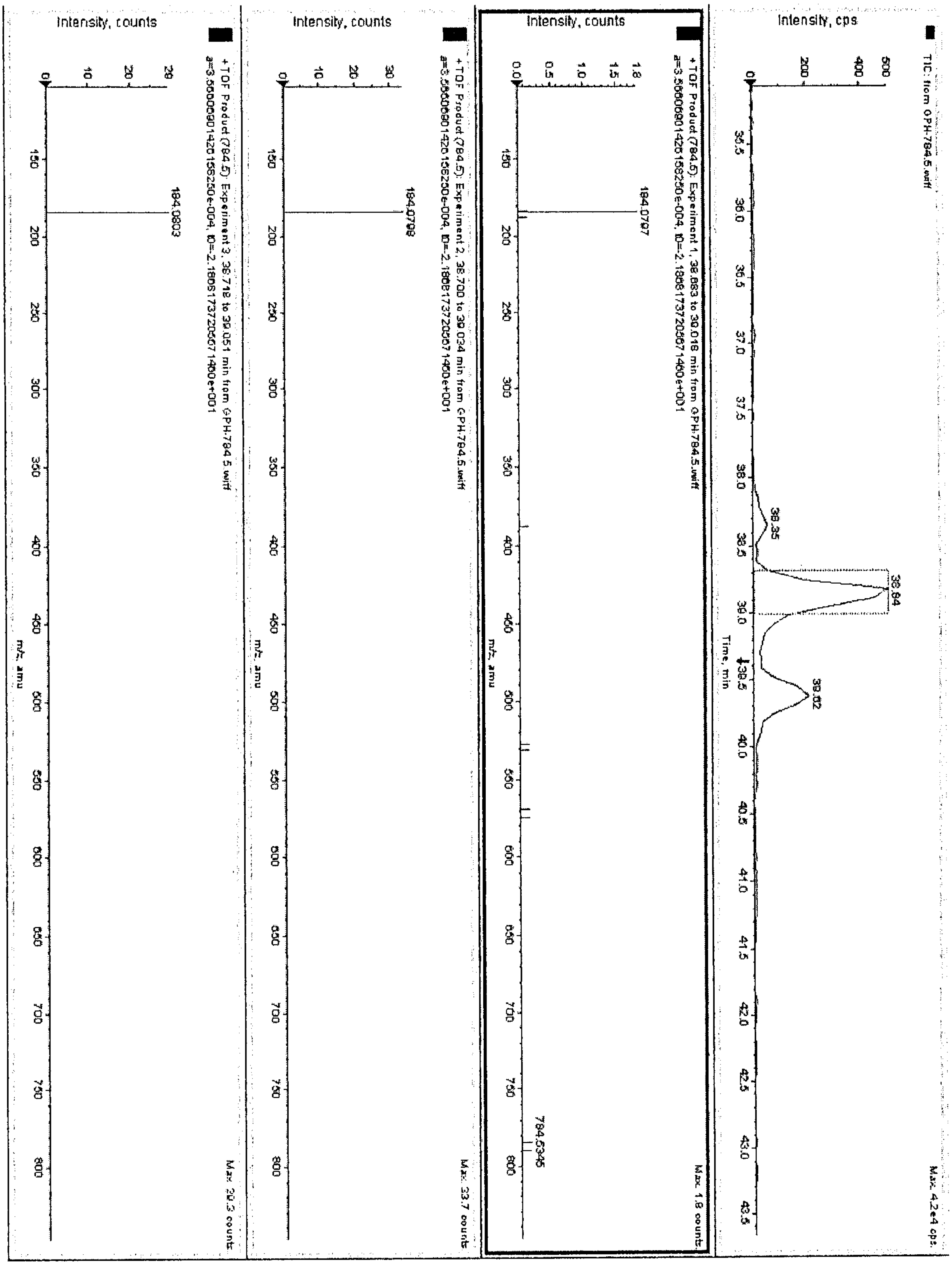

Figure 19 (Cont.)

(c)

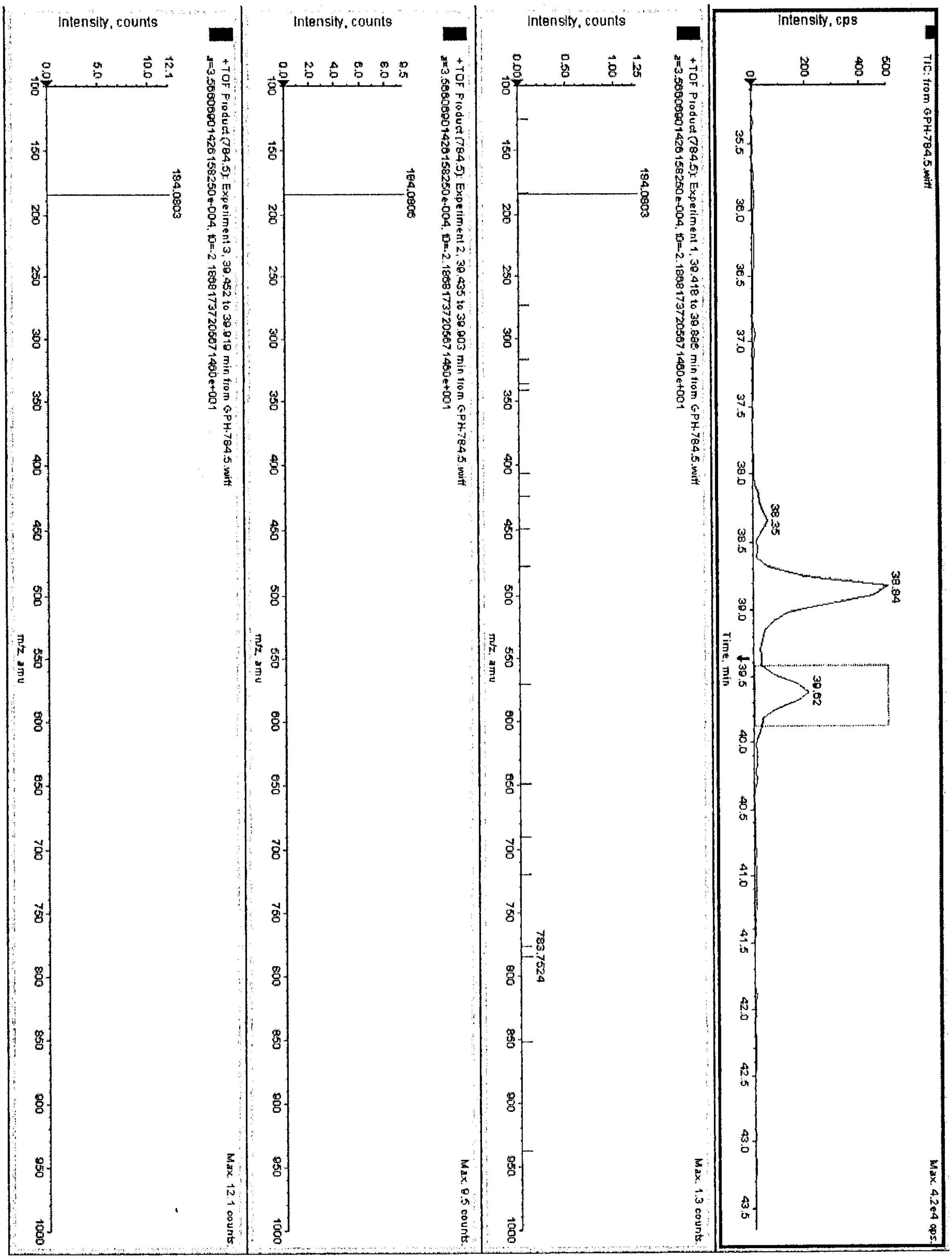

Figure 19 (Cont.)

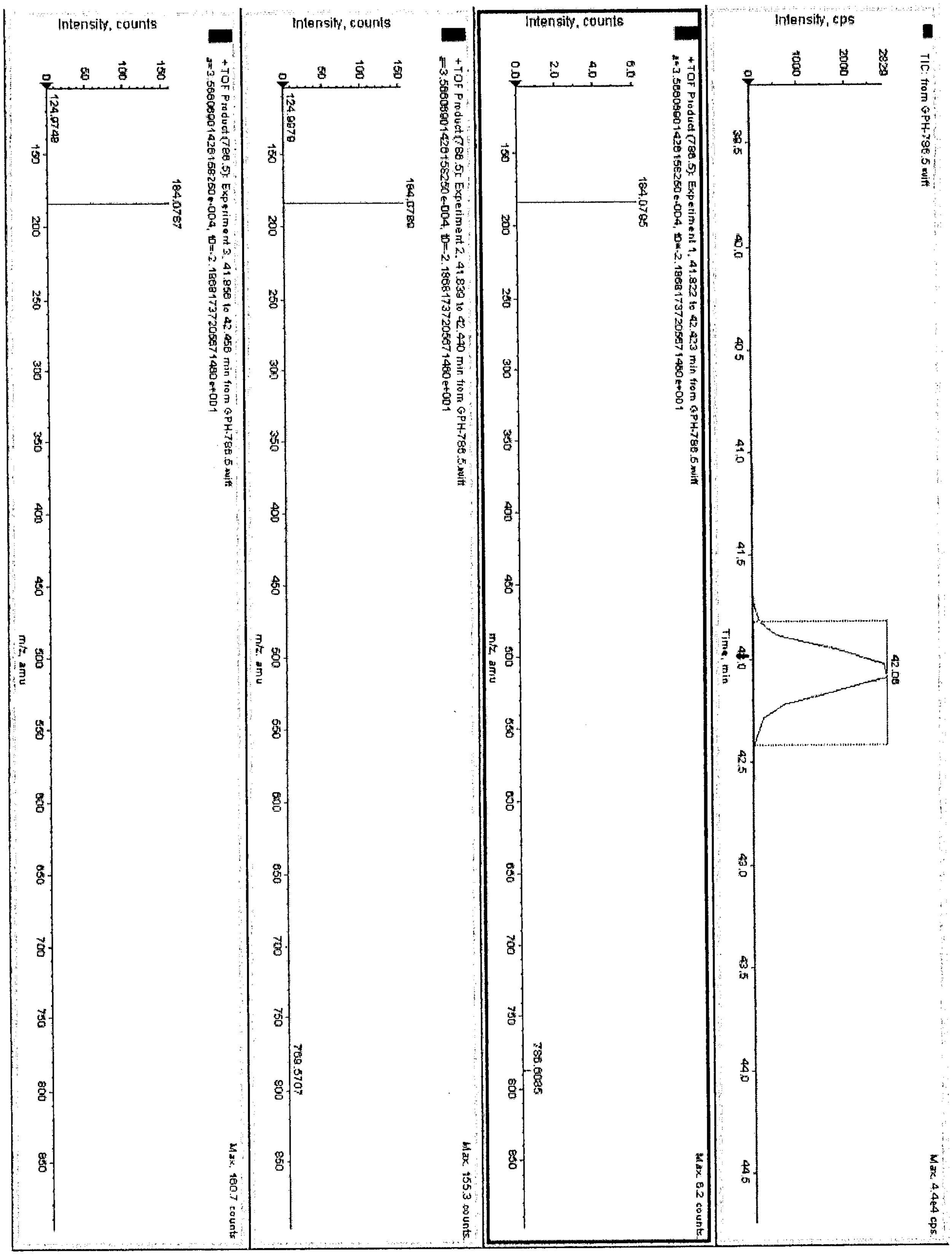
TIC: from GPH-786.5.wiff
Max. 4.4e4 cps.
Intensity, cps
2829
2000
1000
0
42.06
Time, min
39.5
40.0
40.5
41.0
41.5
42.0
42.5
43.0
43.5
44.0
44.5
+TOF Product (786.5): Experiment 1, 41.822 to 42.423 min from GPH-786.5.wiff
a=3.56608901426156250e-004, t0=-2.18681737205671460e+001
Max. 6.2 counts.
Intensity, counts
0.0
2.0
4.0
6.0
184.0785
786.6085
m/z, amu
+TOF Product (786.5): Experiment 2, 41.839 to 42.440 min from GPH-786.5.wiff
a=3.56608901426156250e-004, t0=-2.18681737205671460e+001
Max. 155.3 counts.
Intensity, counts
0
50
100
150
124.9878
184.0780
789.5707
m/z, amu
+TOF Product (786.5): Experiment 3, 41.856 to 42.456 min from GPH-786.5.wiff
a=3.56608901426156250e-004, t0=-2.18681737205671480e+001
Max. 160.7 counts
Intensity, counts
0
50
100
150
124.9748
184.0787
m/z, amu
150
200
250
300
350
400
450
500
550
600
650
700
750
800
850

Figure 20

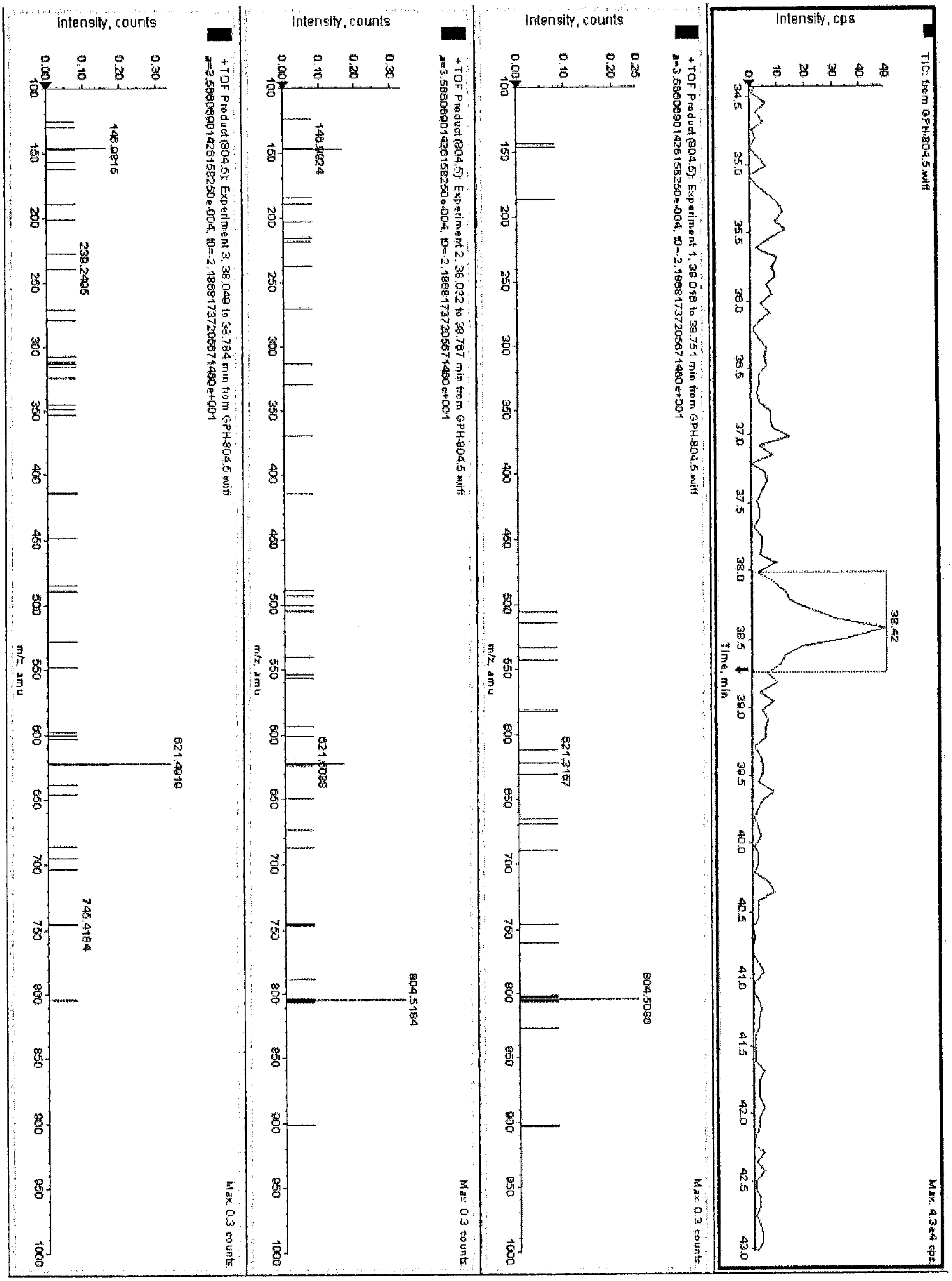
TIC: from GPH-804.5.wiff
Intensity, cps
Max. 4.3e4 cps.
38.42
Time, min
+TOF Product (804.5): Experiment 1, 38.018 to 38.751 min from GPH-804.5.wiff
a=3.58609014261582500e-004, t0=-2.18681737205671480e+001
Intensity, counts
Max. 0.3 counts.
621.3167
804.5086
m/z, amu
+TOF Product (804.5): Experiment 2, 38.032 to 38.767 min from GPH-804.5.wiff
a=3.58609014261582500e-004, t0=-2.18681737205671480e+001
Intensity, counts
Max. 0.3 counts.
146.9024
621.5088
804.5184
m/z, amu
+TOF Product (804.5): Experiment 3, 38.049 to 38.784 min from GPH-804.5.wiff
a=3.58609014261582500e-004, t0=-2.18681737205671480e+001
Intensity, counts
Max. 0.3 counts.
146.0815
238.2485
621.4919
745.4184
m/z, amu

Figure 21

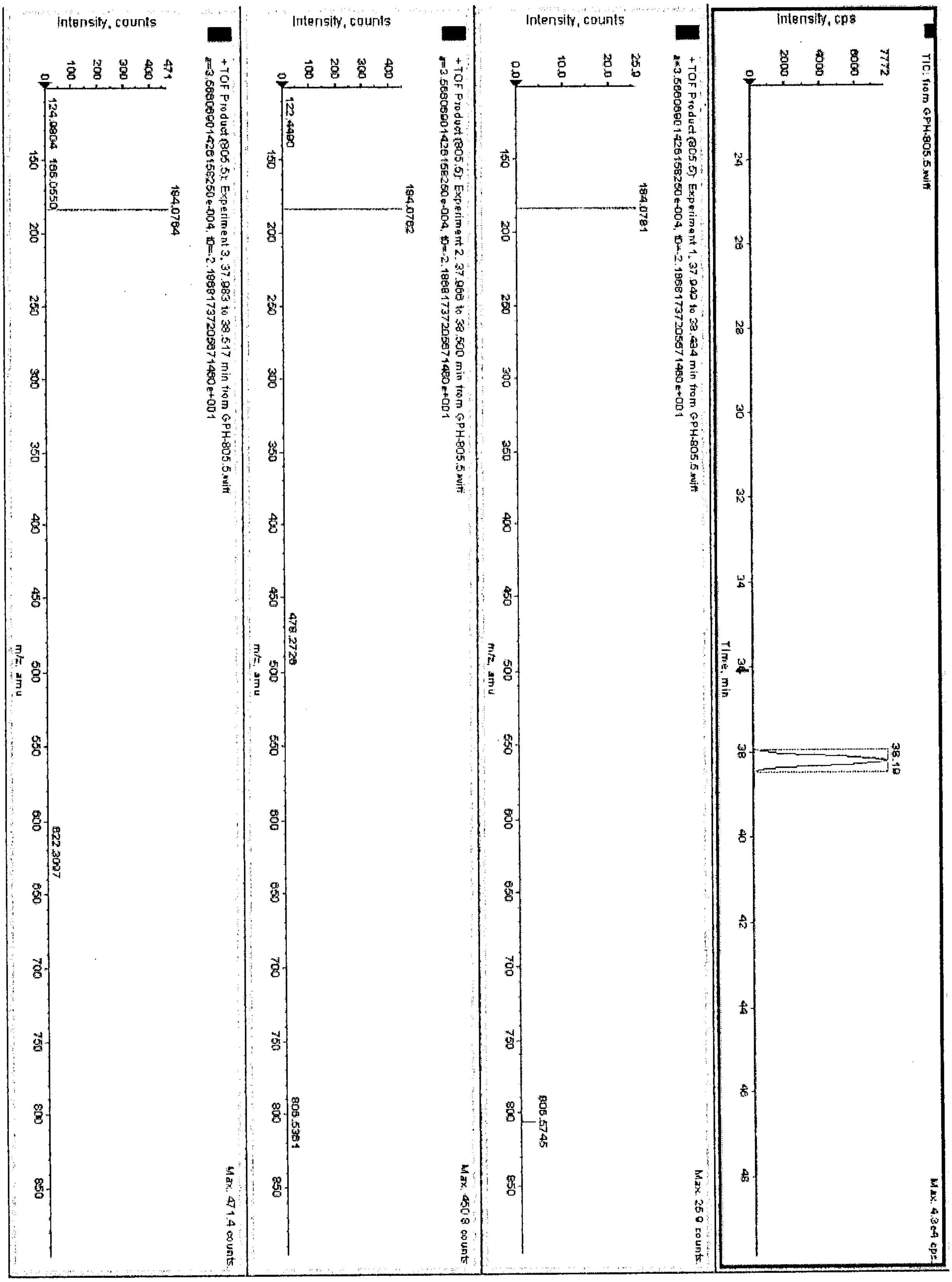
TIC: from GPH-805.5.wiff
Max. 4.3e4 cps
Intensity, cps
7772
6000
4000
2000
0
24
26
28
30
32
34
36
38
40
42
44
46
48
Time, min
38.10
+TOF Product (805.5): Experiment 1, 37.940 to 38.434 min from GPH-805.5.wiff
a=3.56606001426158250e-004, t0=-2.18681737205671480e+001
Max. 25.9 counts
Intensity, counts
25.9
20.0
10.0
0.0
184.0781
806.5745
m/z, amu
+TOF Product (805.5): Experiment 2, 37.966 to 38.500 min from GPH-805.5.wiff
a=3.56606001426158250e-004, t0=-2.18681737205671480e+001
Max. 450.8 counts
Intensity, counts
400
300
200
100
0
122.4480
184.0762
478.2728
806.5361
m/z, amu
+TOF Product (805.5): Experiment 3, 37.983 to 38.517 min from GPH-805.5.wiff
a=3.56606001426158250e-004, t0=-2.18681737205671480e+001
Max. 471.4 counts
Intensity, counts
471
400
300
200
100
0
124.0804
166.0550
184.0784
622.3097
150
200
250
300
350
400
450
500
550
600
650
700
750
800
850
m/z, amu

Figure 22

(a)

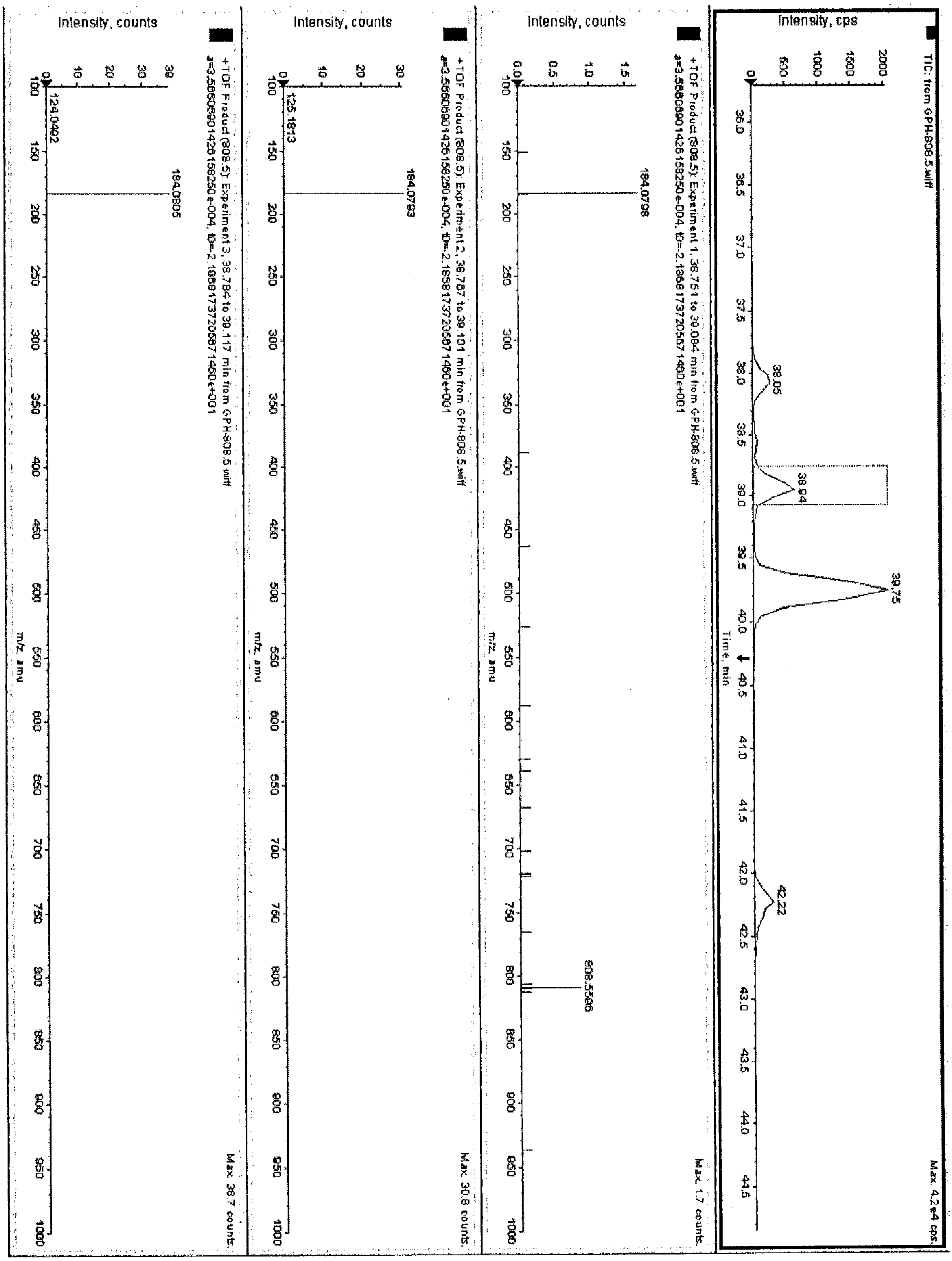
TIC: from GPH-806.5.wiff
Max. 4.2e4 cps.
Intensity, cps
0
500
1000
1500
2000
Time, min
36.0
36.5
37.0
37.5
38.0
38.5
39.0
39.5
40.0
40.5
41.0
41.5
42.0
42.5
43.0
43.5
44.0
44.5
38.05
38.94
39.75
42.22
+TOF Product (808.5): Experiment 1, 38.751 to 39.084 min from GPH-806.5.wiff
a=3.56606901426158250e-004, t0=-2.18681737205671460e+001
Max. 1.7 counts.
Intensity, counts
0.0
0.5
1.0
1.5
184.0798
808.5596
+TOF Product (808.5): Experiment 2, 38.787 to 39.101 min from GPH-806.5.wiff
a=3.56606901426158250e-004, t0=-2.18681737205671460e+001
Max. 30.8 counts.
Intensity, counts
0
10
20
30
125.1813
184.0763
+TOF Product (808.5): Experiment 3, 38.784 to 39.117 min from GPH-806.5.wiff
a=3.56606901426158250e-004, t0=-2.18681737205671460e+001
Max. 38.7 counts.
Intensity, counts
0
10
20
30
38
124.0402
184.0805
m/z, amu
100
150
200
250
300
350
400
450
500
550
600
650
700
750
800
850
900
950
1000

Figure 23

(b)

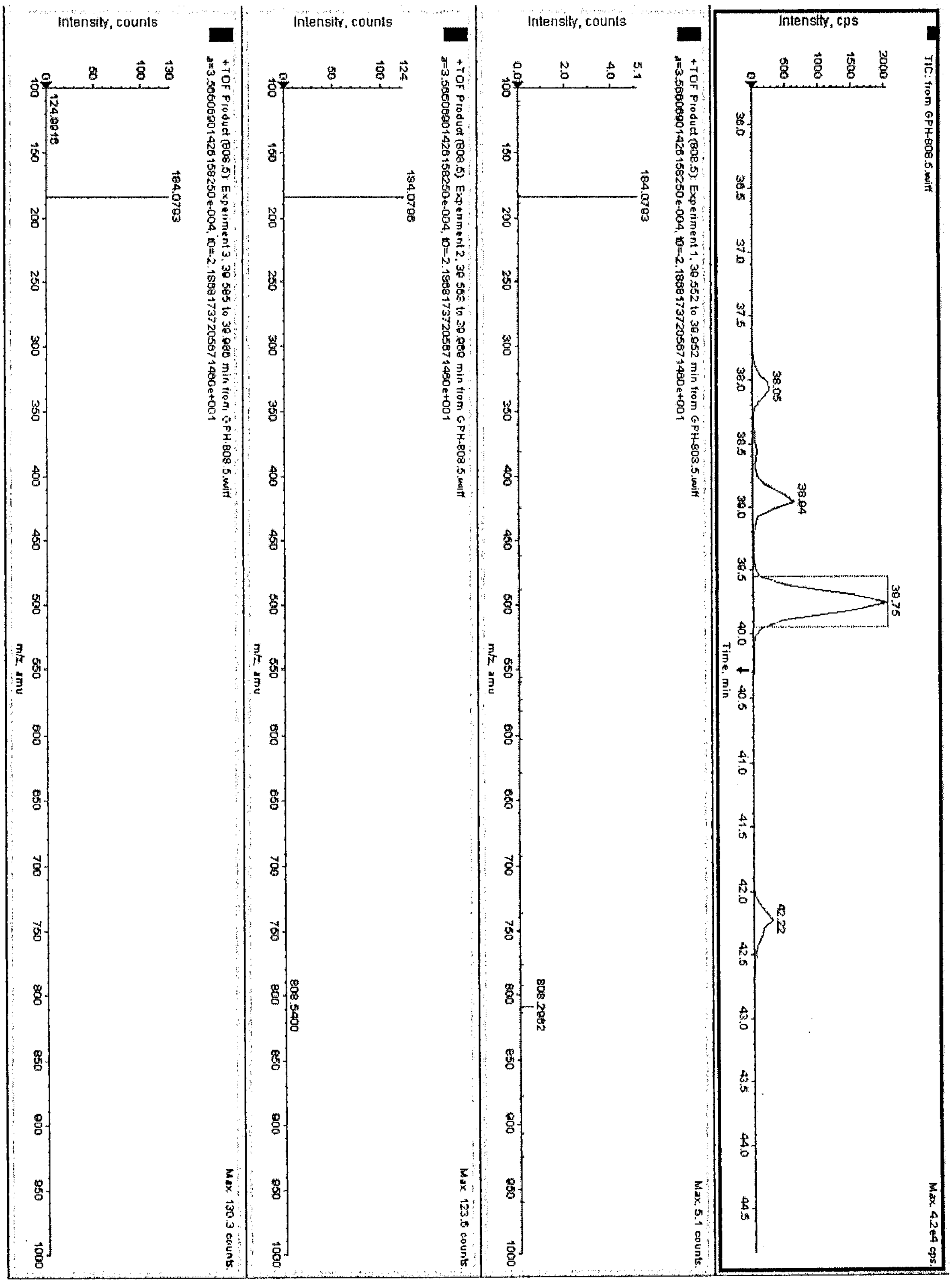

Figure 23 (Cont.)

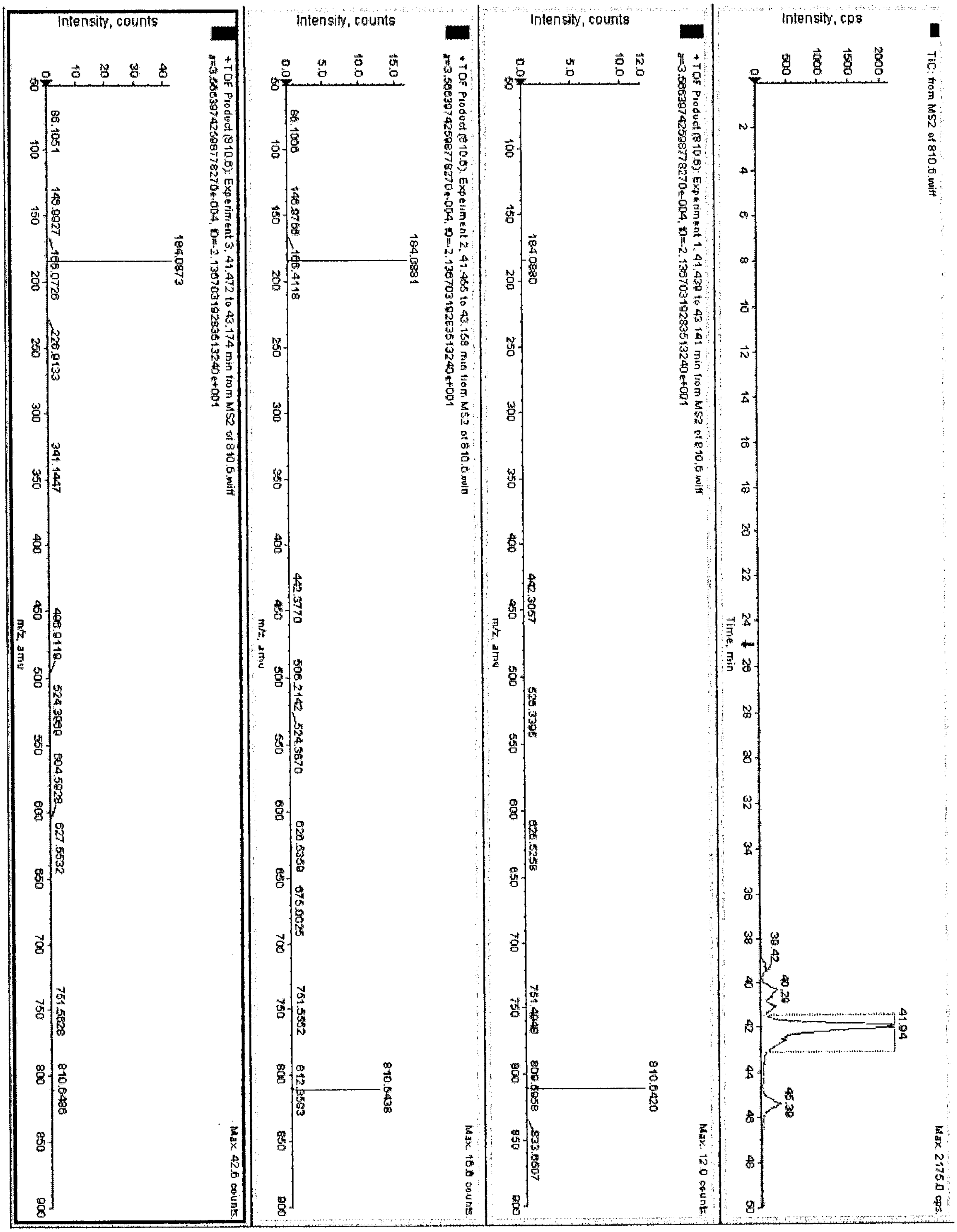
TIC: from MS2 of 810.6.wiff
Max. 2175.0 cps.
Intensity, cps
500
1000
1500
2000
Time, min
38.42
40.29
41.94
45.39
+TOF Product (810.6): Experiment 1, 41.439 to 43.141 min from MS2 of 810.6.wiff
a=3.56639742598778270e-004, t0=-2.13570319283513240e+001
Max. 12.0 counts.
Intensity, counts
184.0880
442.3057
526.3395
626.5258
751.4948
806.5659
810.6420
833.6507
m/z, amu
+TOF Product (810.6): Experiment 2, 41.465 to 43.158 min from MS2 of 810.6.wiff
a=3.56639742598778270e-004, t0=-2.13570319283513240e+001
Max. 16.8 counts.
Intensity, counts
86.1008
146.8766
166.4118
184.0881
442.3770
506.2142
524.3670
626.5359
675.0025
751.5562
810.6438
812.5593
m/z, amu
+TOF Product (810.6): Experiment 3, 41.472 to 43.174 min from MS2 of 810.6.wiff
a=3.56639742598778270e-004, t0=-2.13570319283513240e+001
Max. 42.6 counts.
Intensity, counts
86.1051
146.9027
166.0726
184.0873
226.9133
341.1447
496.9419
524.3869
604.5628
627.5532
751.5628
810.6486
m/z, amu

Figure 24

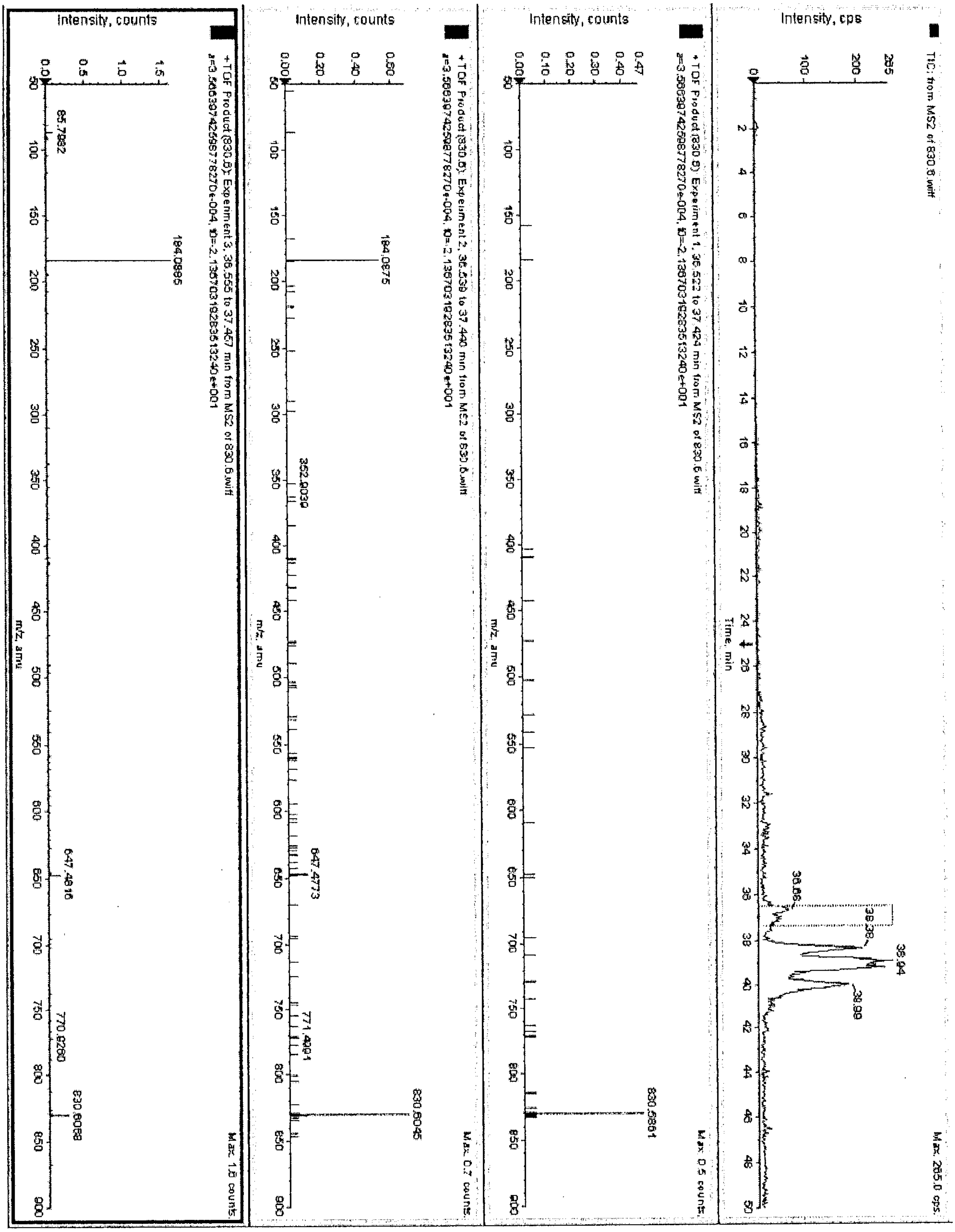
Intensity, cps
TIC: from MS2 of 830.6.wiff
Max. 265.0 cps.
0
100
200
265
2
4
6
8
10
12
14
16
18
20
22
24
26
28
30
32
34
36
38
40
42
44
46
48
50
Time, min
36.86
38.38
38.94
39.99
Intensity, counts
+TOF Product (830.6): Experiment 1, 36.522 to 37.424 min from MS2 of 830.6.wiff
a=3.56839742598778270e-004, t0=-2.13670316283513240e+001
Max. 0.5 counts.
0.00
0.10
0.20
0.30
0.40
0.47
830.5861
Intensity, counts
+TOF Product (830.6): Experiment 2, 36.539 to 37.440 min from MS2 of 830.6.wiff
a=3.56839742598778270e-004, t0=-2.13670316283513240e+001
Max. 0.7 counts.
0.00
0.20
0.40
0.60
184.0875
352.0030
647.4773
771.4091
830.6045
Intensity, counts
+TOF Product (830.6): Experiment 3, 36.555 to 37.457 min from MS2 of 830.6.wiff
a=3.56639742598778270e-004, t0=-2.13670316283513240e+001
Max. 1.6 counts.
0.0
0.5
1.0
1.5
85.7882
184.0885
647.4816
770.6260
830.6068
50
100
150
200
250
300
350
400
450
500
550
600
650
700
750
800
850
900
m/z, amu

Figure 25

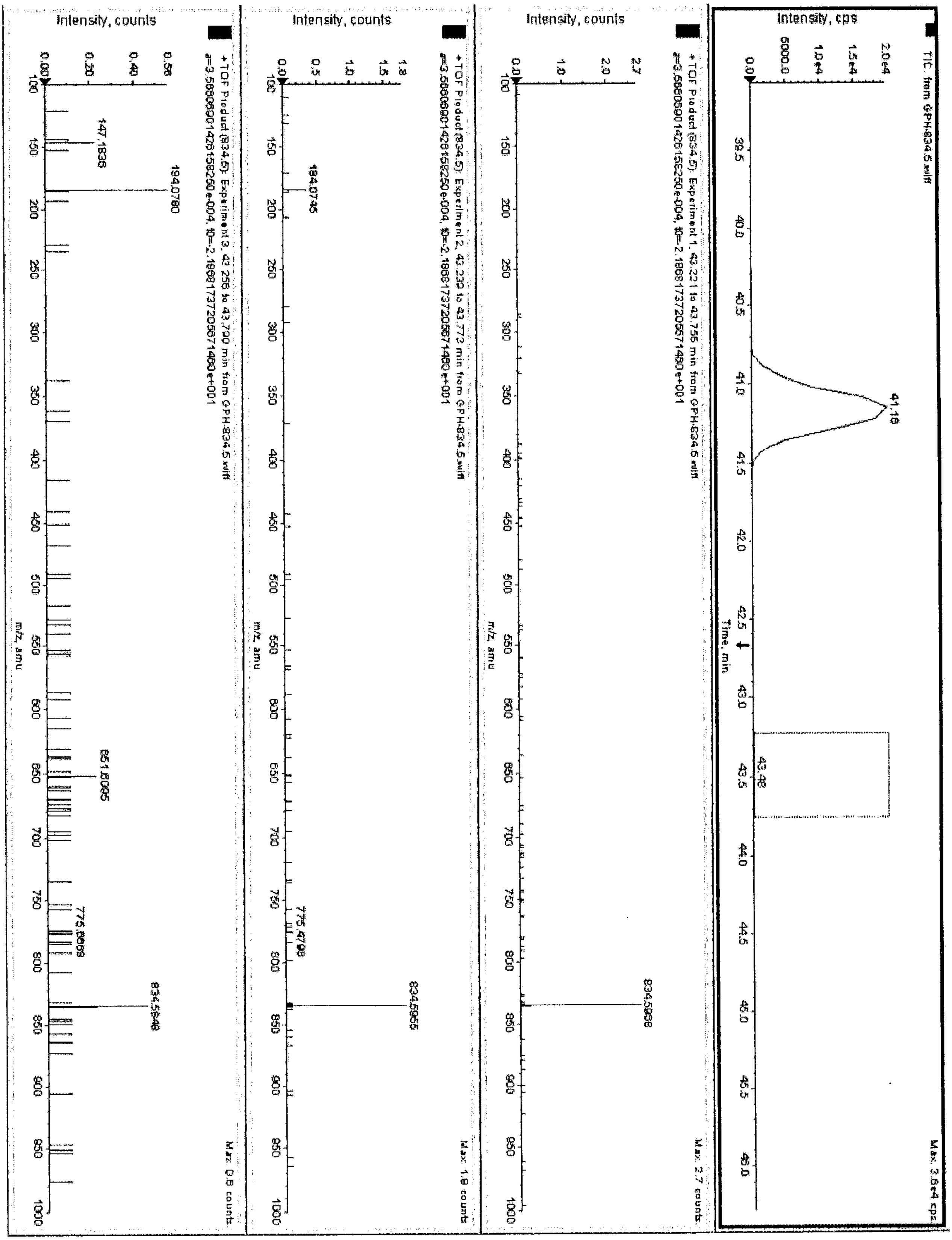
TIC from GPH-834.5.wiff
Max. 3.6e4 cps
Intensity, cps
2.0e4
1.5e4
1.0e4
5000.0
0.0
39.5
40.0
40.5
41.0
41.5
42.0
42.5
43.0
43.5
44.0
44.5
45.0
45.5
46.0
Time, min
41.16
43.48
+TOF Product (834.5): Experiment 1, 43.221 to 43.756 min from GPH-834.5.wiff
a=3.56605901426156250e-004, t0=2.18681737205671480e+001
Max. 2.7 counts
Intensity, counts
2.7
2.0
1.0
0.0
834.5988
+TOF Product (834.5): Experiment 2, 43.239 to 43.773 min from GPH-834.5.wiff
a=3.56605901426156250e-004, t0=2.18681737205671480e+001
Max. 1.8 counts
Intensity, counts
1.8
1.5
1.0
0.5
0.0
184.0745
775.4798
834.5965
+TOF Product (834.5): Experiment 3, 43.256 to 43.790 min from GPH-834.5.wiff
a=3.56605901426156250e-004, t0=2.18681737205671480e+001
Max. 0.6 counts
Intensity, counts
0.58
0.40
0.20
0.00
147.1836
184.0780
651.6095
775.5668
834.5648
m/z, amu
100
150
200
250
300
350
400
450
500
550
600
650
700
750
800
850
900
950
1000

Figure 26

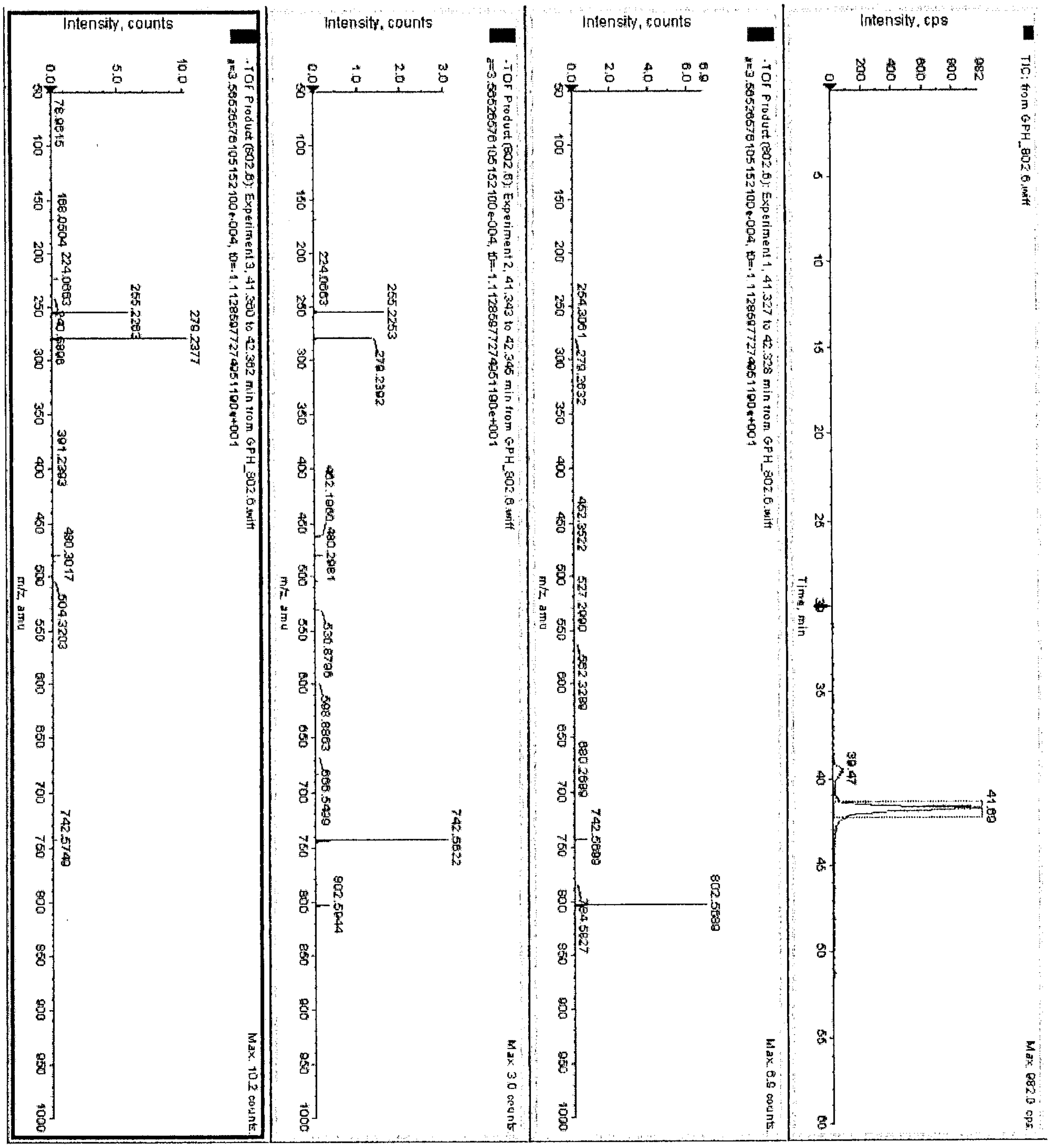
TIC: from GPH_802.6.wiff
Max. 982.0 cps.
Intensity, cps
982
800
600
400
200
0
Time, min
39.47
41.69
.TOF Product (802.6): Experiment 1, 41.327 to 42.328 min from GPH_802.6.wiff
a=3.58526576105152100e+004, t0=-1.11285977274051190e+001
Max. 6.9 counts.
Intensity, counts
254.3061
279.2632
462.3522
527.2990
562.3288
680.2689
742.5689
802.5689
784.5627
.TOF Product (802.6): Experiment 2, 41.343 to 42.346 min from GPH_802.6.wiff
a=3.58526576105152100e+004, t0=-1.11285977274051190e+001
Max. 3.0 counts
Intensity, counts
224.0663
255.2253
279.2392
402.1980
480.2981
530.8795
598.8863
686.5499
742.5622
802.5644
.TOF Product (802.6): Experiment 3, 41.360 to 42.362 min from GPH_802.6.wiff
a=3.58526576105152100e+004, t0=-1.11285977274051190e+001
Max. 10.2 counts.
Intensity, counts
78.9615
166.0504
224.0663
255.2263
240.6806
279.2377
391.2293
480.3017
504.3203
742.5749
m/z, amu

Figure 27

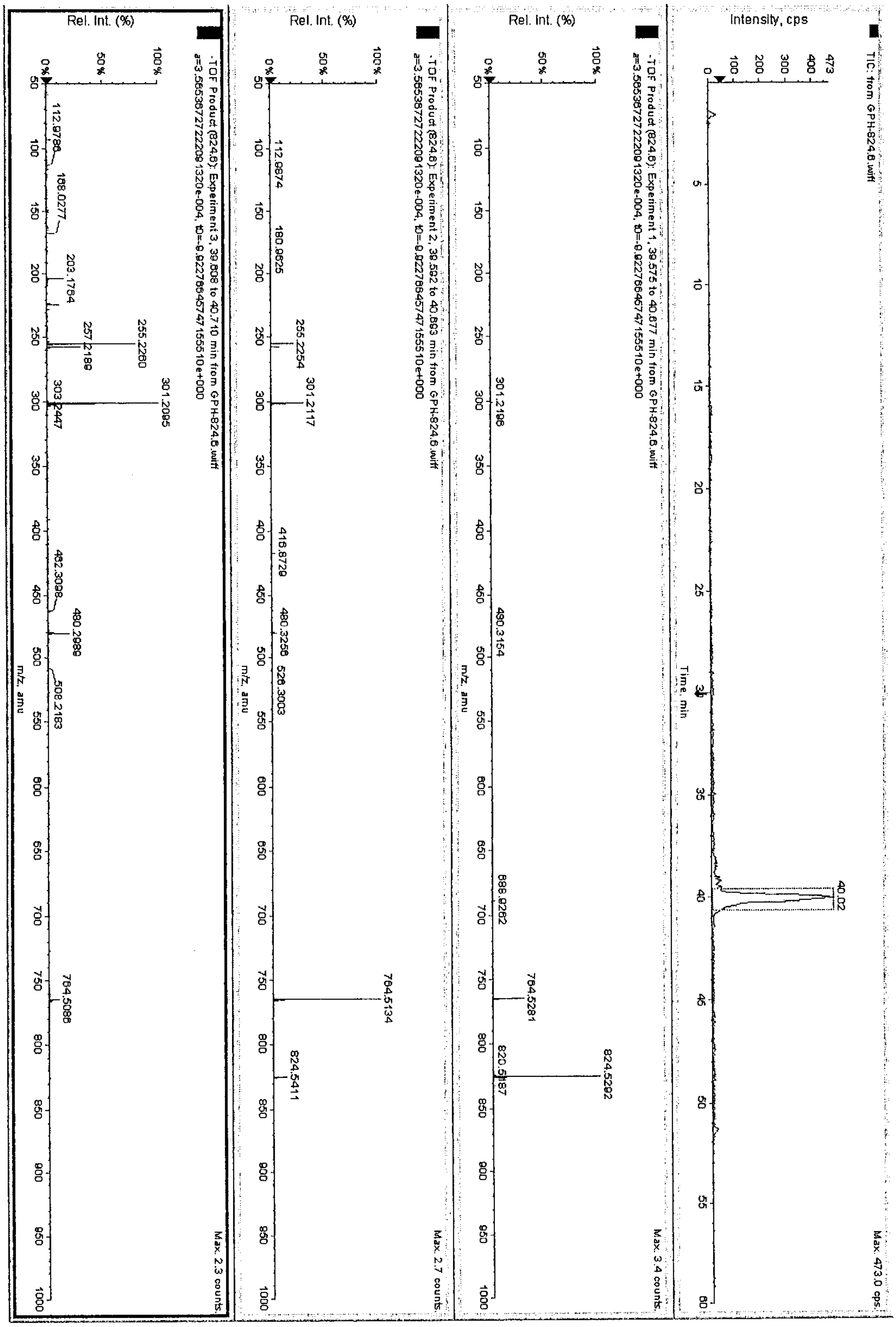
TIC: from GPH-824.6.wiff
Max. 473.0 cps.
Intensity, cps
473
400
300
200
100
0
40.02
Time, min
0
5
10
15
20
25
30
35
40
45
50
55
60
-TOF Product (824.6): Experiment 1, 39.575 to 40.677 min from GPH-824.6.wiff
a=3.56538727222091320e-004, t0=-9.82278645747155510e+000
Max. 3.4 counts.
Rel. Int. (%)
100%
50%
0%
824.5292
820.5187
764.5281
688.8282
490.3154
301.2196
m/z, amu
-TOF Product (824.6): Experiment 2, 39.592 to 40.693 min from GPH-824.6.wiff
a=3.56538727222091320e-004, t0=-9.82278645747155510e+000
Max. 2.7 counts.
Rel. Int. (%)
100%
50%
0%
764.5134
824.5411
528.3003
480.3256
416.8729
301.2117
255.2254
180.9625
112.8874
m/z, amu
-TOF Product (824.6): Experiment 3, 39.608 to 40.710 min from GPH-824.6.wiff
a=3.56538727222091320e-004, t0=-9.82278645747155510e+000
Max. 2.3 counts.
Rel. Int. (%)
100%
50%
0%
301.2095
303.2447
255.2280
257.2189
203.1784
188.0277
112.9788
452.3098
480.2988
508.2183
764.5088
m/z, amu
50
100
150
200
250
300
350
400
450
500
550
600
650
700
750
800
850
900
950
1000

Figure 28

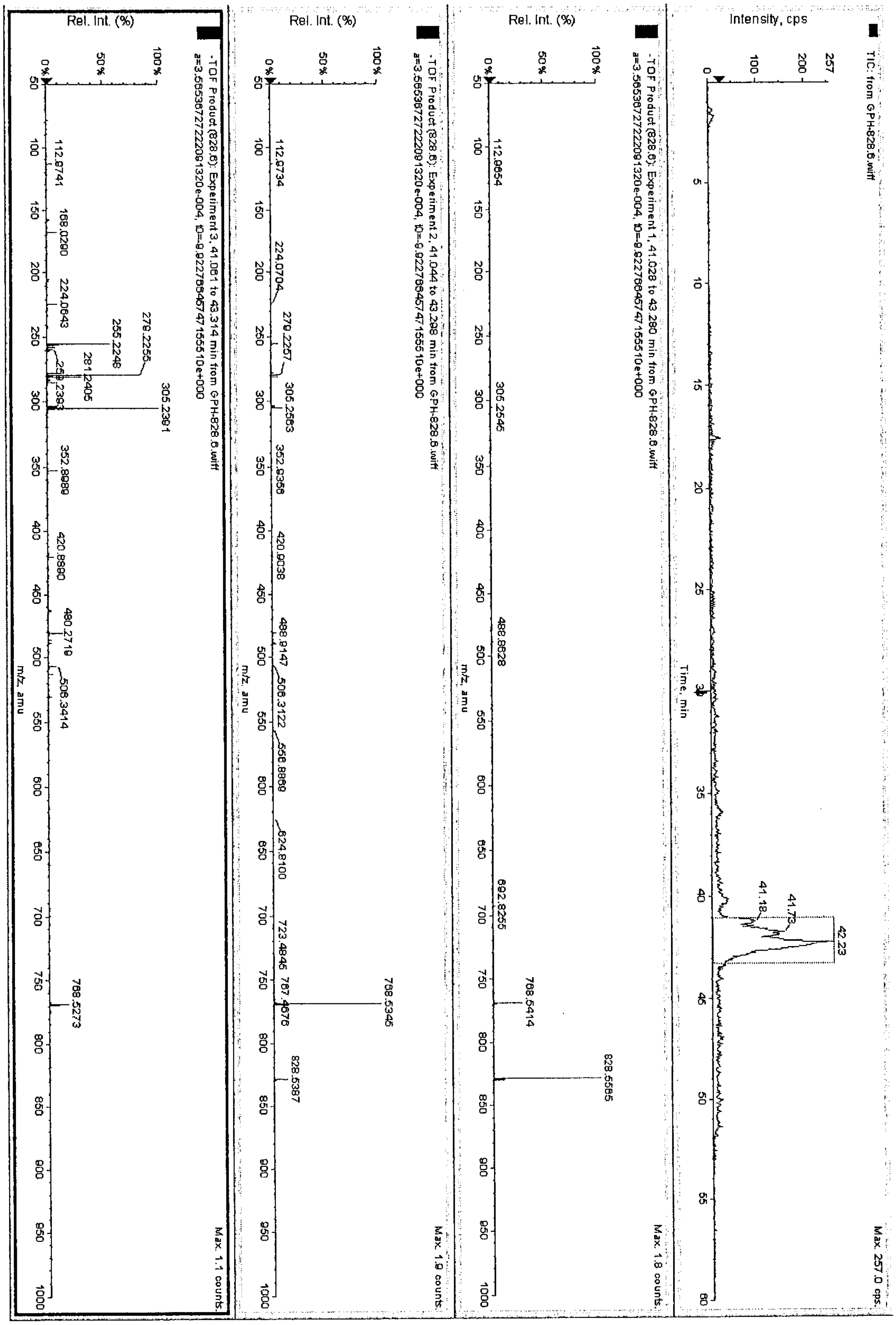
TIC: from GPH-828.6.wiff
Max. 257.0 cps.
Intensity, cps
257
200
100
0
Time, min
41.18
41.73
42.23
-TOF Product (828.6): Experiment 1, 41.028 to 43.280 min from GPH-828.6.wiff
a=3.56536727222091320e-004, t0=9.92276645747155510e+000
Max. 1.8 counts.
Rel. Int. (%)
112.8654
305.2546
488.8628
692.8255
768.5414
828.5585
-TOF Product (828.6): Experiment 2, 41.044 to 43.298 min from GPH-828.6.wiff
a=3.56536727222091320e-004, t0=9.92276645747155510e+000
Max. 1.9 counts.
112.8734
224.0704
279.2257
305.2563
352.9356
420.9038
488.9147
506.3122
556.8869
624.8100
723.4846
767.4676
768.5345
828.5387
-TOF Product (828.6): Experiment 3, 41.061 to 43.314 min from GPH-828.6.wiff
a=3.56536727222091320e-004, t0=9.92276645747155510e+000
Max. 1.1 counts.
112.8741
168.0290
224.0643
255.2246
279.2255
281.2405
297.2393
305.2391
352.8989
420.8880
480.2719
506.3414
768.5273
m/z, amu
100%
50%
0%

Figure 29

(a)

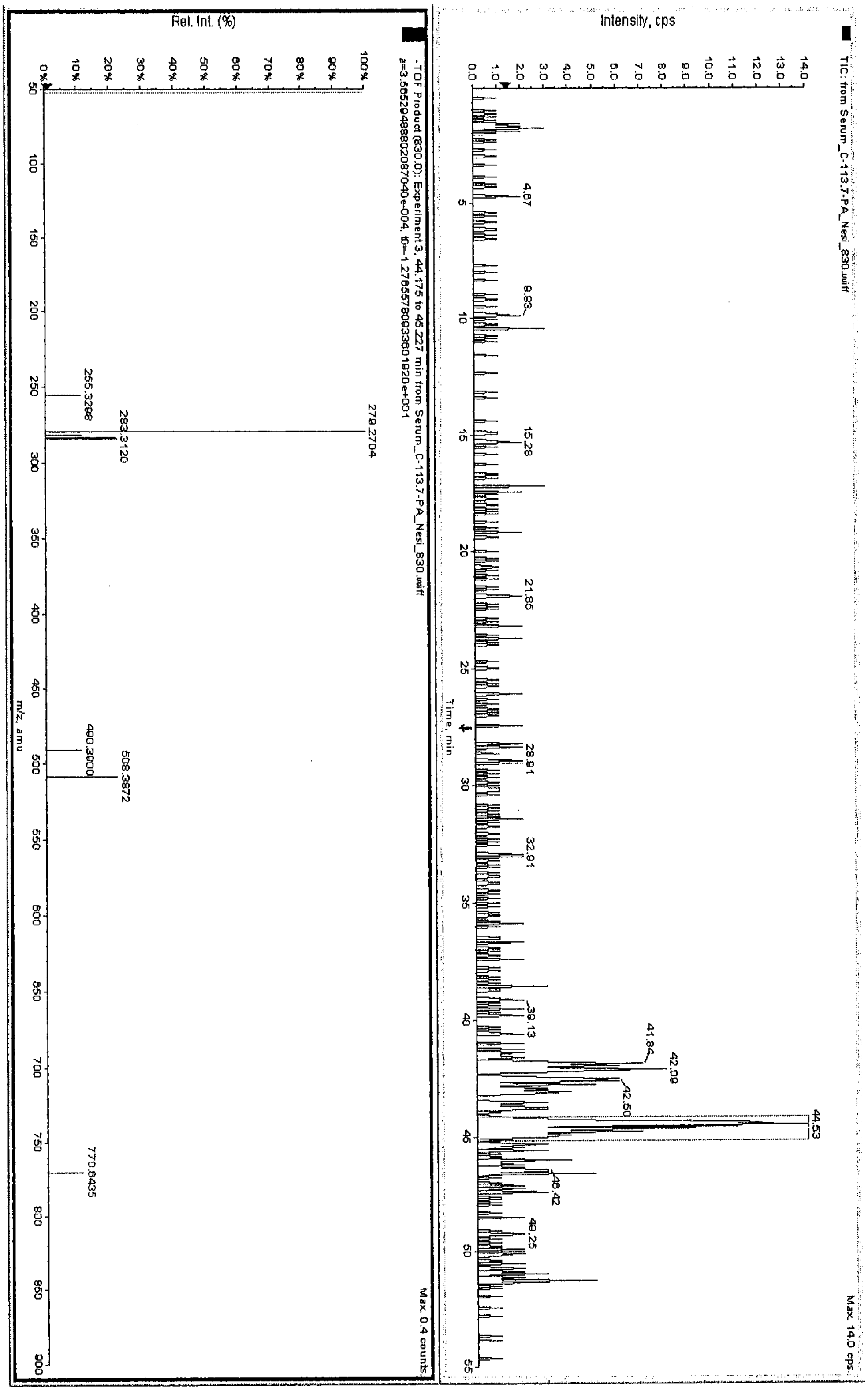
TIC: from Serum_C-113.7-PA_Nesi_830.wiff
Intensity, cps
Max. 14.0 cps
0.0
1.0
2.0
3.0
4.0
5.0
6.0
7.0
8.0
9.0
10.0
11.0
12.0
13.0
14.0
4.87
9.83
15.28
21.85
28.81
32.81
39.13
41.84
42.09
42.50
44.53
46.42
49.25
5
10
15
20
25
30
35
40
45
50
55
Time, min
-TOF Product (830.0): Experiment 3, 44.175 to 45.227 min from Serum_C-113.7-PA_Nesi_830.wiff
a=3.5652948802087040e-004, t0=-1.27655780633601820e+001
Max. 0.4 counts.
Rel. Int. (%)
0%
10%
20%
30%
40%
50%
60%
70%
80%
90%
100%
255.3206
279.2704
283.3120
490.3800
508.3872
770.6435
50
100
150
200
250
300
350
400
450
500
550
600
650
700
750
800
850
900
m/z, amu

Figure 30

(b)

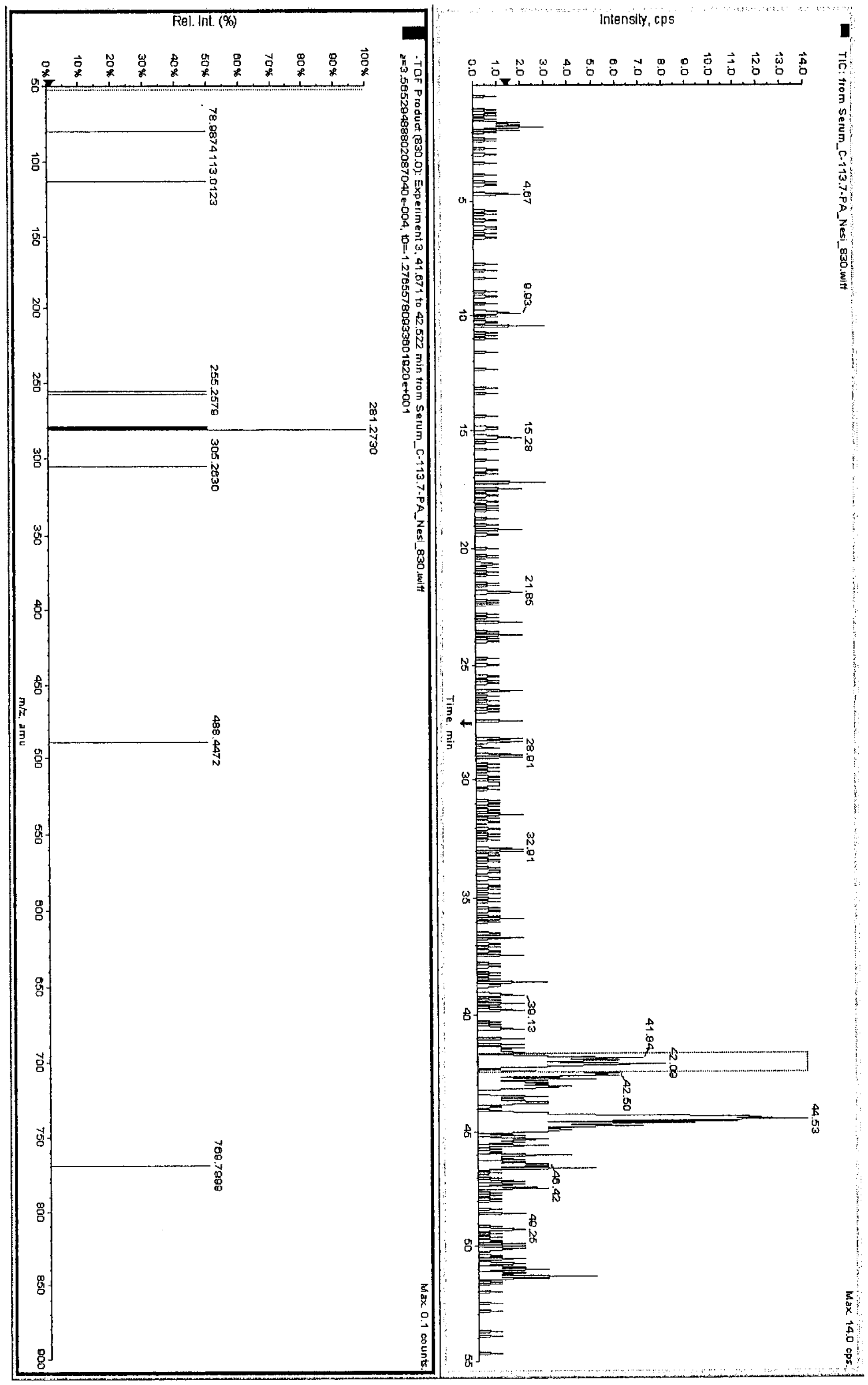

Figure 30 (cont.)

(a)

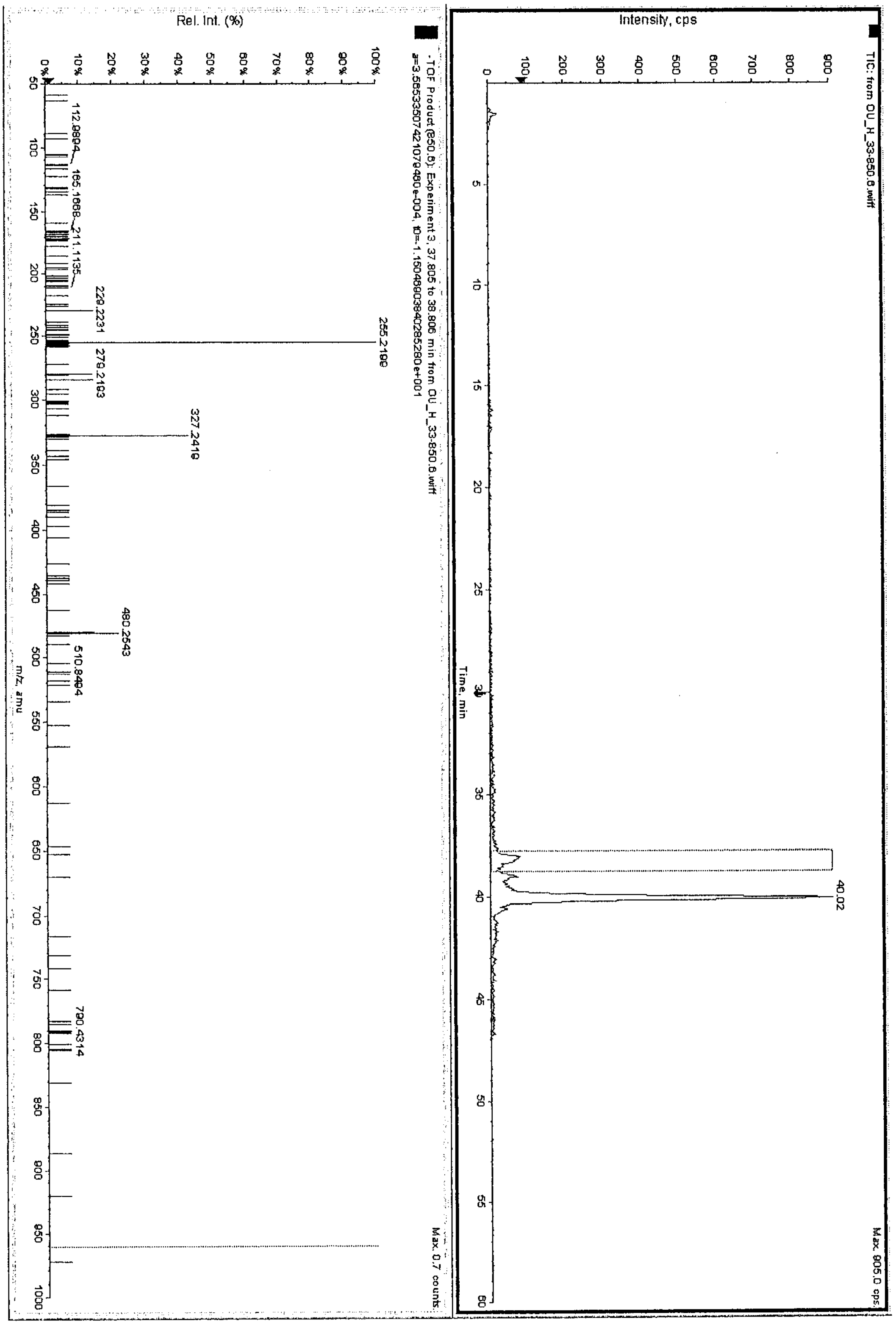
Rel. Int. (%)
-TOF Product (850.6): Experiment 3, 37.805 to 38.806 min from OU_H_33-850.6.wiff
a=3.56533507421079460e-004, t0=-1.15048803840285280e+001
Max. 0.7 counts.
0%
10%
20%
30%
40%
50%
60%
70%
80%
90%
100%
112.0804
165.1668
211.1135
229.2231
255.2199
279.2163
327.2419
480.2543
510.8404
790.4314
50
100
150
200
250
300
350
400
450
500
550
600
650
700
750
800
850
900
950
1000
m/z, amu
Intensity, cps
TIC: from OU_H_33-850.6.wiff
Max. 905.0 cps.
0
100
200
300
400
500
600
700
800
900
40.02
0
5
10
15
20
25
30
35
40
45
50
55
60
Time, min

Figure 31

(b)

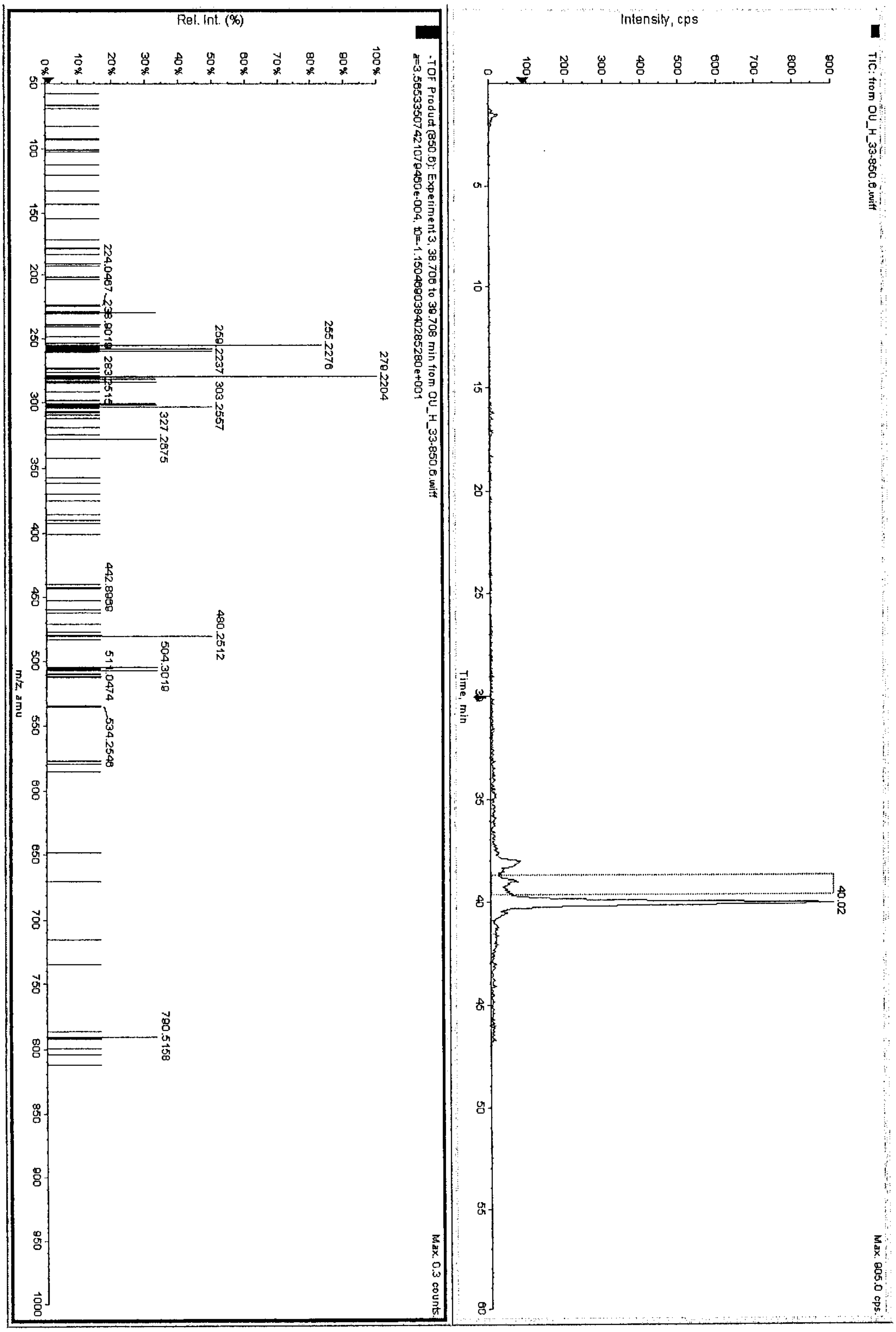

Figure 31 (cont.)

(c)

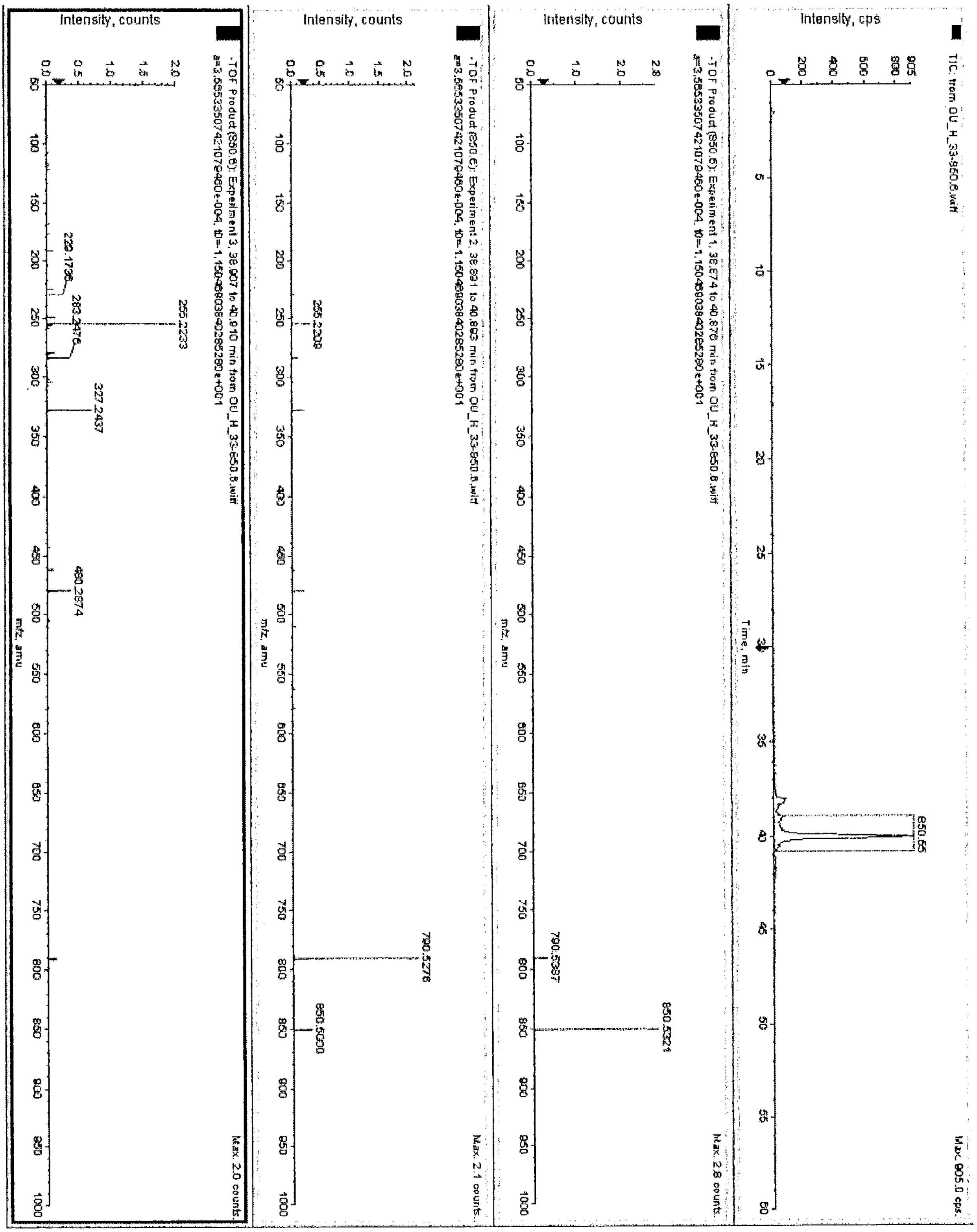

Figure 31 (cont.)

(d)

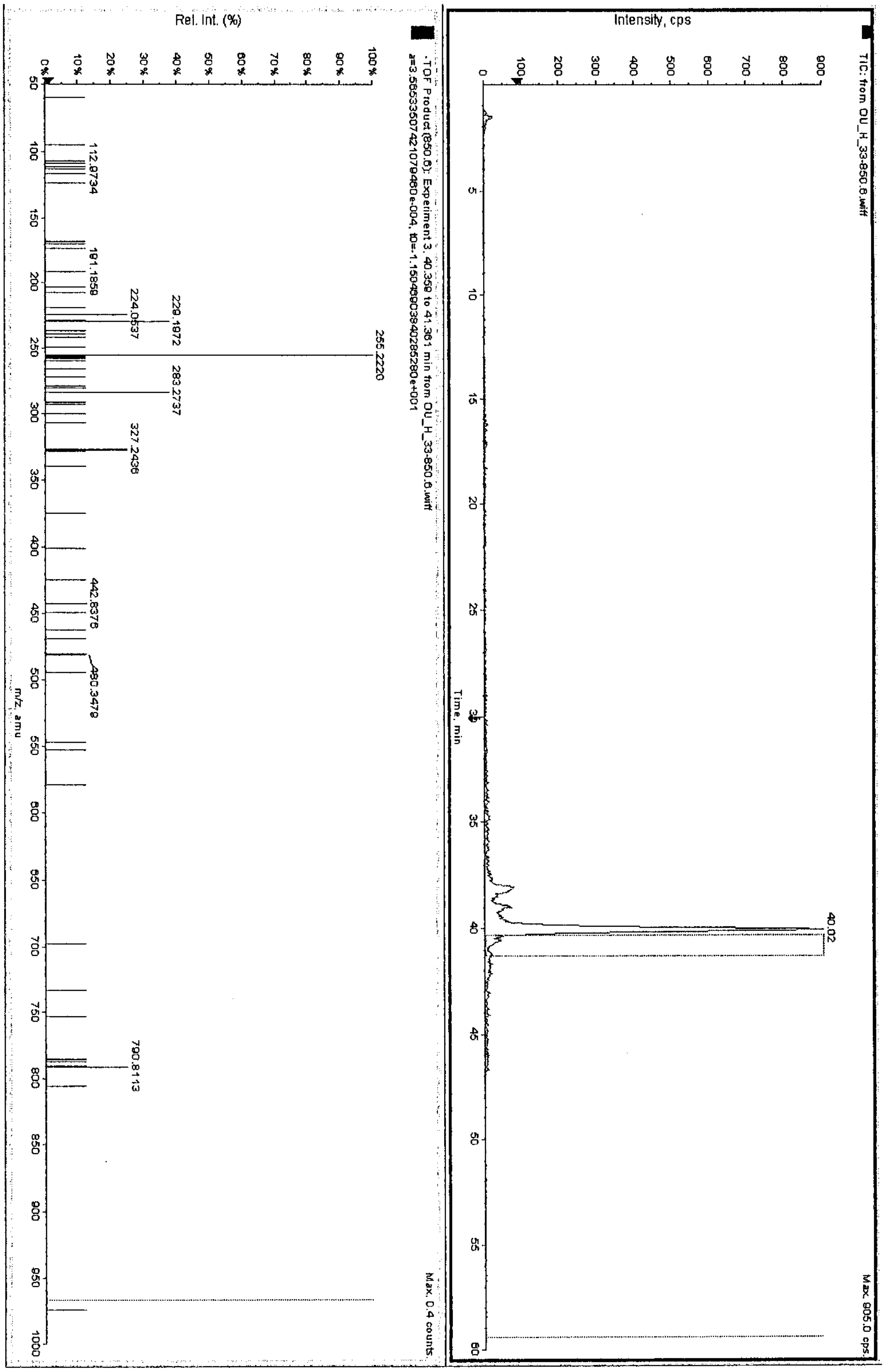

Figure 31 (cont.)

(a)

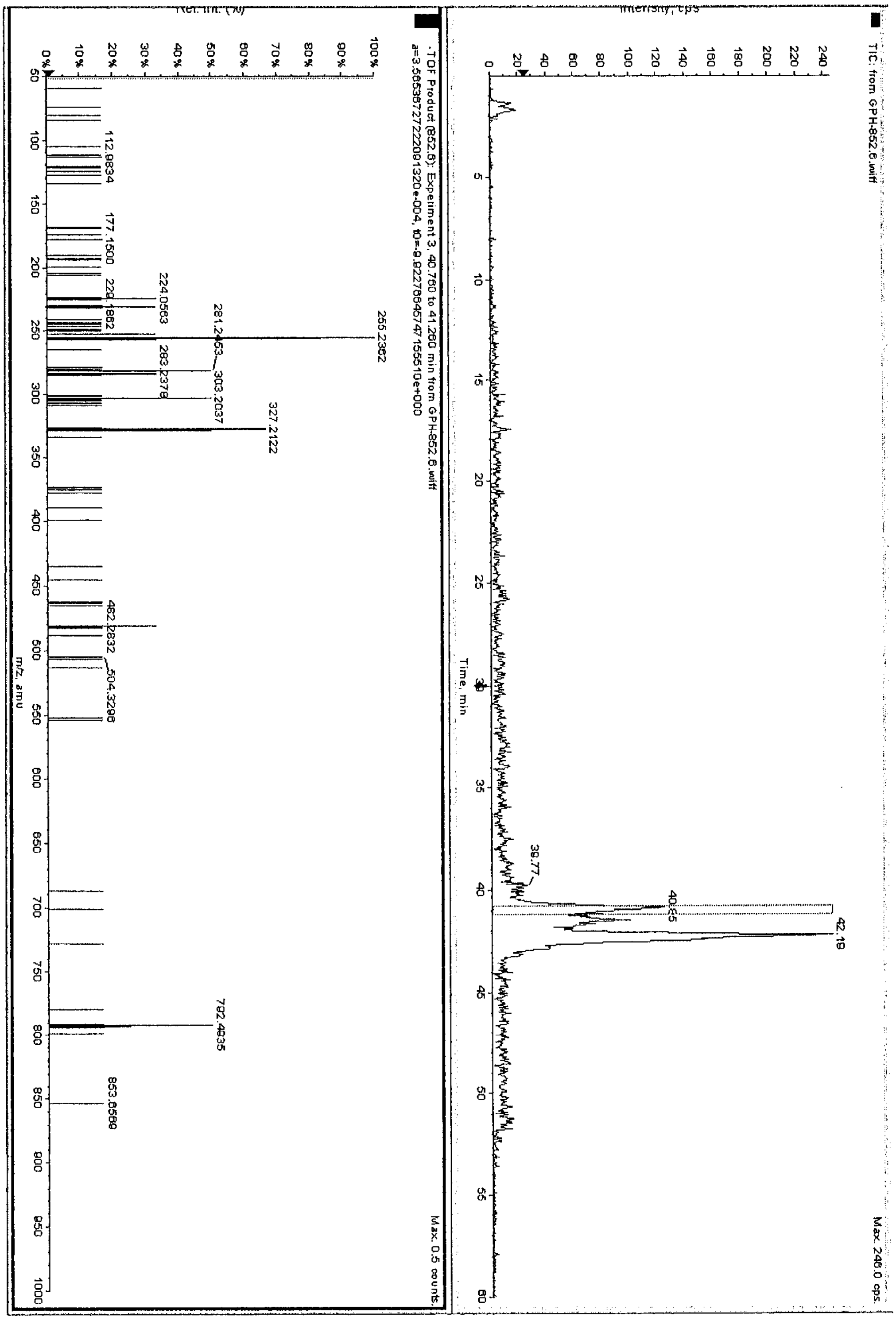
TIC: from GPH-852.6.wiff
Max. 246.0 cps.
Intensity, cps
0
20
40
60
80
100
120
140
160
180
200
220
240
Time, min
5
10
15
20
25
30
35
40
45
50
55
60
38.77
40.65
42.19
-TOF Product (852.6): Experiment 3, 40.760 to 41.260 min from GPH-852.6.wiff
a=3.56538727222091320e-004, t0=-9.82278645747155510e+000
Max. 0.5 counts.
Rel. Int. (%)
0%
10%
20%
30%
40%
50%
60%
70%
80%
90%
100%
m/z, amu
50
100
150
200
250
300
350
400
450
500
550
600
650
700
750
800
850
900
950
1000
112.9834
177.1500
224.0563
229.1882
255.2362
281.2463
283.2378
303.2037
327.2122
482.2832
504.3298
792.4835
853.6569

Figure 32

(b)

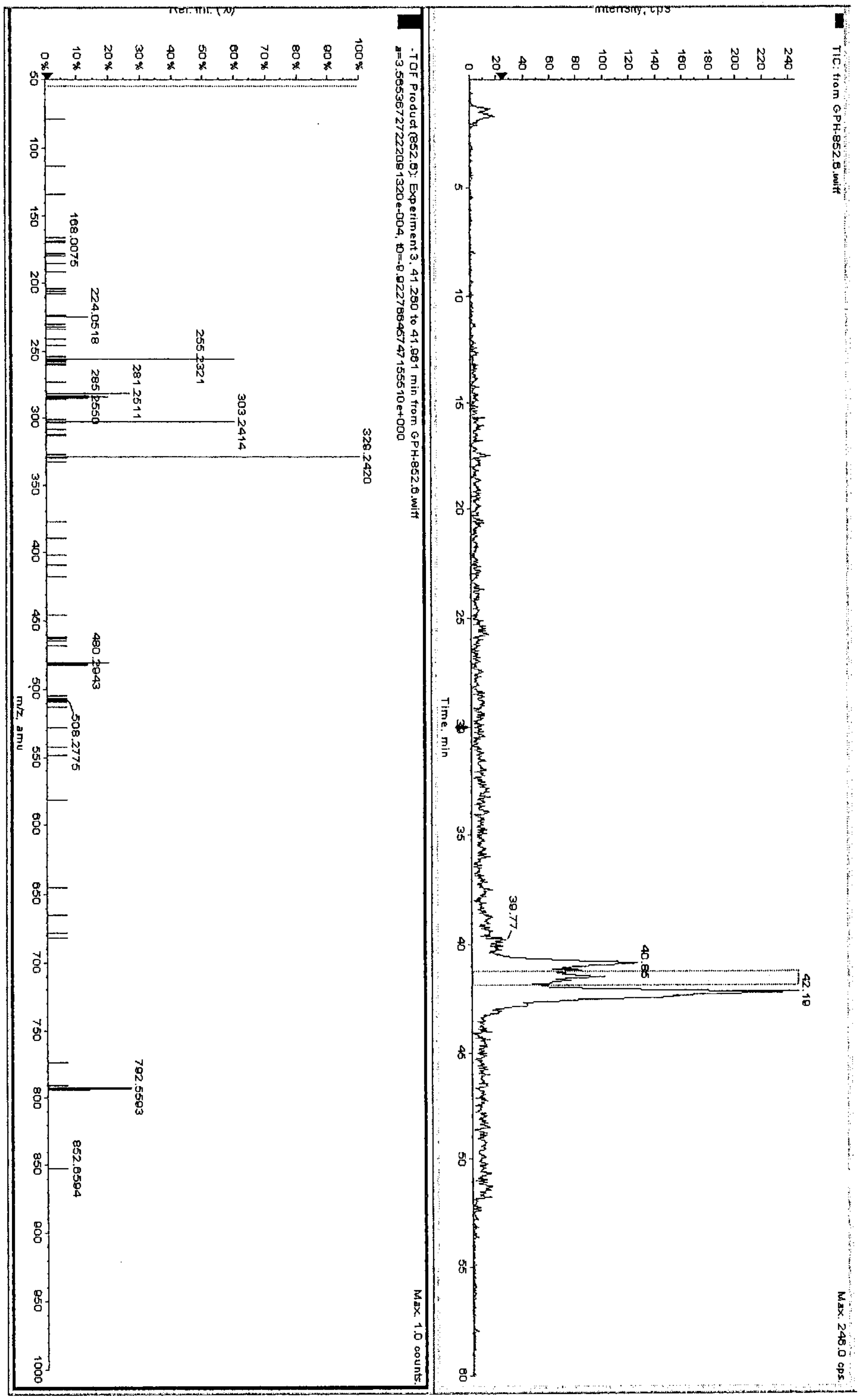

Figure 32 (cont.)

(c)

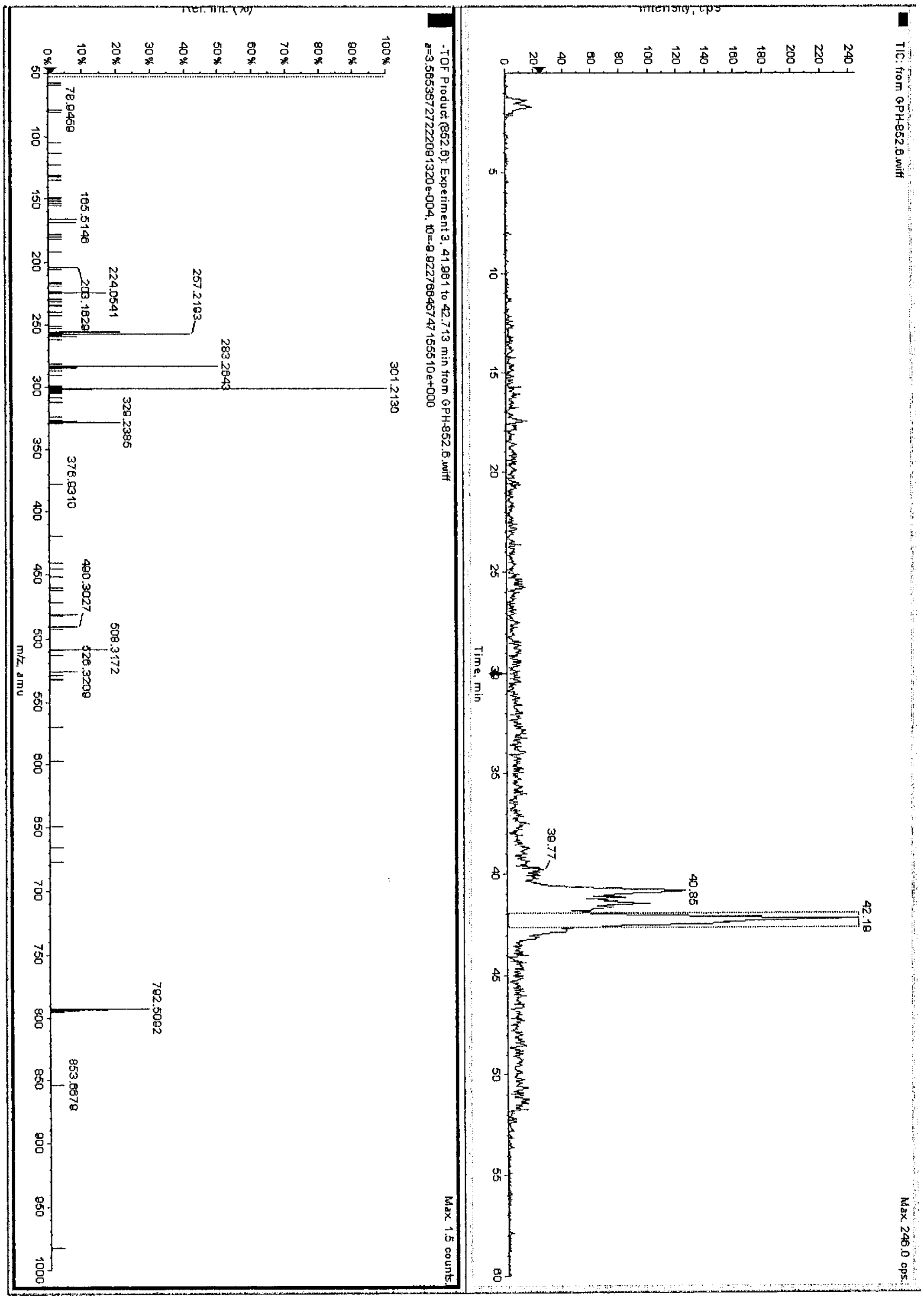

Figure 32 (cont.)

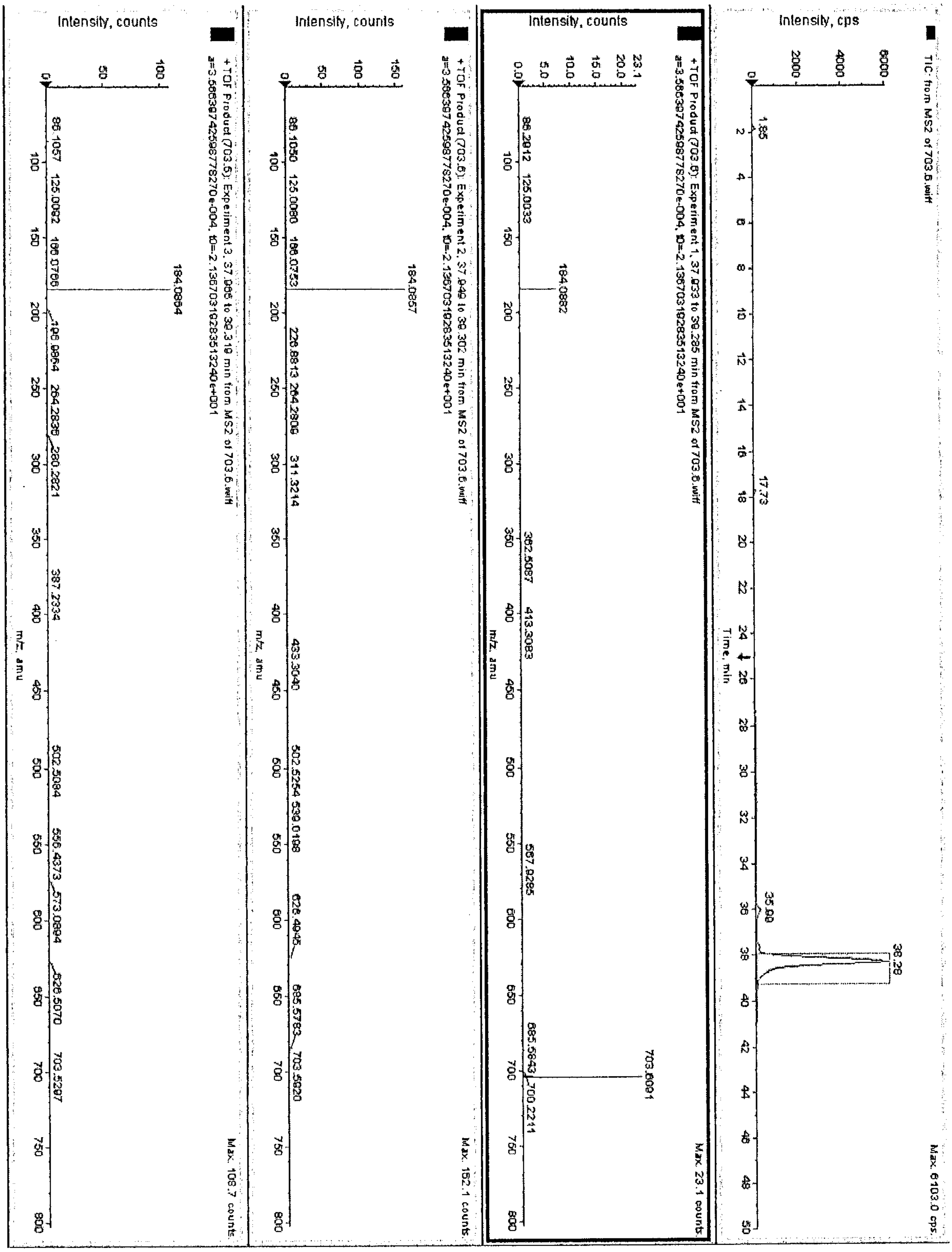
TIC: from MS2 of 703.6.wiff
Max. 6103.0 cps.
Intensity, cps
6000
4000
2000
0
1.85
17.73
35.98
38.28
Time, min
+TOF Product (703.6): Experiment 1, 37.923 to 39.285 min from MS2 of 703.6.wiff
a=3.56639742598778270e-004, t0=-2.13670316283513240e+001
Max. 23.1 counts.
Intensity, counts
23.1
20.0
15.0
10.0
5.0
0.0
86.2912
125.0033
184.0882
362.5087
413.3083
567.9285
685.5643
703.6091
700.2211
m/z, amu
+TOF Product (703.6): Experiment 2, 37.949 to 39.302 min from MS2 of 703.6.wiff
a=3.56639742598778270e-004, t0=-2.13670316283513240e+001
Max. 152.1 counts.
Intensity, counts
150
100
50
0
86.1050
125.0080
166.0753
184.0857
226.8813
264.2806
311.3214
433.3040
502.5254
539.0198
626.4945
685.5783
703.5920
m/z, amu
+TOF Product (703.6): Experiment 3, 37.965 to 39.319 min from MS2 of 703.6.wiff
a=3.56639742598778270e-004, t0=-2.13670316283513240e+001
Max. 106.7 counts.
Intensity, counts
100
50
0
86.1057
125.0062
166.0766
184.0864
196.0864
264.2838
280.2821
387.2334
502.5084
556.4373
573.0894
626.5070
703.5287
m/z, amu

Figure 33

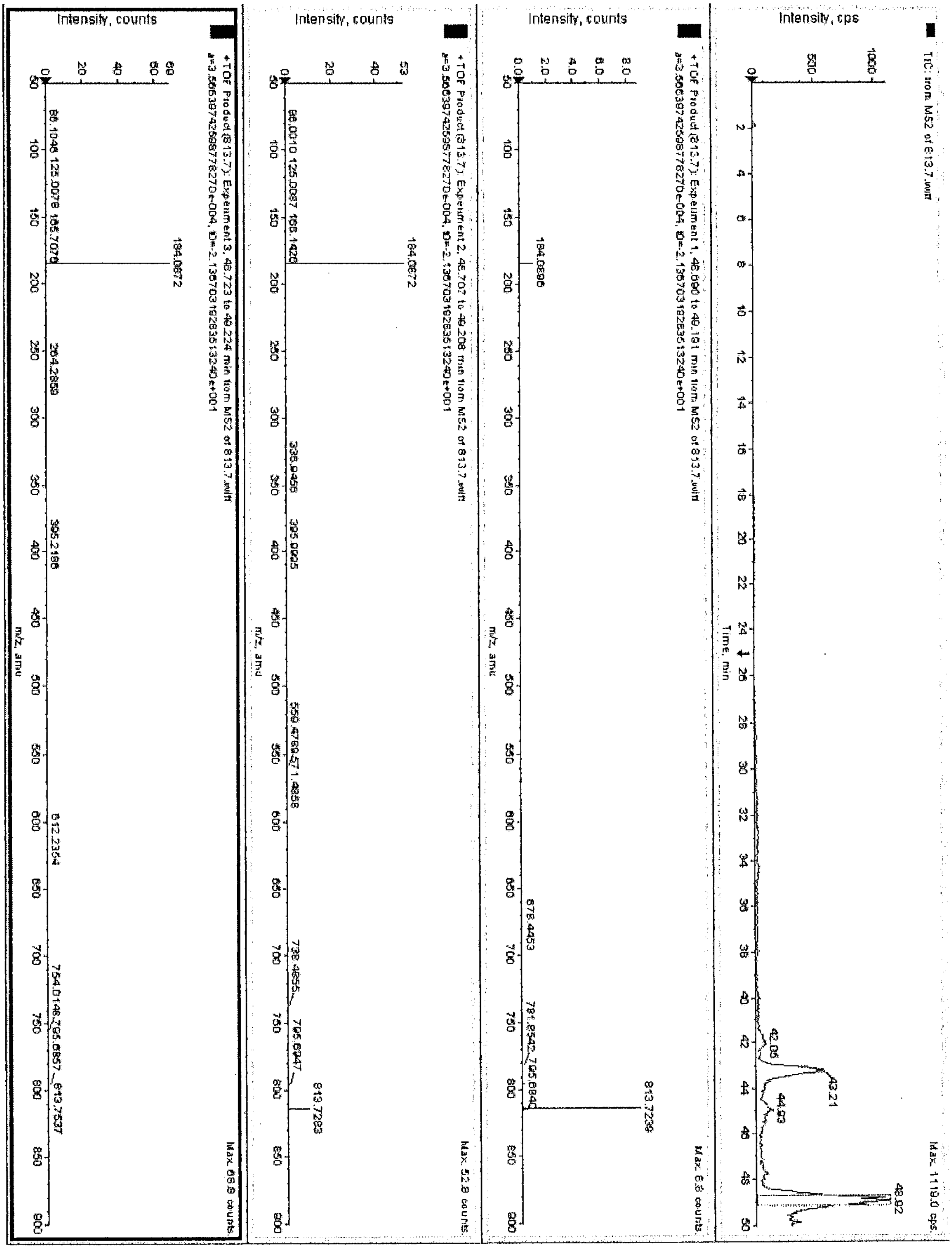
TIC: from MS2 of 813.7.wiff
Intensity, cps
Max. 1119.0 cps.
0
500
1000
Time, min
2
4
6
8
10
12
14
16
18
20
22
24
26
28
30
32
34
36
38
40
42
44
46
48
50
42.05
43.21
44.93
48.92
+TOF Product (813.7): Experiment 1, 48.690 to 49.191 min from MS2 of 813.7.wiff
a=3.56639742568778270e-004, t0=2.13670318263513240e+001
Intensity, counts
Max. 6.6 counts.
0.0
2.0
4.0
6.0
8.0
m/z, amu
50
100
150
200
250
300
350
400
450
500
550
600
650
700
750
800
850
900
184.0896
678.4453
781.8542
785.6840
813.7239
+TOF Product (813.7): Experiment 2, 48.707 to 49.208 min from MS2 of 813.7.wiff
a=3.56639742568778270e-004, t0=2.13670318263513240e+001
Intensity, counts
Max. 52.8 counts.
0
20
40
53
86.0010
125.0087
166.1426
184.0672
336.9456
395.0605
550.4760
571.4856
738.4855
785.6947
813.7283
+TOF Product (813.7): Experiment 3, 48.723 to 49.224 min from MS2 of 813.7.wiff
a=3.56639742568778270e-004, t0=2.13670318263513240e+001
Intensity, counts
Max. 66.9 counts.
0
20
40
60
69
86.1046
125.0076
165.7070
184.0672
264.2859
395.2186
612.2364
754.0146
785.6857
813.7537

Figure 34

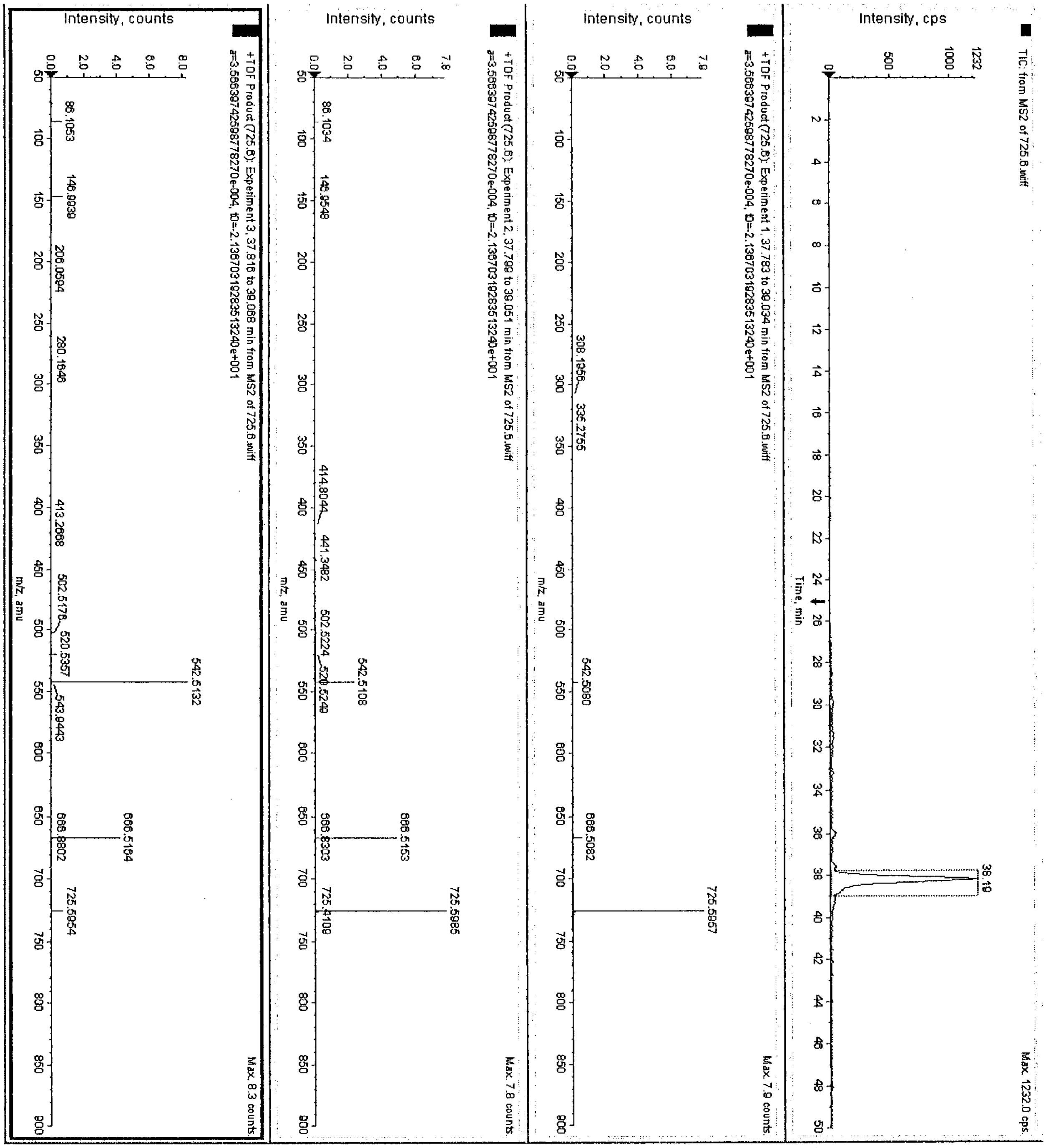
TIC: from MS2 of 725.6.wiff
Max. 1232.0 cps.
Intensity, cps
Time, min
38.19
+TOF Product (725.6): Experiment 1, 37.783 to 39.034 min from MS2 of 725.6.wiff
a=3.56639742598782270e-004, t0=-2.13670318283513240e+001
Max. 7.9 counts.
308.1956
336.2755
542.5080
666.5082
725.5657
+TOF Product (725.6): Experiment 2, 37.799 to 39.051 min from MS2 of 725.6.wiff
a=3.56639742598782270e-004, t0=-2.13670318283513240e+001
Max. 7.8 counts.
86.1034
146.9548
414.8044
441.3482
502.5224
520.5249
542.5106
666.5153
666.8303
725.4108
725.5985
+TOF Product (725.6): Experiment 3, 37.816 to 39.068 min from MS2 of 725.6.wiff
a=3.56639742598782270e-004, t0=-2.13670318283513240e+001
Max. 8.3 counts.
86.1053
146.9939
206.0594
280.1646
413.2666
502.5178
520.5357
542.5132
543.9443
666.5184
666.8802
725.5654
Intensity, counts
m/z, amu

Figure 35

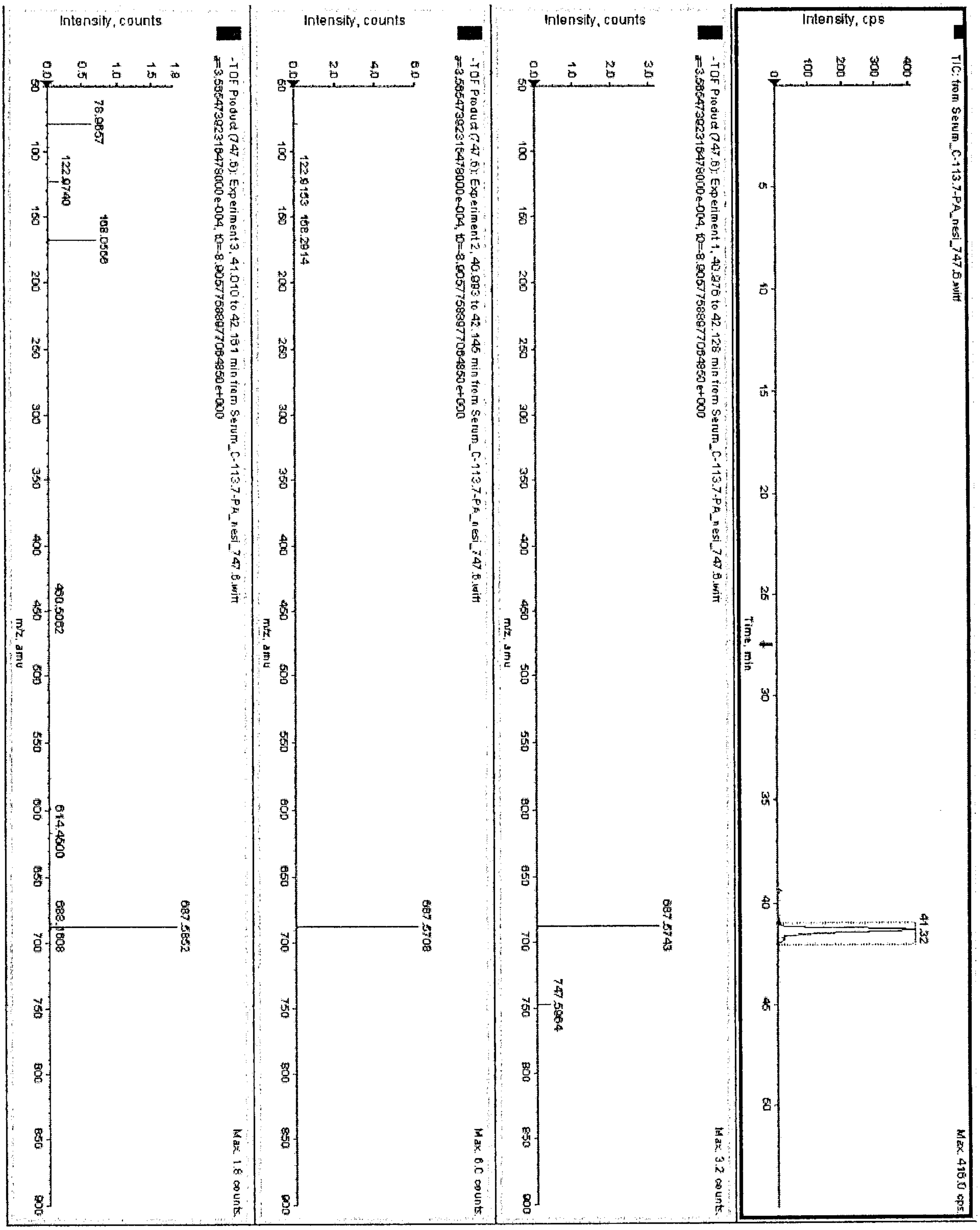
TIC: from Serum_C-113.7-PA_nesi_747.6.wiff
Max. 416.0 cps.
Intensity, cps
0
100
200
300
400
41.32
Time, min
0
5
10
15
20
25
30
35
40
45
50
-TOF Product (747.6): Experiment 1, 40.276 to 42.128 min from Serum_C-113.7-PA_nesi_747.6.wiff
a=3.58547392316478000e-004, t0=-8.90577588977084850e+000
Max. 3.2 counts.
Intensity, counts
0.0
1.0
2.0
3.0
687.5743
747.5864
m/z, amu
-TOF Product (747.6): Experiment 2, 40.993 to 42.145 min from Serum_C-113.7-PA_nesi_747.6.wiff
a=3.58547392316478000e-004, t0=-8.90577588977084850e+000
Max. 6.0 counts.
Intensity, counts
0.0
2.0
4.0
6.0
122.9153
168.2914
687.5708
m/z, amu
-TOF Product (747.6): Experiment 3, 41.010 to 42.151 min from Serum_C-113.7-PA_nesi_747.6.wiff
a=3.58547392316478000e-004, t0=-8.90577588977084850e+000
Max. 1.8 counts.
Intensity, counts
0.0
0.5
1.0
1.5
1.8
78.9857
122.9740
168.0568
460.5062
614.4600
687.5852
688.1608
m/z, amu
50
100
150
200
250
300
350
400
450
500
550
600
650
700
750
800
850
900

Figure 36

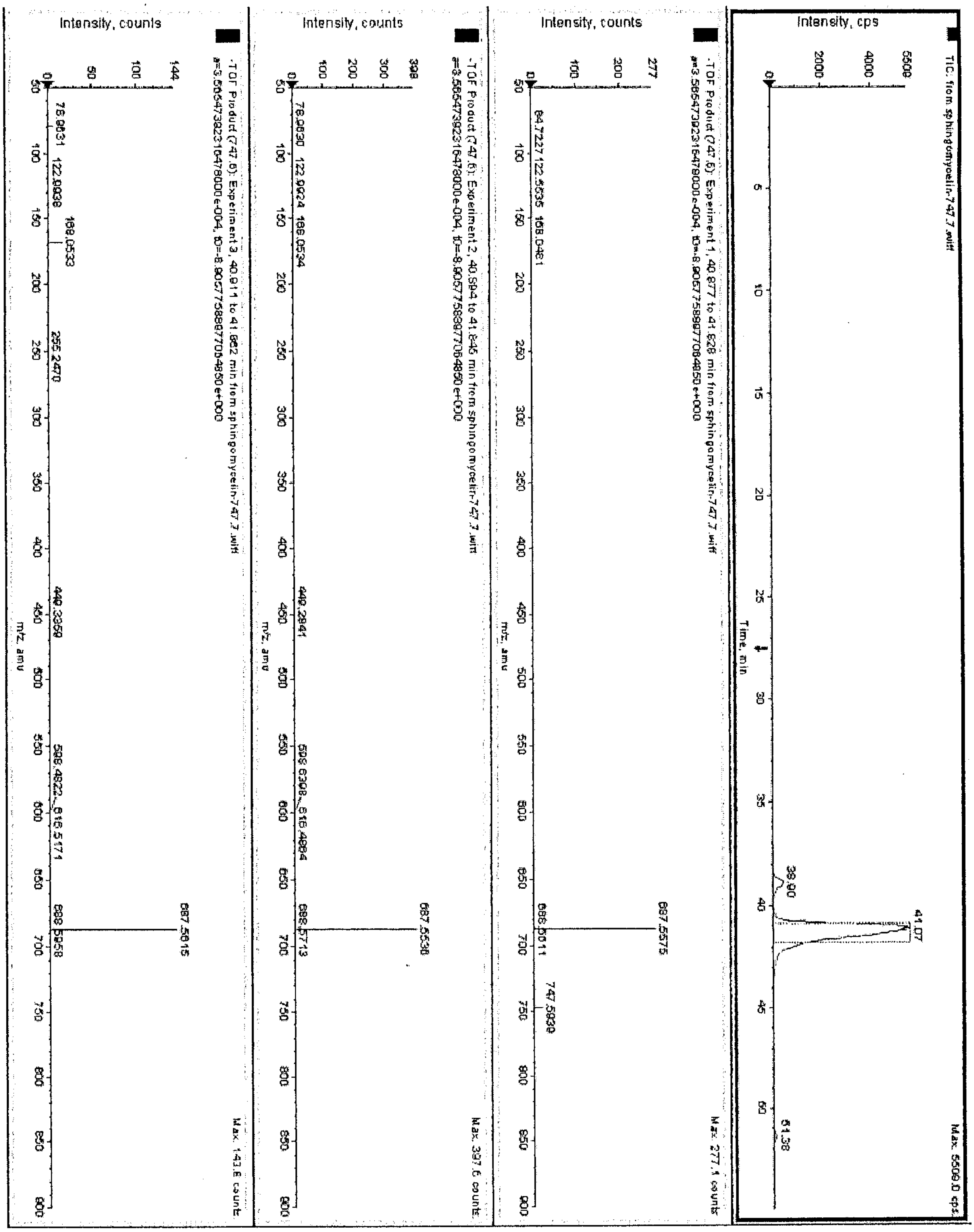
TIC from sphingomyelin-747.7.wiff
Max. 5509.0 cps.
Intensity, cps
Time, min
38.90
41.07
51.38
-TOF Product (747.6): Experiment 1, 40.877 to 41.628 min from sphingomyelin-747.7.wiff
a=3.56547392231647800e-004, t0=-8.90577588977084850e+000
Max. 277.1 counts.
Intensity, counts
84.7227
122.5535
168.0481
686.5611
687.5575
747.5939
-TOF Product (747.6): Experiment 2, 40.894 to 41.845 min from sphingomyelin-747.7.wiff
a=3.56547392231647800e-004, t0=-8.90577588977084850e+000
Max. 397.6 counts.
Intensity, counts
78.9690
122.9924
168.0534
449.2941
599.5308
616.4884
686.5713
687.5538
-TOF Product (747.6): Experiment 3, 40.911 to 41.862 min from sphingomyelin-747.7.wiff
a=3.56547392231647800e-004, t0=-8.90577588977084850e+000
Max. 143.6 counts.
Intensity, counts
78.9831
122.9938
168.0533
255.2470
449.3359
598.4822
616.5171
686.5958
687.5615
m/z, amu

Figure 37

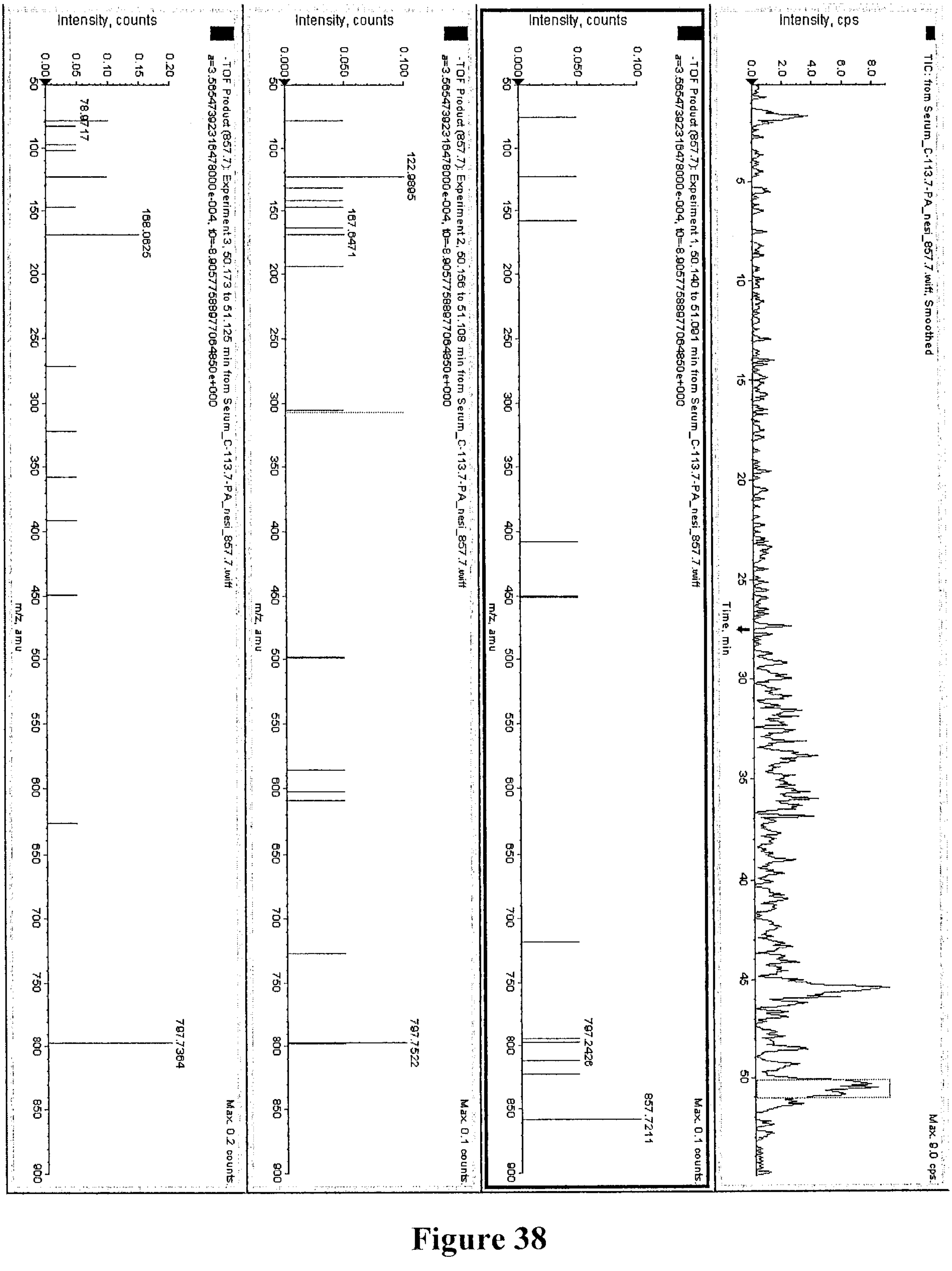
TIC: from Serum_C-113.7-PA_nesi_857.7.wiff, Smoothed
Max. 8.0 cps.
Intensity, cps
0.0
2.0
4.0
6.0
8.0
5
10
15
20
25
30
35
40
45
50
Time, min
-TOF Product (857.7): Experiment 1, 50.140 to 51.081 min from Serum_C-113.7-PA_nesi_857.7.wiff
a=3.56547392316478000e-004, t0=-8.90577588770648500e+000
Max. 0.1 counts.
Intensity, counts
0.000
0.050
0.100
857.7211
797.2426
-TOF Product (857.7): Experiment 2, 50.156 to 51.108 min from Serum_C-113.7-PA_nesi_857.7.wiff
a=3.56547392316478000e-004, t0=-8.90577588770648500e+000
Max. 0.1 counts.
Intensity, counts
0.000
0.050
0.100
122.9805
167.8471
797.7522
-TOF Product (857.7): Experiment 3, 50.173 to 51.125 min from Serum_C-113.7-PA_nesi_857.7.wiff
a=3.56547392316478000e-004, t0=-8.90577588770648500e+000
Max. 0.2 counts.
Intensity, counts
0.00
0.05
0.10
0.15
0.20
78.9717
168.0825
797.7364
50
100
150
200
250
300
350
400
450
500
550
600
650
700
750
800
850
900
m/z, amu

Figure 38

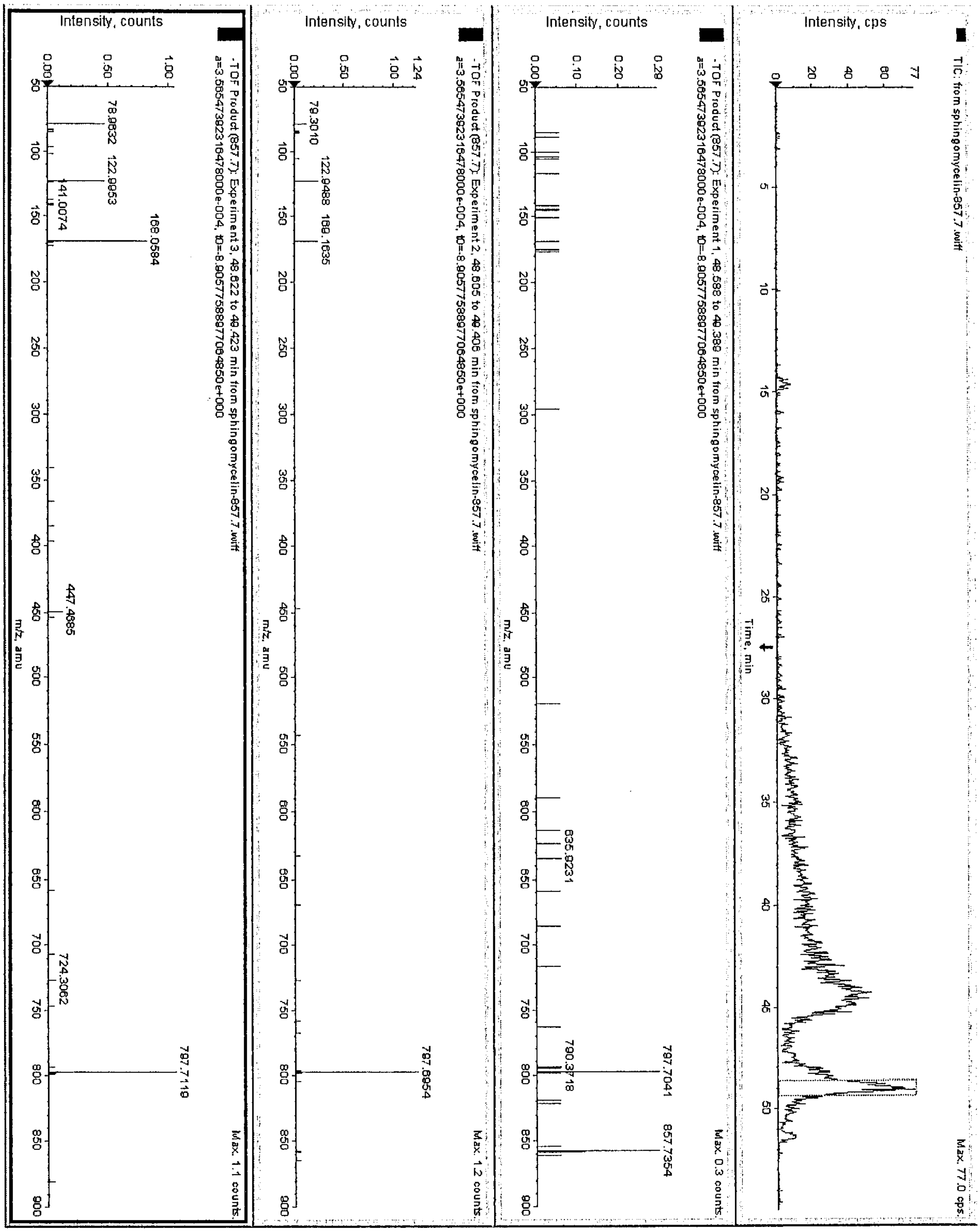
TIC: from sphingomycelin-857.7.wiff
Max. 77.0 cps.
Intensity, cps
77
60
40
20
0
Time, min
0
5
10
15
20
25
30
35
40
45
50
-TOF Product (857.7): Experiment 1, 48.588 to 49.389 min from sphingomycelin-857.7.wiff
a=3.56547392316478000e-004, t0=-8.90577588977064850e+000
Max. 0.3 counts.
Intensity, counts
0.29
0.20
0.10
0.00
797.7041
857.7354
790.3718
635.8231
-TOF Product (857.7): Experiment 2, 48.605 to 49.406 min from sphingomycelin-857.7.wiff
a=3.56547392316478000e-004, t0=-8.90577588977064850e+000
Max. 1.2 counts.
Intensity, counts
1.24
1.00
0.50
0.00
797.6954
168.1635
122.9488
79.3010
-TOF Product (857.7): Experiment 3, 48.622 to 49.423 min from sphingomycelin-857.7.wiff
a=3.56547392316478000e-004, t0=-8.90577588977064850e+000
Max. 1.1 counts.
Intensity, counts
1.00
0.50
0.00
797.7119
724.3062
447.4685
168.0584
141.0074
122.9953
78.9632
m/z, amu
50
100
150
200
250
300
350
400
450
500
550
600
650
700
750
800
850
900

Figure 39

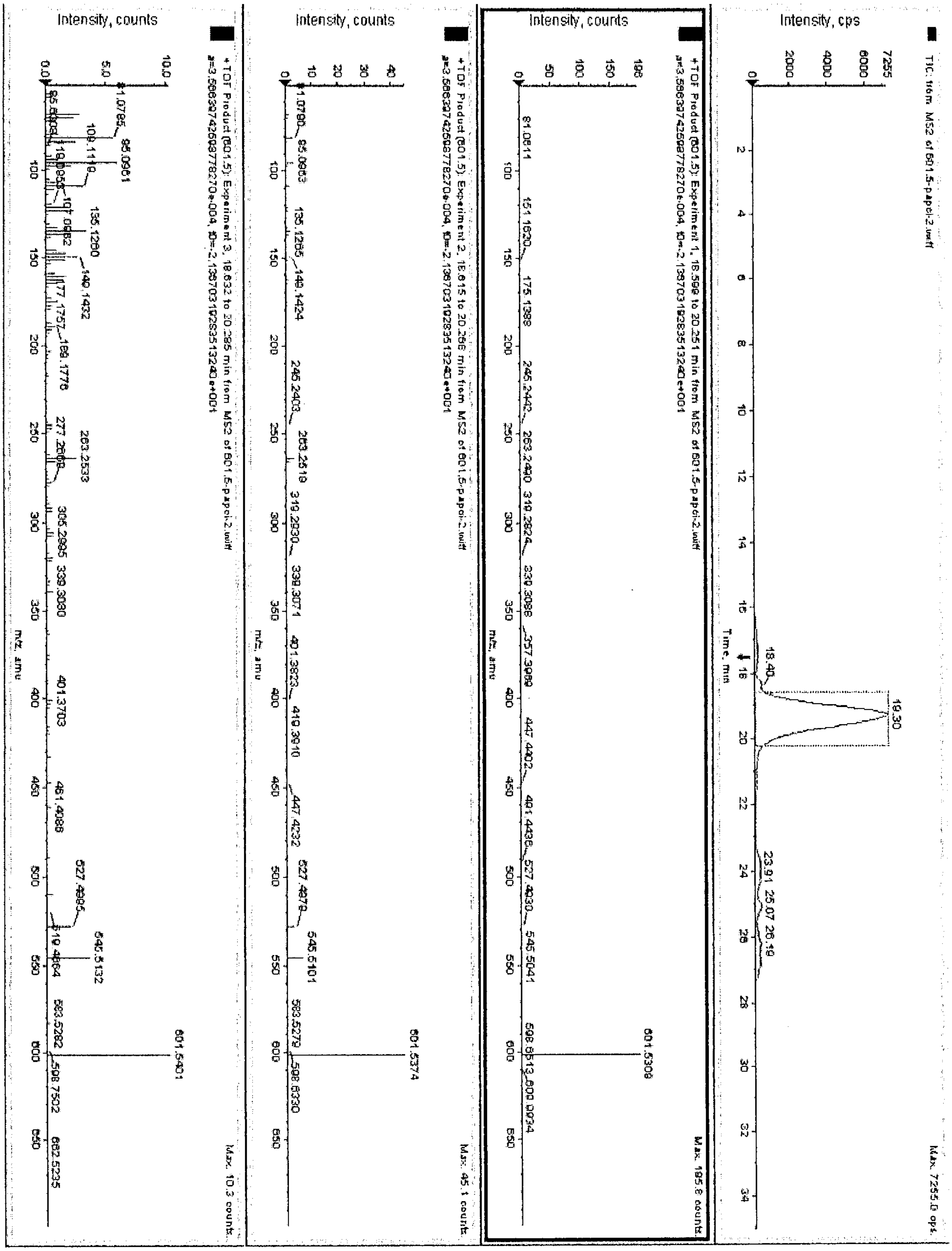
TIC: from MS2 of 601.5-papci-2.wiff
Max. 7255.0 cps.
Intensity, cps
7255
6000
4000
2000
0
Time, min
18.40
19.30
23.91
25.07
26.19
+TOF Product (601.5): Experiment 1, 18.599 to 20.251 min from MS2 of 601.5-papci-2.wiff
a=3.58639742568778270e-004, t0=-2.13870319283513240e+001
Max. 185.8 counts.
Intensity, counts
81.0611
151.1620
175.1388
245.2442
263.2480
319.2824
339.3088
357.3089
447.4402
491.4436
527.4930
545.5041
598.6513
600.0934
601.5308
m/z, amu
+TOF Product (601.5): Experiment 2, 18.615 to 20.266 min from MS2 of 601.5-papci-2.wiff
a=3.58639742568778270e-004, t0=-2.13870319283513240e+001
Max. 45.1 counts.
81.0790
95.0963
135.1265
149.1424
245.2403
263.2519
319.2930
339.3071
401.3823
419.3910
447.4232
527.4879
545.5101
583.5279
601.5374
598.6330
+TOF Product (601.5): Experiment 3, 18.632 to 20.285 min from MS2 of 601.5-papci-2.wiff
a=3.58639742568778270e-004, t0=-2.13870319283513240e+001
Max. 10.3 counts.
81.0785
95.0961
109.1119
135.1280
149.1432
177.1757
189.1776
263.2533
277.2668
305.2985
339.3080
401.3703
461.4088
527.4985
545.5132
519.4864
583.5282
601.5401
598.7502
682.5235

Figure 40

(a)

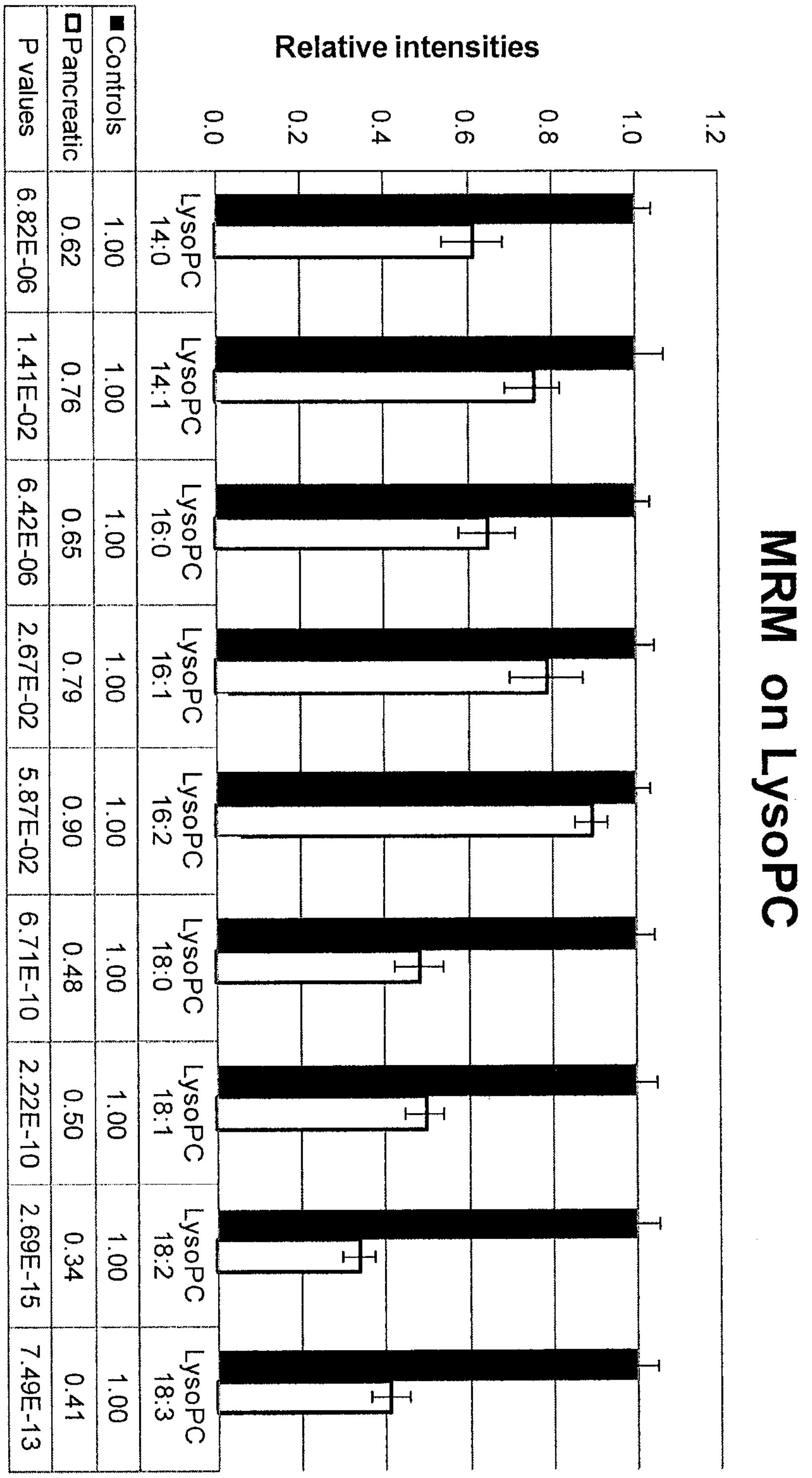

	LysoPC 14:0	LysoPC 14:1	LysoPC 16:0	LysoPC 16:1	LysoPC 16:2	LysoPC 18:0	LysoPC 18:1	LysoPC 18:2	LysoPC 18:3
■ Controls	1.00	1.00	1.00	1.00	1.00	1.00	1.00	1.00	1.00
□ Pancreatic	0.62	0.76	0.65	0.79	0.90	0.48	0.50	0.34	0.41
P values	6.82E-06	1.41E-02	6.42E-06	2.67E-02	5.87E-02	6.71E-10	2.22E-10	2.69E-15	7.49E-13

Figure 41

(b)

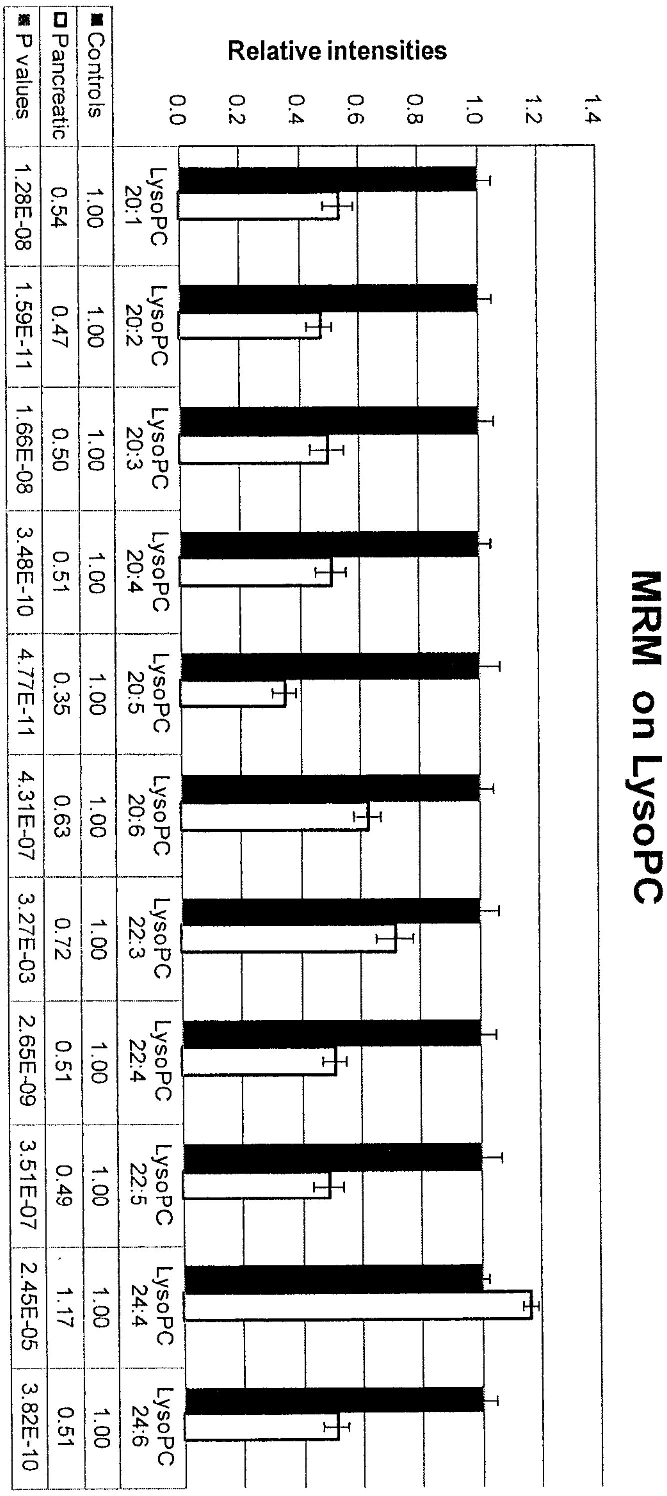

	LysoPC 20:1	LysoPC 20:2	LysoPC 20:3	LysoPC 20:4	LysoPC 20:5	LysoPC 20:6	LysoPC 22:3	LysoPC 22:4	LysoPC 22:5	LysoPC 24:4	LysoPC 24:6
■ Controls	1.00	1.00	1.00	1.00	1.00	1.00	1.00	1.00	1.00	1.00	1.00
□ Pancreatic	0.54	0.47	0.50	0.51	0.35	0.63	0.72	0.51	0.49	1.17	0.51
▩ P values	1.28E-08	1.59E-11	1.66E-08	3.48E-10	4.77E-11	4.31E-07	3.27E-03	2.65E-09	3.51E-07	2.45E-05	3.82E-10

Figure 41 (Cont.)

(c)

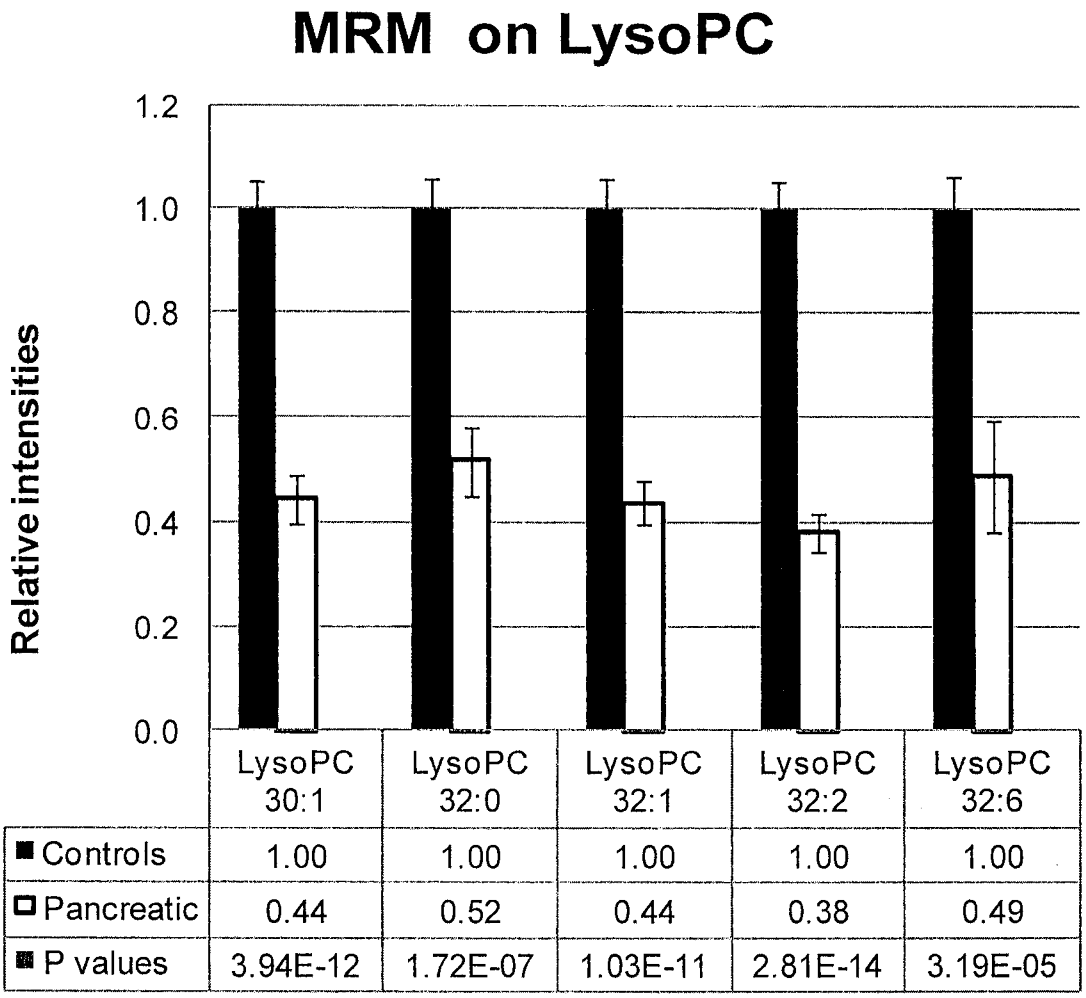

	LysoPC 30:1	LysoPC 32:0	LysoPC 32:1	LysoPC 32:2	LysoPC 32:6
■ Controls	1.00	1.00	1.00	1.00	1.00
□ Pancreatic	0.44	0.52	0.44	0.38	0.49
▨ P values	3.94E-12	1.72E-07	1.03E-11	2.81E-14	3.19E-05

Figure 41 (Cont.)

(d)

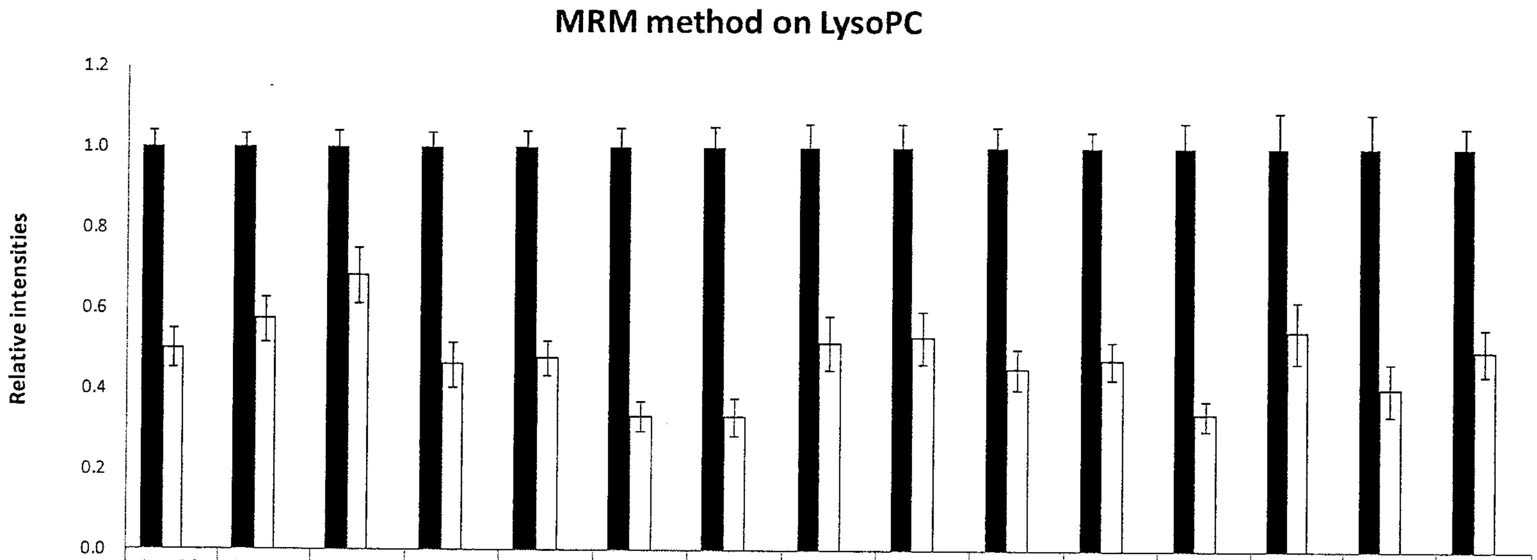

	LysoPC 14:0	LysoPC 16:0	LysoPC 16:1	LysoPC 18:0	LysoPC 18:1	LysoPC 18:2	LysoPC 18:3	LysoPC 20:1	LysoPC 20:2	LysoPC 20:3	LysoPC 20:4	LysoPC 20:5	LysoPC 20:6	LysoPC 22:5	LysoPC 22:6
■ Controls	1.00	1.00	1.00	1.00	1.00	1.00	1.00	1.00	1.00	1.00	1.00	1.00	1.00	1.00	1.00
□ Pancreatic cancer	0.50	0.57	0.68	0.46	0.48	0.33	0.33	0.52	0.53	0.45	0.47	0.34	0.54	0.40	0.49
T test	2.09E-12	5.54E-10	6.42E-05	9.32E-13	1.04E-13	1.34E-17	1.00E-14	4.98E-07	7.67E-07	1.16E-10	7.39E-13	2.37E-13	2.41E-04	8.62E-07	6.29E-09

Figure 41 (Cont.)

a)

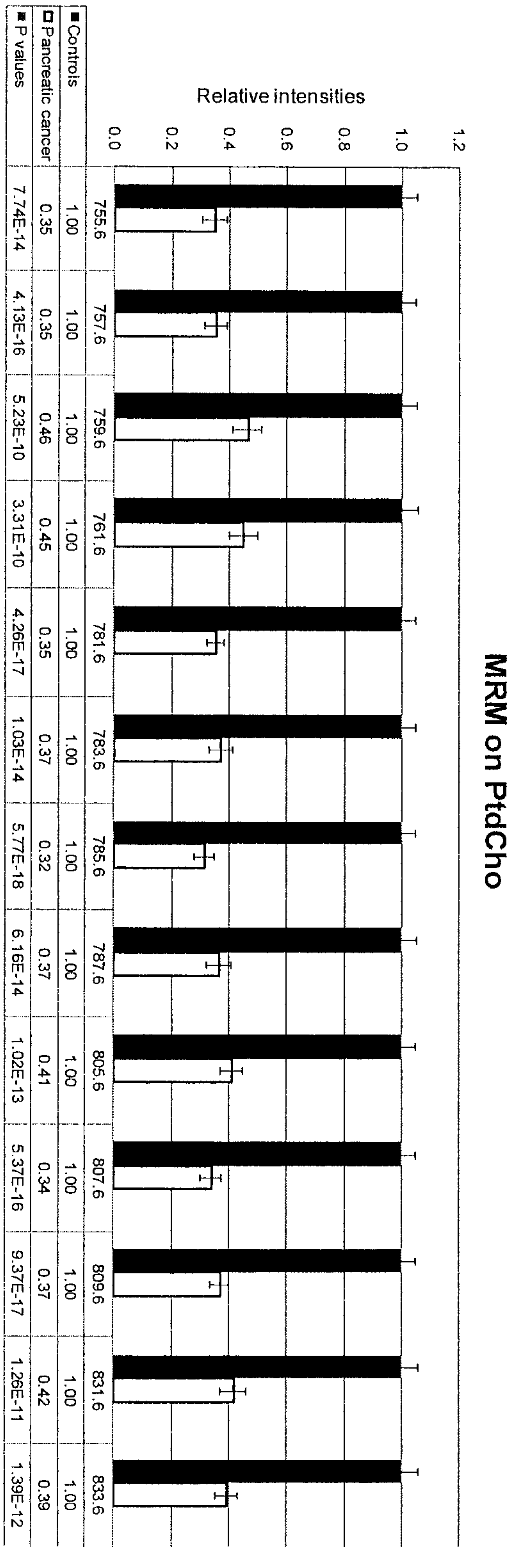

	755.6	757.6	759.6	761.6	781.6	783.6	785.6	787.6	805.6	807.6	809.6	831.6	833.6
■ Controls	1.00	1.00	1.00	1.00	1.00	1.00	1.00	1.00	1.00	1.00	1.00	1.00	1.00
□ Pancreatic cancer	0.35	0.35	0.46	0.45	0.35	0.37	0.32	0.37	0.41	0.34	0.37	0.42	0.39
■ P values	7.74E-14	4.13E-16	5.23E-10	3.31E-10	4.26E-17	1.03E-14	5.77E-18	6.16E-14	1.02E-13	5.37E-16	9.37E-17	1.26E-11	1.39E-12

Figure 42

b)

MRM method on PtdCho (1)

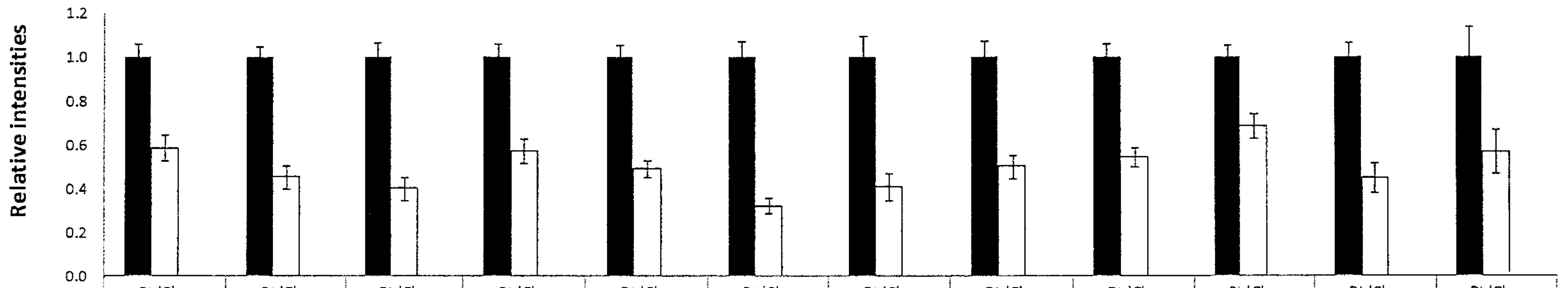

	PtdCho 16:0/18:1	PtdCho 16:0/18:2	PtdCho 16:0/18:3	PtdCho 16:0/20:3	PtdCho 16:0/20:4	PtdCho 16:0/20:5	PtdCho 16:0/22:4	PtdCho 16:0/22:5	PtdCho 16:0/22:6	PtdCho 16:1/18:1	PtdCho 16:1/18:2	PtdCho 16:1/22:6
■ Controls	1.00	1.00	1.00	1.00	1.00	1.00	1.00	1.00	1.00	1.00	1.00	1.00
□ Pancreatic cancer	0.59	0.45	0.40	0.57	0.49	0.32	0.41	0.50	0.54	0.68	0.45	0.57
T test	1.97E-06	6.82E-12	8.22E-10	1.50E-06	1.71E-11	1.98E-12	3.64E-06	2.62E-07	7.19E-08	1.26E-04	1.40E-07	1.69E-02

MRM method on PtdCho (2)

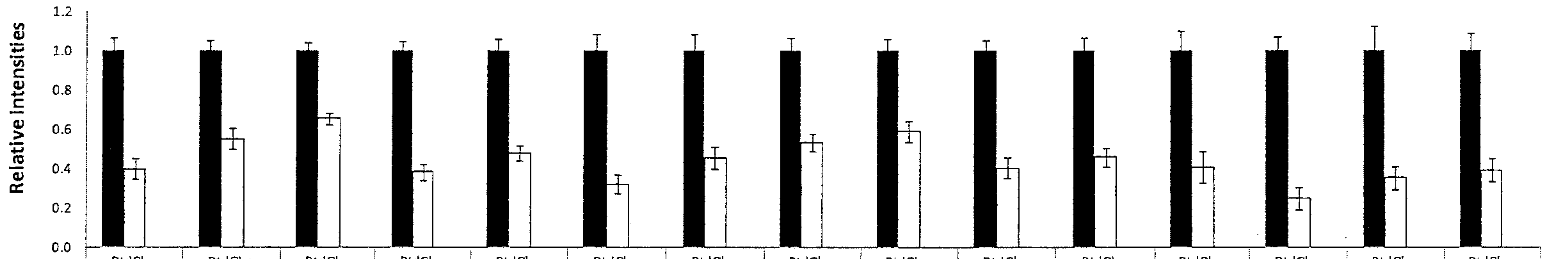

	PtdCho 18:0/16:0	PtdCho 18:0/18:0	PtdCho 18:0/18:1	PtdCho 18:0/18:2	PtdCho 18:0/20:4	PtdCho 18:0/20:5	PtdCho 18:0/22:5	PtdCho 18:0/22:6	PtdCho 18:1/18:1	PtdCho 18:1/18:2	PtdCho 18:1/20:4	PtdCho 18:2/20:5	PtdCho 18:2/18:2	PtdCho 18:2/20:4	PtdCho 18:3/18:2
■ Controls	1.00	1.00	1.00	1.00	1.00	1.00	1.00	1.00	1.00	1.00	1.00	1.00	1.00	1.00	1.00
□ Pancreatic cancer	0.40	0.55	0.66	0.38	0.48	0.32	0.46	0.53	0.59	0.40	0.46	0.41	0.25	0.35	0.39
T test	3.92E-10	5.26E-08	1.09E-08	3.31E-15	3.35E-10	1.17E-09	2.32E-06	3.89E-07	1.82E-06	2.15E-11	9.11E-09	2.98E-05	1.80E-12	4.31E-05	5.80E-07

Figure 42 (cont.)

c)

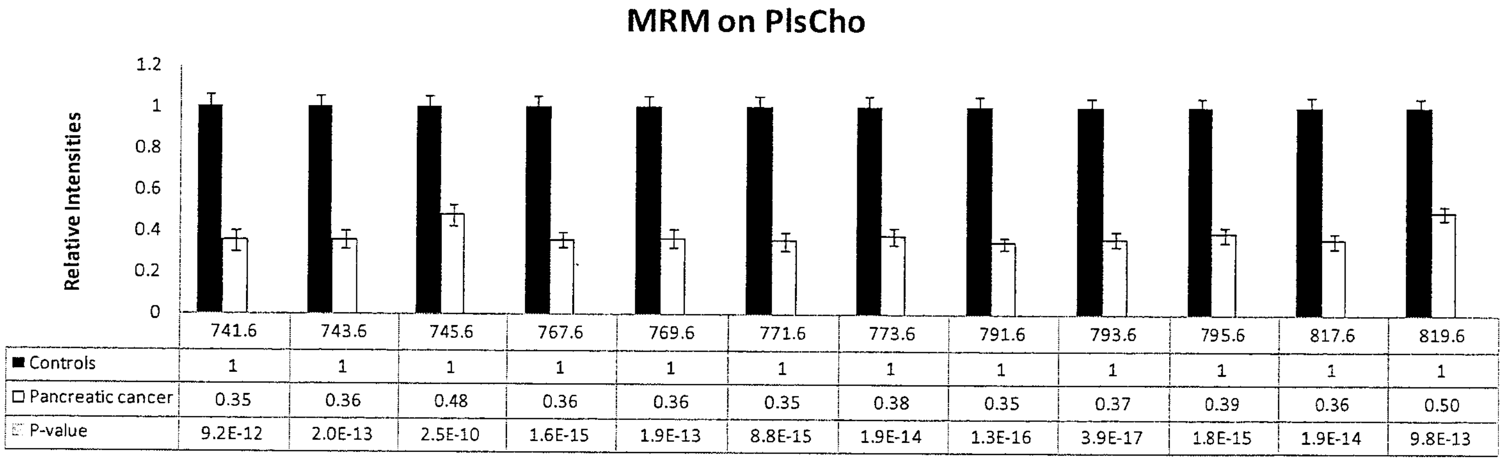

MRM on PlsCho

	741.6	743.6	745.6	767.6	769.6	771.6	773.6	791.6	793.6	795.6	817.6	819.6
■ Controls	1	1	1	1	1	1	1	1	1	1	1	1
☐ Pancreatic cancer	0.35	0.36	0.48	0.36	0.36	0.35	0.38	0.35	0.37	0.39	0.36	0.50
▨ P-value	9.2E-12	2.0E-13	2.5E-10	1.6E-15	1.9E-13	8.8E-15	1.9E-14	1.3E-16	3.9E-17	1.8E-15	1.9E-14	9.8E-13

Figure 42 (Cont.)

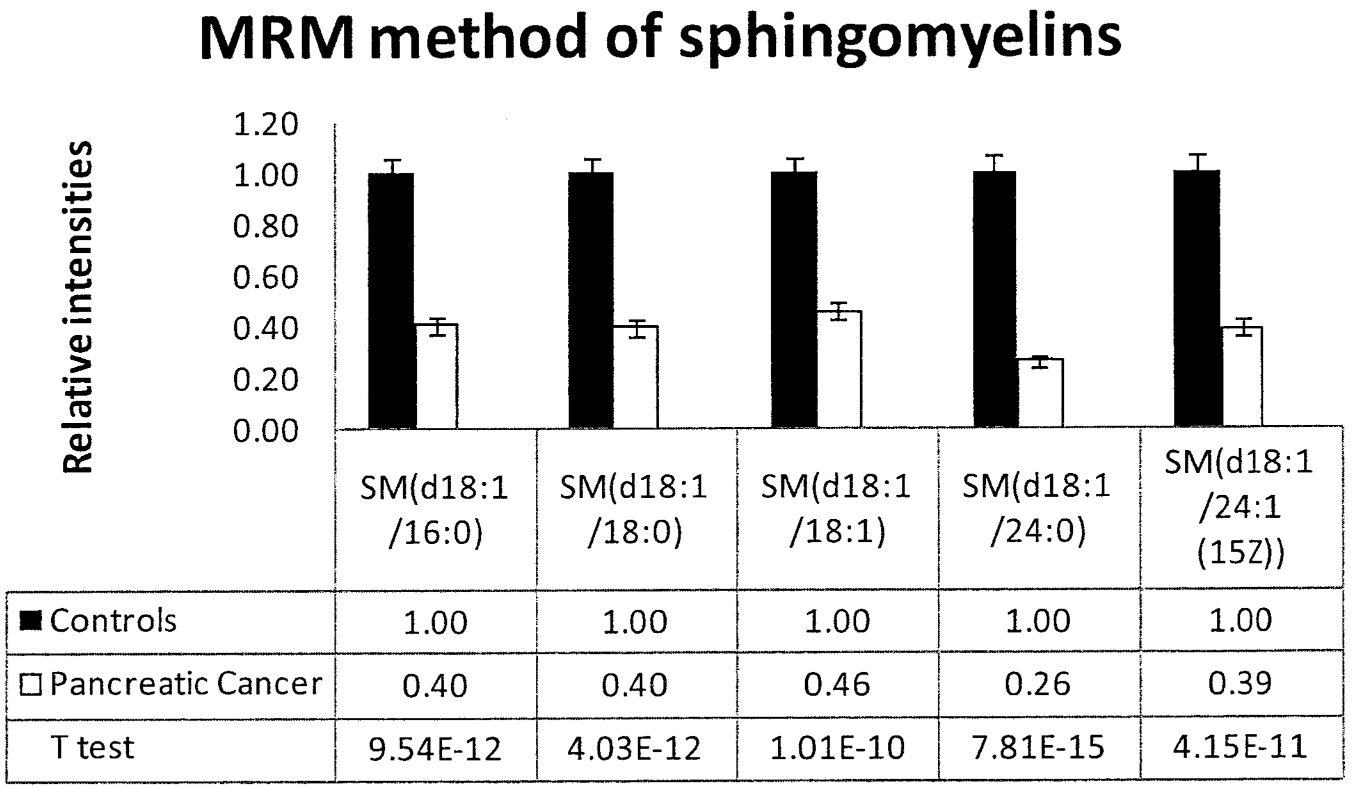

	SM(d18:1 /16:0)	SM(d18:1 /18:0)	SM(d18:1 /18:1)	SM(d18:1 /24:0)	SM(d18:1 /24:1 (15Z))
■ Controls	1.00	1.00	1.00	1.00	1.00
☐ Pancreatic Cancer	0.40	0.40	0.46	0.26	0.39
T test	9.54E-12	4.03E-12	1.01E-10	7.81E-15	4.15E-11

Figure 43

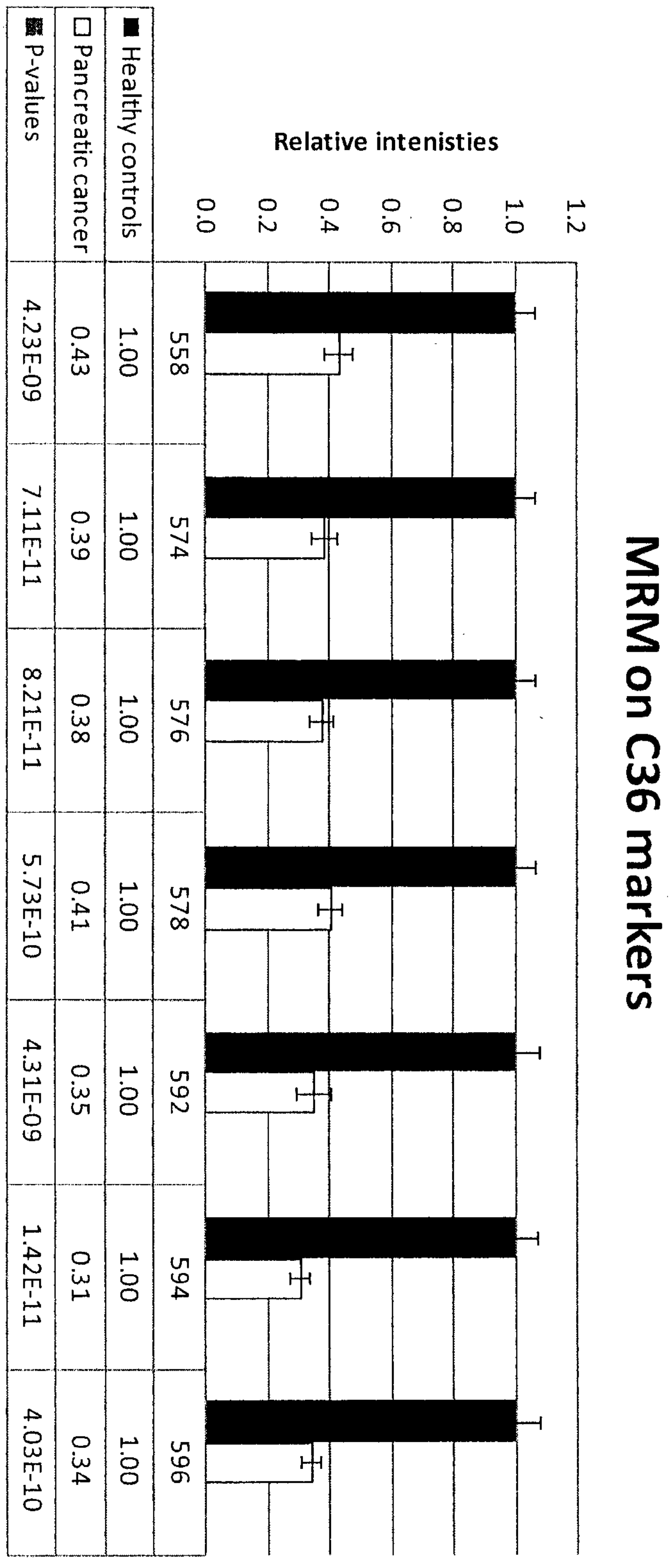

	558	574	576	578	592	594	596
■ Healthy controls	1.00	1.00	1.00	1.00	1.00	1.00	1.00
□ Pancreatic cancer	0.43	0.39	0.38	0.41	0.35	0.31	0.34
▨ P-values	4.23E-09	7.11E-11	8.21E-11	5.73E-10	4.31E-09	1.42E-11	4.03E-10

Figure 44

(a)

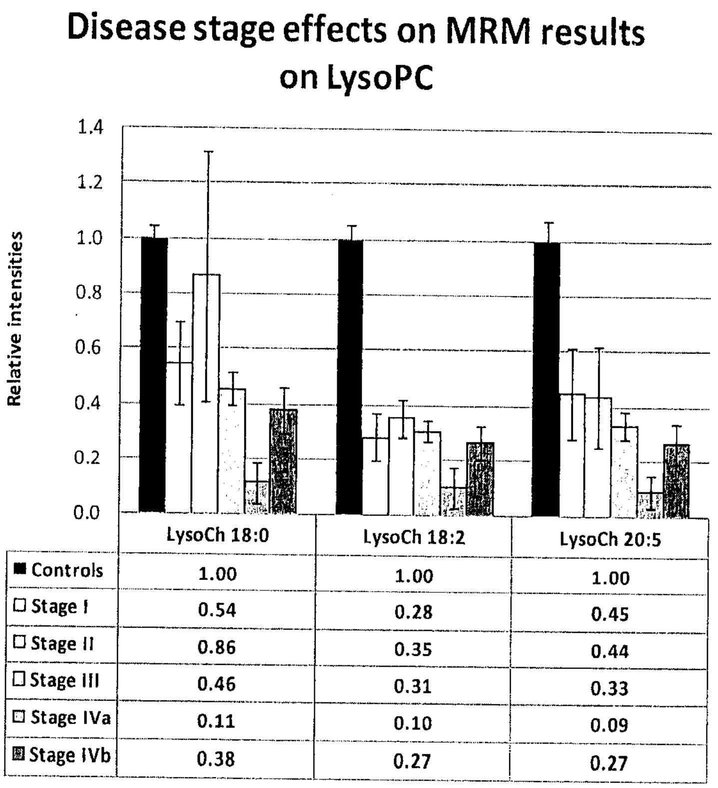
Disease stage effects on MRM results on LysoPC

	LysoCh 18:0	LysoCh 18:2	LysoCh 20:5
■ Controls	1.00	1.00	1.00
□ Stage I	0.54	0.28	0.45
□ Stage II	0.86	0.35	0.44
□ Stage III	0.46	0.31	0.33
▨ Stage IVa	0.11	0.10	0.09
▩ Stage IVb	0.38	0.27	0.27

(b)

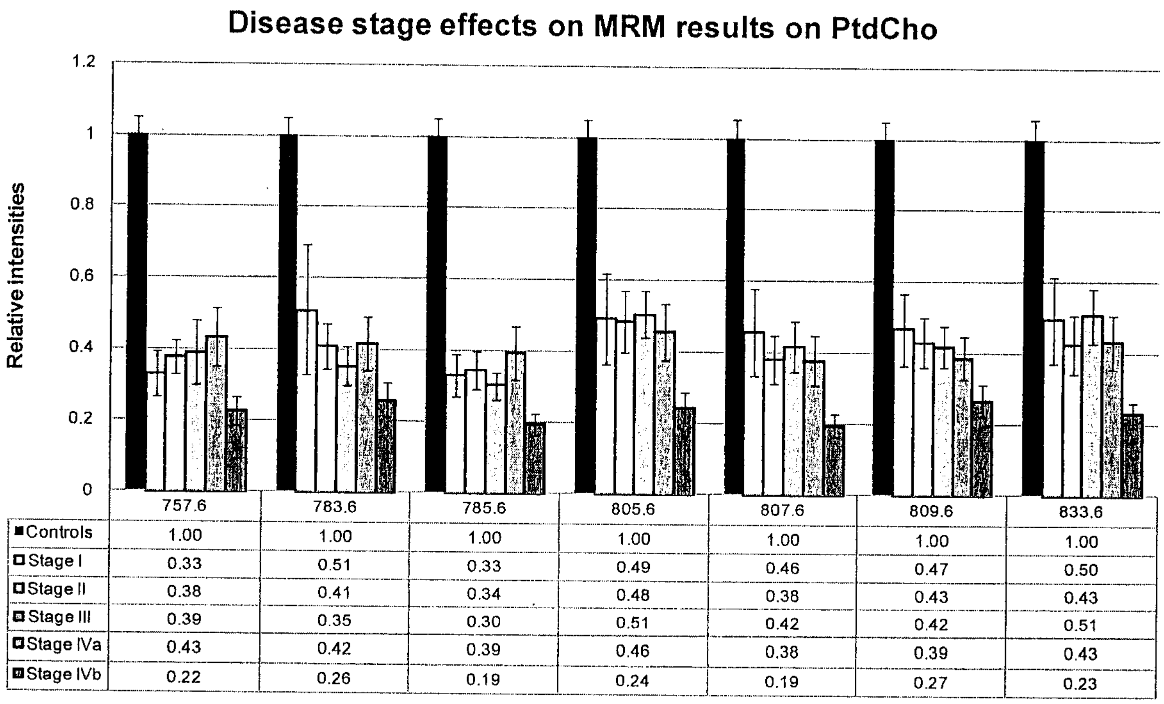
Disease stage effects on MRM results on PtdCho

	757.6	783.6	785.6	805.6	807.6	809.6	833.6
■ Controls	1.00	1.00	1.00	1.00	1.00	1.00	1.00
□ Stage I	0.33	0.51	0.33	0.49	0.46	0.47	0.50
□ Stage II	0.38	0.41	0.34	0.48	0.38	0.43	0.43
□ Stage III	0.39	0.35	0.30	0.51	0.42	0.42	0.51
▨ Stage IVa	0.43	0.42	0.39	0.46	0.38	0.39	0.43
▩ Stage IVb	0.22	0.26	0.19	0.24	0.19	0.27	0.23

Figure 45

(c)

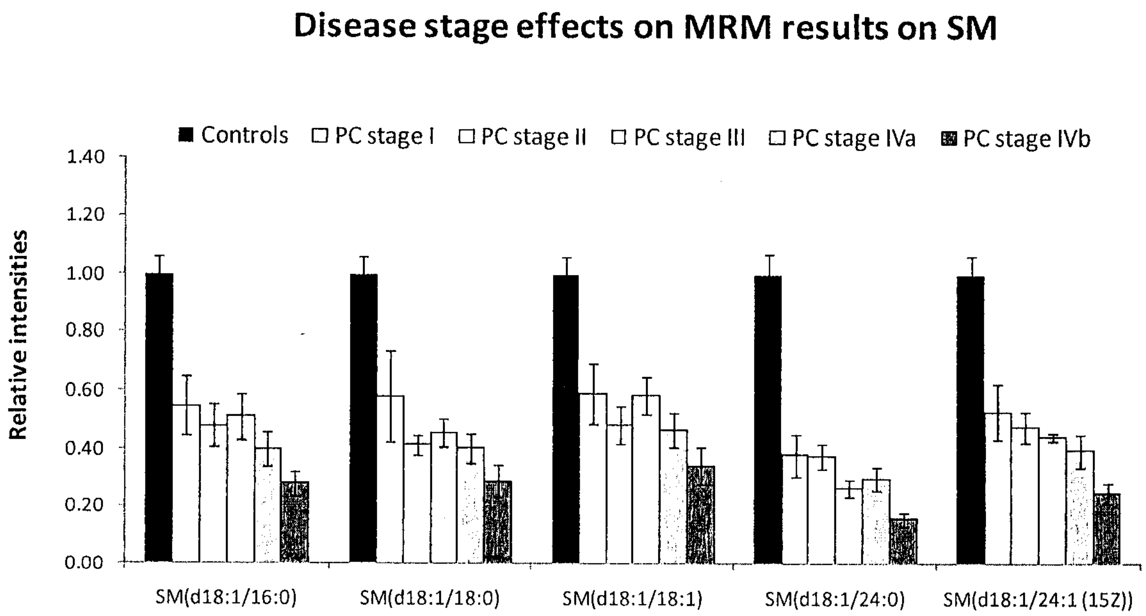

(d)

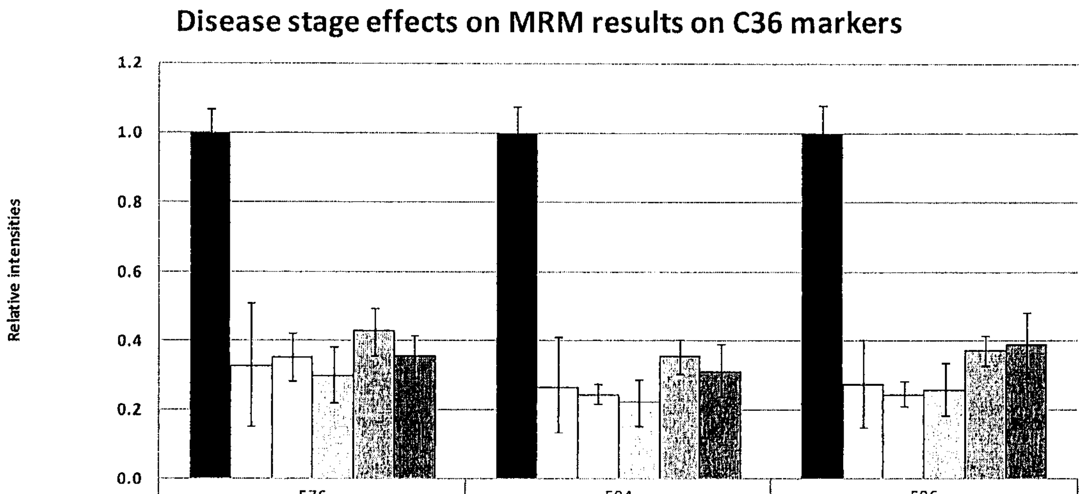

	576	594	596
■ Healthy controls	1.00	1.00	1.00
□ Stage I	0.33	0.27	0.28
□ Stage II	0.36	0.25	0.25
□ Stage III	0.30	0.22	0.26
▨ Stage IVa	0.43	0.36	0.37
▨ Stage IVb	0.36	0.31	0.39

Figure 45 (Cont.)

(a)

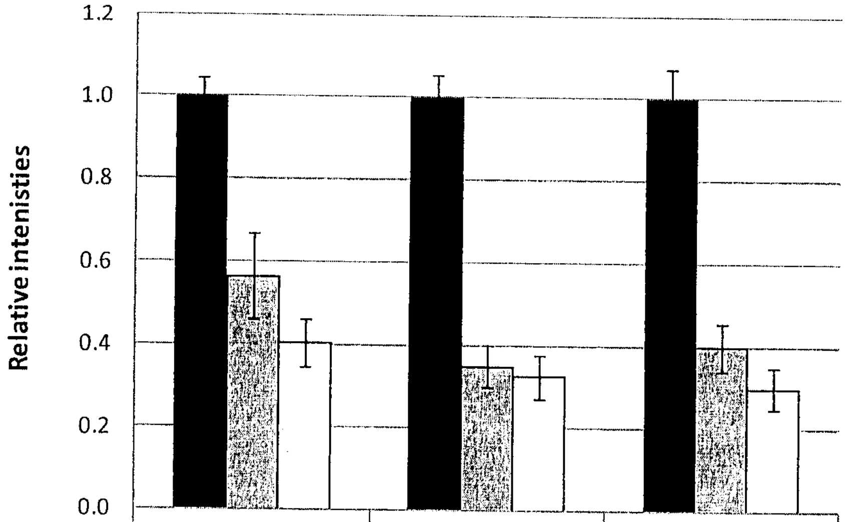

Chemoradiation therapy effects on MRM results on LysoPC

	LysoCh 18:0	LysoCh 18:2	LysoCh 20:5
■ Controls	1.00	1.00	1.00
▨ CRT	0.57	0.35	0.40
☐ No CRT	0.40	0.33	0.30

(b)

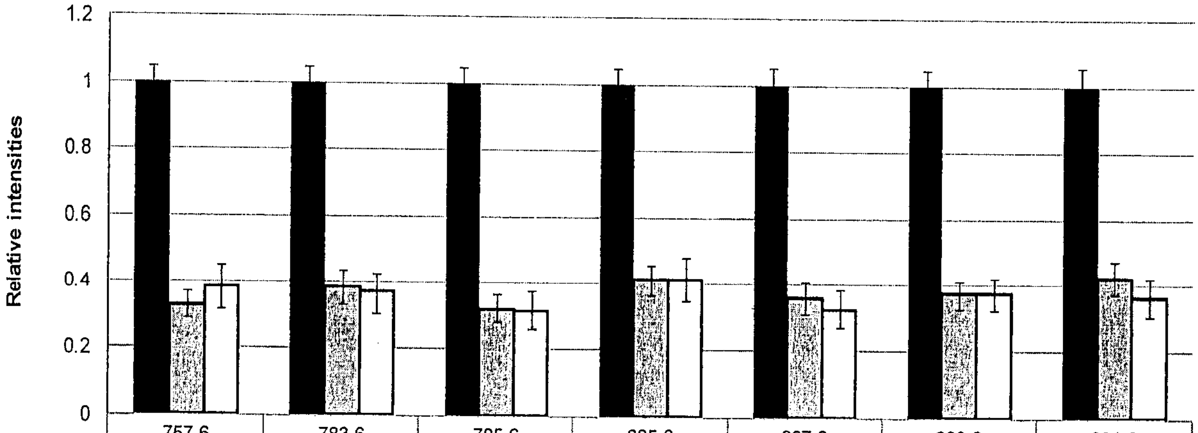

Chemoradiation therapy effects on MRM results on PtdCho

	757.6	783.6	785.6	805.6	807.6	809.6	831.6
■ Controls	1.00	1.00	1.00	1.00	1.00	1.00	1.00
▨ CRT	0.33	0.38	0.32	0.41	0.36	0.37	0.42
☐ No CRT	0.38	0.36	0.31	0.41	0.32	0.37	0.36

Figure 46

(c)

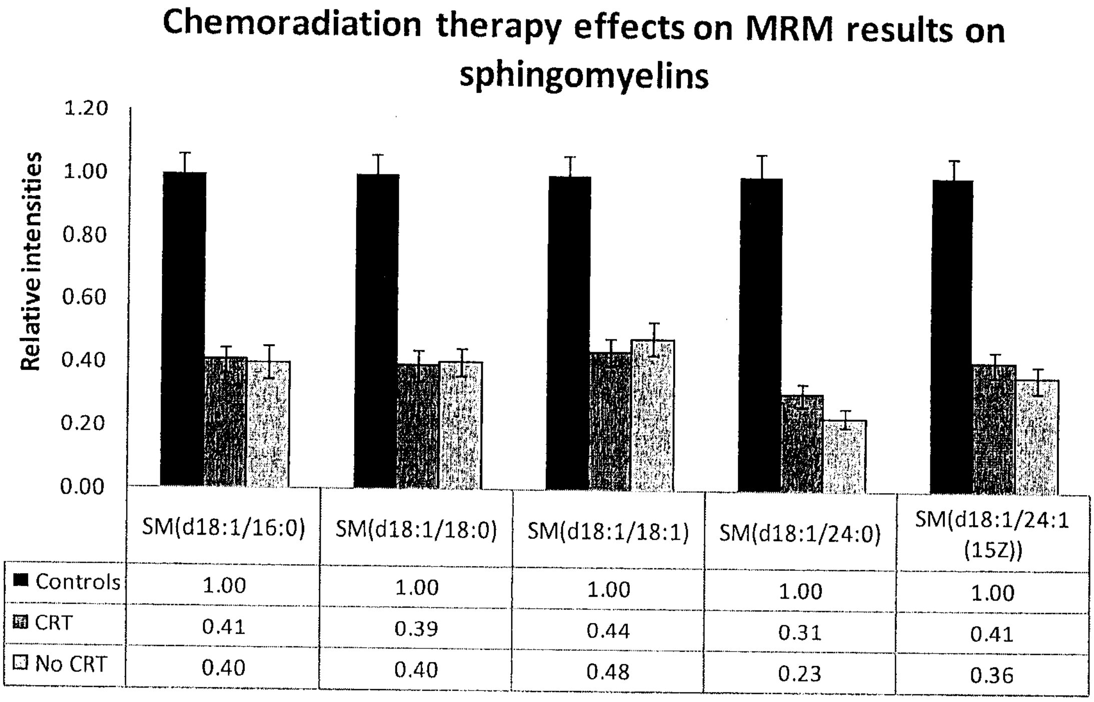

Chemoradiation therapy effects on MRM results on sphingomyelins

	SM(d18:1/16:0)	SM(d18:1/18:0)	SM(d18:1/18:1)	SM(d18:1/24:0)	SM(d18:1/24:1 (15Z))
■ Controls	1.00	1.00	1.00	1.00	1.00
▨ CRT	0.41	0.39	0.44	0.31	0.41
▨ No CRT	0.40	0.40	0.48	0.23	0.36

(d)

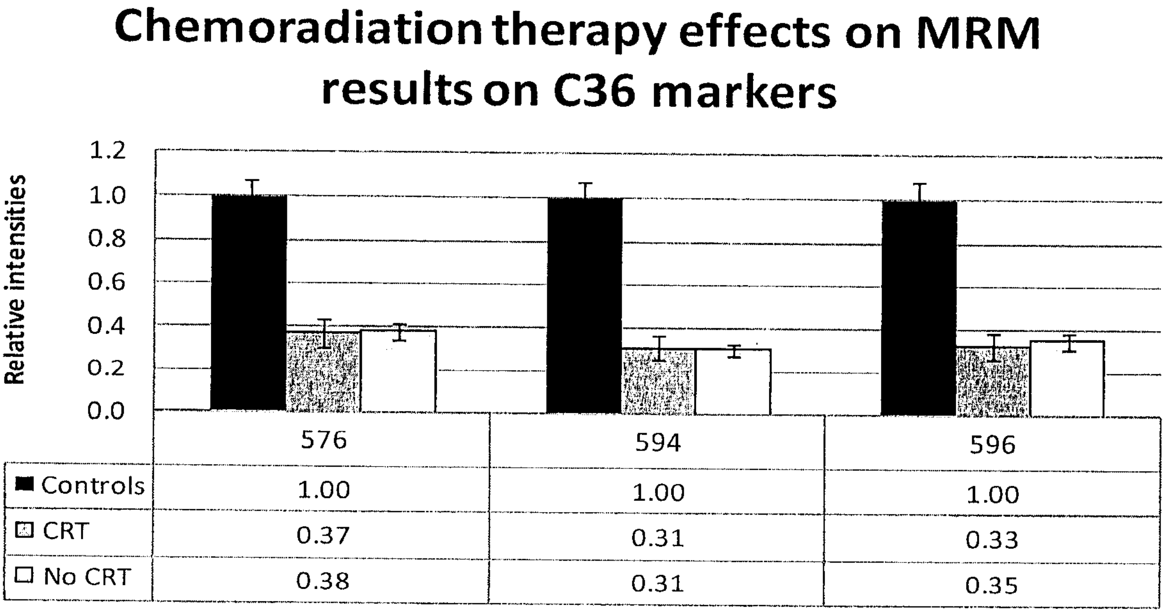

Chemoradiation therapy effects on MRM results on C36 markers

	576	594	596
■ Controls	1.00	1.00	1.00
▨ CRT	0.37	0.31	0.33
☐ No CRT	0.38	0.31	0.35

Figure 46 (Cont.)